

Open Research Online

The Open University's repository of research publications and other research outputs

The rheology of human blood and blood cellular components in suspension measured with a modified Weissenberg rheogoniometer

Thesis

How to cite:

King, Robert G (1984). The rheology of human blood and blood cellular components in suspension measured with a modified Weissenberg rheogoniometer. PhD thesis The Open University.

For guidance on citations see [FAQs](#).

© 1984 The Author



<https://creativecommons.org/licenses/by-nc-nd/4.0/>

Version: Version of Record

Link(s) to article on publisher's website:

<http://dx.doi.org/doi:10.21954/ou.ro.000100f1>

Copyright and Moral Rights for the articles on this site are retained by the individual authors and/or other copyright owners. For more information on Open Research Online's data [policy](#) on reuse of materials please consult the policies page.

oro.open.ac.uk

8014 10740/20
01/83.7
D54465/85

UNRESTRICTED

THE RHEOLOGY OF HUMAN BLOOD AND BLOOD CELLULAR COMPONENTS IN
SUSPENSION MEASURED WITH A MODIFIED WEISSENBERG RHEOGONIOMETER

BY

ROBERT G. KING

A Dissertation for the Degree of
Doctor of Philosophy in the
Open University, Milton Keynes.

Date of submission: 9 March 1984

Date of award: May 1984

ProQuest Number: 27777154

All rights reserved

INFORMATION TO ALL USERS

The quality of this reproduction is dependent on the quality of the copy submitted.

In the unlikely event that the author did not send a complete manuscript and there are missing pages, these will be noted. Also, if material had to be removed, a note will indicate the deletion.



ProQuest 27777154

Published by ProQuest LLC (2020). Copyright of the Dissertation is held by the Author.

All Rights Reserved.

This work is protected against unauthorized copying under Title 17, United States Code
Microform Edition © ProQuest LLC.

ProQuest LLC
789 East Eisenhower Parkway
P.O. Box 1346
Ann Arbor, MI 48106 - 1346

PREFACE

The work described in this thesis was carried out in the Division of Circulatory Physiology and Biophysics of the Department of Physiology, College of Physicians and Surgeons of Columbia University, New York, during the period of May, 1978 to June, 1983. Except where specific reference is made to the work of other authors, the material is original and is not contained in a thesis submitted to any other University.

I am indebted to Dr. Shu Chien, for initiating the investigation and for his advice and encouragement during its course.

January, 1984.

LIST OF CONTENTS

PAGE NO.

Abstract	1
--------------------	---

CHAPTER I

Introduction	3
The development of the Rheogoniometer	5

CHAPTER II

The application of the Weissenberg Rheogoniometer for the study of biological materials	9
Composition and physical properties of human blood . .	10
The design and development of test geometries suitable for use with biological materials	15
Cone and plate geometry	17
Combined couette and cone and plate geometry	19
Double couette concentric cylinder	19
Special geometry for the measurement of surface layers formed at interfaces	21
The couette geometry	23
Special torsion bars	23
The measurement of normal force	24
The attachment of a microscope and video/cine camera .	26
The addition of a mini computer to analyse and store data	28

CHAPTER III

The measurement of viscosity and elasticity of whole blood with varying hematocrits in steady, dynamic and pulsatile flow	31
Experimental method	31
Preparation of blood samples	31
Measurement of plasma viscosity	32
The rheological properties of hemoglobin	33
Effect of concentration	34
Effect of temperature	35

CHAPTER III (continued)

Measurement of viscosity in steady shear of red blood cells resuspended in plasma	35
Measurement of viscosity in steady shear of red blood cells suspended in Ringer-albumin solution	45
Comparison of data from the different preparations	52
The measurement of normal stress in RBCs resuspended in plasma	57
The effect of shear on the sedimentation rate of red blood cells	70
The measurement of viscosity and elasticity of RBCs resuspended in plasma, using oscil- latory shear	75
The measurement of viscosity and elasticity of RBCs resuspended in Ringer-albumin, using oscillatory shear	85
The measurement of viscosity and elasticity of RBCs resuspended in plasma using pulsa- tile flow	93
Rheological measurements of non-anticoagu- lated whole blood	95

CHAPTER IV

The rheological characteristics of preparations of abnormal blood.	102
The effect of changing tonicity of preparations of 80% red cells suspended in Na Cl solutions	103
The effects of deoxygenation on the viscosity and elasticity of packed sickle cell suspensions and sickle hemoglobin	107
The rheology of whole blood and suspensions of leukocytes in leukemia	121

CHAPTER V

Rheological measurements of surface layers of blood proteins at interfaces	132
The measurement of the viscoelasticity of surface layers of solutions of highly purified fibrinogen from different species	136
Measurements of the viscoelasticity of sur- face layers of solutions of human fibrino- gen at varying concentrations	138

CHAPTER V (continued)

The action of highly purified γ globulin and β lipoprotein on the viscous and elastic moduli of fibrinogen surface layers	142
--	-----

The effect of pH on the elasticity of surface layers of fibrinogen	143
--	-----

The inhibitory action on fibrinogen surface layer formation by certain heparins, dextrans and sodium hyaluronate preparations	146
---	-----

The rheology of surface films of extrinsic and intrinsic red cell membrane proteins	158
---	-----

CHAPTER VI

Conclusions and physiological significance	169
--	-----

APPENDIX I

The new Rheogoniometer	183
----------------------------------	-----

Torsion measuring system	185
------------------------------------	-----

Normal Force measuring system	187
---	-----

Oscillatory mechanism	190
---------------------------------	-----

Electronic measuring and recording system	191
---	-----

Material testing techniques	192
---------------------------------------	-----

APPENDIX II

A computer programme for the determination of the amplitude ratio and phase angle during oscillatory flow	196
---	-----

APPENDIX III

A computer programme for the determination of the amplitude ratio and phase angle during pulsatile flow.	201
--	-----

REFERENCES

Chapter I	206
---------------------	-----

Chapter II	207
----------------------	-----

Chapter III	208
-----------------------	-----

Chapter IV	215
----------------------	-----

Chapter V	217
---------------------	-----

Chapter VI	223
----------------------	-----

LIST OF ILLUSTRATIONS

CHAPTER I.

PAGE NO

Fig. 1	The Rheogoniometer designed and built by Freeman, 1947	6
Fig. 2	The Rheogoniometer designed by Roberts 1952, and built by Farol Research Engineers, Ltd., Bognor Regis, Sussex . . .	6

CHAPTER II

Fig. 1.	A scanning electron-micrograph of red cells in single form	12
Fig. 2.	A scanning electron micrograph of red cells in rouleau formation	14
Fig. 3.	A model representation of the red cell membrane (after Singer) showing a possible arrangement of proteins	14
Fig. 4	The development of a microscopic bubble in a sample of whole blood at 40% hematocrit during low shear on the cone of the Rheogoniometer. Elapsed time between the formation of the bubble and the last frame is three minutes	16
Fig. 5	A schematic drawing of the cone and plate geometry together with temperature control	18
Fig. 6	A schematic drawing of the Couette and Cone/Plate combined geometry	20
Fig. 7	A schematic drawing of the Double Couette geometry	20
Fig. 8	A schematic drawing of the Ring in Ring geometry for interface and surface rheological measurements	22
Fig. 9	A schematic drawing of the standard Couette geometry	22
Fig. 10	A sketch of an "I" beam torsion bar . . .	24
Fig. 11	A schematic drawing of the Tangential and Normal Stress measuring system when a cone and plate geometry is fitted	25
Fig. 12	A schematic arrangement of the microscope attachment	26
Fig. 13	A photograph of the Zeiss microscope attached to the Rheogoniometer	27

Fig. 1.	The effect of concentration on the apparent viscosity of cell free RBC hemolysate	33
Fig. 2.	The effect of temperature on the apparent viscosity of cell free RBC hemolysate at a concentration of 32g%	34
Fig. 3.	A recorder trace of tangential stress in steady shear, of RBCs in plasma at 40% hematocrit at 0.05 sec^{-1} . Photomicrographs are taken at the start of shearing, and at one minute intervals thereafter . .	36
Fig. 4.	A recorder trace of tangential stress in steady shear of a preparation of 40% RBCs in plasma at 54 sec^{-1} , together with photomicrographs taken at the start of shearing and then at one minute intervals .	39
Fig. 5.	A recorder trace in steady shear of RBCs resuspended in Ringer-albumin solution at 40% hematocrit, at 0.05 sec^{-1} together with photomicrographs taken at one minute intervals	46
Fig. 6.	Apparent Viscosity versus Rate of Shear in steady shear, of RBCs resuspended in plasma at hematocrits from zero to packed cells	52
Fig. 7.	Apparent Viscosity versus Rate of Shear, of RBCs resuspended in Ringer-albumin at hematocrits from 20 to 95 percent	53
Fig. 8.	A comparison of the Apparent Viscosity versus concentration of RBCs resuspended in plasma with RBCs resuspended in Ringer-albumin solution at 0.1 and 110.0 sec^{-1}	54
Fig. 9.	A comparison of the Relative Viscosity Ratio of RBCs in Ringer-albumin with RBCs in plasma at 0.1 and 110 sec^{-1}	56
Fig. 10.	A plot of the average negative normal stress, plotted against shear rate, of several glycerol solutions at different concentrations	59
Fig. 11a.	Corrected Normal Stress (N^*) versus Rate of Shear for RBCs in plasma at concentrations of 50 to 95 percent, showing the effect of shear rate and concentration . .	60
Fig. 11b.	Normal stress v. Hematocrit at shear rates from 50 to 1000 sec^{-1} with extrapolation to physiological hematocrits	61

Fig. 12. Elasticity (G), versus Rate of Shear, for RBCs in plasma at concentrations of 50 to 95 percent showing the effect of hematocrit	63
Fig. 13. A plot of sedimentation rate (ESR) versus Rate of Shear, showing the effect of increasing shear rate on sedimentation . .	73
Fig. 14. Viscosity (η^l) versus Frequency in oscillatory shear, of suspension of RBCs in plasma at concentrations of 20 to packed cells, showing the effect of frequency and hematocrit	86
Fig. 15. Elasticity (G^l) versus Frequency in oscillatory shear, of suspensions of RBCs in plasma at concentrations from 40% to packed cells, showing the effect of frequency and hematocrit on the elastic component	86
Fig. 16. Viscosity (η^l), versus frequency in oscillatory shear, of suspensions of RBCs in Ringer-albumin solution at concentrations from 20 to 90 percent and including packed cells, showing the effect of hematocrit and frequency on viscosity . .	87
Fig. 17. Elasticity (G^l) versus Frequency in oscillatory shear, of suspensions of RBCs in Ringer-albumin solution at hematocrits from 40% to packed cells, showing the effect of hematocrit and frequency on the elastic modulus	88
Fig. 18 Viscosity (η^l) versus hematocrit of RBCs in Ringer-albumin measured at 0.01 Hertz .	89
Fig. 19. Elasticity (G^l) versus hematocrit of RBCs in Ringer-albumin measured at 0.1 Hertz	90
Fig. 20. A comparison of Elasticity (η^l) versus Frequency, of RBCs in plasma with RBCs resuspended in Ringer-albumin solution at 50 and 80 percent hematocrit	91
Fig. 21. Elasticity (G^l) versus Frequency, of suspensions of RBCs in plasma at 50 and 80 percent hematocrits, showing the separate contributions of rouleau formation and the red cell to the elastic component	92

Chapter III (continued)

- Fig. 22. Viscosity (η') versus frequency, of a suspension of 80 percent RBCs in plasma, showing the change in viscosity when steady shear at 0.1, 1.0 and 10.0 sec^{-1} is superimposed on the oscillatory motion 94
- Fig. 23. A plot of elasticity (G') versus frequency, of a suspension of 80 percent RBCs in plasma, showing the effect on the elastic modules when steady shear at 0.1, 1.0 and 10.1 sec^{-1} is superimposed 94
- Fig. 24. A typical recorder trace of torque (γ) showing the clotting profile of non-anticoagulated whole blood of 44% hematocrit versus time 96
- Fig. 25. A plot of amplitude ratio versus time of a 44% Hct non-anticoagulated human blood measured in oscillatory shear 98
- Fig. 26. Phase lag versus time of a 44% Hct non-anticoagulated human blood measured in oscillatory shear 99
- Fig. 27. The viscosity (η') and elasticity (G') versus time, of a non-anticoagulated normal whole blood, of 44% hematocrit showing the effect on η' and G' of the coagulation process 100

CHAPTER IV

- Fig. 1. A scanning electron micrograph showing a red cell in crenated form 104
- Fig. 2. A scanning electron micrograph showing many red cells in crenated form 104
- Fig. 3. A plot of Viscosity (η') versus Osmolarity of 50 percent RBCs in Ringer-albumin solution showing the effect of changing Osmolarity and frequency 105
- Fig. 4. A plot of Elasticity (G') versus Osmolarity of 80 percent RBCs in Ringer-albumin solution showing the effect on the elastic modulus of changing osmolarity and frequency 106
- Fig. 5. A scanning electron micrograph of a tethered sickled red cell showing the typical crescent form 108
- Fig. 6. A scanning electron micrograph showing aggregated Hb molecules in typical rod-like structures 109

- Fig. 7. The Viscosity (η') of SS and AA cell suspensions in Ringer-albumin at a concentration of 90 percent as a function of O_2 saturation. Data were obtained at a frequency of 0.01 Hertz 112
- Fig. 8. The dynamic elastic modulus (G') of AA RBCs (—▲—) and SS RBCs(—●—) versus O_2 saturation measured in oscillatory shear² at 0.01 Hertz 113
- Fig. 9. The viscosity (η') of HbS and HbA solutions at a concentration of 32g/dl as a function of O_2 saturation. The data was obtained at a²frequency of 0.01 Hertz . . . 114
- Fig. 10. The elasticity (G') of HbS and HbA solutions at a concentration of 32g/dl as a function of O_2 saturation, measured at a frequency of² 0.01 Hertz 115
- Fig. 11. A comparison of the viscosity (η') versus O_2 saturation of 90% SS RBCs from sickle cell patients in an active and quiescent phase of the disease 116
- Fig. 12. A comparison of the elasticity (G') versus O_2 saturation of 90% SS RBCs from sickle cell patients in an active and quiescent phase of the disease 117
- Fig. 13. A comparison of the viscosity (η') versus O_2 saturation of 90% RBCs in Ringer-albumin and a HbS preparation at 32g/dl at a frequency of 0.01 Hertz 119
- Fig. 14. A comparison of the elastic modulus (G') versus O_2 saturation of 90% RBCs in Ringer-albumin and a HbS preparation at 32g/dl at a frequency of 0.01 Hertz 120
- Fig. 15. The Apparent Viscosity versus Rate of Shear, of suspensions of white blood cells (WBC) in a tris-saline-albumin (TSA) buffer solution, showing the effect of concentration. At low leukocrits the viscosity is Newtonian, but at a concentration of 40% and above, it becomes markedly non-Newtonian 121
- Fig. 16. A plot of Apparent Viscosity v. concentration of WBCs from both CLL and CML patients measured at 0.01 sec^{-1} . A change of slope occurs at between 30 and 40% concentration 125

Chapter IV (continued)

- Fig. 17. Viscosity (η') versus Frequency in oscillatory shear, of suspensions of WBCs from a CML patient, showing the effect on η' of increasing concentration 126
- Fig. 18. The Elasticity (G') versus Frequency, in oscillatory shear, of WBCs from a CML patient resuspended in TSA, showing the effect on G' of increasing concentration of WBCS 127
- Fig. 19. The viscosity (η') measured in oscillatory shear at 0.01 Hertz, of WBCs from patients with CML and CLL resuspended in TSA showing the effect of increasing leukocrit 128
- Fig. 20. The elasticity (G'), measured in oscillatory shear at 0.01 Hertz, of WBC in TSA of patients with CML and CLL showing the effect of increasing concentrations 129
- Fig. 21. Viscosity (η') versus frequency, showing the effect on whole blood viscosity of leukophoresis treatment. The values of hematocrit and leukocrit measured in the pre-leukophoresis blood samples were 35 and 16 percent. In the post leukophoresis blood sample the values were 33 and 12 percent 130
- Fig. 22. A scanning electron micrograph of white cells from a patient with CLL, showing the surface roughness of the membrane 131

CHAPTER V

- Fig. 1. Apparent Viscosity, measured in steady shear of normal human plasma plotted against Rate of Shear. The measurements were made with ($-\bigcirc-$) and without ($-\bullet-$) a detachable guard ring 133
- Fig. 2. Apparent Viscosity, measured in steady shear with and without a guard ring, of a solution of 0.4% human fibrinogen. 135
- Fig. 3. A typical recorder trace, obtained during an oscillatory experiment using the "Ring in Ring" geometry, of surface layers on a 0.4% solution of human fibrinogen, at a frequency of 0.01 Hertz. The solid trace represents the input motion, while the dotted trace represents the output from the torsion head. The phase difference between the two traces is 15 degrees 137

- Fig. 4. Surface Viscosity (η_s^I) measured in oscillatory shear at very low frequencies, of surface layers of solutions of fibrinogen from human, bovine and sheep 138
- Fig. 5. Surface Elasticity (G_s^I) measured in oscillatory shear at very low frequencies, of solutions of fibrinogen from human, bovine and sheep 139
- Fig. 6. Surface Viscosity (η_s^I) measured in oscillatory shear of surface layers from preparations of human fibrinogen at concentrations of 0.4, 0.004 and 0.00004 percent 140
- Fig. 7. Surface Elasticity (G_s^I) measured in oscillatory shear, of surface layers of preparations of human fibrinogen at concentrations of 0.4, 0.004 and 0.00004 per cent. 141
- Fig. 8. The effect on G_s^I of a surface layer of a 0.4% fibrinogen solution, when γ globulin at 0.01 and 1.0% concentration is added 142
- Fig. 9. The effect on G_s^I of the surface layer of a solution of 0.4% fibrinogen when β lipoprotein is added at a concentration of 0.029% and 0.25%. The addition of 0.25% eliminates the layer altogether. 144
- Fig. 10. The effect of pH on G_s^I of surface layers of a preparation of 0.4% fibrinogen. As pH is lowered, G_s^I increases, while at pH 8.6 it is weakest. There is a plateau over the pH range 6.8 to 7.6 which are approximately physiological normal values 145
- Fig. 11. Comparisons of the surface elasticity (G_s^I) of surface layers of 0.4% human fibrinogen as control, compared with 0.5% fibrinogen preparations to which 100 and 500 NIH units of heparin (Organon) are added 148
- Fig. 12. A plot of the Surface Elasticity (G_s^I) of 0.4% Human Fibrinogen compared with a 0.4% fibrinogen plus 0.2% heparin prepared by Lindahl. This heparin preparation does not show any affinity for antithrombin, but still considerably weakens G_s^I 149

- Fig. 13. Plots showing the effect on surface elasticity (G_s^I) of surface layers of 0.4% human fibrinogen when two different low molecular weight heparin fractions are added 150
- Fig. 14. Plots showing the effect on G_s^I of surface layers of 0.4% fibrinogen solutions when a sodium heparin and calcium preparations (Chaoy) are added) 151
- Fig. 15. The viscous (η_s^I) and elastic (G_s^I) moduli versus frequency of surface layers of a 0.2% fibrinogen solution in a tris-saline buffer of pH 7.4, compared with a similar preparation containing the addition of 5mM Ca Cl_2 152
- Fig. 16. Surface viscosity (η_s^I), versus frequency of a 0.4% fibrinogen solution as control, compared with three fibrinogen preparations to which heparin depolymerization products of MW 4400, 5300 and 5900 Daltons have been added 153
- Fig. 17. Surface Elasticity (G_s^I) versus Frequency of a 0.4% fibrinogen solution as control, compared with 0.4% fibrinogen solutions plus 0.2% of heparin depolymerization products of 4400, 5300 and 5900 molecular weight 154
- Fig. 18. The elasticity (G_s^I) of a surface layer of a 0.4% solution as control, compared with fibrinogen solutions to which chondroitin A, B and C were added 155
- Fig. 19. The viscous (η_s^I) and elastic moduli (G_s^I) of surface layers of a 0.4% solution of human fibrinogen plus 0.2% dextran, MW 20,000 compared to a 0.4% human fibrinogen preparation as control 156
- Fig. 20. Surface elasticity (G_s^I) of surface layers of 0.2% dextran sulfate (MW 17,000) compared to 0.2% fibrinogen solution as control 157
- Fig. 21. The viscous (η_s^I) and elastic (G_s^I) moduli of 0.2% sodium hyaluronate plus 0.2% human fibrinogen solution surface layers, compared to a 0.2% fibrinogen solution as control 157
- Fig. 22. The Surface Viscosity (η_s^I) and the Surface Elasticity (G_s^I) of spread Spectrin/Actin surface films, plotted as a function of time, showing the effect of age on the surface film 160

- Fig. 23. The Surface Viscosity (η_s^l) of spread Spectrin/Actin surface films as a function of surface at four different frequencies of oscillation 162
- Fig. 24. The Surface Elasticity (G_s^l) of spread Spectrin/Actin surface films plotted as a function of approximate film thickness in angstroms at four different frequencies of oscillation 163
- Fig. 25. The surface viscosity (η_s^l) of spread layers of intrinsic red cell membrane proteins plotted as a function of the thickness of the film, at three different frequencies of oscillation 165
- Fig. 26. The surface elasticity (G_s^l), of surface layers of intrinsic red cell membrane proteins, plotted as a function of the estimated thickness of the film at three different frequencies 166
- Fig. 27. The Surface Viscosity (η_s^l) and the Surface Elasticity (G_s^l) of spread layers of intrinsic red cell membrane proteins of approximately 100Å thick, plotted as a function of frequency 167

APPENDIX I.

- Fig. 1. An illustration of the complete assembly of the new Rheogoniometer 184
- Fig. 2. A cut away section of the torsion measuring system 186
- Fig. 3. A sketch of the Normal Force Diaphragm assembly 187
- Fig. 4. A schematic layout of the Normal Force measuring system 188
- Fig. 5. A sketch of the mechanical parts of the Normal Force Measuring System 189
- Fig. 6. A schematic arrangement of the variable sine wave generator 190
- Fig. 7. Arrangement of the gearing for oscillatory and rotational motions 191
- Fig. 8. A representation of the steady shear and oscillatory modes 192
- Fig. 9. A plot of Tangential and Normal Stress versus Shear Rate for Nylon 6. at 270°C . 194

APPENDIX I. (continued)

Fig. 10.	A plot of Tangential and Normal Stress versus Shear Rate for Polystyrene at 200 °C	194
Fig. 11.	A plot of Tangential and Normal Stress versus Shear Rate of polypropylene at 190 °C	195
Fig. 12.	A plot of Tangential and Normal Stress versus Shear Rate for Milk Chocolate at 40 °C	195

ABSTRACT

The development of the Weissenberg Rheogoniometer is described, together with details of the modifications that were required to adapt it for hemorheological studies.

The rheological parameters, viscosity and elasticity of whole blood from healthy human donors, prepared in concentrations of red cells from 10 to 95 percent, were measured in steady, oscillatory and pulsatile flow. The viscosity and elasticity of red cells resuspended in buffer solution at similar concentrations are also reported. The changing rheological properties of the clotting process of non-anticoagulated human blood have been studied with time.

Preparations of red cells and white cells in abnormal states (in sickle cell disease and leukemia) have been studied and the rheological data reported.

Surface rheological investigations are also made of preparations of blood proteins such as fibrinogen, albumin and spectrin/actin derived from the red cell membrane. These materials are deployed both at air-fluid and fluid-fluid interfaces. The effect of the addition of such materials as coagulating and anticoagulating agents to these preparations are also studied.

The results of these investigations serve to establish the mechanism regulating the viscoelastic behavior of blood in health and to elucidate the pathophysiological changes in blood rheology in disease.

CHAPTER I.

Introduction.

The purpose of this study is to apply the theories and spatial concepts of Weissenberg (1,2,3,4) to elucidate and widen the knowledge of the mechanical behavior of blood cellular elements in suspension, and of whole blood itself in healthy condition and in some diseased states using a modified Weissenberg Rheogoniometer. The aim is to specifically measure the viscous and elastic moduli of normal whole blood and of suspensions of its individual components, and to investigate their interaction with one another, and to discuss their physiological significance. There are many diseases in which difficulties in the circulatory system arise, marked by abnormalities in size, shape and concentration of one or more of the constituents of blood. It is therefore important to observe what effect these abnormalities may have on the flow characteristics and to compare them with the normal state.

The studies reported in this thesis comprise a series of separate investigations of the rheological properties of suspensions of different blood cellular elements and of whole blood. As these materials exhibit a wide range of different mechanical properties, different measuring techniques are required to precisely evaluate their rheological characteristics. Together, these measurements comprise a unifying study describing the rheological properties of blood in normal and in some diseased conditions which is aimed at broadening our knowledge of the dynamics of the circulatory system.

For this study, Weissenberg's concepts have been translated into two main types of experimental approach which have been applied to the measurement of the rheological characteristics of these materials by means of a modified Rheogoniometer, these are:-

a) In continuous laminar shearing motion, the tangential and normal components of stress are measured in preparations of whole blood at a series of rates of shear. From these parameters, the apparent viscosity, an elastic modulus, and the recoverable strain (Weissenberg Number), are calculated as functions of the rate of shear.

b) Harmonic oscillatory shearing tests are carried out at small strain amplitudes and at a series of frequencies, and the frequency dependent moduli of viscosity and elasticity are calculated. The effect of pulsatile flow on these parameters is also investigated.

These two experimental techniques will give different values depending on the type of structure present in the material. Only simple Newtonian liquids will give the same answer, but viscoelastic liquids will exhibit different properties in the different tests and coincident values of the moduli can only be expected in extrapolation to zero rate of shear or frequency.

In continuous unidirectional laminar shearing action, or "continuous flow" the structure present in the material is continuously broken down and reformed. The material at any given rate of shear may be physically quite different from the material in its rest state or at any other rate of shear. Orientation of component molecules or particles may occur under the action of the shearing motion and the thermodynamic properties of the material will be different in the sheared state if free energy is stored. This type of test will not, in

general, give information about the material in its rest state except by extrapolation to zero rate of shear. This information is of use to the clinician and physiologist who requires to know the flow properties of the material in the sheared state, which may account for some specific clinical condition or event.

In harmonic oscillatory motion, the material is subjected to a harmonic laminar shear about its rest state at different frequencies. When the amplitude of the strain vibration is sufficiently small, this becomes a test of the material in its natural state. It is this type of test that is most likely to yield the colloidal structural information of interest to the biochemist and bioengineer.

The development of a Rheogoniometer.

Weissenberg (3) pointed out that in materials of a general nature, additional forces were generated in other directions than the applied strain, and in his theoretical approach, the application of three fundamental principles were required, which are:- a) The dynamic equilibrium of forces at all points in the flowing material. b) The maintenance of continuity, and c) The stress/strain relationship with time.

It was not until the late 1940s that Weissenberg and Freeman, 1949, (5,6) set out to establish this hypothesis by constructing an apparatus which they termed the "Rheogoniometer". This instrument, in its ideal form, would yield a complete specification of rheological data concerning a particular material by measuring the development with time of the stresses and strains present throughout the whole solid angle. Although this instrument approximated to these ideals, it did not in fact achieve Weissenberg's goal of the measurement of all the stresses and strains in all directions. Figure 1 is an illustration of the Rheogoniometer designed and constructed by

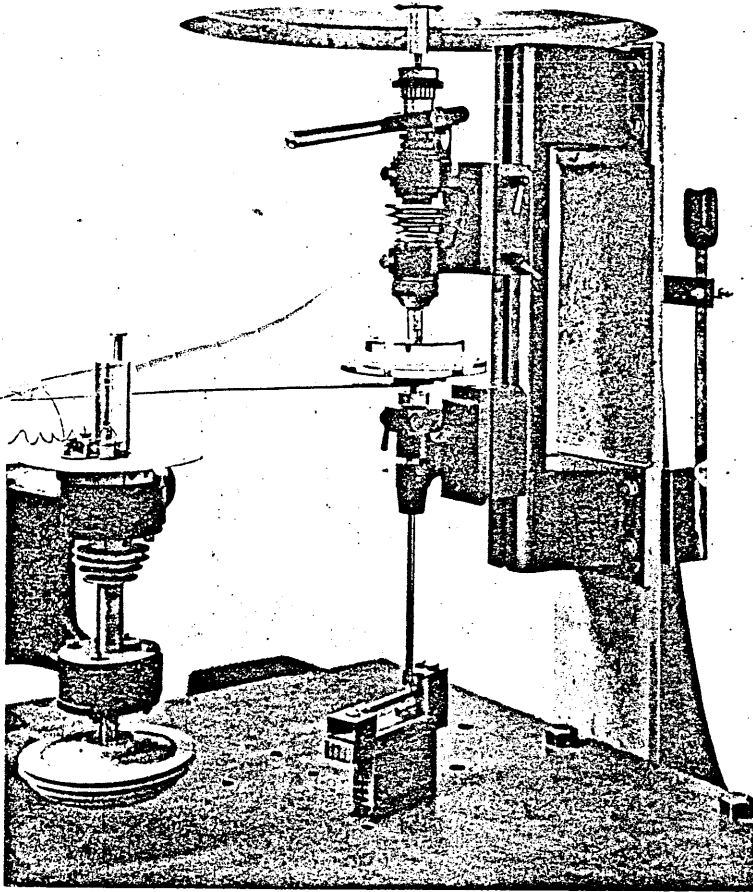


Figure 1. The Rheogoniometer designed and built by Freeman, 1949.

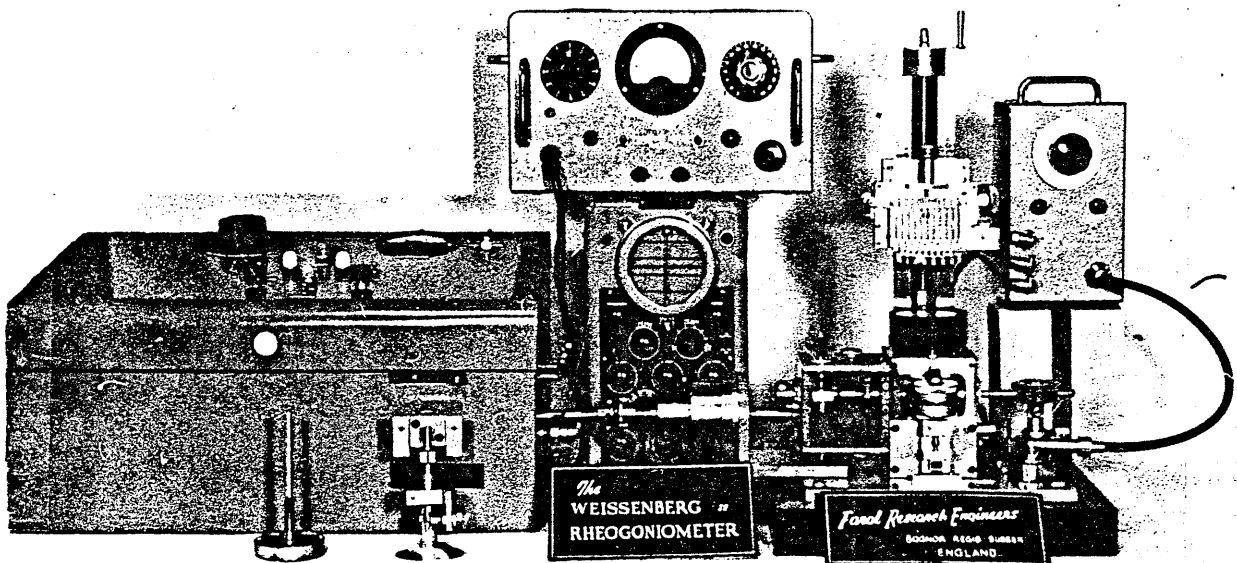


Figure 2. The Rheogoniometer designed by Roberts, 1952, and built by Farol Research Engineers, Ltd., Bognor Regis, Sussex.

The usual analysis of flowing materials using conventional viscometers is limited to the relationship of the stress in the same direction as the displacement. Weissenberg's concept of measuring the properties of fluids in a goniometric pattern was to become increasingly important when solving flow problems associated with complex new materials such as plastics and other synthetic materials that were developed at this time.

Weissenberg's concept of goniometric measurements of "distributions of stresses and strains within the flowing material at every point in space around the full solid angle" appeared essential to the research and development effort concerning these new materials. Accordingly, Weissenberg who was at that time Director of Physics Research at the Shirley Institute, Manchester was invited to act as consultant on the process of formulating a method to investigate these problems. He proposed that his idea for an instrument (the Rheogoniometer) be further developed, and accordingly, an improved version of the Rheogoniometer was developed and constructed under the direction of J. Roberts, with the advice of K. Weissenberg (7). Figure 2 is an illustration of the Roberts version of the Rheogoniometer which was made available to Farol Research Engineers, Ltd., Bognor Regis, Sussex, to be manufactured commercially, but this instrument had limited sensitivity and could only measure a comparatively narrow viscosity range (8). It was proposed by Roberts (9), that the Rheogoniometer should be redesigned so that it could cover a complete range of materials of all viscosities, from solid to water, and so have the widest possible application for industrial and academic research. Accordingly, the development of an improved Rheogoniometer was commenced, chiefly by R. G. King who was the senior engineer of Farol Research Engineers, Ltd.,

The general specification of the new Rheogoniometer included the capability to subject materials, over a wide range

of temperatures to:-

- a) Unidirectional laminar shear.
- b) Vibrational (reciprocating) shear.
- c) Both unidirectional laminar shear and vibrational shear at the same time.

The new Rheogoniometer was developed by a small team at Farol Research Engineers, Ltd., and the improved design was reported by King (10).

Weissenberg's theories and concepts in the field of fluid dynamics have been discussed by Weissenberg (1,2,3,4,6) Freeman (5), Roberts (7), Jobling (8), Grossman (11,12,13,14) Giesekeus (15), Lodge (16), Scott-Blair (17) and others.

Formulae for the calculation of the various rheological parameters measured by the Rheogoniometer have been described by Weissenberg (18) and Walters (19). These formulas have been used to calculate the values of the various rheological parameters of the materials measured, that are described in this thesis.

Appendix I contains a short description of the Rheogoniometer used in this study. Modifications that were found necessary to adapt the instrument for the measurement of hemorheological fluids are described in Chapter II.

CHAPTER II.

THE APPLICATION OF THE WEISSENBERG RHEOGONIOMETER FOR THE STUDY OF THE RHEOLOGICAL PROPERTIES OF BIOLOGICAL MATERIALS.

As previously described in Chapter I, the new Rheogoniometer was primarily designed for the measurement of phenomeological fluids of interest to industry. Most of these materials were of high or comparatively high viscosity. The application of the Rheogoniometer to study biological materials was not seriously considered from a commercial point of view, as only a small number of researchers were interested in such measurements. These were notably, Weissenberg 1961, (1); Scott-Blair 1952, (2); Copley 1960, (3); Whitmore 1963, (4); Dintenfass 1962 (5); Wells 1964, (6); and Gregersen 1963, (7); King 1962, (8), did make an attempt to use the standard Rheogoniometer to measure bovine synovial fluid and blood. These materials were supplied by G. W. Scott-Blair who was Director of the Dairy Research Institute, Reading, Berks.

With the great advances of medical sciences, many diseases no longer remained the killers they once were. Cardiovascular diseases have persisted, and have increased statistically. During most recent years, there has been an increasing interest in the nature of the rheological characteristics of flowing blood and blood components, as research into the cause of cardiovascular problems widened. Most of the early rheological investigations however, were made with capillary viscometers.

These instruments will measure accurately only ideal fluids that are Newtonian. As most biological materials are non-Newtonian, the capillary viscometer is not completely suitable for these measurements. It was felt that the uniqueness of the Rheogoniometer and its ability to measure the elastic component of a fluid would make it an excellent tool for hemorheological research, if certain adaptations were made to meet the rather special requirements of these fluids.

Blood is a complex suspension of several types of deformable particles, some more deformable than others, in an aqueous solution of many proteins. Its purpose is to circulate throughout the vascular system bringing oxygen and nourishment to cells, while removing metabolites.

This study is aimed at further elucidating the rheological behavior, specifically with measurements of the viscous and elastic moduli of healthy whole blood and also the rheological properties of its individual components and their interaction with one another.

There are many diseases in which difficulties in the circulatory system arise, marked by abnormalities in size, shape and concentration of one or more of the constituents of the blood. It is therefore important to see what effect these abnormalities may have on the flow properties of human blood.

Composition and properties of Human Blood

Human blood is a suspension of three general types of particles in a continuous medium, the plasma.

The three types of particles are the red cells (erythrocytes), white cells (leukocytes), and platelets.

Plasma is a solution of inorganic salts and organic macromolecules in water. The normal human red cell has the shape of a biconcave disk with a general diameter of eight microns and a thickness of two microns. Its average volume is 85 cubic microns. The shape of the erythrocyte can be seen in Fig. 1. It is quite flexible and is deformed into many shapes during its circulation around the circulatory system. The red cell is a membrane container filled with a solution rich in hemoglobin.

In health, the human male has about 5.4 million red cells per cubic millimeter of blood, while the human female has about 4.6 million per cubic centimeter. This gives an average volume percentage of red cells (hematocrit) in man of 45 percent, and in woman 42 percent. At normal pH of 7.4 the red cells have a negative charge. They will aggregate face to face in a rod like structure called rouleaux, if fibrinogen or other macromolecules are present in the suspending medium. The mechanism of rouleaux formation has been postulated to be due to macromolecular bridging between adjacent cell surfaces. The bridging energy is a function of the nature of binding sites between the macromolecules and cell surfaces. The red cell surface is negatively charged due to the presence of sialic acids. The interaction of surface potentials results in a significant mutual repulsion between the cells, especially in the presence of macromolecules. The magnitude of the repulsion is a function of surface charge density and ionic composition of fluid medium. Aggrega-

tion occurs when the bridging force due to surface adsorption of macromolecules overcomes the electrostatic repulsive force. Figure 1 is an electronmicrograph of single

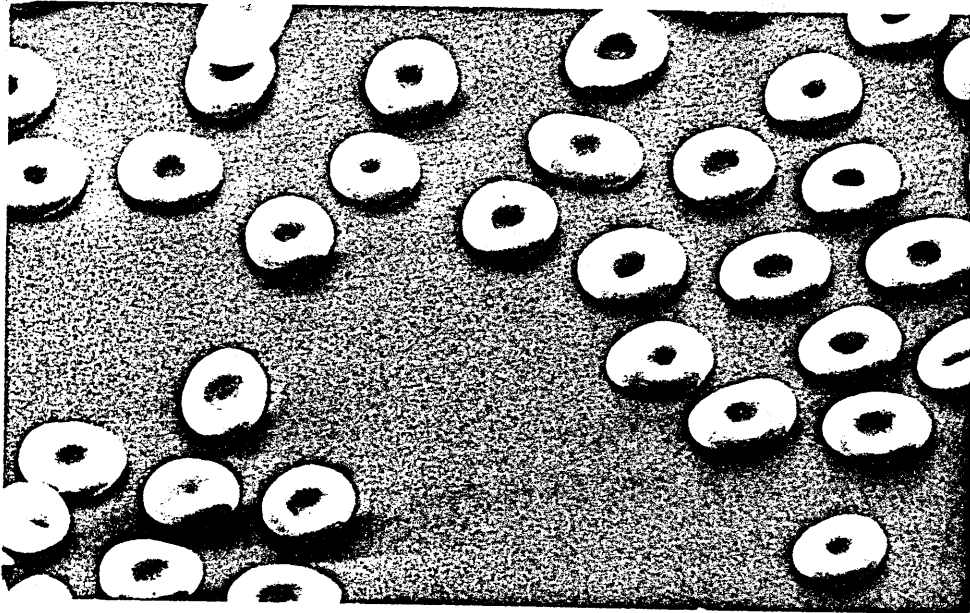


Figure 1. A scanning electron-micrograph of red cells in single form.

red cells, and Figure 2 is an illustration of the red cells in rouleaux formation.

The red cells when in rouleaux formation are only weakly held together and when the blood is sheared, the rouleaux decrease in length, or break up into single cells. The rouleaux are not rigid, but can bend without the red cells breaking open, demonstrating the flexibility of the red cell membrane.

The formation of these rouleaux has been extensively studied by Fahraeus, 1929 (9), who showed that the plasma protein albumin prevented rouleaux formation, while the globulins aided rouleaux formation weakly, but fibrinogen greatly enhanced the formation of rouleaux.

The red cell membrane strongly determines the

physical and chemical properties of the whole erythrocyte.

An interpretation of the structure of the membrane, Singer, 1974 (10), is shown in Figure 3. It consists of an asymmetric lipid bilayer with proteins interjected at intervals, some of which traverse the thickness of the bilayer, affording the possibility of communication and transport across the membrane. The protein spectrin is present, possibly in a continuous network together with other proteins, lining the cytoplasmic surface of the bilayer and appears to be involved in the regulation of cell shape as well as anchoring membrane, holding spanning proteins in place.

The red cell membrane has an elastic memory. This has been investigated by Katchalsky et al, 1960 (11); Rand, 1964 (12); Hochmuth et al, 1973 (13); Evans and La Celle, 1975 (14); Chien et al, 1978 (15).

Special techniques required for handling blood systems.

The measurement of blood and blood systems in the Rheogoniometer requires the observance of several precautions:-

a) Blood has a corrosive action on metals and some other materials, so that metals and metal alloys which are usually used for the test geometries cannot be used.

b) Blood cellular elements tend to form clumps or clots and the plasma coagulates rapidly after the blood is shed. These processes can be slowed by siliconization of those parts of the viscometer that come into contact with these blood components.

c) Certain anticoagulants will have to be employed

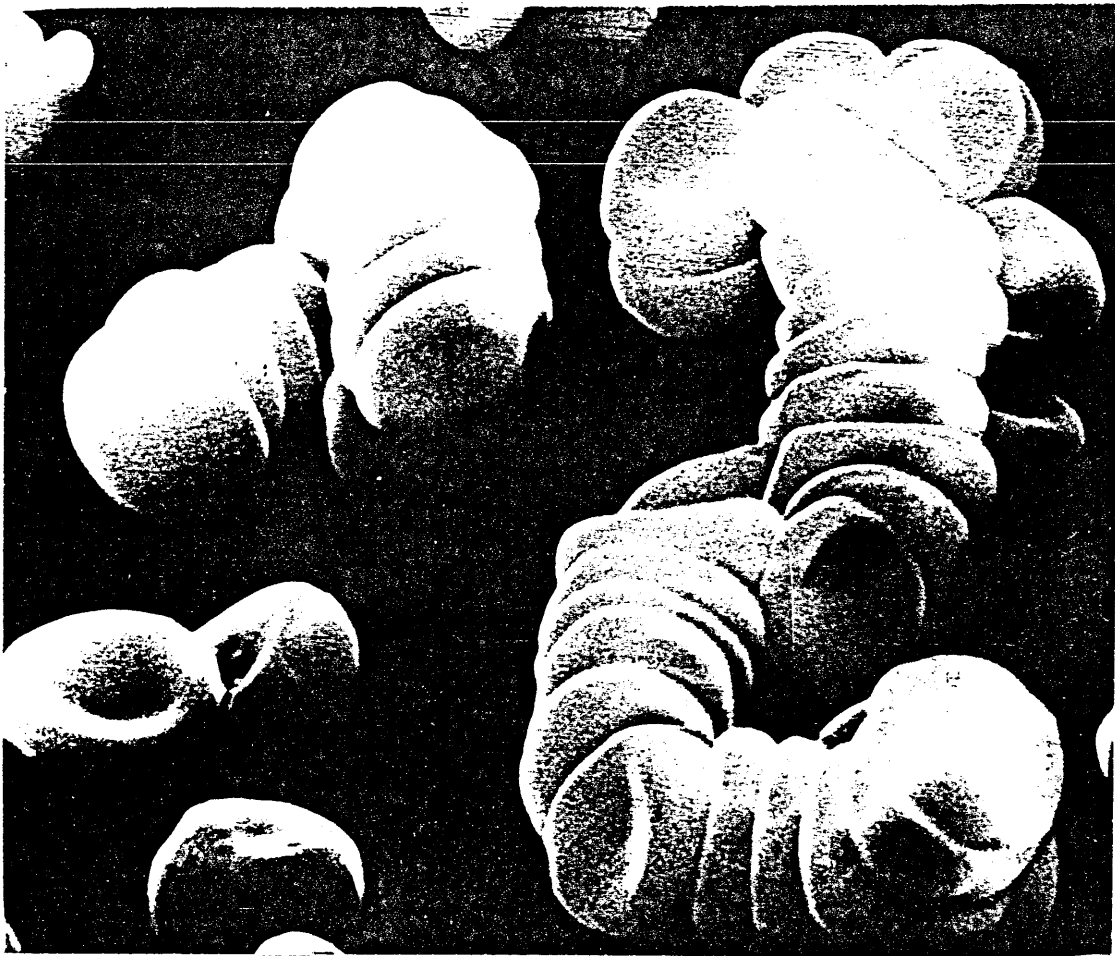


Figure 2. A scanning electron-micrograph of red cells in rouleau formation.

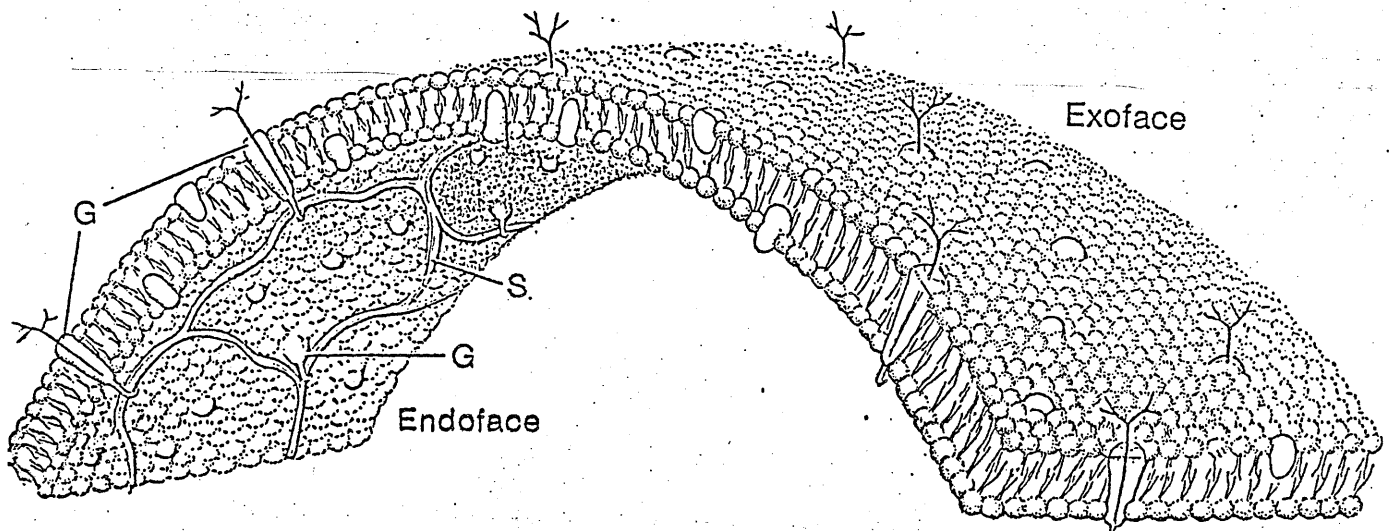


Figure 3. A model representation of the red cell membrane (after Singer) showing a possible arrangement of proteins.

to prevent coagulation but do not necessarily prevent blood cellular clumping or aggregation.

The action of the shear in the Rheogoniometer,

if prolonged, can cause the formation of macroscopically visible clumps, which could not be seen unless the viscometer geometry was transparent. These clumps, which were microscopically found to be mostly composed of platelets (when measuring whole blood) can cause the measurements to be unreliable. Small bubbles can form, which, if in large enough numbers, will cause an apparent increase in viscosity. The evolution of such a bubble has been photographed with a microscope attached to the Rheogoniometer, and is shown in Fig.4 . It is important, therefore, that the test sample be observed at least macroscopically during the measurement.

d) Blood and systems of blood components as well as other biological fluids are sometimes in short supply and necessitate the use of small volumes. The instrument therefore must be compatible with small sample sizes but still give accuracy of measurement. It may even be necessary, in some instances, to pool the material to obtain a sufficient quantity.

e) Biological materials, which may quickly degrade, should be measured in the shortest possible time.

The design and development of test geometries suitable for use with biological materials

In order to satisfy the requirements that are predicated previously, the components that come into direct contact with the biological materials to be tested were the immediate targets for design changes, and accordingly four new geometric measuring heads were designed and constructed. These geometries are described and their preferred application is explained as follows:-

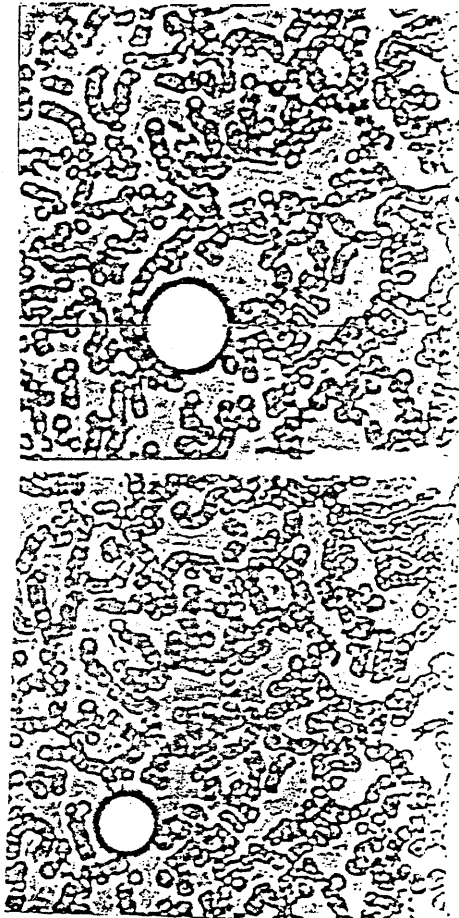
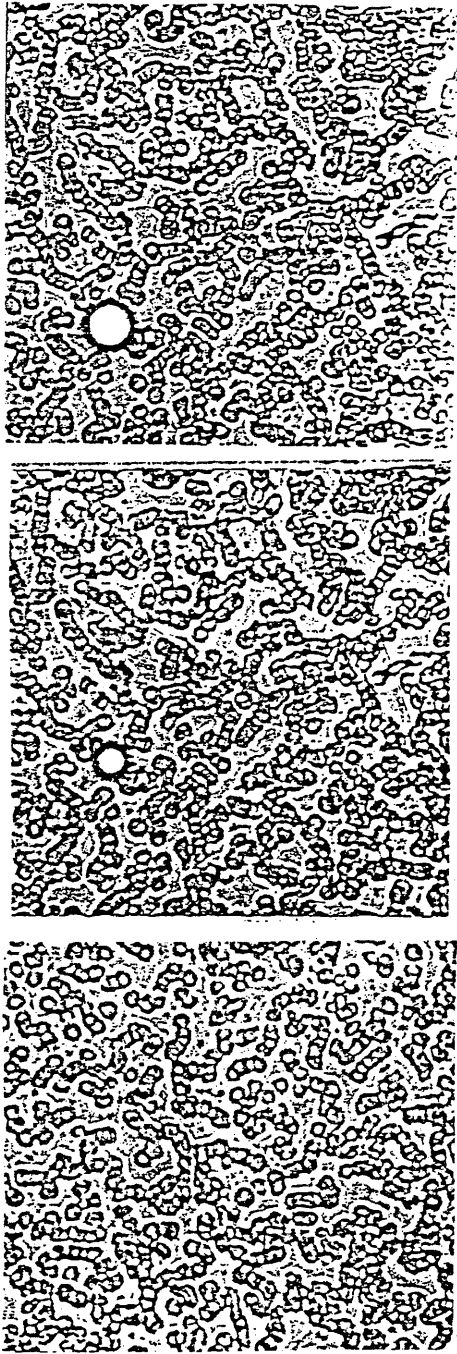


Figure 4. The development of a microscopic bubble in a sample of whole blood at 40% hematocrit during low shear on the cone of the Rheogoniometer. Elapsed time between the formation of the bubble and the last frame is three minutes.

The cone and plate.

A cone and plate which carries its own temperature control jacket together with a guard ring, is illustrated in Fig. 5. The advantage of using a cone and plate when compared to some other geometries is that the shear rate in steady shear, remains virtually constant along the radius of the cone when the angle of the cone remains small. This makes it ideal for the measurement of non-Newtonian fluids where the viscosity is dependent on the rate of shear.

The geometry is constructed of plexiglass which is lightly polished so that it is transparent. This enables the test sample to be observed during the experiment and the appearance of small bubbles or aggregates of particulate material can then be seen, which may explain unexpected data.

A cone angle of 1° was chosen as being the most suitable. This angle will give a reasonable amount of room for the development of chains or aggregates of molecules which may be present in the test material to allow their effects to be measured. There would also be sufficient room for the red cell (erythrocyte) either singly or in clumps, or for the development of complicated rouleau formations. These events are responsible for much of the interesting rheological behavior found in whole blood systems.

The 1° angle cone and plate does not require a large volume of material to fill the gap. This is important when materials are in short supply. This geometry

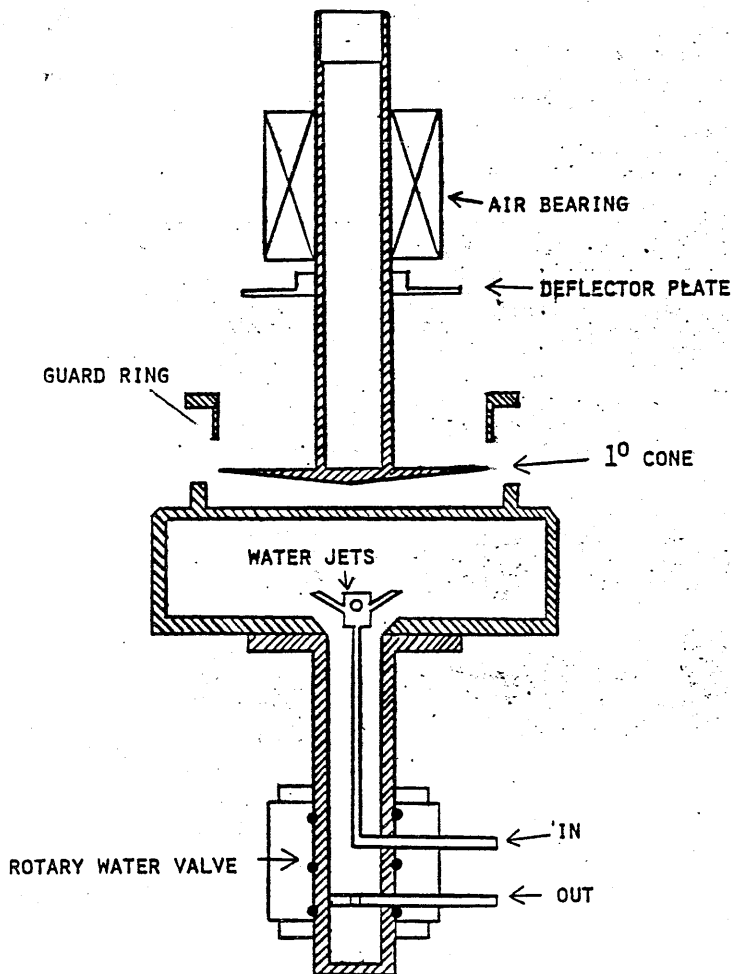


Figure 5. A schematic drawing of the cone and plate geometry together with temperature control.

was made in two diameters, 5cm. and 7cm. requiring 3 and 5ml. of sample respectively.

The 5cm diameter cone is particularly useful for coagulation studies, either for whole blood clotting, plasma systems, or for gels of selected plasma proteins.

The 5 and 7cm. diameter cones have low inertia because of their very thin section, making them particularly sensitive to transient changes of stress in the test material. The low mass make them particularly suitable for dynamic (oscillatory) experiments.

A guard ring is used with this geometry to

avoid the measurement of spurious torque derived from surface layers of material either by drying or the action of surface active proteins, that develop at the sample/air interface giving increased torque readings.

Combined Couette concentric cylinder and cone and plate.

This geometry illustrated in Fig. 6, is particularly suitable for the measurement of biological fluids of very low viscosity such as serum, plasma, hemoglobin solutions or solutions of plasma proteins, because of its large surface area (130 sq.cm.).

The diameter of the inner cylinder is 5cm. and the height is 7cm. The radial gap is .05cm. The radial gap chosen, is one that gives the same shear rate in the parallel part of the geometry as the coned end, again making it suitable for the measurement of non-Newtonian materials.

Double Couette concentric cylinder.

A double Couette concentric cylinder is also a suitable geometry for the measurement of biological materials of low viscosity. This is illustrated in Fig. 7. The geometry has a large surface area of 132sq.cm. as torque is measured on both sides of the inner cylinder. The diameters of the inner cylinder are 2.9 and 3.1 cm. The radial gap on the inner surface is .047cm and on the outer surface is .053cm. The difference is to ensure a constant rate of shear when the inner surface is compared to the outer surface and to compensate for the effect of radius. The height is 7cm.

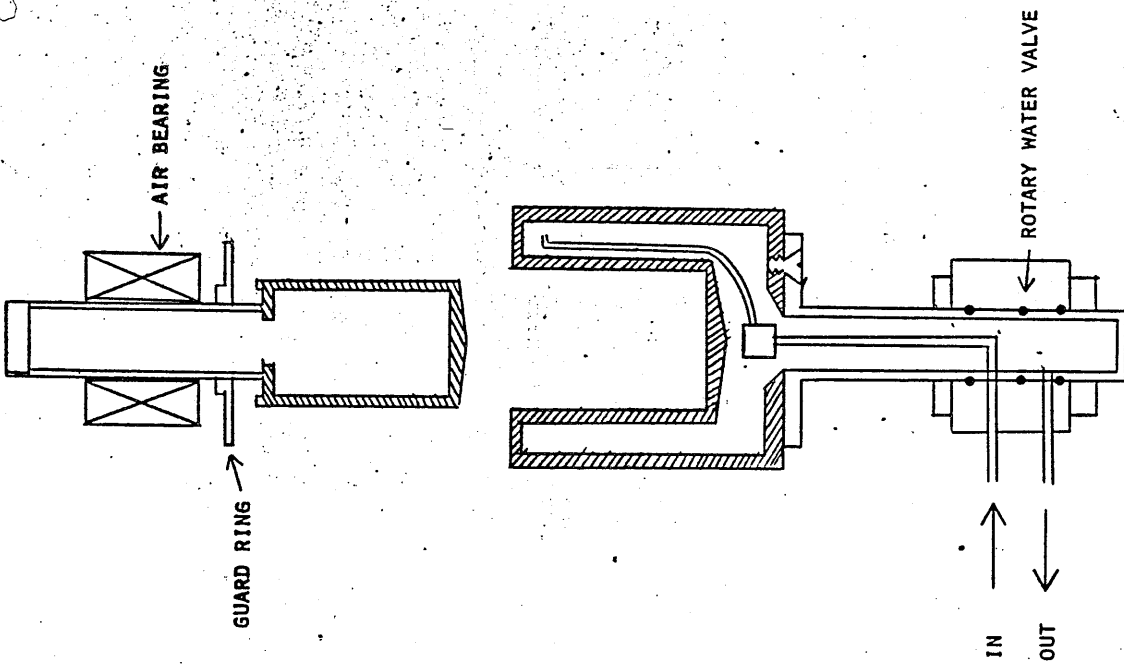


Figure 6, A schematic drawing of the Couette and Cone/Plate combined geometry.

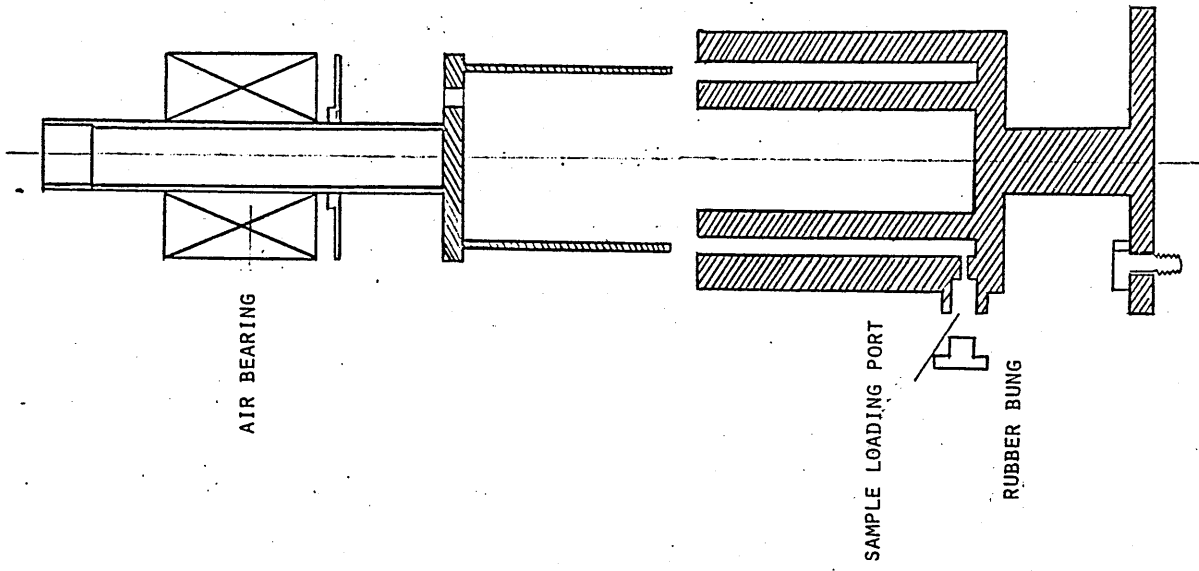


Figure 7. A schematic drawing of the Double Couette geometry.

Provision is made for the direct infusion of the test sample by means of a syringe which injects the test sample through a rubber bung at the sample loading port at the bottom of the outer cylinder after the inner cylinder is set in place. The material can be retrieved in the same way if further tests of any kind are required on the test material. This geometry is also manufactured in Plexiglass and siliconized.

A special geometry for the measurement of torque (τ) from surface layers formed on solutions of plasma proteins.

The geometry is illustrated in Fig. 8. It is based on the design of the double Couette concentric cylinder to measure torque from surface layers which form or can be spread at interfaces. This geometry is made of plexiglass and is siliconized. Temperature control is affected by circulating temperature controlled water around the circular trough which contains the test material, from an external water bath.

The diameters of the inner and outer surface of the top ring are 8.36cm. and 8.62cm. respectively, while the internal and outer diameters of the trough are 8cm. and 9cm. respectively.

In its operation the upper ring is set so that it just penetrates the top layer of the test material in the trough. 5ml. of material is required to fill the trough to the required height.

The geometry is most suitably used in dynamic shear, as in steady shear these protein layers tend to tear, particularly if heavily cross-linked.

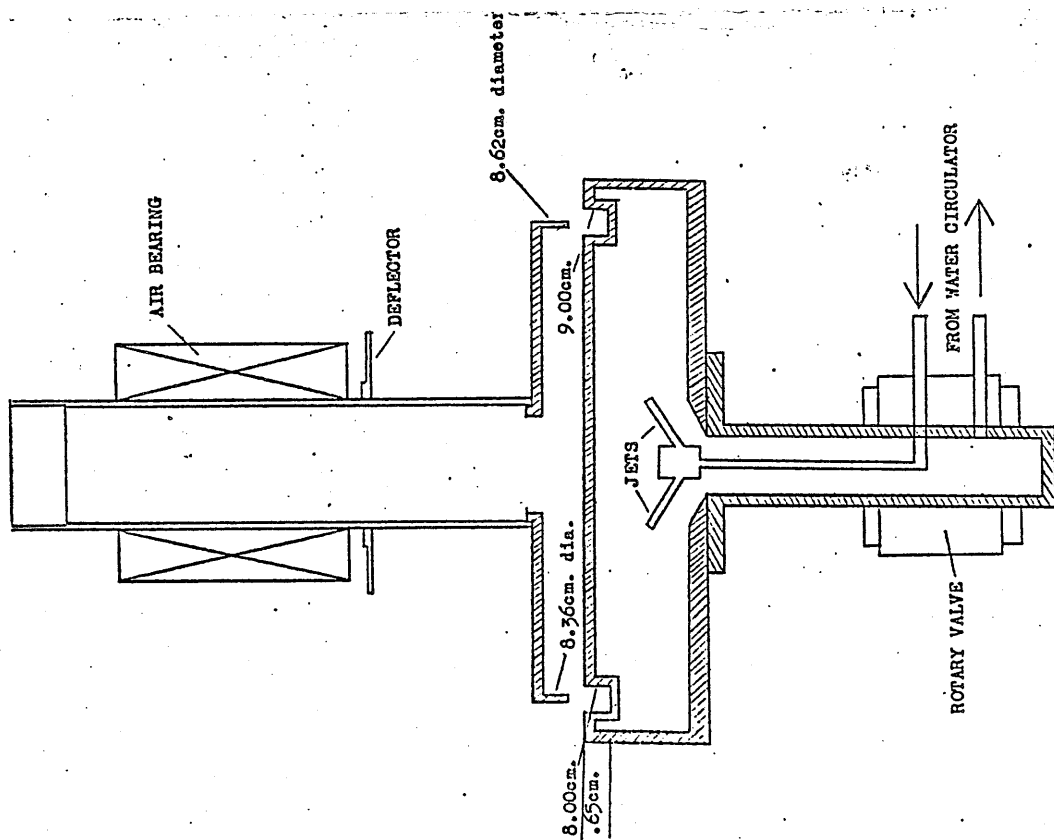


Figure 8. A schematic drawing of the Ring in Ring geometry for interface and surface rheological measurements.

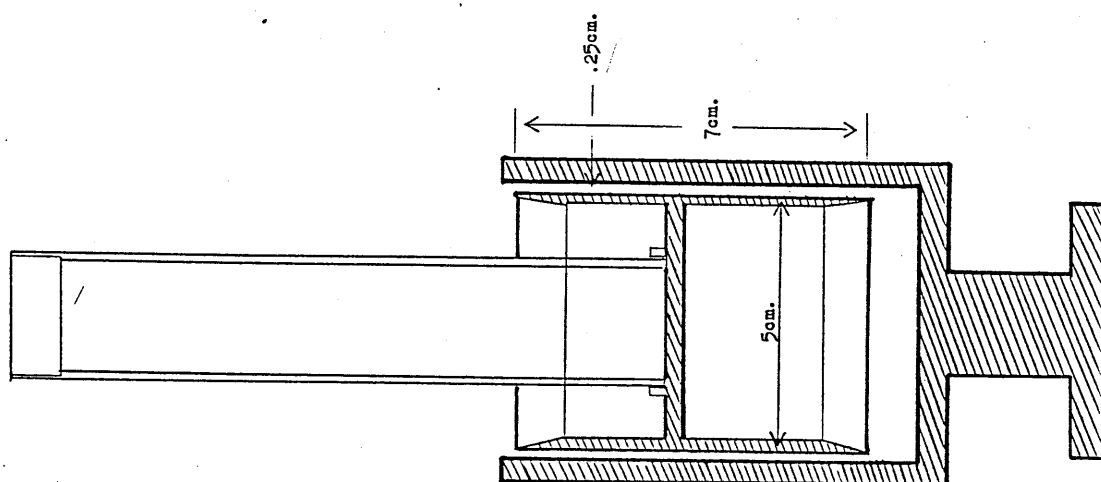


Figure 9. A schematic drawing of the standard Couette geometry.

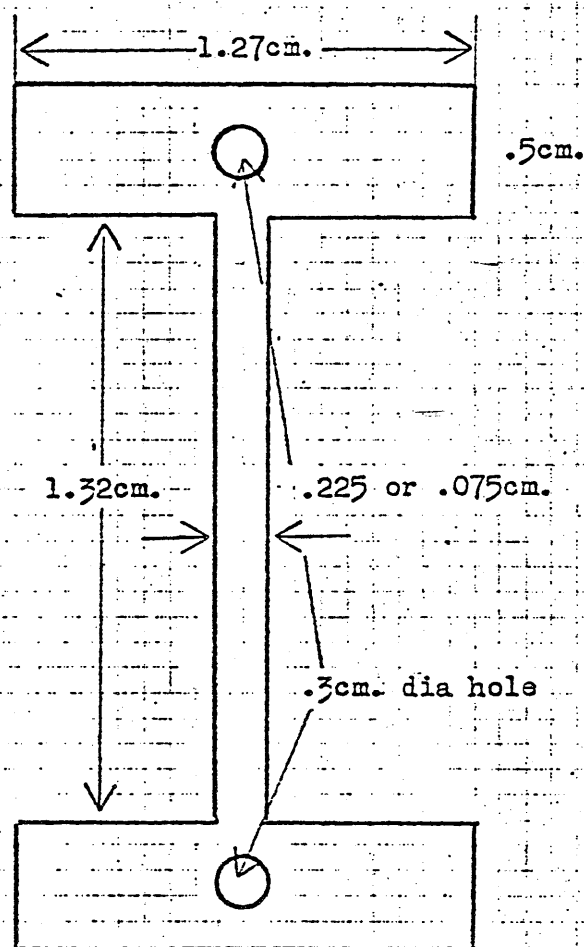
The "Couette" type geometry

A "Couette" type geometry has been manufactured in plexiglass, and is illustrated in Fig. 9. The diameter of the inner cylinder has been chosen as 5cm. and the height is 7cm. The radial gap is .25cm. The advantage of the Couette geometry of 5cm in diameter when compared with a cone and plate system of the same diameter, is that the Couette geometry will give about eight times the torque (t) when testing at the same rate of shear. This is particularly useful when measuring materials of low viscosity. On the other hand it has the disadvantage of requiring a large volume of material to fill, as there is a space (1cm. high by 5cmdiameter) under the trapped air bubble in the lower annulus which must be filled with the test sample. This geometry is also more susceptible to sedimentation when measuring suspensions such as whole blood. 10ml. of material is required to fill this geometry.

Special Torsion Bars

Two special torsion bars in "I" beam form with low rate constants (K_t) were found necessary to adapt the Rheogoniometer to allow measurements of materials of low viscosity at low shear rates. These are illustrated in Fig.10. They are manufactured in beryllium copper of .045cm. in thickness, with dimensions as described in the illustration. Beryllium copper is chosen because of the very low hysteresis evident with this material. The finished torsion bar is tempered at 225°C. for two hours.

The rate constants of the torsion bars with the two widths described in the illustration are nominally 5 dyne.cm/micron and 30 dyne.cm/micron.



Beryllium copper .045cm. thick

Figure 10. A sketch of an "I" beam torsion bar.

The Measurement of Normal Force

The normal force unit that is supplied with the commercially available Rheogoniometer, was designed to measure the extensive normal stress, sometimes amounting to several kilograms, encountered in materials such as polymer melts, and bitumens etc. This unit is not sensitive enough to measure the very small forces that might be predicted to occur in

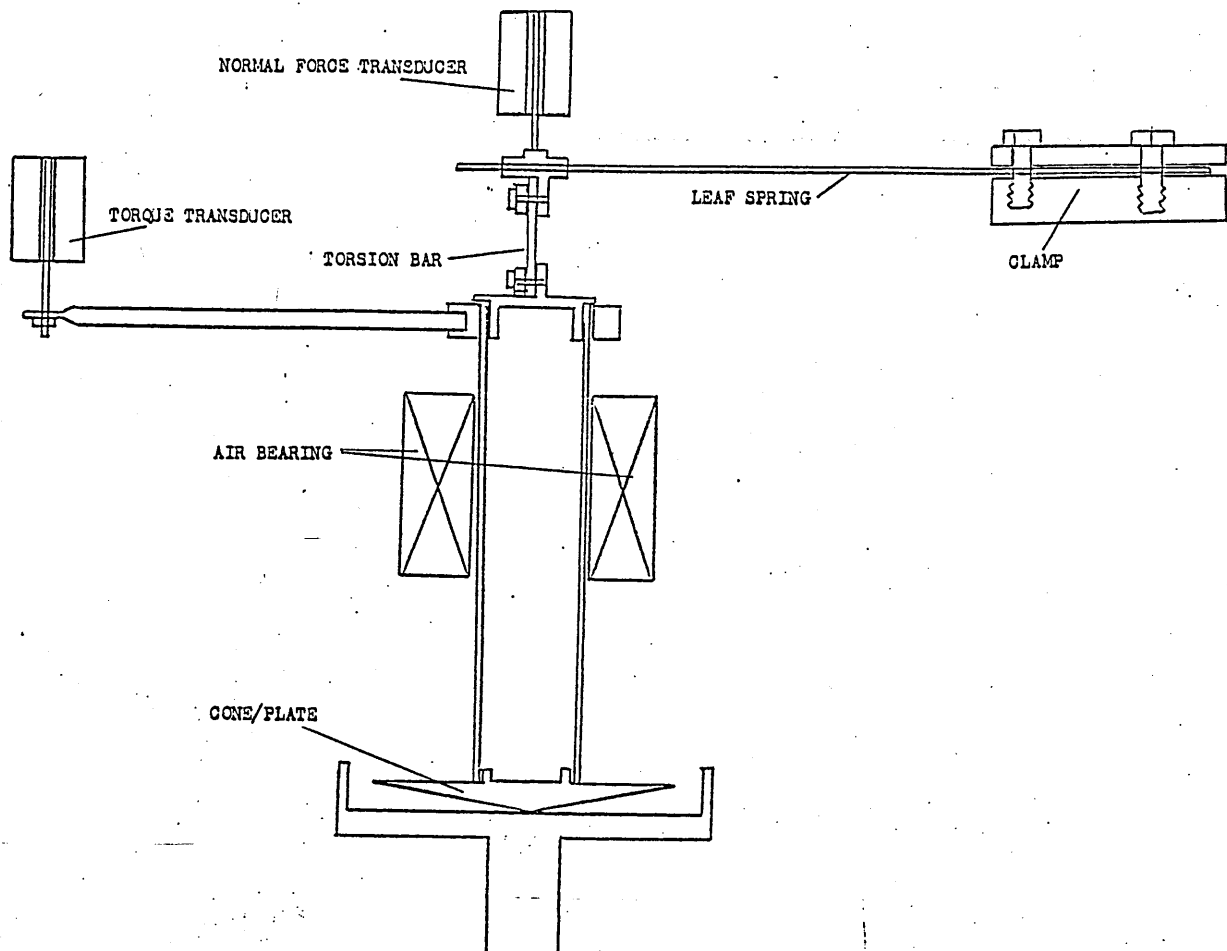


Figure 11. A schematic drawing of the Tangential and Normal Stress measuring system when a cone and plate geometry is fitted.

whole blood in view of reports in the literature of measurement of a small elastic component in blood by Lessner et al, 1970 (16); Thurston, 1972 (17) and Chien et al, 1975 (18). Accordingly a special unit was designed. This is illustrated in Fig.11. In this system, the flat plate together with its rotor and torsion bar is suspended from a thin beryllium copper leaf spring anchored to the Rheogoniometer frame. Stress normal to the rotational plane is measured by a sensitive transducer connected to the instrument frame and having contact with the leaf spring. The unit is calibrated by weights placed in a tray attached to the upper platen by a thread over a pulley.

The attachment of a microscope and video camera and video recorder to the Rheogoniometer for the visualization of flowing whole blood and suspensions of blood components during steady and oscillatory shear.

A special transparent cone and plate together with a modified microscope and video camera is fitted to the Rheogoniometer by removing the torsion head, and in its place, a special carrying bracket is attached to the instruments upright column to support a special flat plate made of plexiglass and carefully polished. A $\frac{1}{2}^\circ$ cone, 5cm. in diameter is used together with the flat plate, also made of plexiglass.

A part of a Zeiss microscope which includes the objective holder and focusing arrangement is bolted to

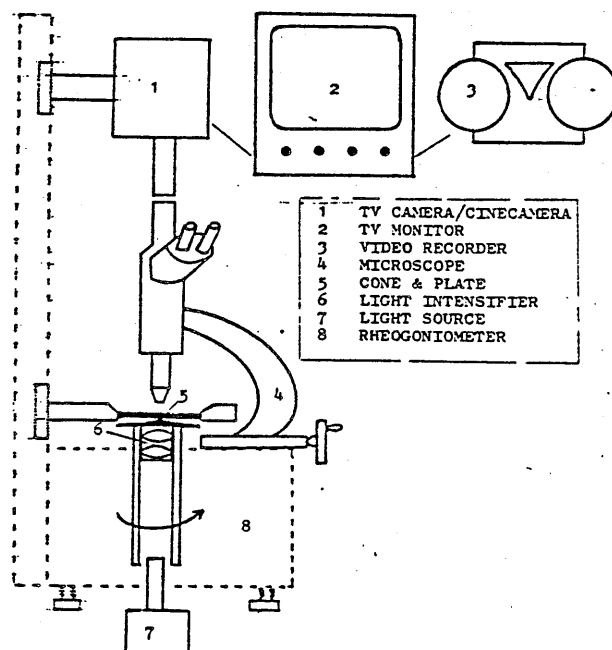


Figure 12. A schematic drawing of the microscope attachment.

the base of the Rheogoniometer's column. This bracket has an anti-vibration device to prevent vibrations from reaching the microscope.

Provision is made for the microscope to be moved horizontally across the cone, so that the observations can be made at or near the apex of the cone and also at other points across its radius. Illumination of the sample is achieved by a light source which, via a fiber optic arrangement, directs cool light on to the cone and plate from the underside. A schematic drawing of this instrumentation is shown in Fig.12. Fig. 13, is a photograph of the assembly.

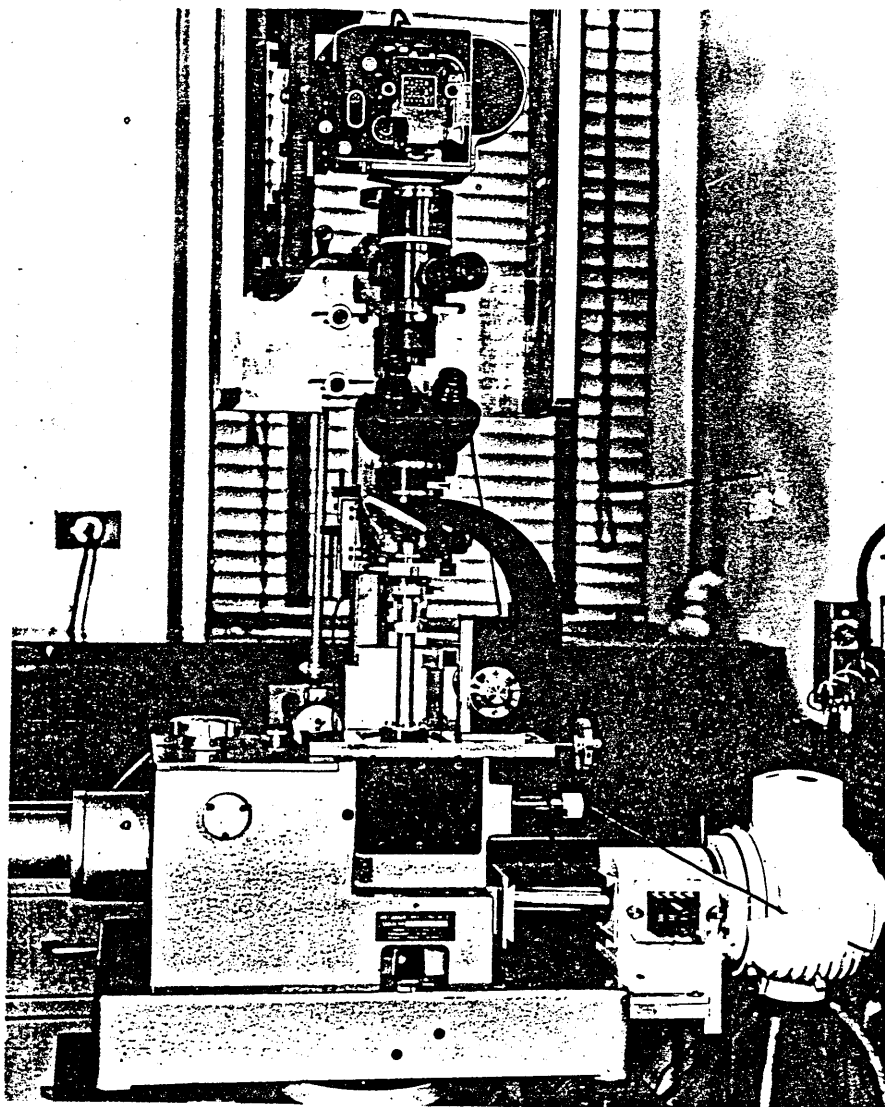


Figure 13. The Rheogoniometer with microscope attachment.

The addition of a Digital PDP11/10 computer to analyse
and store data from the Rheogoniometer

As the calculation, reduction, and storage of the data from the Rheogoniometer is time consuming, a PDP11/10 (Digital) computer was connected, on line, to the Rheogoniometer to collect, analyse and store the data from the measurements.

Two programs were developed, one to collect and process data from the oscillatory experiments, and the other to collect and process data for the pulsatile flow experiments. These two programs solve and measure the phase angles and amplitude ratios for given frequencies, that are necessary for the calculation of the viscous and elastic moduli of the test materials. A listing of these programs and their operating procedures are given in Appendix II and III.

The addition of the computer completes the modifications and additions made to the Weissenberg Rheogoniometer to make it more suitable for the rheological measurement of blood and blood components in suspension.

In subsequent chapters, rheological measurements of blood and blood components in suspension using these modifications will be described.

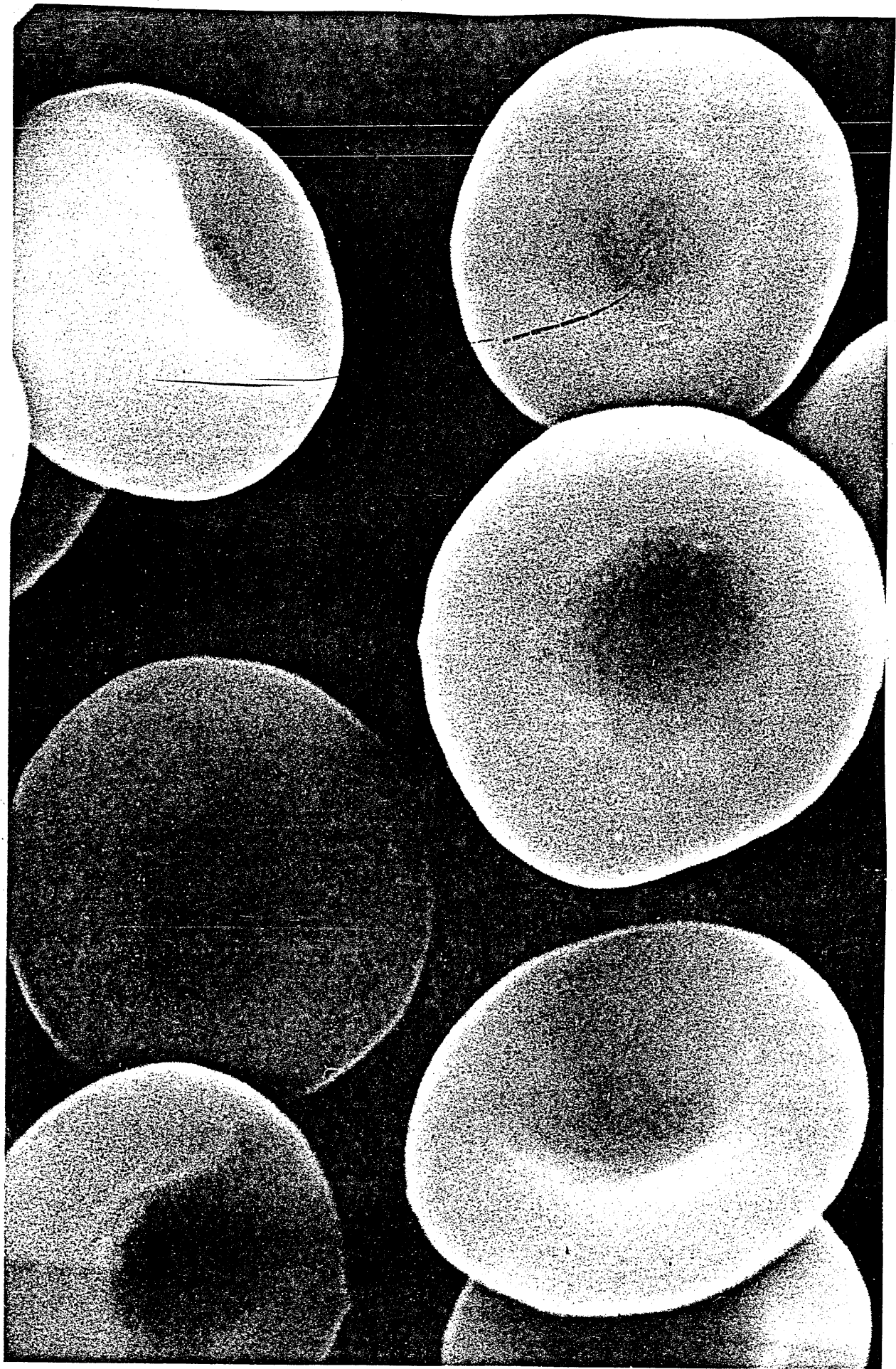
CHAPTER III.

THE MEASUREMENT OF THE VISCOSITY AND ELASTICITY OF WHOLE BLOOD AND SUSPENSIONS OF BLOOD COMPONENTS.

Introduction.

There are reports in the literature that whole blood exhibits viscoelastic properties. These properties are attributed to the viscoelastic characteristics of the individual blood cells, reported by Chien et al. 1978 (1), and others, and to cellular-protein interactions during aggregation reported by Brooks 1974 (2). Lessner, et al. 1970 (3), reported the measurement of an elastic component in anticoagulated human blood by employing a visco-elastometer developed by Silberberg and Mijnlief 1979 (4). Thurston, 1972 (5,6), could also show that blood is a viscoelastic material in his oscillating pressure tube flow studies. Chien, King, Skalak and Usami, 1975 (7), reported the measurement of an elastic component in whole blood when hematocrits were above 45 percent, using dynamic shear.

In view of these determinations it would be reasonable to expect that in steady shear, whole blood, as well as displaying viscosity should also display elasticity. This would take the form of a demonstrable "Normal Stress" or "Weissenberg effect". In oscillatory (dynamic) shear, the elastic component should be indicated



The Red Cell

by a phase shift between the input and output sinus motions, while both of these should occur in pulsatile flow.

The measurement of viscosity ($\eta_{app.}$) and elasticity (G) of whole blood with varying hematocrits in steady shear, dynamic shear and pulsatile flow.

Experimental Method

The Rheogoniometer was used together with a cone and plate geometry of 7cm. in diameter. The cone angle was 1° and a guard ring was used. The temperature of all test samples was maintained at 37°C by circulating temperature controlled water through the lower plate. An "I" beam torsion bar was used for these measurements which had a constant (K_T) of 5 dyne.cm per micron deflection of the torque reading transducer. A schematic illustration of this measuring system is shown in Figure 2 of Chapter II.

Preparation of Blood Samples

Blood was drawn from the antecubital vein of healthy human donors. EDTA (ethylenediaminetetracetate) was present in dry form in the collecting tubes (Becton-Dickinson, N.J.). The concentration of EDTA was 1 mg/ml of blood.

Plasma protein determinations were made of each blood donation. The mean and standard deviations of the major protein components are given in Table 1.

The blood was centrifuged at 3000 RPM, for five minutes, and a white cell-platelet coating left on the top layer of red cells was removed by suction. The red

cells were recombined with plasma or Ringers-albumin solution to obtain red cell hematocrits of from 10 to 95 percent. Preparations of packed cells were also prepared. An aliquat of plasma was retained from each blood donation for viscosity determination.

Table I.

Protein Component	Mean. (gram /100ml)	Standard deviation
Albumin	4.34	0.31
Alpha globulin	0.22	0.49
Alpha globulin	0.63	0.15
Beta globulin	0.73	0.15
Beta globulin	0.42	0.18
Gamma globulin	0.72	0.27
Fibrinogen	0.31	0.04
Total protein	7.43	0.31

Measurement of plasma viscosity

A cone of 7.0cm. diameter with a 1° angle, together with a flat plate and guard ring, was used for viscosity measurements. Shear rates of from 0.054 to 540 sec^{-1} were used. The temperature was maintained at 37°C . All samples were found to be Newtonian and an average viscosity of 1.30 centipoise was calculated from

measurements of fifty preparations. A standard deviation of 0.055 was calculated.

The rheological properties of hemoglobin (RBC hemolysate)

Hemoglobin has been reported to be a crystalline material which has a molecular weight of 64,000. It is present in the normal red cell interior at a concentration of about 32gram/100ml. Ponder, 1948 (8), Prankerd, 1961 (9).

As the hemolysate exhibits Newtonian flow characteristics over the range of shear rates used in this study, its viscosity will qualify the relaxation time of the red cell. Only in a diseased state, such as in sickle cell anemia, where deoxygenated hemoglobin exhibits non-Newtonian flow characteristics, and in some conditions,

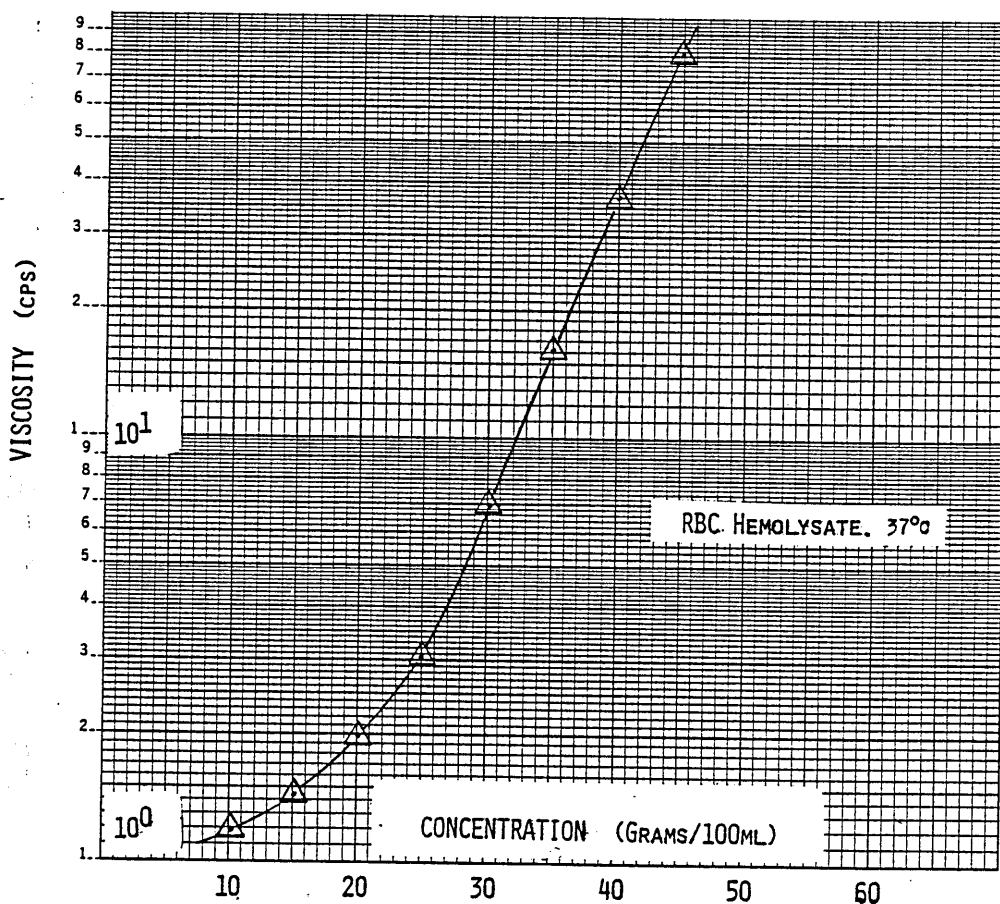


Figure 1. The effect of concentration on the apparent viscosity of cell free RBC hemolysate.

an elastic modulus, (see Chapter 4, page 115) will the elastic modulus of the red cell and of whole blood itself, be changed.

Effect of Concentration

The effect of hemoglobin concentration was investigated and a plot of these measurements is shown in Figure 1. As can be seen, small changes in concentration can cause considerable change in viscosity.

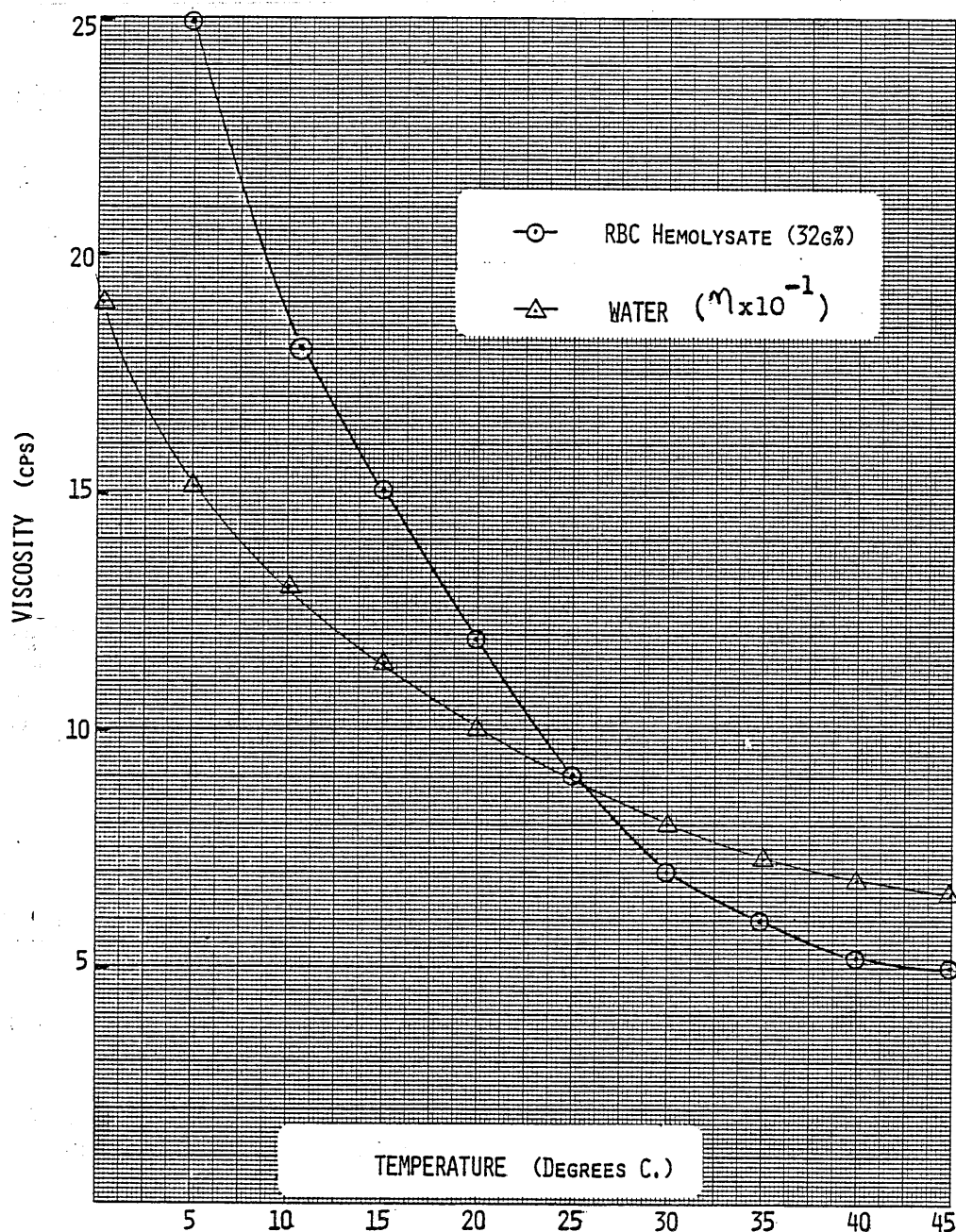


Figure 2. The effect of temperature on the apparent viscosity of cell free RBC hemolysate at a concentration of 32g%. The effect of temperature on the viscosity of water is also shown as a comparison.

Effect of Temperature

The effect of temperature on the viscosity of hemoglobin was investigated and the data is shown in Figure 2. The effect of temperature on the viscosity of water is also included in this figure as a comparison. It can be seen that hemoglobin viscosity at a concentration of 32g/dl is more sensitive to temperature change when compared to water, but it also has a higher viscosity.

The measurement of viscosity in steady shear of red blood cells resuspended in plasma.

Shear rates of from 0.011 to 1100 sec^{-1} were chosen for these measurements. The lowest shear rates were measured first. Between each shear rate increment, the blood sample was stirred vigorously to remix the red cells and break up rouleaux (red cells aggregated together in rod like structures). The chosen shear rate was then applied as quickly as possible after remixing.

Huang et al. 1975 (10), and Dintenfass 1971 (11), have reported that whole blood is thixotropic.

There appears to be some confusion about the term "thixotrophy". Many workers consider that only materials that have comparatively high viscosities and long relaxation times, where only moderate strain rates will cause time dependent viscosity, are thixotropic. It is the opinion of the author that all materials will exhibit thixotropic behavior provided the applied rate of strain is greater than the rate of relaxation.

Cokelet et al. 1963 (12), attributed this apparent time dependence of torque to the development of a

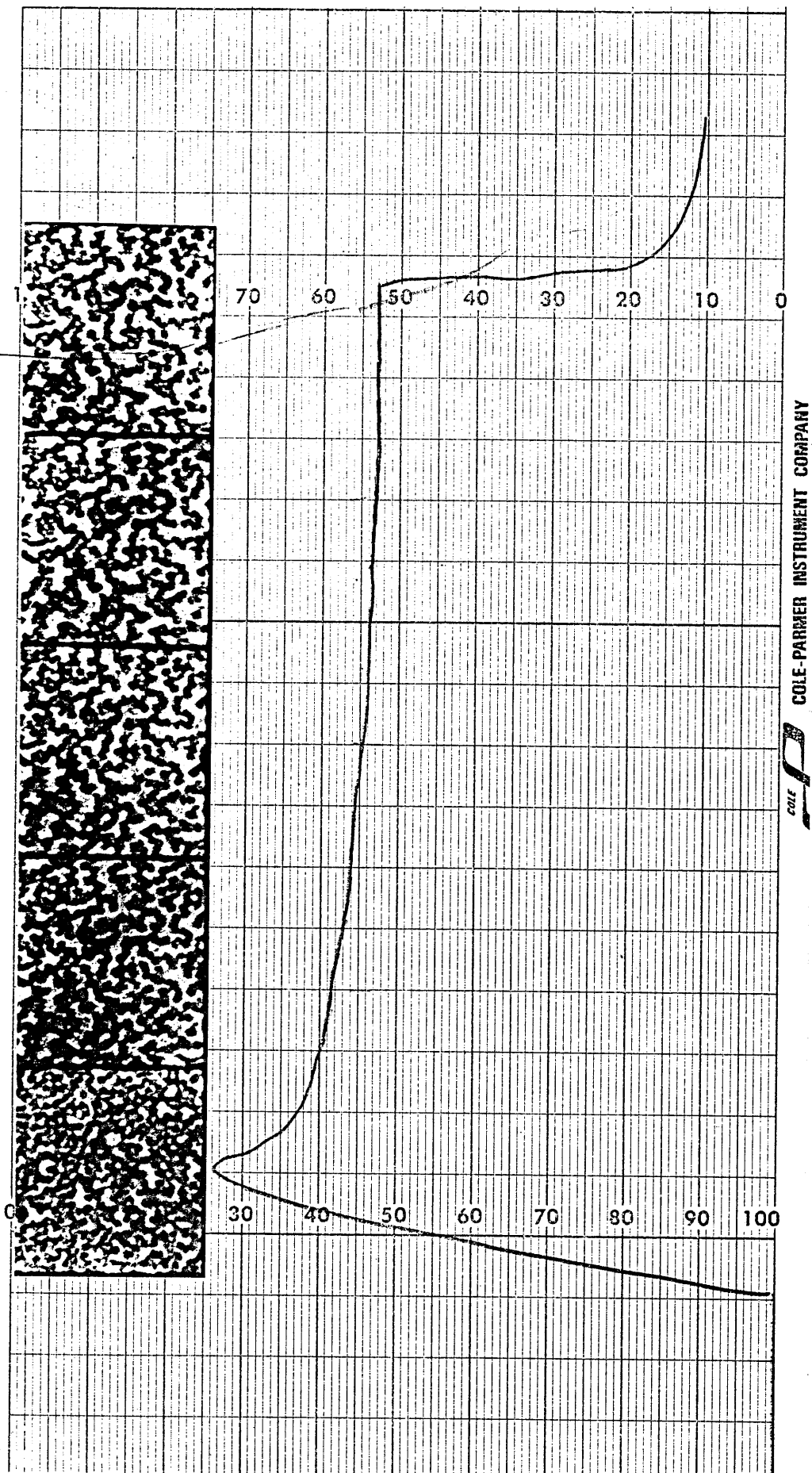


Figure 3. A recorder trace of tangential stress in steady shear, of RBCs in plasma at 40% hematocrit at 0.05 sec^{-1} . Photomicrographs are taken at the start of shearing, and at one minute intervals thereafter.

cell free plasma layer at the sample geometry interface. He proposed a method of extrapolation to a peak shear stress at zero time, from which to derive a "true" torque from which viscosity can be calculated.

Copley and King 1970 (13), suggested that this torque reduction was caused by "slip" of a three dimensional system of red cells in rouleau formation on a plasma layer at the geometry interface. Figure 3 shows a recorder trace made at 0.054 sec^{-1} , together with photomicrographs, taken in a time sequence when shearing the blood at a constant shear rate. This shows the development of a system of red cells which are forming into a system of continuous rouleau. It is clear from this figure that the apparent reduction in viscosity with time of shearing, is due to a change in homogeneity which progresses with time.

It can be seen also in Figure 3 that after the shearing has stopped, the torsion measuring system does not return to zero, but remains deflected, indicating that the blood system exhibits an apparent yield stress. This effect is not seen at the very low shear rates (below 0.01 sec^{-1}), or at the very high ones. The value of the apparent yield stress derived from the relaxation curve after the shear has been discontinued was 0.01 dyne/cm^2 for a hematocrit of 40%. Copley and King 1970 (13), reported the measurement of viscosity in whole blood at physiological hematocrits at very low shear rates down to 0.0009 sec^{-1} . They reported their findings that, at these very low shear rates, the viscosity of blood reaches a plateau. This would appear to discount the presence of a yield stress in whole blood, however,

these authors contended that at these low shear rates, slip occurs at the geometry wall and a plug of red cells behaves as a plastic solid which slips on a layer of plasma. If this is the case, it may be further confirmation that blood exhibits a yield stress. The finding that blood exhibits an apparent yield stress, and plug flow occurs below the yield point, is of utmost significance in the physiology and pathology of the circulation.

At higher shear rates, above 10.0 sec^{-1} , the tangential stress recording remains constant with time. Examination of the photomicrographs at these higher shear rates, shows that there is little change in the configuration of the red cells with time of shearing. Figure 4 is an example of the recorder tracing of tangential stress at 54.0 sec^{-1} of a sample of whole blood at 40% hematocrit, together with the appropriate photomicrographs taken during shearing. At these higher shear rates the tangential stress remains constant and the torsion head returns directly to zero, and there is no indication of a residual yield stress. It can be concluded that at 40% hematocrit an apparent yield stress will only be measurable if rouleaux are present.

Tables 2 to 10 list the data obtained from the various preparations of red cells resuspended in plasma. The measured viscosity at each shear rate used is averaged, and a standard deviation calculated.

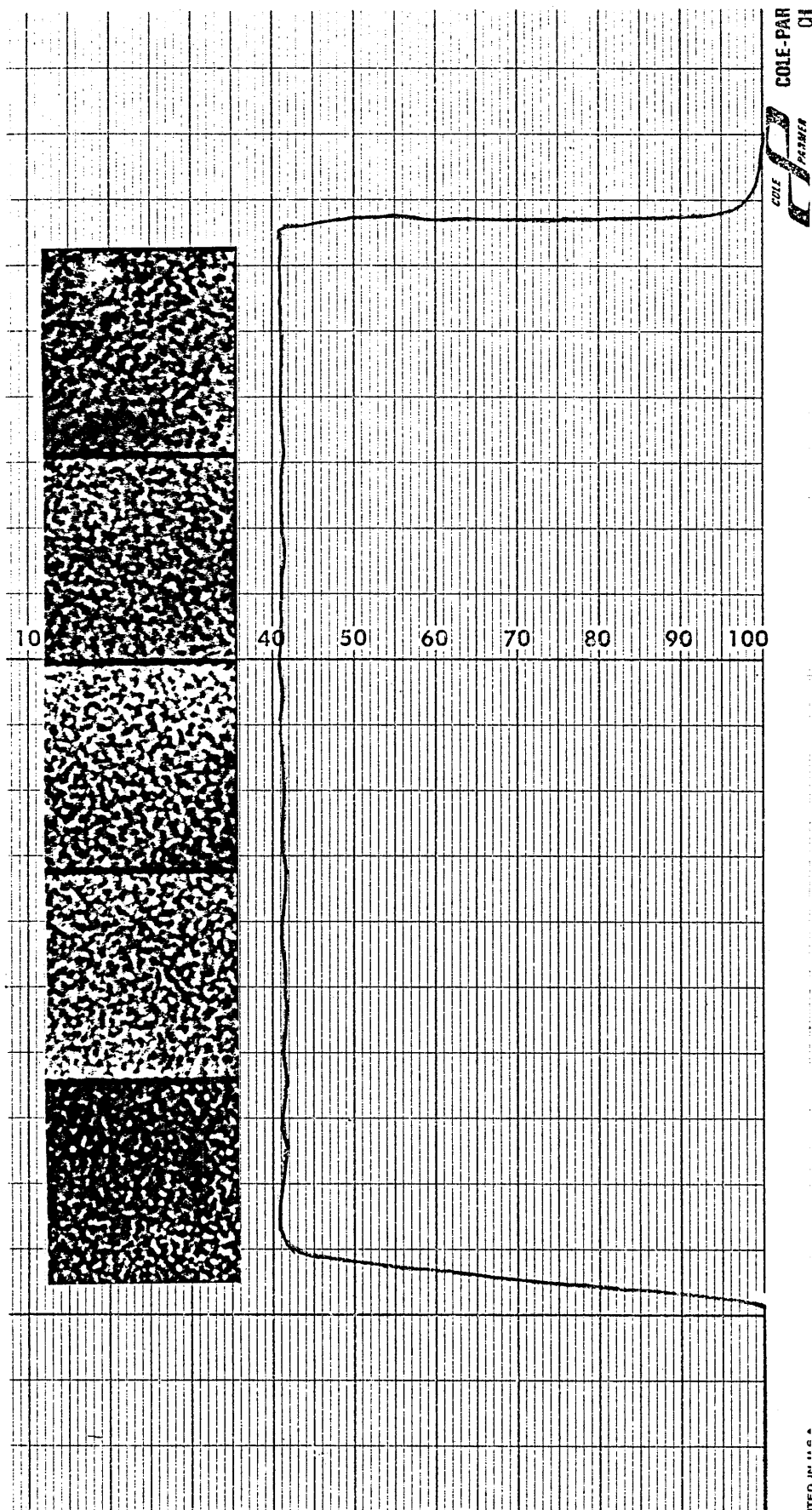


Figure 4. A recorder trace of tangential stress in steady shear of a preparation of 40% RBCs in plasma at 54 sec^{-1} , together with photomicrographs taken at the start of shearing and then at one minute intervals.

RHEOGONIOMETER IN STEADY SHEAR.

Table No. 2

Preparation RBCs in Plasma											Hematocrit 20%		Number of samples 15			
Rate of Shear (sec ⁻¹)	.011	.022	.054	.11	.22	.54	1.10	2.20	5.40	11.0	21.6	54.0	110.0	220.0	540.0	1100
Viscosity (η_{app}) (cps) (average)	22.13	17.73	13.0	9.92	7.5	5.48	4.5	3.8	3.17	2.89	2.71	2.57	2.50	2.45	2.45	2.40
Standard deviation	5.03	3.89	3.0	2.12	1.36	.79	.57	.40	.314	.23	.17	.14	.12	.10	.10	.11

Table No. 3

Preparation RBCs in Plasma											Hematocrit 30%		Number of samples 9			
Rate of Shear (sec ⁻¹)	.011	.022	.054	.11	.22	.54	1.10	2.20	5.40	11.0	21.6	54.0	110.0	220.0	540.0	1100
Viscosity (η_{app}) (cps) (average)	65.33	50.90	35.06	25.78	18.28	11.78	8.71	6.68	4.92	4.23	3.73	3.43	3.32	2.16	3.10	2.99
Standard deviation	18.33	13.89	9.36	6.6	4.27	2.39	1.46	1.05	.59	.42	.37	.26	.23	.26	.28	.28

RHEOGONIOMETER IN STEADY SHEAR.

Table No. 4

RBCs in Plasma										Hematocrit 40%			Number of samples 9			
Preparation																
Rate of Shear (sec ⁻¹)	.011	.022	.054	.11	.22	.54	1.10	2.20	5.40	11.0	21.6	54.0	110.0	220.0	540.0	1100
Viscosity (η_{app}) (cps) (average)	14.22	96.33	71.44	54.89	38.22	23.78	16.5	11.78	8.02	6.48	5.63	4.74	4.46	4.29	4.13	4.03
Standard deviation	19.1	7.04	8.44	9.82	7.36	4.84	3.14	1.94	.82	.58	.55	.41	.44	.53	.55	.57

Table No.5

RBCs in Plasma										Hematocrit 50%			Number of samples 11			
Preparation																
Rate of Shear (sec ⁻¹)	.011	.022	.054	.11	.22	.54	1.10	2.20	5.40	11.0	21.6	54.0	110.0	220.0	540.0	1100
Viscosity (η_{app}) (cps (average))	187.27	153.64	119.36	91.0	65.18	41.81	28.5	19.36	12.59	9.33	7.57	6.4	5.8	5.6	5.4	5.2
Standard deviation	49.16	25.87	9.77	8.74	7.13	5.62	3.84	1.96	.80	.67	.54	.52	.37	.27	.29	.26

RHEOGONIOMETER IN STEADY SHEAR.

Table No.6

RBCs in Plasma										Hematocrit 60%			Number of samples 12			
Preparation	.011	.022	.054	.11	.22	.54	1.10	2.20	5.40	11.0	21.6	54.0	110.0	220.0	540.0	1100
Rate of Shear (sec ⁻¹)																
Viscosity (η_{app}) (cps) (average)	292.27	245.0	182.7	139.6	99.73	64.27	44.64	30.27	19.0	14.1	10.81	8.52	7.65	7.15	6.56	6.40
Standard deviation	49.67	30.82	23.8	18.26	12.72	9.58	7.47	5.02	2.78	1.88	1.22	1.10	.89	.99	.89	.89

Table No.7

RBCs in Plasma										Hematocrit 70%			Number of samples 12			
Preparation																
Rate of Shear (sec ⁻¹)	.011	.022	.054	.11	.22	.54	1.10	2.20	5.40	11.0	21.6	54.0	110.0	220.0	540.0	1100
Viscosity (η_{app}) (cps) (average)	685.8	497.5	330.8	220.5	145.0	90.3	62.5	43.0	27.0	20.0	17.0	13.0	11.4	10.25	9.50	.12
Standard deviation	249.9	121.8	57.9	38.0	33.0	16.0	11.0	7.75	4.2	3.2	2.5	2.2	1.9	1.7	1.5	1.4

RHEOGONIOMETER IN STEADY SHEAR.

Table No. 8

RBCs in Plasma										Hematocrit 80%			Number of samples 10			
Preparation																
Rate of Shear (sec ⁻¹)	.011	.022	.054	.11	.22	.54	1.10	2.20	5.40	11.0	21.6	54.0	110.0	220.0	540.0	1100
Viscosity ('lapp) (cps) (average)	1451	893	486	324	217	128	86.0	60.6	40.5	29.9	23.5	17.95	15.55	13.7	12.35	11.55
Standard deviation	496	228	99.0	47.4	31.6	18.0	11.5	10.1	5.8	3.5	3.0	2.6	2.0	1.7	1.6	1.5

Table No. 9

Preparation RBCs in Plasma										Hematocrit 90%				Number of samples 10			
Rate of Shear (sec-l)	.011	.022	.054	.11	.22	.54	1.10	2.20	5.40	11.0	21.6	54.0	110.0	220.0	540.0	1100	
Viscosity (η_{app}) (cps) (average)	2340	1438	772	495	329	193	137	102	70.2	55.4	45.3	34.8	29.7	25.2	21.25	19.6	
Standard deviation	687	412	180	84.6	41.2	16.4	9.8	8.2	6.0	5.0	5.2	4.6	3.7	3.0	3.0	2.7	

RHEOGONIOMETER IN STEADY SHEAR.

Table No. 10

Preparation 95% RBCs in Plasma										Hematocrit 95			Number of samples 4			
Rate of Shear (sec ⁻¹)	.011	.022	.054	.11	.22	.54	1.10	2.20	5.40	11.0	21.6	54.0	110.0	220.0	540.0	1100
Viscosity ("lapp) (cps) (average)	5850	3525	1837	1195	785	485	342	248	174	139	115	95.6	86.0	78.0	72.0	67.0
Standard deviation	2635	1322	512	276	152	90.0	61.3	39.5	27.5	26.6	21.2	24.8	23.9	22.4	20.0	17.0

Measurement of Viscosity in Steady Shear of Red Blood cells resuspended in Ringer/albumin solution

Red Cells separated from plasma by centrifugation, were washed three times and resuspended in Ringers/albumin solution. The viscosity of the Ringers/albumin solution (Abbott Laboratories, Chicago, Ill.) was found to be 0.75 centipoise at 37°C.

The viscosity of the RBC suspensions in Ringers/albumin were measured in the same way and at the same shear rates as RBCs suspended in plasma. Figure 5 shows a typical recorder trace of the measurements at 0.05 sec^{-1} together with photomicrographs taken at the time intervals indicated.

It can be seen that the characteristics shown by the red cells resuspended in plasma at low shear rates are not repeated in suspensions in Ringers/albumin. The tangential stress value does not vary with time, and the stress decays to zero when the shearing is stopped indicating the absence of a residual yield stress. Photomicrographs taken as time elapses do not show the build up of rouleaux.

Tables 11 to 19 list the number of experiments, the average viscosity and standard deviation for the various hematocrits from 10 to 90% as well as packed cells.

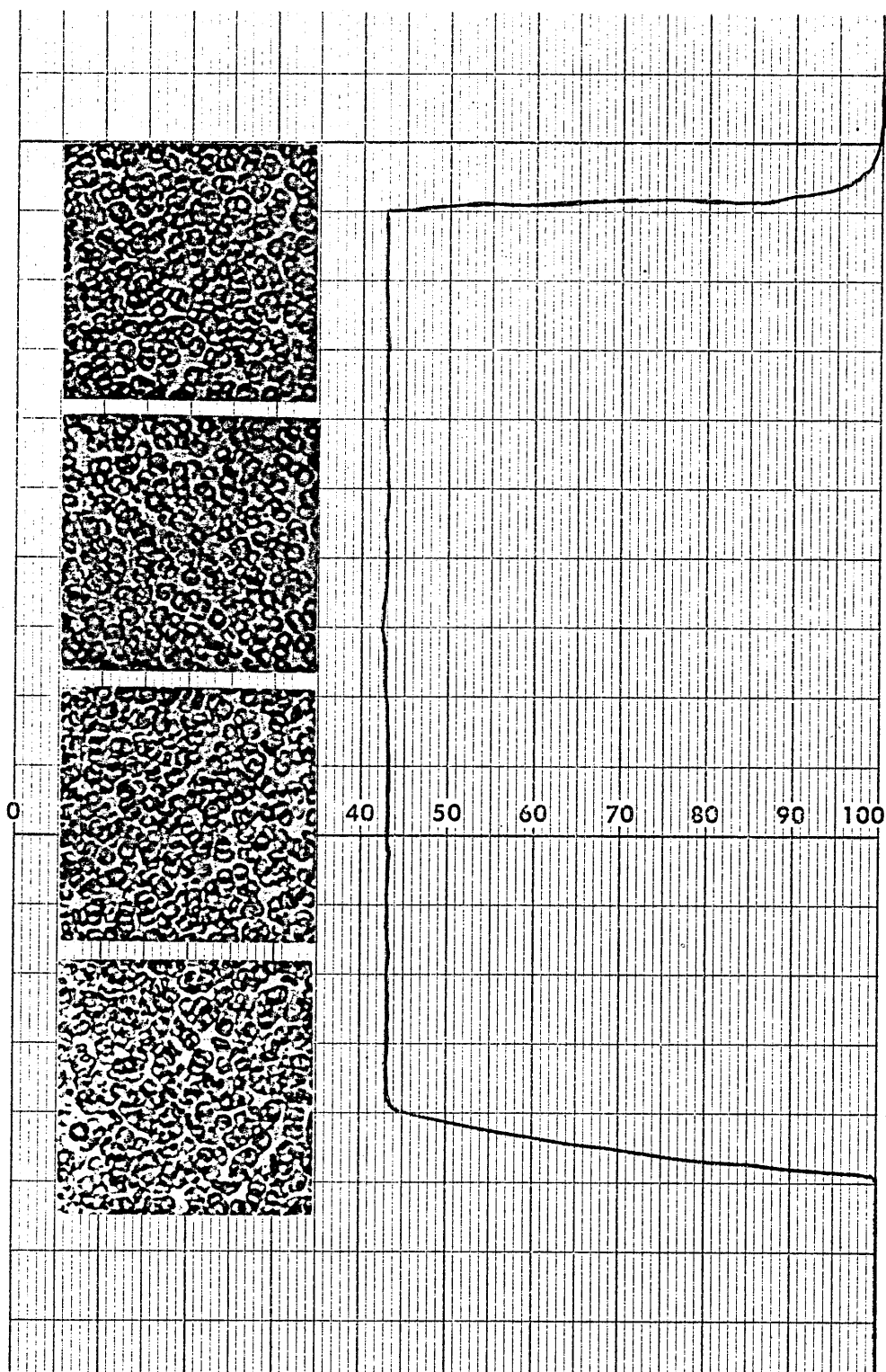


Figure 5. A recorder trace at 0.05 sec^{-1} in steady shear, of RBCs resuspended in Ringer-albumin solution at 40% hematocrit, together with photomicrographs taken at one minute intervals.

Table No. 11

Preparation RBCs in Ringer/albumin										Hematocrit 20%				Number of samples 8			
Rate of Shear (sec-1)	.011	.022	.054	.11	.22	.54	1.10	2.20	5.40	11.0	21.6	54.0	110.0	220.0	540.0	1100	
Viscosity (η_{lapp}) (cps (average))			2.53	2.29	2.06	1.89	1.79	1.72	1.65	1.60	1.59	1.58	1.58	1.58	1.58	1.58	
Standard deviation			.7	.49	.34	.20	.14	.75	.038	.03	.03	.046	.046	0.53	.053	.053	

RHEOGONIOMETER IN STEADY SHEAR.

Table No.12

RBCs in Ringer/alubumin										Hematocrit 30%			Number.of samples 9			
Preparation																
Rate of Shear (sec ⁻¹)	.011	.022	.054	.11	.22	.54	1.10	2.20	5.40	11.0	21.6	54.0	110.0	220.0	540.0	1100
Viscosity (η_{app}) (cps) (average)	3.42	3.28	3.16	3.00	2.9	2.74	2.63	2.53	2.47	2.41	2.32	2.25	2.18	2.12	2.06	2.00
Standard deviation	.77	.70	.62	.53	.45	.32	.22	.16	.15	.14	.14	.14	.10	.10	.085	.11

Table No.13

RBCs in Ringer/albumin										Hematocrit 40%			Number of samples 8			
Preparation																
Rate of Shear (sec ⁻¹)	.011	.022	.054	.11	.22	.54	1.10	2.20	5.40	11.0	21.6	54.0	110.0	220.0	540.0	1100
Viscosity (η_{app}) (cps (average)	6.47	6.24	5.9	5.62	5.23	4.84	4.54	4.30	4.0	3.71	3.52	3.30	3.2	3.00	2.9	2.8
Standard deviation	1.29	1.12	1.0	.97	.76	.64	.53	.52	.43	.37	.38	.43	.45	.47	.52	.5

RHEOGONIOMETER IN STEADY SHEAR.

Table No. 14

Preparation		RBCs in Ringer/albumin								Hematocrit 50				Number of samples 10			
Rate of Shear (sec ⁻¹)	.011	.022	.054	.11	.22	.54	1.10	2.20	5.40	11.0	21.6	54.0	110.0	220.0	540.0	1100	
Viscosity (η _{app}) (cps) (average)	19.3	15.8	12.7	11.1	10.2	8.6	7.8	7.0	6.23	5.6	5.0	4.5	4.0	3.7	3.4	3.21	
Standard deviation	7.3	4.5	2.4	1.5	1.4	.9	.8	.6	.43	.37	.34	.3	.3	.26	.24	.27	

Table No. 15

Preparation		RBCs in Ringer/albumin								Hematocrit 60%				Number of samples 12			
Rate of Shear (sec ⁻¹)	.011	.022	.054	.11	.22	.54	1.10	2.20	5.40	11.0	21.6	54.0	110.0	220.0	540.0	1100	
Viscosity (η _{app}) (cps) (average)	56.7	48.0	36.8	30.0	24.3	18.8	15.5	12.8	10.2	8.6	7.3	6.1	5.23	4.82	4.46	4.25	
Standard deviation	23.2	16.5	11.6	8.40	5.9	4.2	3.11	2.2	1.14	.75	.52	.32	.28	.24	.29	.31	

RHEOGONIOMETER IN STEADY SHEAR.

Table No. 16

RBCs in Ringer/albumin													Hematocrit 70			Number of samples 11			
Preparation	.011	.022	.054	.11	.22	.54	1.10	2.20	5.40				11.0	21.6	54.0	110.0	220.0	540.0	1100
Rate of Shear (sec ⁻¹)																			
Viscosity (η_{app}) (cps) (average)	264	173	106	75.0	54.4	35.8	27.0	21.0	15.4	12.9	10.35	8.15	7.25	6.64	6.2	6.0			
Standard deviation	63.0	40.0	19.4	12.4	8.75	5.21	3.47	2.65	1.4	.81	.68	.40	.35	.25	.28	.26			

Table No. 17

Preparation	RBCs in Ringer/albumin										Hematocrit 80				Number of samples 14			
	.011	.022	.054	.11	.22	.54	1.10	2.20	5.40	11.0	21.6	54.0	110.0	220.0	540.0	1100		
Rate of Shear (sec-1)																		
Viscosity η_{app} (cps) (average)	882	530	297	193	133	79.2	54.6	39.8	26.3	20.1	16.4	13.21	11.8	10.8	10.0	9.5		
Standard deviation	267	166	96.4	60.0	41.0	24.5	15.4	11.2	6.26	4.4	3.14	1.72	1.36	1.0	10	.79		

RHEOGONIOMETER IN STEADY SHEAR.

Table No. 18

Preparation RBCs in Ringer/albumin										Hematocrit 90				Number of samples 23			
Rate of Shear (sec ⁻¹)	.011	.022	.054	.11	.22	.54	1.10	2.20	5.40	11.0	21.6	54.0	110.0	220.0	540.0	1100	
Viscosity (η_{app}) (cps) (average)	2611	1345	672	406	260	146	98.1	71.0	48.6	38.4	32.0	25.7	22.4	19.8	17.8	16.8	
Standard deviation	733	400	111	65.0	34.0	20.0	13.5	10.0	8.5	7.1	6.0	5.0	5.0	5.1	5.52	5.6	

Table No. 19

Preparation RBCs in Ringer/albumin										Hematocrit 95			Number of samples 3			
Rate of Shear (sec-1)	.011	.022	.054	.11	.22	.54	1.10	2.20	5.40	11.0	21.6	54.0	110.0	220.0	540.0	1100
Viscosity (η_{app}) (cps (average)	11167	5867	2750	1617	1010	530	350	247	150	114	85.7	61.0	50.0	42.0	35.3	32.3
Standard deviation	1040	902	427	202	135	70.0	50.0	30.0	20.0	14.9	8.6	4.6	3.5	2.0	.59	.58

Comparison of data from the different preparations

Figure 6 is a plot of the average apparent viscosity versus shear rate, of red cells suspended in plasma at the various hematocrits prepared. It can be seen that at low shear rates, the slope of the suspensions of

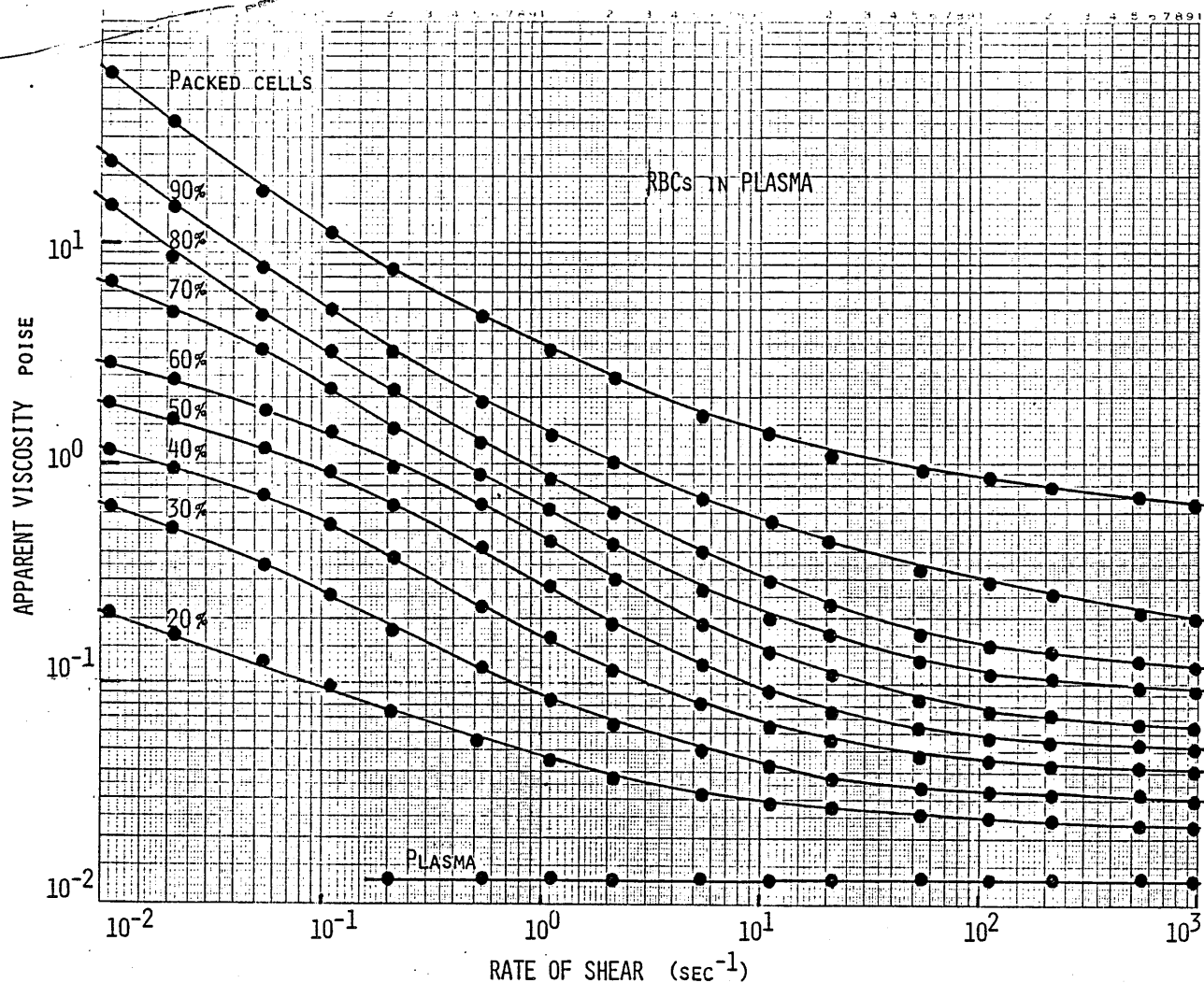


Figure 6. Apparent Viscosity versus Rate of Shear in steady shear, of RBCs resuspended in plasma at hematocrits from zero to packed cells.

30 to 70% hematocrits appear to approach a plateau. This would be inconsistent with the behavior of a fluid that exhibits a yield stress, but not inconsistent with the findings of Cokelet 1963 (12), that the development of a plasma layer at the viscometer geometry interface, and

Copley and King 1970 (13), who described the formation of a three dimensional network of rouleau which slips at the geometry interface, causing the change of slope. The curves of the hematocrits of 80% and above, do not show this effect. This is probably due to pressure caused by crowding, which tends to hold the outer layer of red cells against the geometry wall.

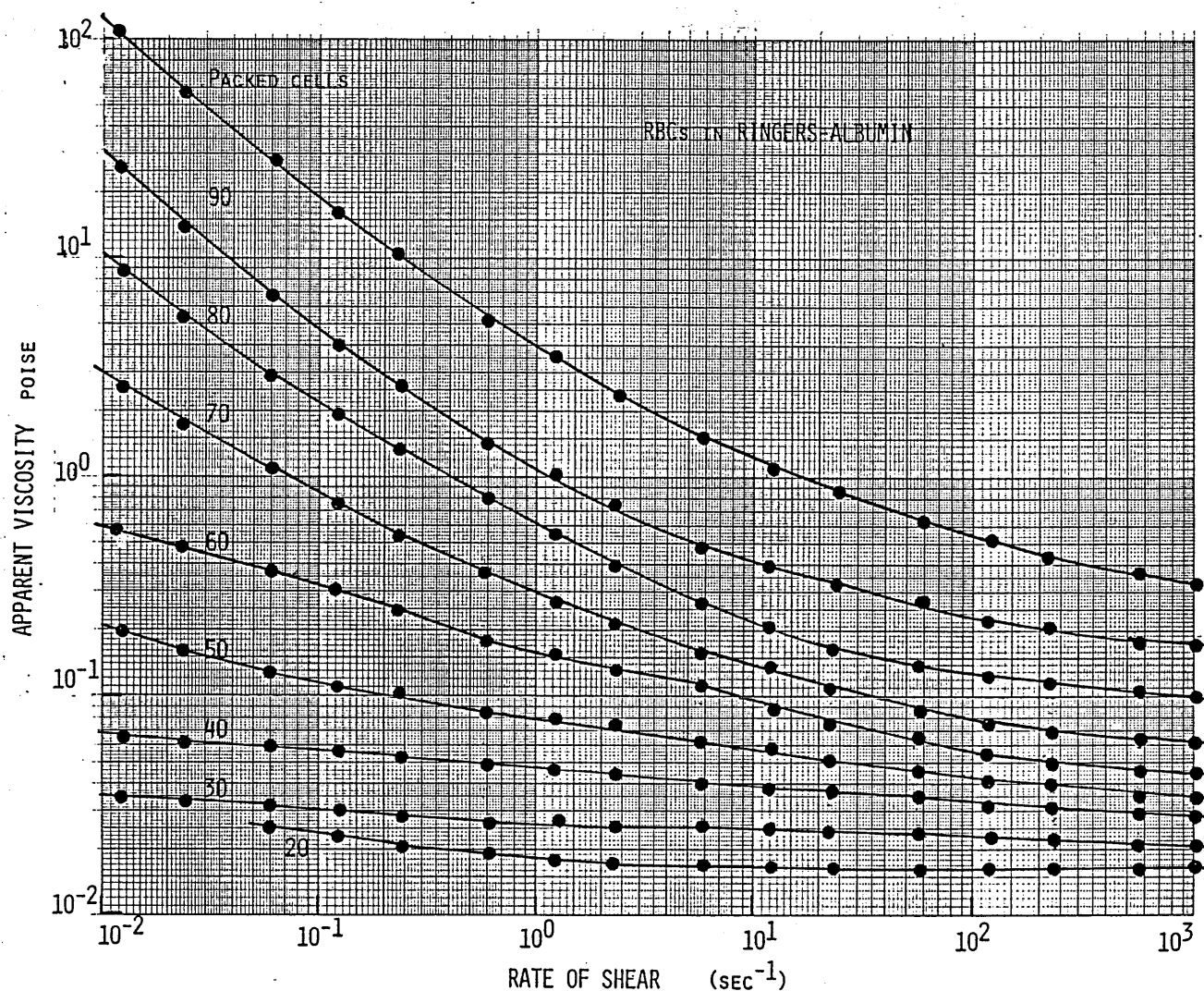


Figure 7. Apparent Viscosity versus Rate of Shear, of RBCs resuspended in Ringer-albumin solution at hematocrits from 20 to 95 percent.

Figure 7 is a plot of the average apparent viscosity versus shear rate of washed red cells resuspended in Ringer/albumin solution. The change of slope seen at low shear rates, of RBCs in plasma at 30 to 70% hemato-

crits, in Figure 6 is much less pronounced in the RBCs in Ringer/albumin preparations at similar hematocrits. This is probably due to the lack of aggregation and rouleau formation. If a cell-free layer develops at the geometry interface, it appears to be narrow and it has only a minor effect on the torque measurements.

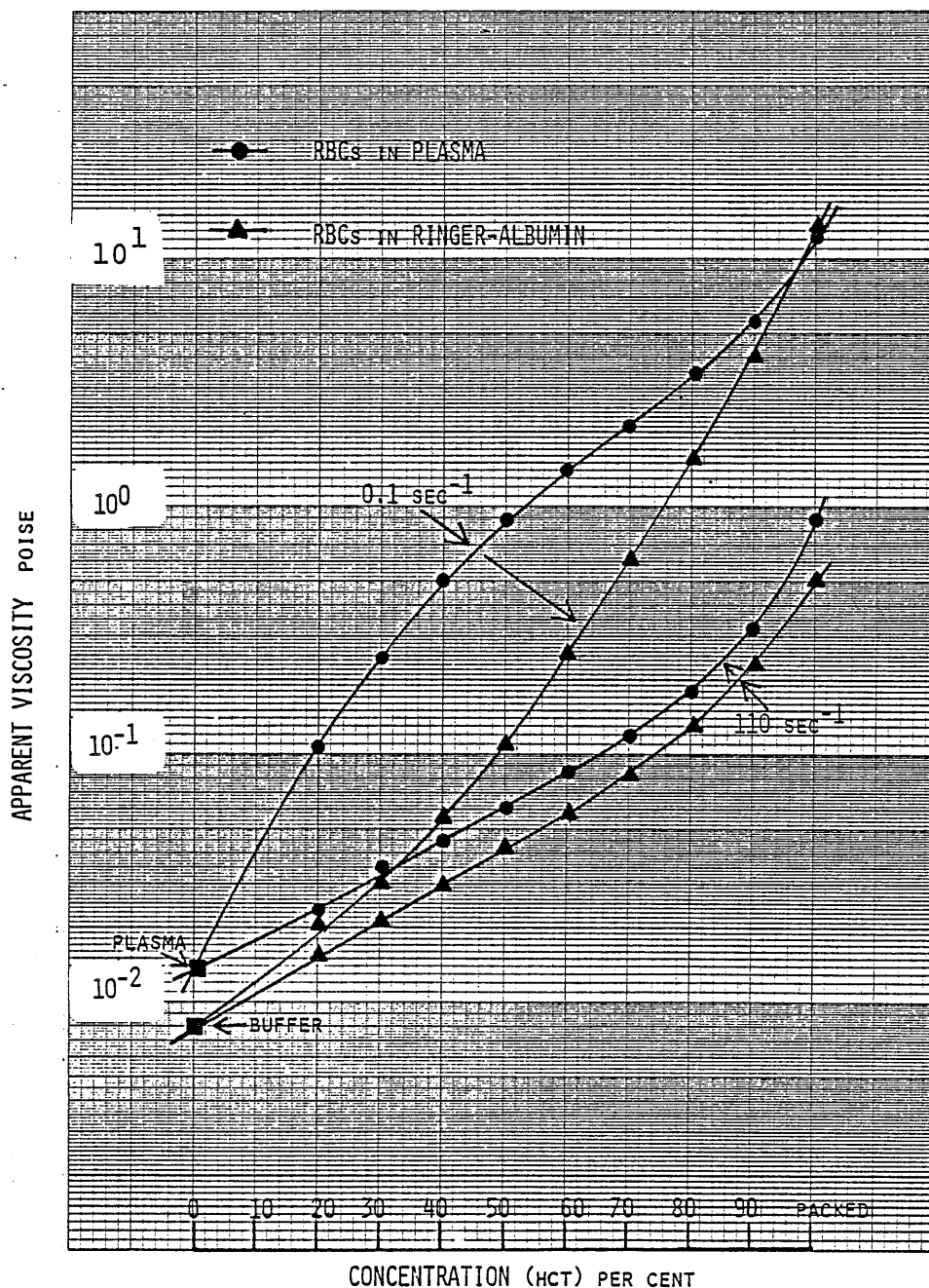


Figure 8. A comparison of the Apparent Viscosity versus concentration of RBCs resuspended in plasma with RBCs resuspended in Ringer-albumin solution at 0.1 and 110.0 sec⁻¹.

Figure 8 is a plot of the viscosity versus hematocrit of both the RBCs in plasma and the washed RBCs in Ringer/albumin at 0.1 sec^{-1} and at 100 sec^{-1} . The RBCs suspended in plasma show approximately a ten times increase in viscosity at hematocrits of from 20 to 60% at the lower shear rate. This shear rate does not generate sufficient stress to prevent aggregation of RBCs into rouleau due to the presence of the plasma proteins. The aggregation and rouleau development causes greatly increased viscosity values to be measured. The absence of the plasma proteins in the preparation of washed RBCs does not allow aggregation due to the lack of bridging macromolecules, resulting in lower viscosity measurements. Another contributing factor, though a lesser one, is the differing viscosities of the suspending medium.

As the concentration of red cells increases, the viscosity difference at 0.1 sec^{-1} reduces until the viscosities of the two preparations become similar at 90% hematocrit. Eventually the viscosity of the washed cells becomes slightly greater.

A comparison of the two red cell preparations at 110 sec^{-1} shows that the viscosities remain similar at all hematocrits when allowance is made for the different viscosities of the suspending medium, indicating that aggregation is the major factor for the increased viscosity of the RBCs in plasma preparation. If we divide the viscosity of the suspending media into the bulk viscosity, we can derive the "Relative Viscosity". Figure 9 is a plot of Relative Viscosity Ratio versus Concentration. At the low shear rate (0.1 sec^{-1}), the actual effect of aggregation of red cells can be seen, causing the elevated vis-

cosity of the RBCs in plasma curve. At high shear rates the relative viscosity ratio of the RBCs in Ringer/albumin solution is higher than the RBCs suspended in plasma. This may indicate that the higher shear stress present in the RBCs in plasma, due to the higher viscosity of the suspending medium, is enough to deform the red cell to a greater extent, thereby lowering the relative viscosity of the RBCs in plasma preparations at the highest hematocrits.

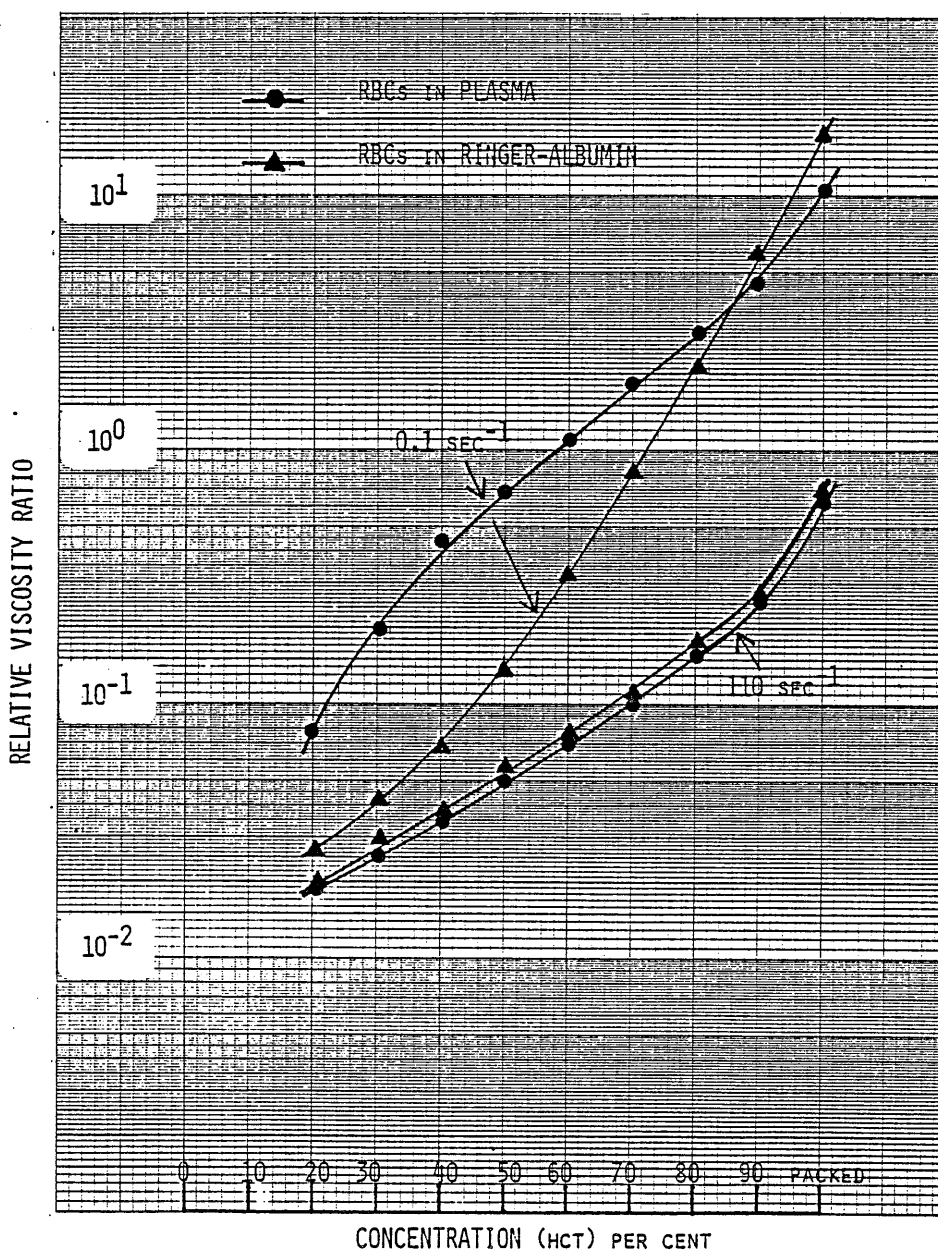


Figure 9. A comparison of the Relative Viscosity Ratio of RBCs in Ringer-albumin solution with RBCs in plasma at 0.1 and 110 sec^{-1} .

The Measurement of Normal Stress in RBCs resuspended Plasma

It has been established that suspension of RBCs in Plasma or Ringers/albumin solution exhibit an elastic component. (1-7). It can be expected therefore, that, in steady flow, this elastic component would cause the display of normal forces, (see Chapter I, page 5). This study was undertaken in an effort to discover whether anticoagulated whole blood from healthy human subjects would exhibit an elastic component by the display of normal forces in study shear.

Copley and King 1975 (14), described investigations of Normal Stress in blood of healthy humans of from 35 to 45% hematocrit. They concluded that Normal Forces were probably present, when whole blood of physiological hematocrits was sheared between a cone and plate of a modified Rheogoniometer. However, they estimated the amount of stress present was outside the sensitivity of their measuring system. In this study the measurement of Normal Stress was undertaken using RBCs resuspended in plasma at 50 to 95% Hematocrit.

Experimental method

The normal forces in response to shear in preparation of RBCs in plasma from 50 to 95% Hematocrit, were measured using a 7cm. diameter cone and plate geometry. The arrangement of the normal force measuring system used is shown in Chapter II, Figure 8. The unit was carefully calibrated by adding weights, and a spring constant of 1 dyne/cm² per micron deflection of the normal force transducer was derived. Rates of shear from 0.01 to 1080 sec⁻¹ were applied in equal increments to the test samples.

Results

No deflection of the Normal Force transducer could be detected at rates of shear from 0.01 to 5.0 sec⁻¹. At 54 sec⁻¹, a slight indication of negative pressure was indicated when measuring hematocrits of 50 and 60%. As shear rates were increased, the negative normal stress increased. King 1965 (15), who first reported this effect, and called it the "Negative Normal Stress Effect". It is caused by centrifugal forces operating in an undisturbed spiraling flow across the flat plate and back across the cone. This negative normal stress occurs when materials of low viscosity are measured with the cone and plate geometry. It was shown by King that when measuring a viscoelastic fluid of low viscosity, a positive normal stress could be reduced, or completely overcome, by the negative normal stress effect.

For the determination of normal stress in fluids of low viscosity at high shear rates, it is necessary to obtain an indication of the negative normal stress that may be present. This can be derived from a fluid of similar viscosity and density to that of the test sample, but which known not to exhibit viscoelasticity, and which should, preferably, be Newtonian.

Solutions of glycerol in distilled water have about the same viscosity and density as normal whole blood, and this material is known to be Newtonian. Solutions of 25, 40 and 50% glycerol in water were therefore used for the estimation of the negative normal stress that may be present in the preparations of blood cells.

Figure 10 is a plot of the negative normal

stress measured in the glycerol solutions. The points are the average values of several measurements of each concentration employed. These values were used to correct the normal stresses measured in the RBC preparations. There did not seem to be any significant difference in negative stress between the three glycerol concentrations.

Both positive and negative normal stresses were exhibited by the suspensions of red cells at 50, 60 and 70% hematocrits, while the preparations of 80, 90 and 95% gave positive normal stress only. Tables 20 to 25 give the average values of the tangential stress (P_{12}), the viscosity (η app.), the negative (N-) and the positive

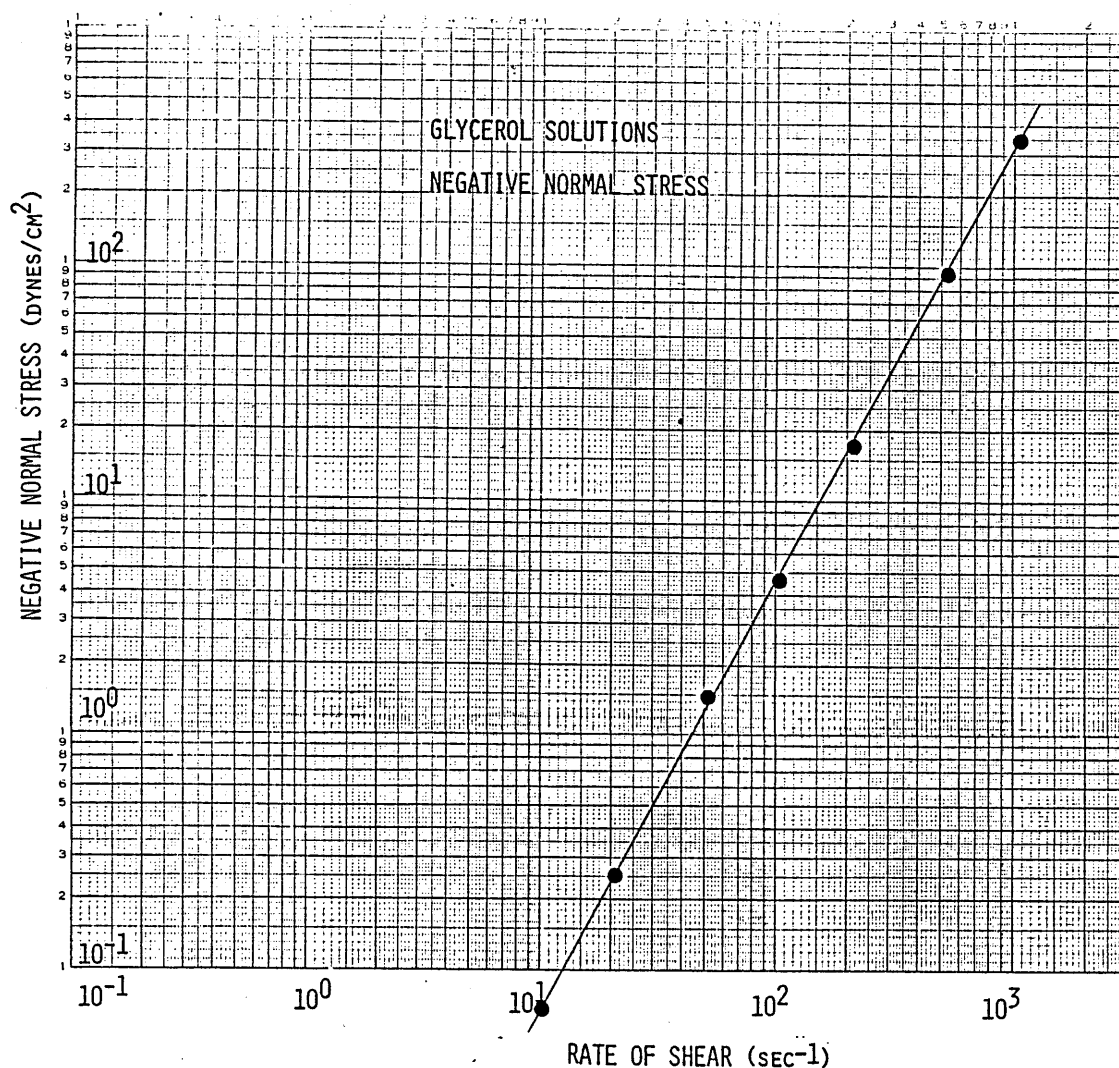


Figure 10. A plot of the average negative normal stress, plotted against shear rate, of several glycerol solutions at different concentrations.

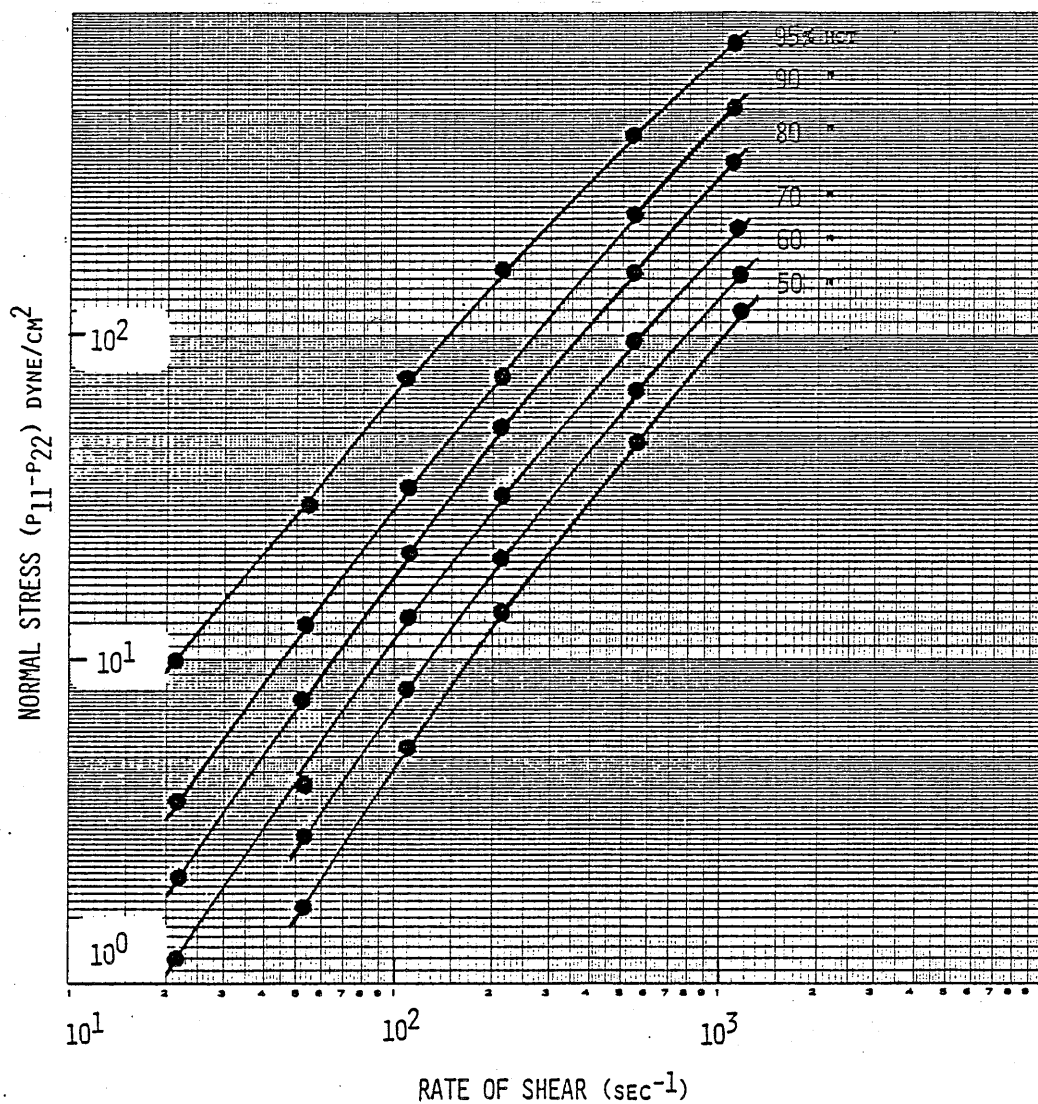


Figure 11a Corrected Normal Stress (N^*) versus Rate of Shear for RBCs in plasma at concentrations of 50 to 95 percent, showing the effect of hematocrit and concentration.

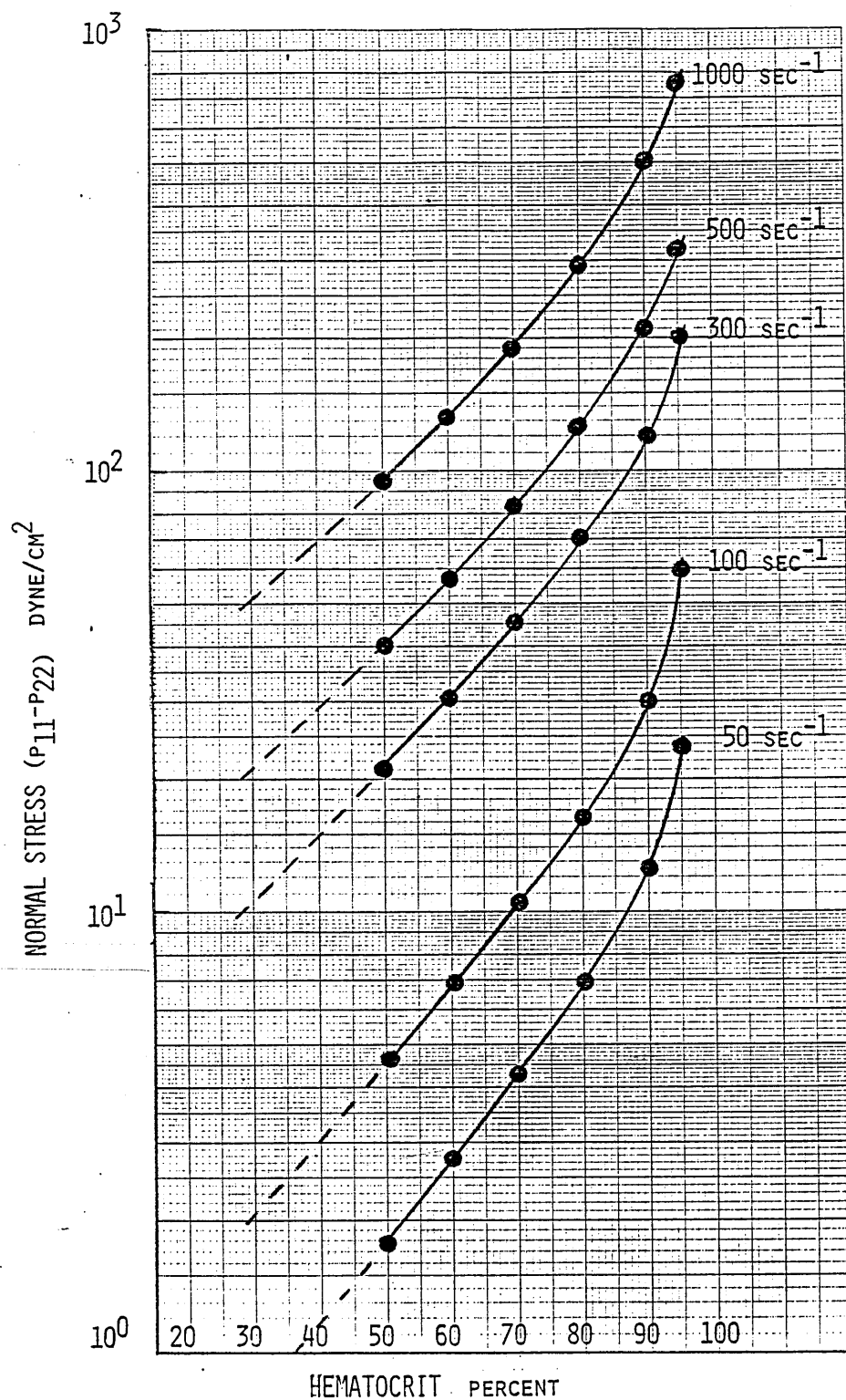


Figure 11b. Normal Stress v. Hematocrit at shear rates from 50 to 1000 sec⁻¹ with an extrapolation to physiological hematocrits.

(N+) normal stresses. Also tabulated is the normal stress correction factor (N_c) derived from the glycerol solutions, and also the corrected normal stress (N^*). From these values, the elasticity (G) is calculated, as well as Weissenberg's recoverable strain (C) and the relaxation time (T_{app}). Figure 11a is a plot of corrected normal stress (N^*), versus rate of shear for the various red cell concentrations prepared. Figure 11b is the same data but plotted against hematocrit. The curves have been extrapolated to 30 percent hematocrit which shows the possible values of normal stress that might occur at physiological values. Figure 12 is a plot of the calculated values of elasticity (G) versus rate of shear for the preparations of red cells in plasma at hematocrits of from 50 to 95 percent.

Discussion

No reliable measurement of normal stress could be made below a hematocrit of 50%. This was also reported by Copley and King 1975 (14). It is envisioned that due to the reduced crowding at this and lower hematocrits, the elongation of the red cells due to the shear stress, is less felt due to the extra free plasma space. This allows only weak "hoop stresses" to develop which are too small for reliable measurement..

These measurements confirm that normal stress can be measured in suspensions of RBCs in plasma from 50 to 95% hematocrit. At physiological hematocrits, no reliable measurements of normal stress could be made, but it is considered likely that normal stress is present, albeit at a low value, in regions with high rates of shear.

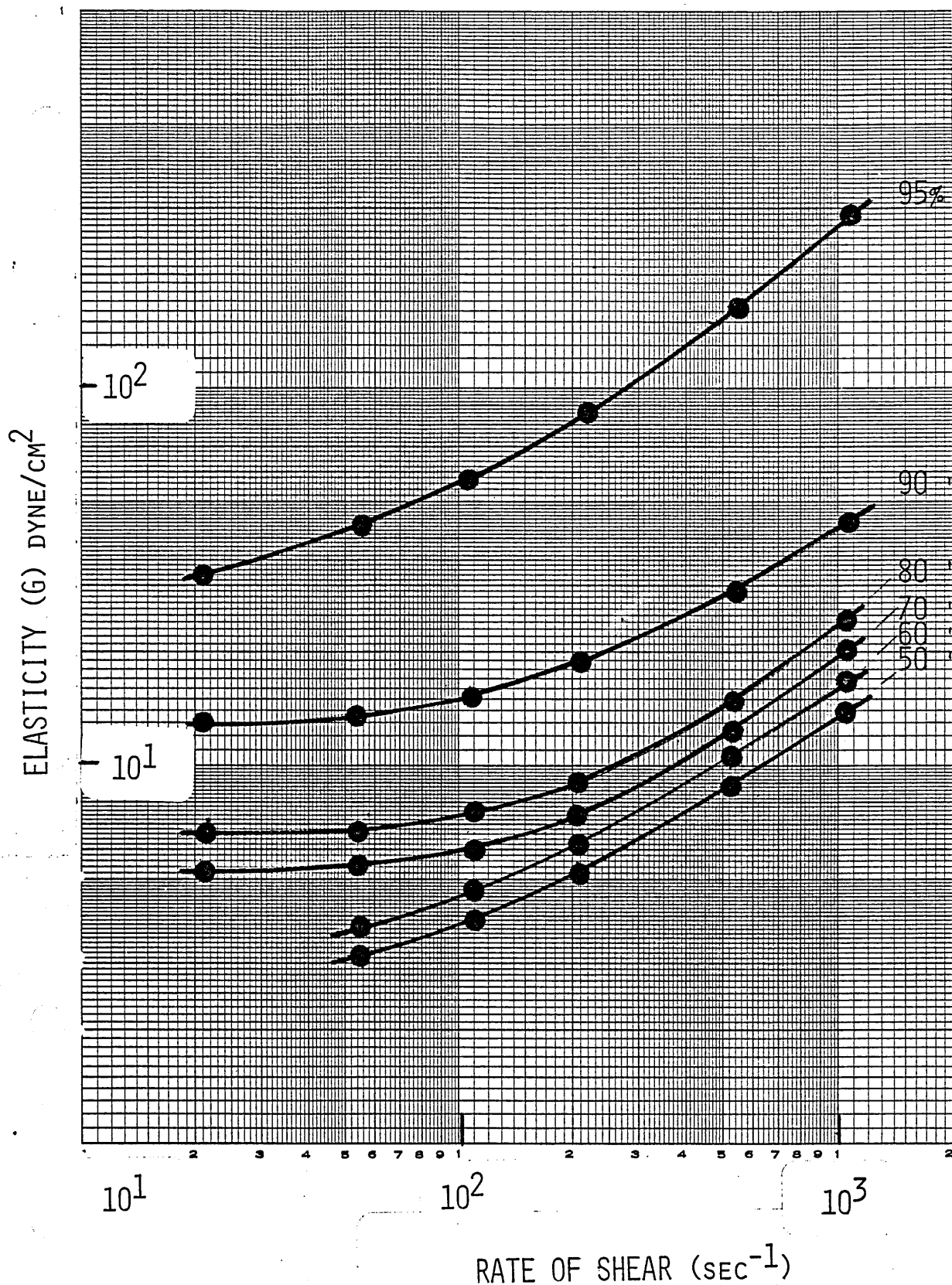


Figure 12. Elasticity (G), calculated from the normal stress values, versus rate of shear, for RBCs in plasma at concentrations of 50 to 95 per cent showing the effect of hematocrit.

RHEOGONIOMETER IN STEADY SHEAR.
(Mean average values)

Table No. 20

Preparation	RBCs in Plasma							Hematocrit		Number of preparations
	1.10	2.16	5.40	11.0	21.6	54.0	108.0	216.0	540.0	8
Rate of Shear (sec^{-1})	1.10	2.16	5.40	11.0	21.6	54.0	108.0	216.0	540.0	1080.0
Tangential Stress (P_{12}) (dyne/cm^2)	.32	.41	.70	1.00	1.60	3.46	6.26	12.1	29.2	56.2
Apparent Viscosity (η app) (Poise)	.29	.19	.13	.093	.076	.064	.058	.056	.054	.052
Positive Normal Stress (N+) (dyne/cm^2)	-	-	-	-	-	.3	.6	-	-	-
Negative Normal Stress (N-) (dyne/cm^2)	-	-	-	-	-	-	-	3.0	37.0	240.0
Correction for Normal Stress (θ) (dyne/cm^2)	-	-	-	-	-	1.50	4.8	17.0	95.0	350.0
Corrected Normal Stress (N*) (dyne/cm^2)	-	-	-	-	-	1.80	5.4	14.0	48.0	110.0
Elasticity (G) (dyne/cm^2)	-	-	-	-	-	3.32	3.63	5.22	8.82	14.25
Recoverable Strain (C)	-	-	-	-	-	1.00	1.72	2.32	3.28	3.92
Relaxation Time (sec)	-	-	-	-	-	.019	.016	.011	.006	.0036

RHEOGONIOMETER IN STEADY SHEAR.
(Mean average values)

Table No. 21

Preparation	RBCs in Plasma						Hematocrit		Number of preparations	
							60		10	
Rate of Shear (sec ⁻¹)	1.10	2.16	5.40	11.0	21.6	54.0	108.0	216.0	540.0	1080.0
Tangential Stress (P ₁₂) (dyne/cm ²)	.5	.65	1.00	1.54	2.38	4.59	8.32	15.55	35.60	69.12
Apparent Viscosity (η _{app}) (Poise)	.45	.30	.19	.14	.11	.085	.077	.072	.066	.064
Positive Normal Stress (N ⁺) (dyne/cm ²)	-	-	-	-	.55	1.30	3.20	4.0	-	-
Negative Normal Stress (N ⁻) (dyne/cm ²)	-	-	-	-	-	-	-	-	27.0	200.0
Correction for Normal Stress (θ) (dyne/cm ²)	-	-	-	-	-	1.50	4.80	17.0	95.0	350.0
Corrected Normal Stress (N*) (dyne/cm ²)	-	-	-	-	-	2.8	8.0	21.0	68.0	150.0
Elasticity (G) (dyne/cm ²)	-	-	-	-	-	3.76	4.32	5.75	9.35	16.0
Recoverable Strain (C)	-	-	-	-	-	1.22	1.92	2.70	2.80	4.34
Relaxation Time (sec)	-	-	-	-	-	.022	.018	.013	.007	.004

RHEOGONIOMETER IN STEADY SHEAR.
(Mean average values)

Table No. 22

Preparation	RBCs in Plasma						Hematocrit 70%		Number of preparations 12	
	1.10	2.16	5.40	11.0	21.6	54.0	108.0	216.0	540.0	1080.0
Rate of Shear (sec ⁻¹)										
Tangential Stress (P ₁₂) (dyne/cm ²)	.69	.93	1.46	2.20	3.67	7.00	12.0	21.6	51.3	98.28
Apparent Viscosity (η app) (Poise)	.63	.43	.27	.20	.17	.13	.11	.10	.095	.091
Positive Normal Stress (N+) (dyne/cm ²)	-	-	-	-	1.00	3.50	10.20	18.0	15.0	-
Negative Normal Stress (N-) (dyne/cm ²)	-	-	-	-	-	-	-	-	-	120.0
Correction for Normal Stress (θ) (dyne/cm ²)	-	-	-	-	.25	1.5	4.80	17.0	95.0	350.0
Corrected Normal Stress (N*) (dyne/cm ²)	-	-	-	-	1.25	5.0	15.0	35.0	110.0	230.0
Elasticity (G) (dyne/cm ²)	-	-	-	-	5.49	5.4	5.5	6.65	12.0	21.0
Recoverable Strain (C)	-	-	-	-	.68	1.42	2.50	3.24	4.28	4.68
Relaxation Time (sec)	-	-	-	-	.03	.024	.02	.015	.008	.004

RHEOGONIOMETER IN STEADY SHEAR.
(Mean average values)

Table No. 23

Preparation	RBCs in Plasma						Hematocrit 80%		Number of preparations 9	
	1.10	2.16	5.40	11.0	21.6	54.0	108.0	216.0	540.0	1080.0
Rate of Shear (sec ⁻¹)										
Tangential Stress (P ₁₂) (dyne/cm ²)	.95	1.32	2.16	3.3	5.2	9.72	17.28	30.24	64.8	129.6
Apparent Viscosity (η app) (Poise)	.86	.61	.40	.30	.24	.18	.16	.14	.12	.12
Positive Normal Stress (N+) (dyne/cm ²)	-	-	-	-	1.85	5.9	17.20	35.0	65.00	-
Negative Normal Stress (N-) (dyne/cm ²)	-	-	-	-	-	-	-	-	-	-
Correction for Normal Stress (θ) (dyne/cm ²)	-	-	-	-	.25	1.50	4.80	17.0	95.0	350.0
Corrected Normal Stress (N*) (dyne/cm ²)	-	-	-	-	2.10	7.4	22.0	52.0	160.0	350.0
Elasticity (G) (dyne/cm ²)	-	-	-	-	6.45	6.38	6.78	8.8	13.1	24.0
Recoverable Strain (C)	-	-	-	-	.8	1.52	2.54	3.44	4.94	5.40
Relaxation Time (sec)	-	-	-	-	.037	.028	.024	.016	.0092	.005

RHEOGONIOMETER IN STEADY SHEAR.
(Mean average values)

Table No. 24

Preparation	RBCs in Plasma							Hematocrit		Number of preparations	
	1.10	2.16	5.40	11.0	21.6	54.0	108.0	216.0	540.0	1080.0	14
Rate of Shear (sec^{-1})	1.10	2.16	5.40	11.0	21.6	54.0	108.0	216.0	540.0	1080.0	
Tangential Stress (P_{12}) (dyne/cm ²)	1.50	2.16	3.78	6.1	9.72	18.9	32.4	56.16	113.4	205.2	
Apparent Viscosity (η app) (Poise)	1.37	1.00	.70	.55	.45	.35	.30	.26	.21	.19	
Positive Normal Stress (N+) (dyne/cm ²)	-	-	-	-	3.25	11.5	30.20	59.0	135.0	150.0	
Negative Normal Stress (N-) (dyne/cm ²)	-	-	-	-	-	-	-	-	-	-	
Correction for Normal Stress (θ) (dyne/cm ²)	-	-	-	-	.25	1.5	4.8	17.	95.0	350.0	
Corrected Normal Stress (N*) (dyne/cm ²)	-	-	-	-	3.5	13.0	35.0	76.0	230.0	500.0	
Elasticity (G) (dyne/cm ²)	-	-	-	-	13.5	13.75	15.0	21.0	28.0	42.10	
Recoverable Strain (C)	-	-	-	-	.72	1.38	2.2	2.7	4.00	4.88	
Relaxation Time (sec)	-	-	-	-	.033	.025	.02	.013	.0075	.0045	

RHEOGONIOMETER IN STEADY SHEAR.
(Mean average values)

Table No. 25

Preparation	RBCs in Plasma							Hematocrit 95%		Number of preparations 6	
	1.10	2.16	5.40	11.0	21.6	54.0		108.0	216.0	540.0	1080.0
Rate of Shear (sec^{-1})											
Tangential Stress (P_{12}) (dyne/cm ²)	3.77	5.36	9.4	15.29	24.80	51.84		93.0	168.5	388.8	723.6
Apparent Viscosity (η_{app}) (Poise)	3.43	2.48	1.74	1.39	1.15	.96		.86	.78	.72	.67
Positive Normal Stress (N+) (dyne/cm ²)	-	-	-	-	9.75	28.5		71.2	143.0	345.0	440.0
Negative Normal Stress (N-) (dyne/cm ²)	-	-	-	-	-	-		-	-	-	-
Correction for Normal Stress (0) (dyne/cm ²)	-	-	-	-	.25	1.5		4.8	17.0	95.0	370.0
Corrected Normal Stress (N*) (dyne/cm ²)	-	-	-	-	10.0	30.0		76.0	160.0	440.0	810.0
Elasticity (G) (dyne/cm ²)	-	-	-	-	30.85	44.8		57.0	88.70	176.0	323.2
Recoverable Strain (C)	-	-	-	-	.8	1.2		1.64	1.90	2.26	2.20
Relaxation Time (sec)	-	-	-	-	.087	.021		.015	.0088	.0041	.0021

The Effect of Shear on the Sedimentation Rate of Red Blood Cells

The phenomenon of the erythrocyte sedimentation was first investigated by Fahraeus 1921 (16,17). In this classical work on erythrocyte sedimentation, he demonstrated that the main cause of the increased settling rate is the aggregation of erythrocytes. It was shown by Ruhenstroth-Bauer, et al. 1960 (18), that chemical factors are involved in the sedimentation rate. Gomulkiewicz 1973 (19), Boyd and Sanderson 1969 (20) pointed out that the electrostatic effect the surface charge of erythrocytes is affected by the ionic concentration in the plasma. The erythrocyte sedimentation rate (ESR), standardised in a number of methods as a clinical test, has been in use for many years (21-23). The ESR test consists of placing blood in a tube of standard bore and recording the drop of the interface separating the supernatant plasma from the sedimented erythrocytes for one hour or any other given length of time. The ESR from a healthy human subject is usually about 1 cm/hr. An increase of the ESR was found in the blood of pregnant women and of patients with a large variety of diseases and clinical disorders. In making the test more meaningful for clinical considerations as an indicator of pathological changes, it is necessary to understand more about the physical phenomena, erythrocyte sedimentation. The latter is affected by many factors, such as those mentioned above and also by imposed shear.

Experimental method

In order to investigate the effect of shear on the sedimentation rate of RBCs, the Couette geometry was used for this investigation. This geometry is described in Chapter II, Fig. 9. Two bands of thin black tape were secured around the outer cylinder 0.6 cm apart, with the top band 0.5cm down from the liquid/air interface.

Blood samples were secured from the antecubital vein of four healthy donors whose blood had hematocrits varying from 38 to 44 percent. The blood was anticoagulated upon withdrawal with EDTA (1.0mg. per ml of blood). After being applied to the test geometry the blood samples were first mixed thoroughly to break up aggregates of red cells, and to ensure even distribution of the red cells throughout the plasma. Thereafter, the desired shear rate was applied and, by the use of a stop watch, the time was recorded for the red cell/plasma interface to pass downward between the two bands of tape.

The erythrocyte sedimentation rate (ESR) was calculated using the formula - $ESR = \frac{d \times 60}{t}$ cm/hr

where d = distance in cm between the two marks

t - time in minutes taken by the red cells/plasma interface to pass between the two marks.

The first measurement was made with the cylinder stationary at zero shear. Thereafter, the shear rate was increased from 1.0×10^{-4} up to 10.0 sec^{-1} , and the sedimentation time was measured and recorded as described.

Results

Figure 13 shows the plots of the calculated ESR versus the rate of shear of the samples from the four donors. No significant change of the characteristics of the ESR was found with the blood samples of three donors between zero and shear rates up to 1.0×10^{-2} . One donor, however, exhibits a slight increase of ESR, beginning at $1.0 \times 10^{-3} \text{ sec}^{-1}$. Above the shear rate of 1.0×10^{-2} , there is a significant increase in ESR of all donors, with a peak value occurring at 1.0×10^{-1} . Thereafter, there are decreasing values as shear rate is increased up to $1.0 \times 10 \text{ sec}^{-1}$, above which the ESR becomes nonexistent.

Discussion

It has been demonstrated that at these very low shear rates, ($0 - 0.01 \text{ sec}^{-1}$) slip occurs at the wall of the test geometry and so the effect of the shear will not be felt within the system of rouleau which has developed. The sedimentation rate should not therefore be affected by the shear between zero and 0.01 sec^{-1} .

In the region of the shear rates between 0.01 and 1.0 sec^{-1} the blood is now flowing. The relative movement of erythrocytes and the plasma will enhance the probability of cell-cell encounters and allow greater

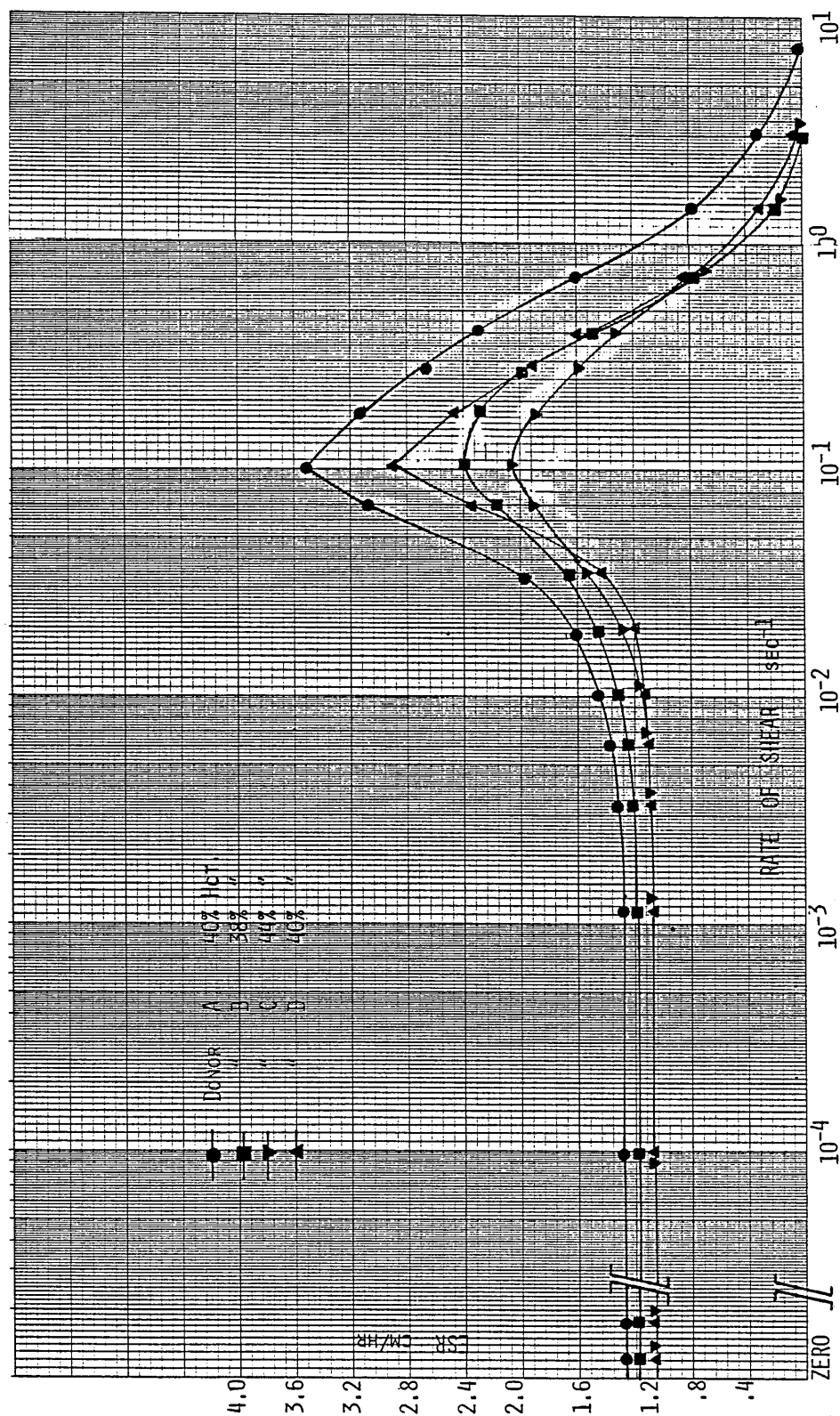


Figure 13. A plot of sedimentation rate (ESR) versus Rate of Shear, showing the effect of increasing shear rate on sedimentation.

numbers of them to be bridged by red cell-protein-red cell bonds which would allow large clumps or rafts of rouleaux to respond to gravitational pull and to settle downward at an increased rate. This effect reaches a peak at 0.1 sec^{-1} .

An increase in flow velocity gradient would cause an increase in shear stress which will break up the rouleaux formations. Therefore, the sedimentation of erythrocytes will be slowed down and eventually stop as the shear rate reaches a certain value. It is evident in Figure 13, that both effects influence the ESR when the shear rate is between 0.01 and 0.10 sec^{-1} . The first effect, of increasing cell to cell encounters, is predominant at this range of shear rates, and so ESR increases. When the shear rate is higher than 0.10 sec^{-1} , the second effect, viz., the effect of shear dispersing of rouleaux becomes predominant. Therefore, the ESR decreases and eventually approaches zero when the shear is higher than 10 sec^{-1} .

The studies of Fahraeus, as well as the photomicroscopic observations of rouleau formation at low shear in Figure 3, and the lack of it in Figure 6, are of particular interest physiologically. Here, as was emphasized by Fahraeus 1961 (24), the red cell aggregates or rouleaux, can actually facilitate the flow of blood in certain conditions.

The measurement of viscosity and elasticity in oscillatory shear of RBCs resuspended in plasma, and also in Ringer/albumin solution

Macrorheological and microrheological studies on RBCs suspended in plasma and Ringers/albumin solution, have suggested the presence of an elastic component in

these blood systems, (1-7). The dynamic viscosity and dynamic elasticity of these systems are conveniently measured by the oscillatory mode of testing in which the phase lag and amplitude ratios between the input and output sinus motions are determined.

Measurements of RBCs resuspended in plasma

Red cells were prepared as previously described (page 31) and resuspended in the donor's plasma at concentration of from 20 to 95%.

The rheogoniometer is fitted with a cone and plate geometry of 7cm diameter with 1° angle, and measurements of the dynamic viscosity (η') and dynamic elasticity (G') were made in oscillatory shear from 0.0019 to 19.0 Hertz.

The data obtained from these measurements are tabulated in Tables 26 to 34. Figure 14 shows the variation of viscosity (η') with frequency at varying hematocrits and Figure 15 shows the variation of the elastic component (G') with frequency at the same hematocrits. The plateau effect at low frequencies is still present as is seen in the steady shear experiments presented in Figure 5. It can be presumed that the same conditions that have been described are still present, and that there is a three dimensional network of rouleau, which slips at the boundary wall.

RHEOGONIOMETER IN OSCILLATORY SHEAR.
(Mean average values)

Table No. 26

Preparation	RBCs in Plasma					Hematocrit 20%		Number of samples. 32		
	.0006	.0019	.006	.019	.06	.19	.6	1.9	6.0	19.0
Frequency (Hertz)										
Dynamic Viscosity (η') (poise)	-	-	-	.038	.035	.032	.028	.024	.020	.017
Dynamic Elasticity (G') (dynes/cm ²)	-	-	-	-	-	-	-	-	-	-

Table No. 27

Preparation	RBCs in Plasma					Hematocrit 30%		Number of samples. 28		
	.0006	.0019	.006	.019	.06	.19	.6	1.9	6.0	19.0
Frequency (Hertz)										
Dynamic Viscosity (η') (poise)	-	-	-	.072	.064	.058	.046	.036	.025	.019
Dynamic Elasticity (G') (dynes/cm ²)	-	-	-	-	-	-	-	-	-	-

RHEOGONIOMETER IN OSCILLATORY SHEAR.
(Mean average values)

Table No. 28

Preparation	RBCs in Plasma					Hematocrit 40%		Number of samples. 34		
Frequency (Hertz)	.0006	.0019	.006	.019	.06	.19	.6	1.9	6.0	19.0
Dynamic Viscosity (η') (poise)	-	.020	.17	.14	.12	.084	.056	.042	.030	.022
Dynamic Elasticity (G') (dynes/cm ²)	-	-	-	-	.014	.033	.075	.17	.40	1.2

Table No. 29

Preparation	RBCs in Plasma					Hematocrit 50%		Number of samples. 36		
Frequency (Hertz)	.0006	.0019	.006	.019	.06	.19	.6	1.9	6.0	19.0
Dynamic Viscosity (η') (poise)	-	.45	.40	.29	.20	.13	.09	.062	.044	.030
Dynamic Elasticity (G') (dynes/cm ²)	-	-	-	.015	.032	.069	.14	.30	.65	1.8

RHEOGONIOMETER IN OSCILLATORY SHEAR.
(Mean average values)

Table No. 30

Preparation	RBCs in Plasma				Hematocrit 60%		Number of samples. 31		
Frequency (Hertz)	.0006	.0019	.006	.019	.06	.19	.6	1.9	6.0
Dynamic Viscosity (η') (poise)	-	.88	.70	.50	.36	.22	.13	.09	.06
Dynamic Elasticity (G') (dynes/cm ²)	-	-	.016	.032	.064	.14	.27	.56	1.02
									3.0

Table No. 31

Preparation	RBCs in Plasma				Hematocrit 70%		Number of samples. 36		
Frequency (Hertz)	.0006	.0019	.006	.019	.06	.19	.6	1.9	6.0
Dynamic Viscosity (η') (poise)	-	1.9	1.7	1.3	.73	.42	.23	.14	.10
Dynamic Elasticity (G') (dynes/cm ²)	-	.016	.036	.081	.15	.28	.53	.98	1.8
									4.0

RHEOGONIOMETER IN OSCILLATORY SHEAR.
(Mean average values)

Table No. 32

Preparation	RBCs in Plasma					Hematocrit 80%		Number of samples. 42		
Frequency (Hertz)	.0006	.0019	.0006	.019	.06	.19	.6	1.9	6.0	19.0
Dynamic Viscosity (η') (poise)	-	5.0	3.2	1.9	1.0	.56	.32	.19	.13	.082
Dynamic Elasticity (G') (dynes/cm ²)	-	.04	.09	.19	.33	.60	1.0	1.8	3.2	6.6

Table No. 33

Preparation	RBCs in Plasma				Hematocrit 90%		Number of samples. 46			
	.0006	.0019	.0006	.019	.06	.19	.6	1.9	6.0	19.0
Frequency (Hertz)										
Dynamic Viscosity (η') (poise)	-	13.0	6.0	3.0	1.5	.76	.4	.25	.16	.12
Dynamic Elasticity (G') (dynes/cm ²)	-	.22	.34	.54	.84	1.3	2.0	3.2	4.9	9.0

RHEOGONIOMETER IN OSCILLATORY SHEAR.
(Mean average values)

Table No. 34

Preparation	RBCs in Plasma					Hematocrit 95%		Number of samples. 18		
Frequency (Hertz)	.0006	.0019	.0006	.019	.06	.19	.6	1.9	6.0	19.0
Dynamic Viscosity (η') (poise)	-	70.0	32.0	14.0	6.0	2.7	1.3	.66	.34	.17
Dynamic Elasticity (G') (dynes/cm ²)	-	.50	.74	1.10	1.6	2.3	3.5	5.2	7.6	13.0

Table No. 35

Preparation	RBCs in Ringer/albumin					Hematocrit 20%		Number of samples. 22		
Frequency (Hertz)	.0006	.0019	.0006	.019	.06	.19	.6	1.9	6.0	19.0
Dynamic Viscosity (η') (poise)	-	-	-	-	.019	.017	.016	.015	.014	.012
Dynamic Elasticity (G') (dynes/cm ²)	-	-	-	-	-	-	-	-	-	-

RHEOGONIOMETER IN OSCILLATORY SHEAR.
(Mean average values)

Table No. 36

Preparation	RBCs in Ringer/albumin					Hematocrit 30%		Number of samples. 28		
	.0006	.0019	.006	.019	.06	.19	.6	1.9	6.0	19.0
Frequency (Hertz)	.0006	.0019	.006	.019	.06	.19	.6	1.9	6.0	19.0
Dynamic Viscosity (η') (poise)	-	-	-	-	.027	.025	.022	.02	.017	.016
Dynamic Elasticity (G') (dynes/cm ²)	-	-	-	-	-	-	-	-	-	-

Table No. 37

Preparation	RBCs in Ringer/albumin					Hematocrit 40%		Number of samples. 26		
	.0006	.0019	.006	.019	.06	.19	.6	1.9	6.0	19.0
Frequency (Hertz)	.0006	.0019	.006	.019	.06	.19	.6	1.9	6.0	19.0
Dynamic Viscosity (η') (poise)	-	-	.07	.056	.046	.037	.032	.026	.023	.018
Dynamic Elasticity (G') (dynes/cm ²)	-	-	-	-	-	-	-	-	-	-

RHEOGONIOMETER IN OSCILLATORY SHEAR.
(Mean average values)

Table No. 38

Preparation	RBCs in Ringer/albumin					Hematocrit 50%		Number of samples. 30		
	.0006	.0019	.006	.019	.06	.19	.6	1.9	6.0	19.0
Frequency (Hertz)	.0006	.0019	.006	.019	.06	.19	.6	1.9	6.0	19.0
Dynamic Viscosity (η') (poise)	-	.018	.13	.11	.083	.066	.052	.04	.03	.023
Dynamic Elasticity (G') (dynes/cm ²)	-	-	-	-	.013	.033	.086	.22	.57	1.5

Table No. 39

Preparation	RBCs in Ringer/albumin					Hematocrit 60%		Number of samples. 28		
	.0006	.0019	.006	.019	.06	.19	.6	1.9	6.0	19.0
Frequency (Hertz)	.0006	.0019	.006	.019	.06	.19	.6	1.9	6.0	19.0
Dynamic Viscosity (η') (poise)	-	.54	.36	.25	.17	.12	.086	.062	.044	.032
Dynamic Elasticity (G') (dynes/cm ²)	-	-	-	.011	.027	.067	.17	.40	1.0	2.5

RHEOGONIOMETER IN OSCILLATORY SHEAR.
(Mean average values)

Table No. 40

Preparation	RBCs in Ringer/albumin				Hematocrit 70%		Number of samples. 24		
Frequency (Hertz)	.0006	.0019	.006	.019	.06	.19	.6	1.9	6.0
Dynamic Viscosity (η') (poise)	-	1.8	.96	.58	.36	.22	.14	.092	.06
Dynamic Elasticity (G')	-	-	.01	.025	.058	.13	.30	.70	1.7
									3.6

Table No. 41

Preparation	RBCs in Ringer/albumin				Hematocrit 80%		Number of samples. 48		
Frequency (Hertz)	.0006	.0019	.006	.019	.06	.19	.6	1.9	6.0
Dynamic Viscosity (η') (poise)	-	7.4	3.0	1.50	.80	.44	.26	.16	.09
Dynamic Elasticity (G')	-	.013	.027	.062	.13	.29	.60	1.5	2.9
									6.2

Table No. 42 RHEOGONIOMETER IN OSCILLATORY SHEAR.
(Mean average values)

Preparation	RBCs in Ringer/albumin					Hematocrit 90%		Number of samples. 62		
Frequency (Hertz)	.0006	.0019	.006	.019	.06	.19	.6	1.9	6.0	19.0
Dynamic Viscosity (η') (poise)	-	25.0	9.65	4.2	1.9	.92	.48	.27	.155	.096
Dynamic Elasticity (G') (dynes/cm ²)	-	.036	.072	.145	.28	.56	1.15	2.20	4.4	8.5

Table No. 43

Preparation	RBCs in Ringer/aluminum					Hematocrit 95%		Number of samples. 26		
Frequency (Hertz)	.0006	.0019	.006	.019	.06	.19	.6	1.9	6.0	19.0
Dynamic Viscosity (η') (poise)	-	85.0	30.0	11.5	4.6	2.20	1.00	.52	.27	.15
Dynamic Elasticity (G') (dynes/cm ²)	-	.086	.16	.32	.56	1.10	2.0	3.7	7.0	14.0

Red cells were prepared as described on page 31 of this chapter, and resuspended in Ringer/albumin solution at hematocrits of from 20% to 95%. These were measured in oscillatory shear in the same way as the RBCs resuspended in plasma.

Tables 35 to 43 list the data obtained by these measurements. Figure 16 is a plot of η' versus frequency. It can be seen that the plateau effect at the low frequencies is not evident, indicating that rouleau formation is not present in these preparations. A comparison of η' with the viscosity of RBCs in plasma preparation shows that at hematocrits above 85%, the viscosities are similar, but at the lower hematocrits, the η' of the RBCs in Ringer/albumin has a much lower viscosity, again reflecting the absence of rouleau formation.

Figure 17 is a plot of elasticity (G') versus frequency. The values of RBCs in Ringer/albumin are much lower than those in plasma, indicating that a considerable part of the elastic modulus measured in the RBCs in plasma preparation is derived, at the low frequencies, from the rouleau formations. As the frequency is increased, the rouleaux are broken down, and the two sets of data become similar at around 1.0 Hertz.

Figure 18 shows a comparison of the dynamic viscosity (η') plotted against hematocrit at 0.01 Hertz of both RBCs in plasma and washed RBCs in Ringer/albumin solution. At low hematocrits, the difference is approximately 3 fold, but at hematocrits of 90% and above, η' is similar in both preparations.

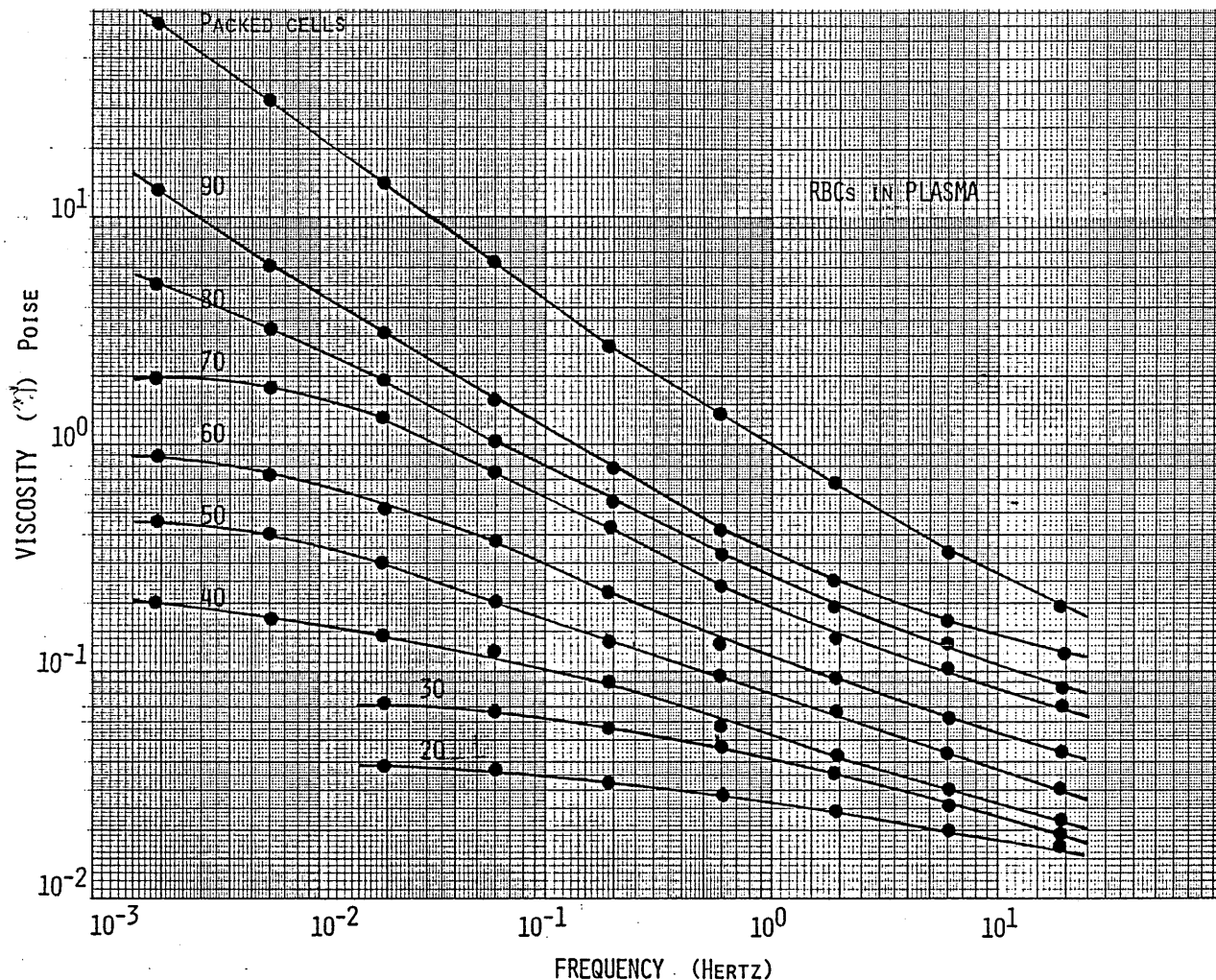


Figure 14. Viscosity (η') versus Frequency in oscillatory shear, of suspensions of RBCs in plasma at concentrations of 20% to packed cells, showing the effect of frequency and hematocrit.

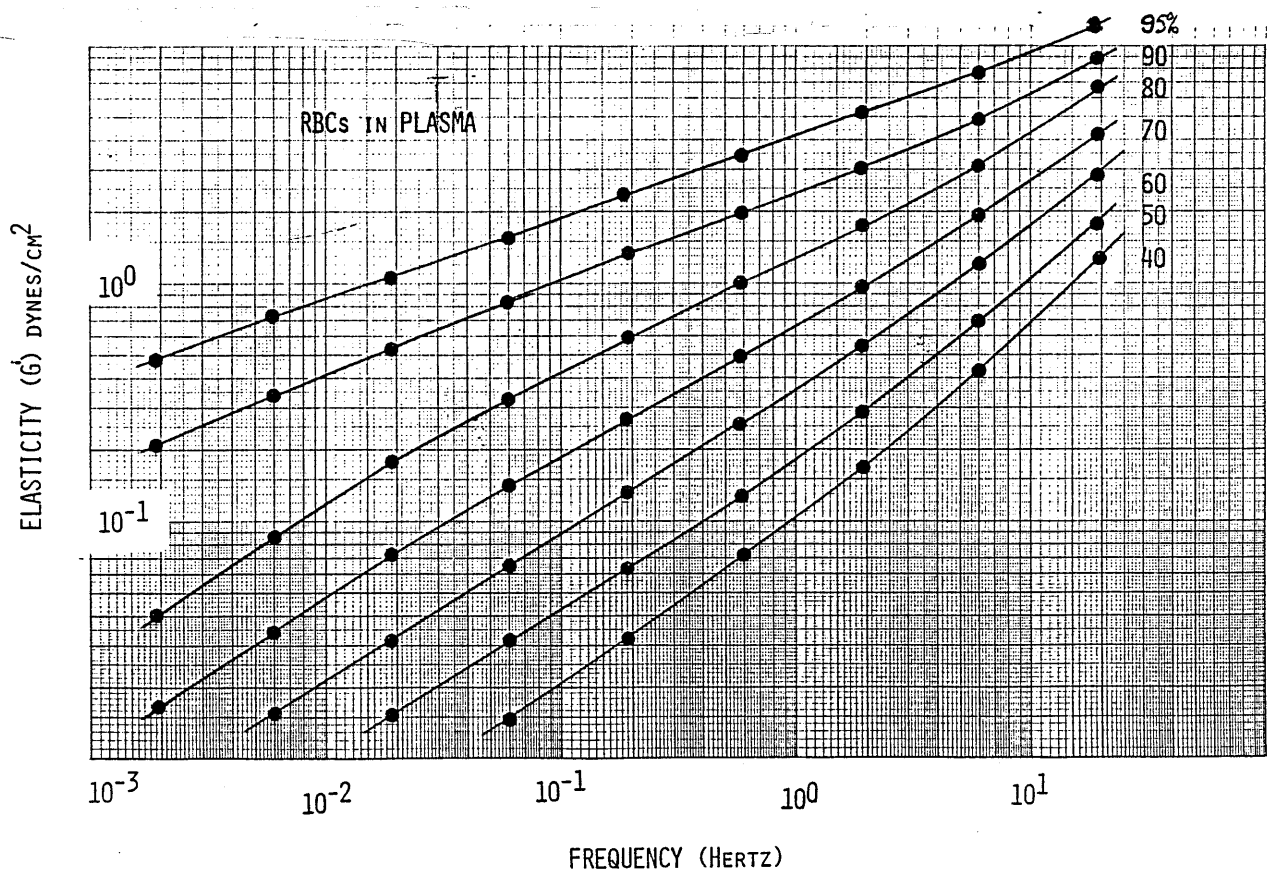


Figure 15. Elasticity (G') versus Frequency in oscillatory shear, of suspensions of RBCs in plasma at concentrations from 40% to 95%, showing the effect of frequency and hematocrit on the elastic component.

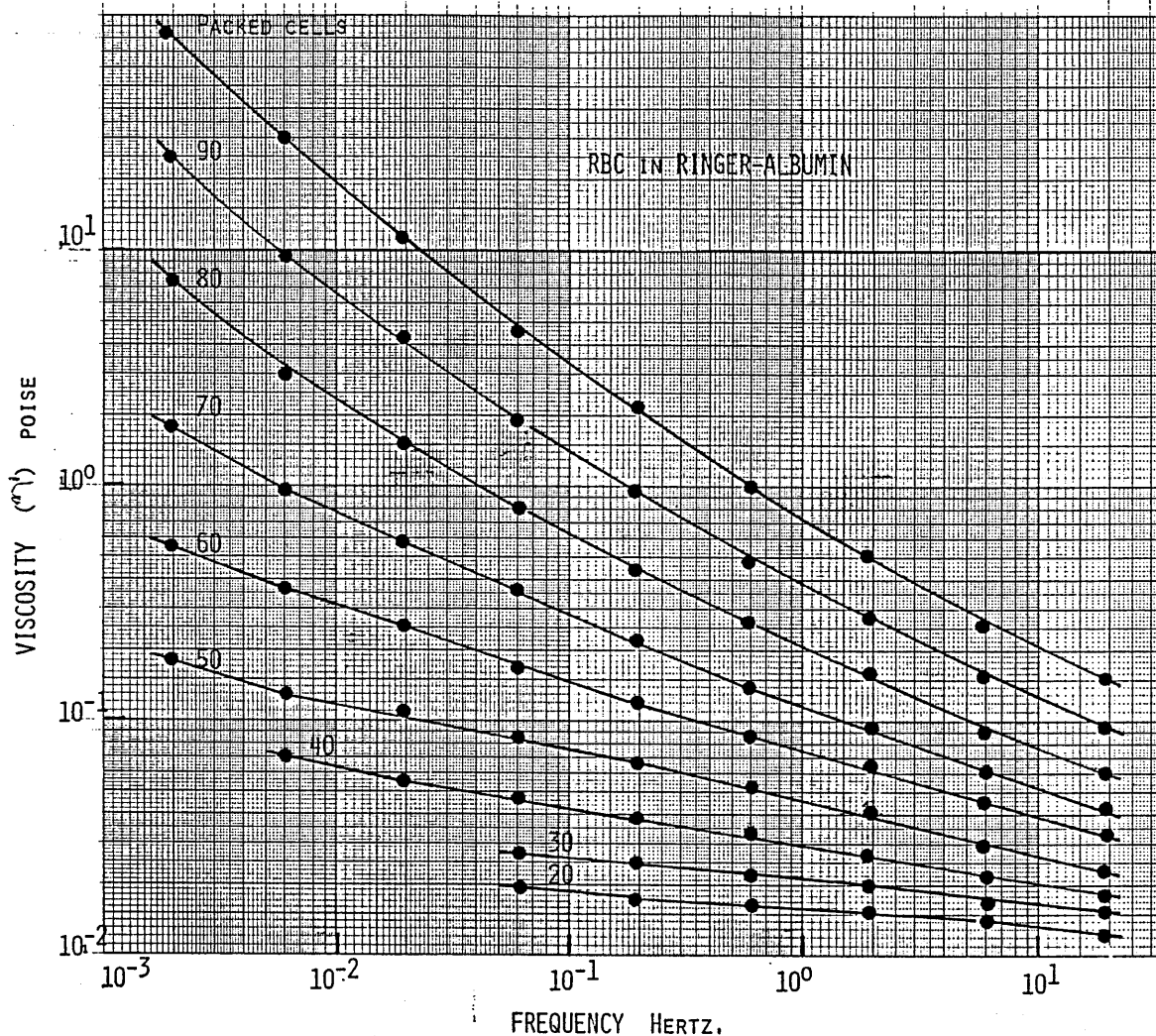


Figure 16. Viscosity (η') versus frequency in oscillatory shear, of suspensions of RBCs in Ringer-albumin solution at concentrations from 20 to 90 per cent and packed cells, showing the effect of hematocrit and frequency on viscosity.

Figure 19 shows a comparison of the dynamic elasticity (G') plotted against hematocrit at 0.1 Hertz of both RBCs in plasma and washed RBCs in Ringer/albumin solution. It can be seen that the RBCs in plasma preparation has the higher elastic modulus which is maintained at all hematocrits.

Figure 20 is a comparison of G' of RBC suspensions in plasma and also Ringer/albumin solution at 50 and 80% hematocrits. The higher elastic modulus of the RBCs in plasma can be explained as being due to the addition of the elasticity of the rouleaux formations.

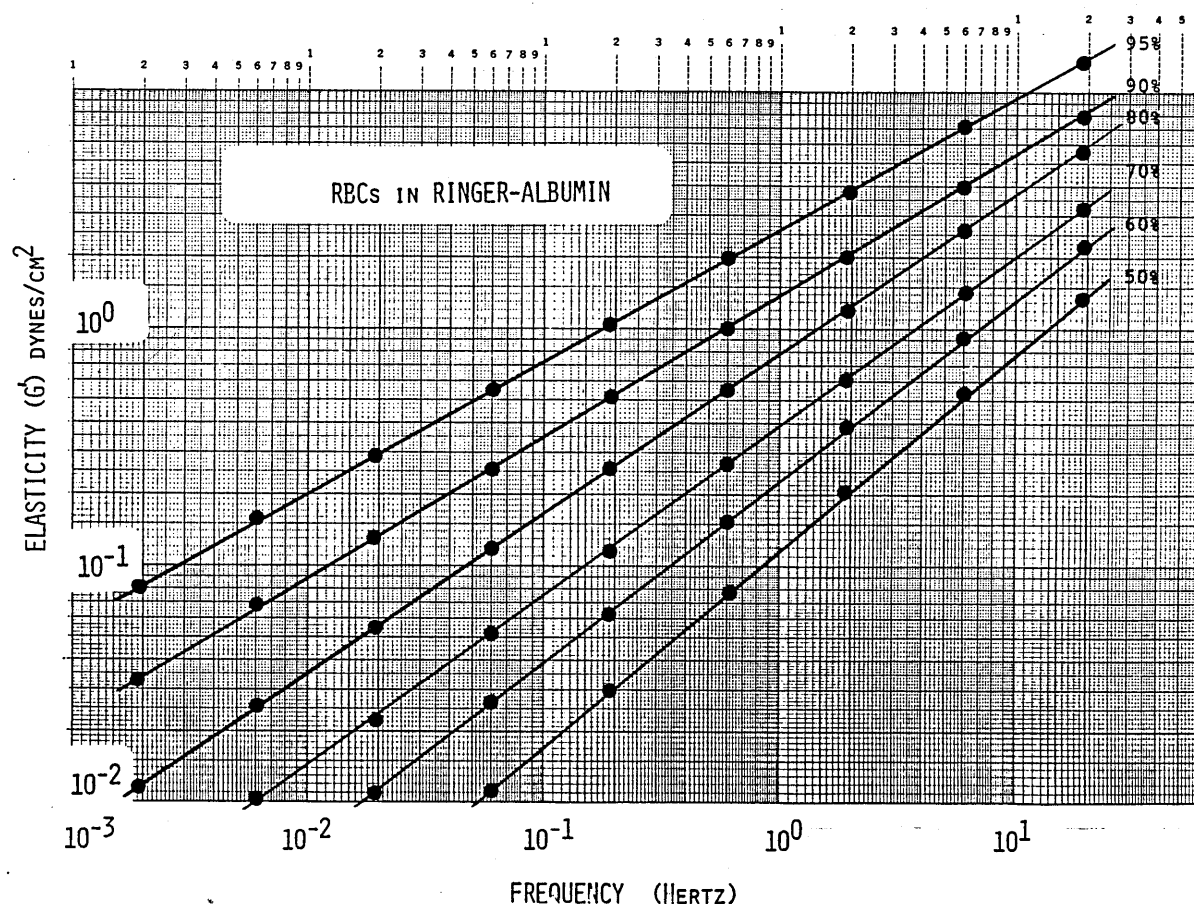


Figure 17. Elasticity (G') versus frequency in oscillatory shear of suspensions of RBCs in Ringer-albumin solution at hematocrits from 50 to 95%, showing the effect on the elastic modulus of

If the difference between the two curves is attributed to aggregation and rouleaux formation, then their contribution to G' can be differentiated by subtracting the values obtained with the Ringer-albumin preparations, from the values of the RBC in plasma preparations. Figure 21 shows the contribution to G' of these rouleaux formations at the various hematocrits measured. It can be seen that as the frequency is increased, the contribution of the rouleaux formations decrease as they are progressively broken down by the increasing frequency. It can be said therefore, that the values of G' shown in Figure 17 are derived from the red cell itself.

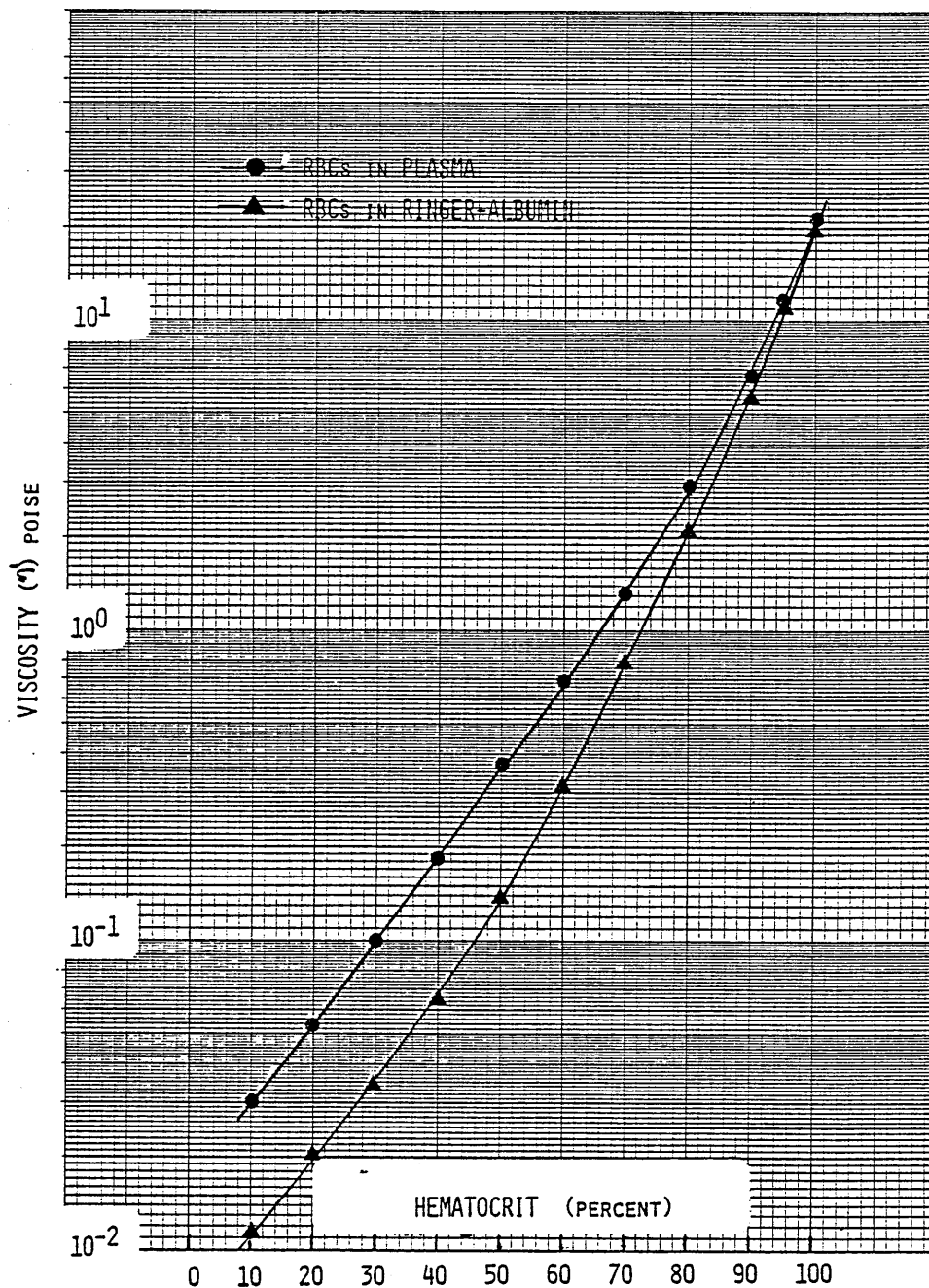


Figure 18. Viscosity (η) versus hematocrit of RBCs in plasma compared with RBCs in Ringer-albumin measured at 0.01 Hertz.

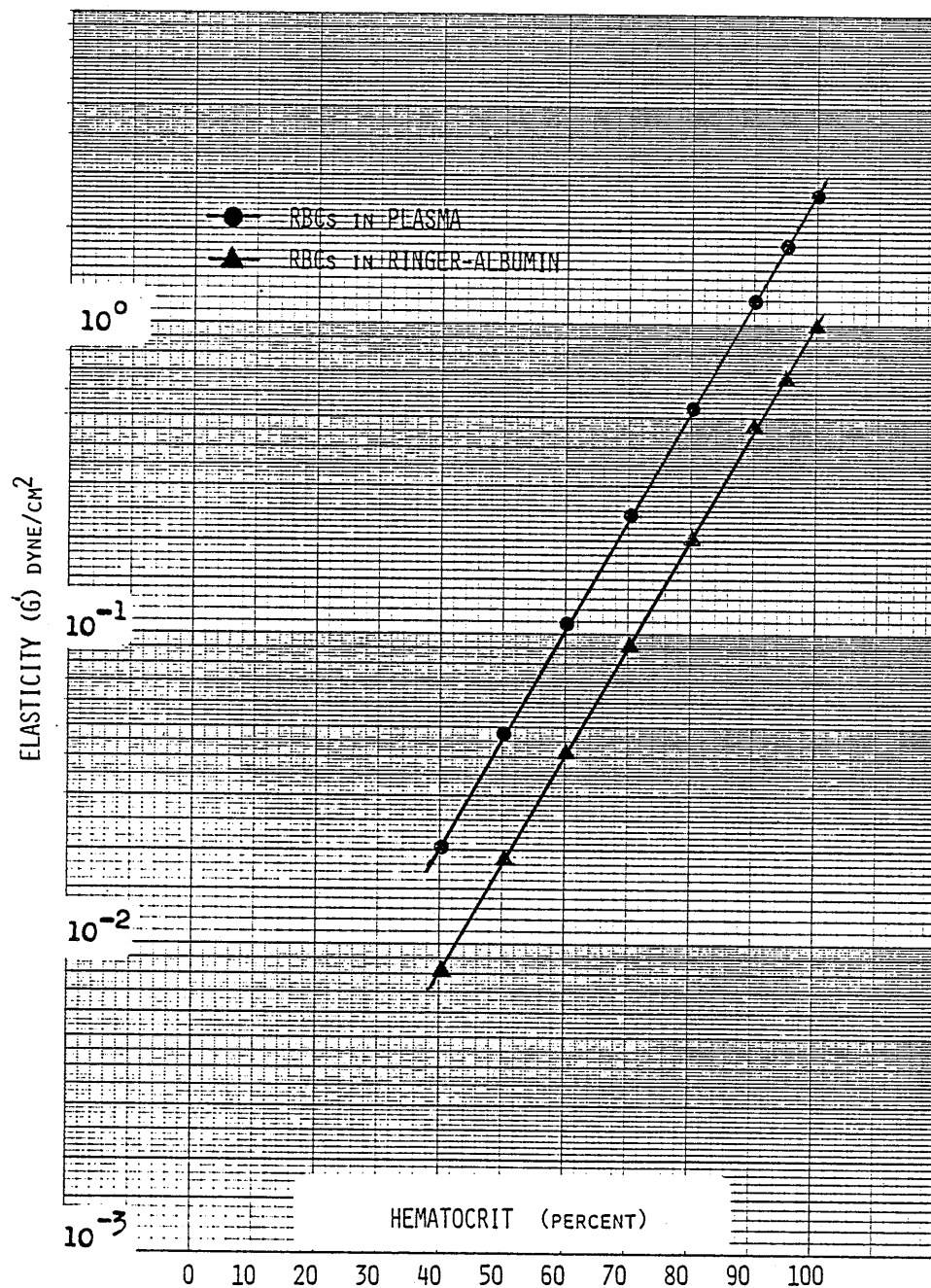


Figure 19. Elasticity (G') versus hematocrit of RBCs in plasma compared with RBCs in Ringer-albumin measured at 0.1 Hertz.

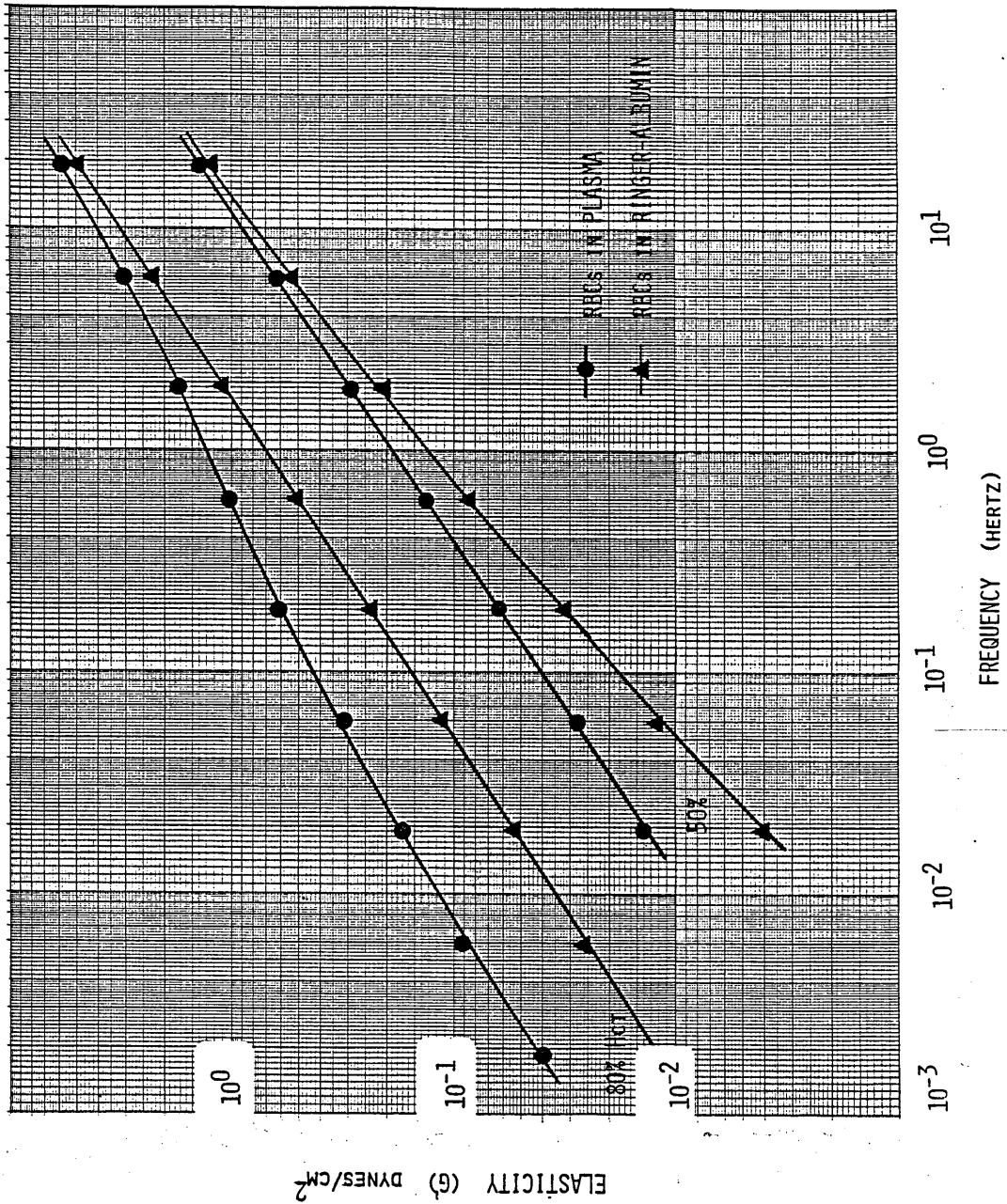


Figure 20. Elasticity (G) versus frequency of RBCs in plasma compared with RBCs resuspended in Ringer-albumin solution at 50 and 80 per cent hematocrit.

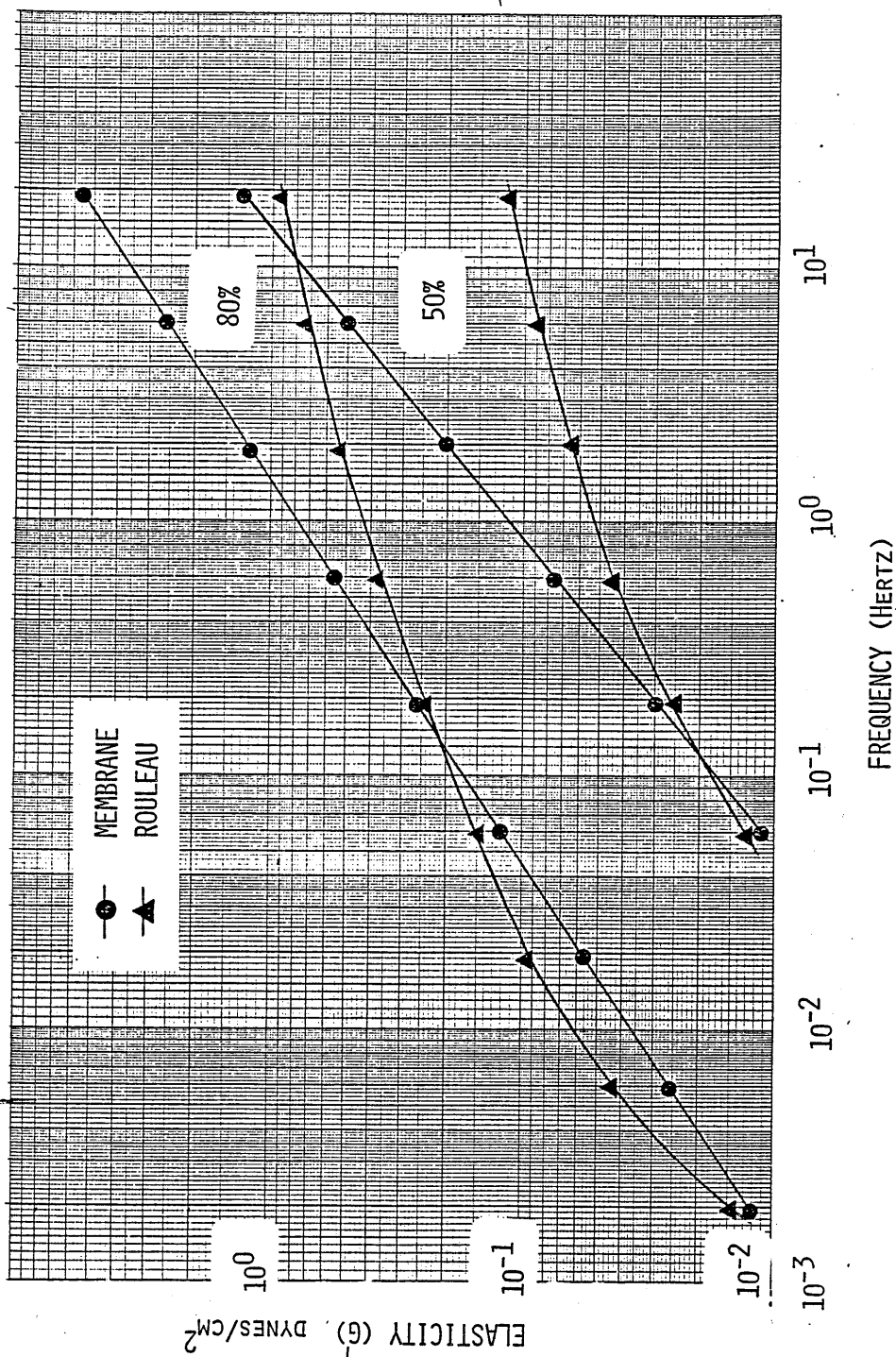


Figure 21. Elasticity (G') versus frequency, of suspensions of RBCs in plasma at 50 and 80% hematocrits, showing the separate contributions of rouleau formation and the red cell to the elastic component.

The measurement of dynamic viscosity (η') and dynamic elasticity of (G') of red cells in plasma using pulsatile flow.

Measurements of η' and G' were made of RBCs re-suspended in plasma in pulsatile flow. The range of frequencies employed was from 0.0006 to 19 Hertz, while steady shear, at a rate of 0.1, 1.0 and 10.0 sec^{-1} , was superimposed on the oscillatory flow.

Figure 22 is a typical plot of the calculated dynamic viscosity of a preparation of 80% red cells in plasma versus frequency. The highest viscosity was found when no superimposed steady flow was applied. As increasing rates of steady flow are superimposed, the viscosity at the low frequencies was reduced considerably, indicating that the superimposed shear alters the state of the blood sample, probably by breaking up rouleau formations. Above a frequency of 2 Hertz the applied steady shear had little or no influence on the viscosity, which is probably because the oscillatory shear stress at this frequency is already high enough to break down the rouleau formation.

Figure 23 is a plot of the dynamic elasticity (G') versus frequency of the same preparation. Again the highest value is measured when no superimposed steady shear is applied. As the superimposed steady shear is increased, G' is progressively reduced, reflecting the change in the extent of rouleau formation.

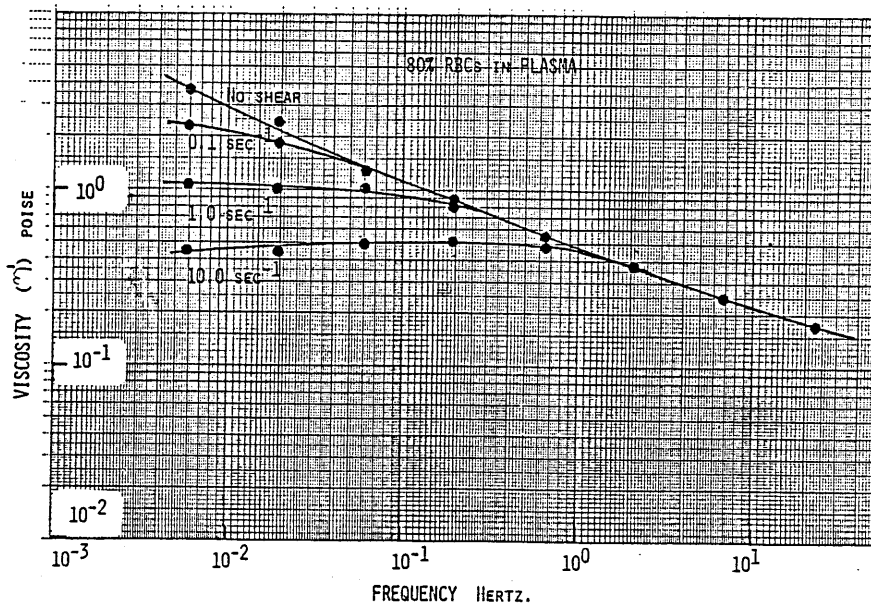


Figure 22. Viscosity (η') versus frequency, of a suspension of 80 per cent RBCs in plasma, showing the change in viscosity when steady shear at 0.1, 1.0 and 10.0 sec^{-1} is superimposed on the oscillatory motion.

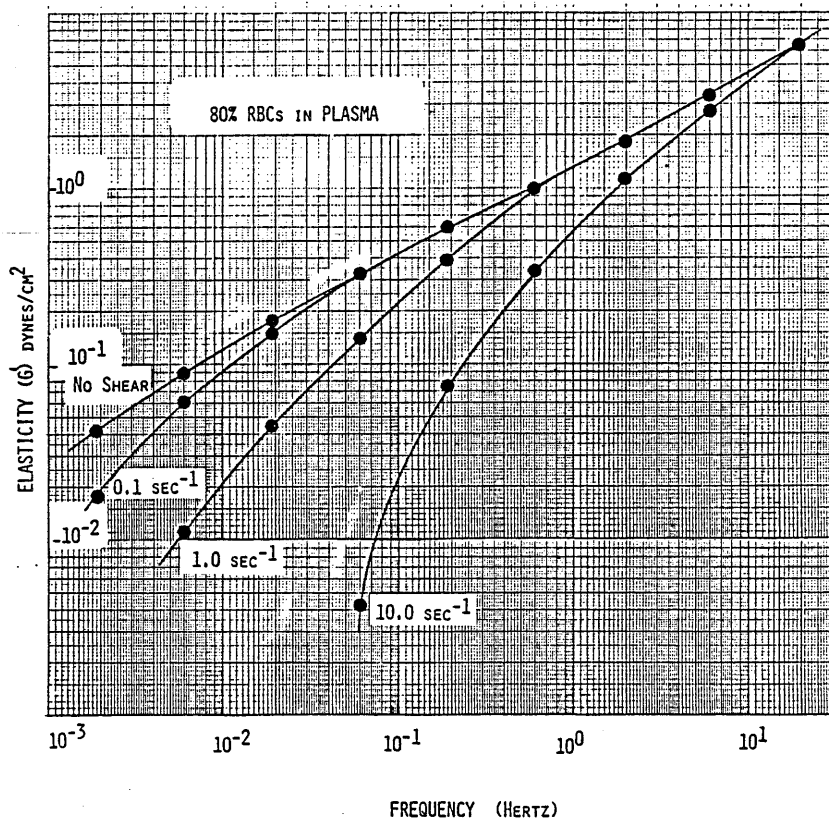


Figure 23. Dynamic elasticity (G') versus frequency of a suspension of 80 per cent RBCs in plasma, showing the effect on the elastic modulus when steady shear at 0.1, 1.0 and 10.0 sec^{-1} is superimposed.

The rheology of non-anticoagulated whole blood

Introduction

When drawn into a glass container, whole blood will quickly clot unless anticoagulants are added. The clotting process is initiated by the contact of certain enzyme factors in the blood with a surface that is different from the normal vascular endothelium. The mechanism of the clotting process has been described in detail by Macfarlane 1964 (25), 1966 (26). The measurement of the clotting time, i.e., the time required for blood to solidify in a glass tube, has long been a diagnostic procedure to detect hematological disorders. A more sophisticated method of monitoring clotting abnormalities is by the use of an instrument known as a "Thrombelastograph". This instrumental method has been extensively described by Hartert and others (27-75). The Thrombelastograph is a Viscometer that uses a concentric cylinder measuring geometry and the outer cylinder is oscillated slowly at a large amplitude about its axis, while the inner cylinder is constrained by a torsion wire. A mirror is attached to the inner cylinder, and a light beam is reflected on light sensitized paper. As the blood clots, the movement of the inner cylinder, which increases in amplitude as the clotting process continues, is recorded on a chart, and the clotting profile, (stress v. time) or "Thrombelastogram" is drawn. This instrument does not measure the phase angle between the input and output motions of the

cylinders, so only the complex viscosity (η^*) can be calculated. It does not record a true clotting profile, as the shear rate used is large enough to accelerate the clotting process.

Extensive use of the Thrombelastograph has been made for the diagnoses of clotting disorders. Marchal et al. 1962 (76), has prepared an "Atlas de Thrombodynamographie" which describes the changing shape a thrombelastogram can take in various clotting disorders, and offers diagnoses to fit the profiles encountered.

Dintenfass 1966 (77, 78, 79), has used his cone in cone viscometer or "Thromboviscometer" to follow the clotting process in a similar manner. He used a large input amplitude (220° peak to peak) and comparatively

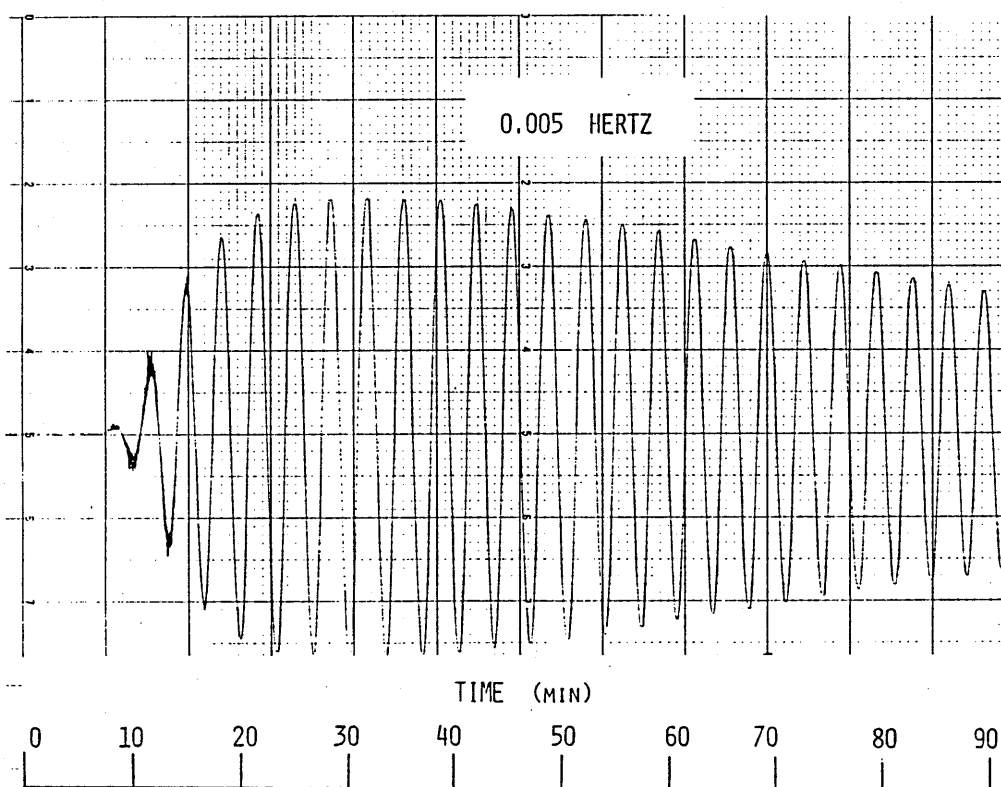


Figure 24. A typical recorder trace at 0.005 Hertz of stress versus time, showing the development of a clot of non-anticoagulated healthy blood of 44% hematocrit.

high frequencies of oscillation, from 1.6 to 230 Hertz, to obtain a clotting profile. Again the amplitude ratio and phase difference between the input and output motions are not measured, and so the viscosity and the elasticity of the clot are not known. Dintenfass, however, reports that the large amplitude and high frequencies he employed grossly affect the rigidity and structure of the clot and accelerate the rate of the clotting process. This makes his data difficult to interpret.

The Rheogoniometer, on the other hand, has a very wide range of frequencies and input amplitudes available, beginning at 0.0001 Hertz, and 0.0005 radians. The amplitude and phase angle between the cone and plate are measured so that the dynamic viscosity (η') and elasticity (G') can be monitored continuously with time.

Experimental method and measurements

A small input amplitude of 0.0005 radians and a frequency of oscillation of .005 Hertz was chosen to follow the clotting process and also to determine the dynamic viscosity (η') and dynamic elasticity (G') of the growing clot with time. The small amplitude and low frequency chosen was found to cause no disturbance to the natural rate of the clotting process.

Blood was drawn from healthy donors and fed directly by a plastic tube to the cone and plate geometry of the rheogoniometer which is already set in motion. The input and output sine wave signals were fed on line to the PDP 11/10 computer which measures the amplitude ratio and phase angle between the signals. Figure 24 shows a

typical clotting profile measured by the rheogoniometer, of a blood sample of 44% hematocrit. After 10 minutes elapsed time the output amplitude begins to increase, reaching a plateau in about 30 minutes. Figure 25 is a plot of the amplitude ratio between the input and output motions of the cone and plate versus time. Figure 26 is a plot of the phase angle between the input motion and

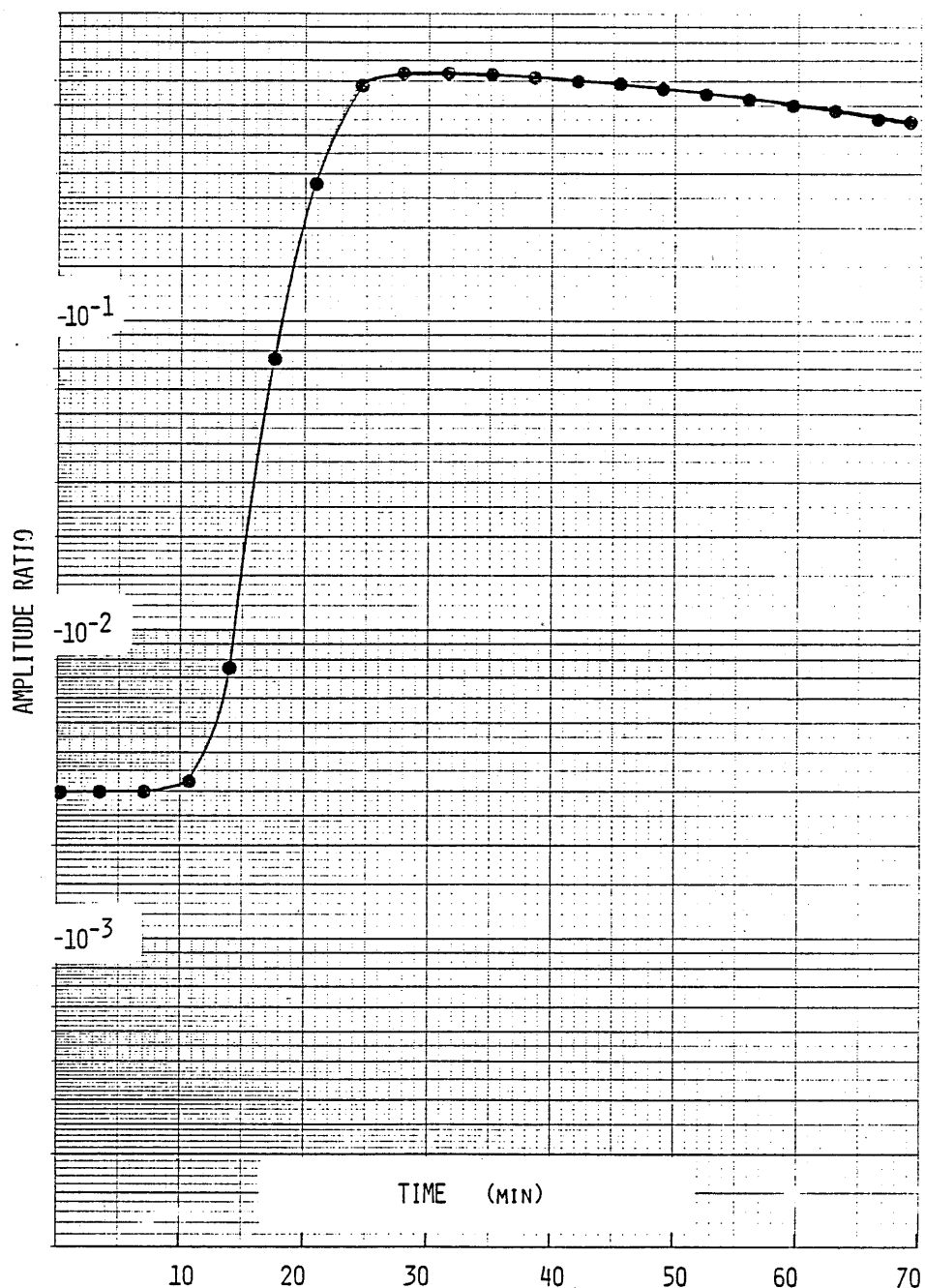


Figure 25. The amplitude ratio (θ'/θ'') versus time at 0.005 Hertz, of non-anticoagulated healthy blood of 44% hematocrit.

output stress of the torsion head. The phase angle during the first few minutes of the experiment is similar to that found with anticoagulated blood when of the same hematocrit. The phase angle changes as the clotting process continues, until the two sine waves are in phase, or the phase angle between them is zero. This indicates

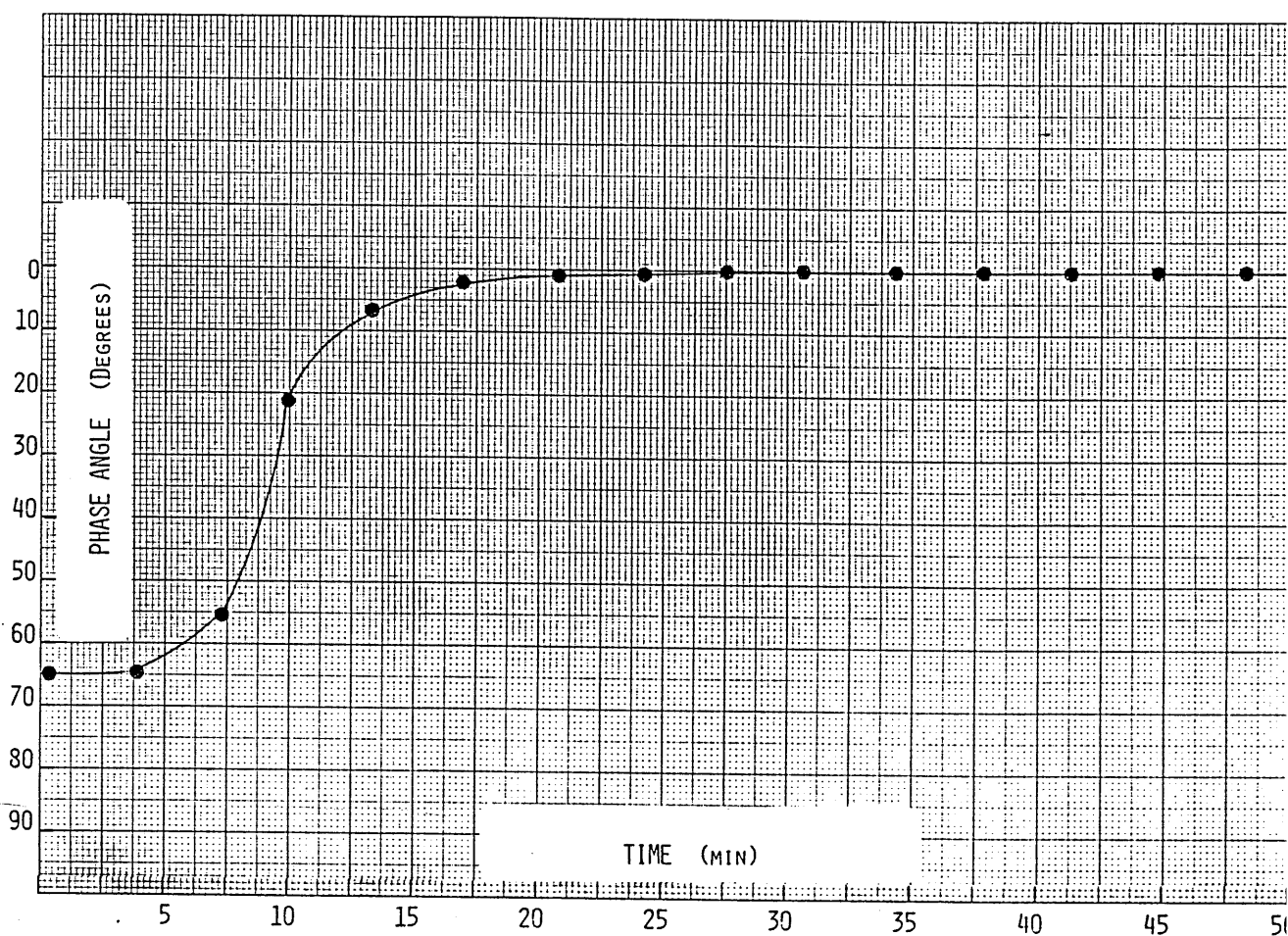


Figure 26. The phase angle versus time of a non-anticoagulated healthy blood sample measured at 0.005 Hertz.

that the clot has become a crosslinked gel and is completely elastic. All the input strain is stored in the first half cycle, and is recovered in the next, and none is lost as heat. There is, therefore, no "loss modulus" (viscosity), and only the "storage modulus" (elasticity) can be calculated.

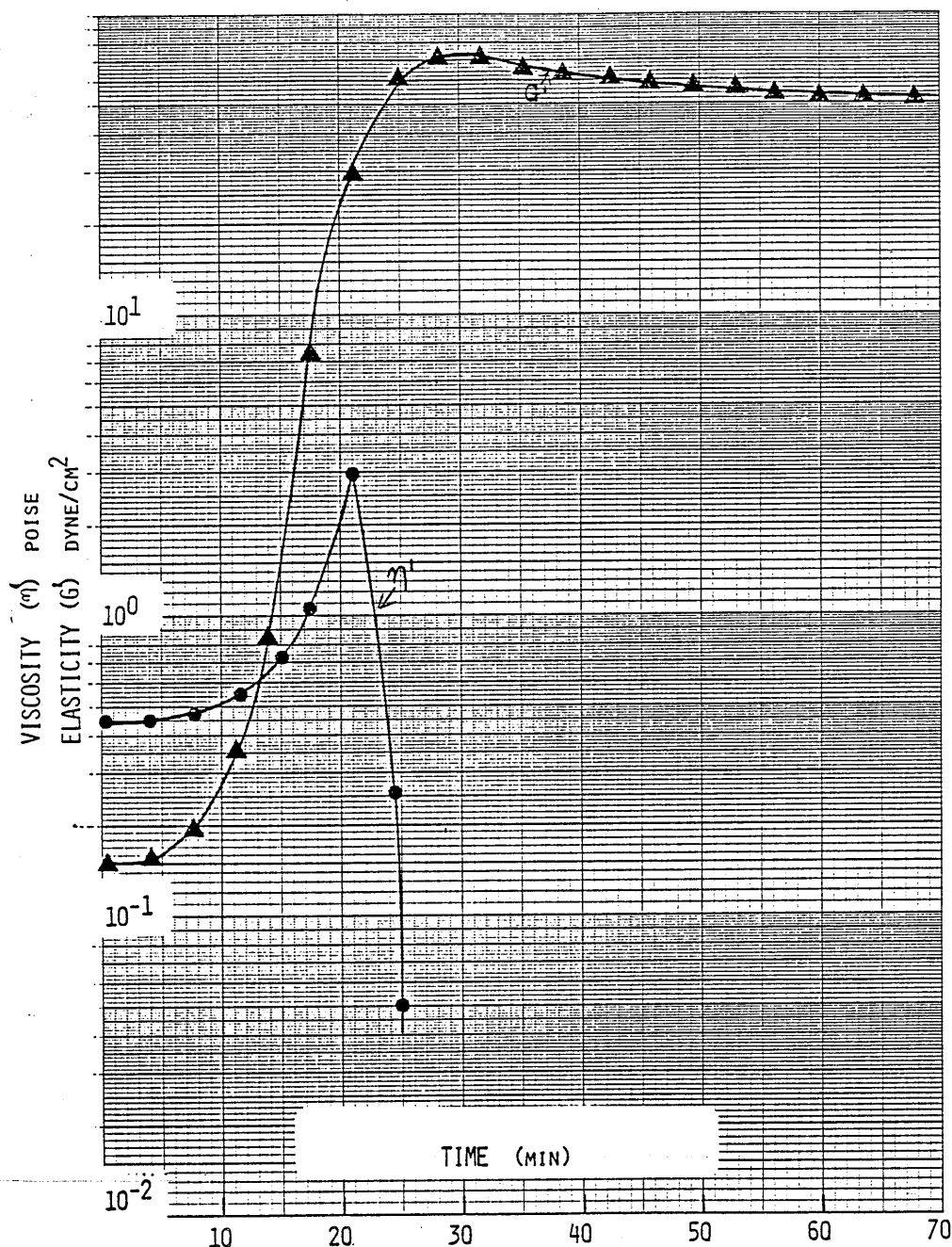


Figure 27. The dynamic viscosity (η')—●— and elasticity (G') —▲— versus time of non-anticoagulated healthy human blood at 44% hematocrit.

Figure 27 is a plot of the viscosity and elasticity of a non-anticoagulated blood sample of 44% hematocrit versus time, measured at a frequency of 0.005 Hertz. The viscosity and elasticity increase sharply at about 10 minutes elapsed time from blood withdrawal. The viscosity continues to increase for 20 minutes and then drops as the phase angle nears zero. The elastic modulus increases and reaches a peak at 30 minutes. Thereafter,

the clot retraction process commences and the elastic modulus drops gradually.

The techniques of measuring the viscosity and elasticity as well as the clotting profile, using the Rheogoniometer is considered to be an improved method when compared to the Thrombelastograph of Hartert, or the Thromboviscometer of Dintenfass. The small amplitudes and frequencies employed do not interfere with the natural clotting process and the measurement of viscosity and elasticity of the clot will allow the more subtle differences, such as variations in the ratios of η' and G' , to be seen, which may give a more definitive evaluation of clotting abnormalities.

CHAPTER IV.

THE RHEOLOGICAL CHARACTERISTICS OF ABNORMAL BLOODS.

Introduction.

An extensive rheological study of blood in diseased conditions has been reported by Dintenfass, 1971 (2). Whitmore 1968 (1), discusses the possible implications of abnormal blood and blood components on the rheology of the circulation. These rheological abnormalities may be severe, as in sickle cell disease, or leukemia, or more subtle, as in hypertension.

Time does not permit in this study, a wide ranging investigation of the rheological abnormalities that may be present in all diseases. There are still many gaps in the knowledge of these parameters still to be filled. However, measurements have been made in this study of the rheological abnormalities that are found in suspensions of artificially deformed red cells in buffer solutions of different osmolarities, and in the blood of persons suffering from sickle cell disease and leukemia. The rheological abnormalities found are reported in this chapter.

The effect of changing tonicity on the rheology of 80% red cells suspended in Na Cl solutions

Below normal osmolarity (300 mOsm) the red cell will gain water and the cell will swell. This has the effect of reducing the concentration of the hemoglobin contents, which will render the cell more deformable. With very low tonicity, the red cell will eventually hemolyse.

Hypertonic osmolarities above 300 mOsm will cause the red cell to shrink, and it may assume crenated form. Figures 1 and 2 are scanning electron micrographs showing red cells in this condition. The shrinkage of the red cell will increase the concentration of hemoglobin and cause the viscosity and elasticity to increase.

Experimental Method

Normal red cells were washed three times in Tris-Ringer-albumin solution, the buffy coat was removed and the cells were resuspended in buffered NaCl solutions. The hematocrit was adjusted to 80% for each osmolarity value prepared. The viscosity (η') and elasticity (G') of these preparations were measured using the Rheogoniometer in the oscillatory mode. Figure 3 is a plot of viscosity (η') versus osmolarity of 80% RBCs in buffered NaCl solutions at frequencies of 0.006, 0.06, and 0.6 Hertz. As osmolarity increases, η' increased by a factor of 10. At higher frequencies the slope of η' versus osmolarity is reduced. Figure 4 is a plot of elasticity (G') versus osmolarity at three different frequencies. The G' is also increased by a factor of 10, reflecting the increased rigidity of the red cells and the increased concentration of the red cell contents.

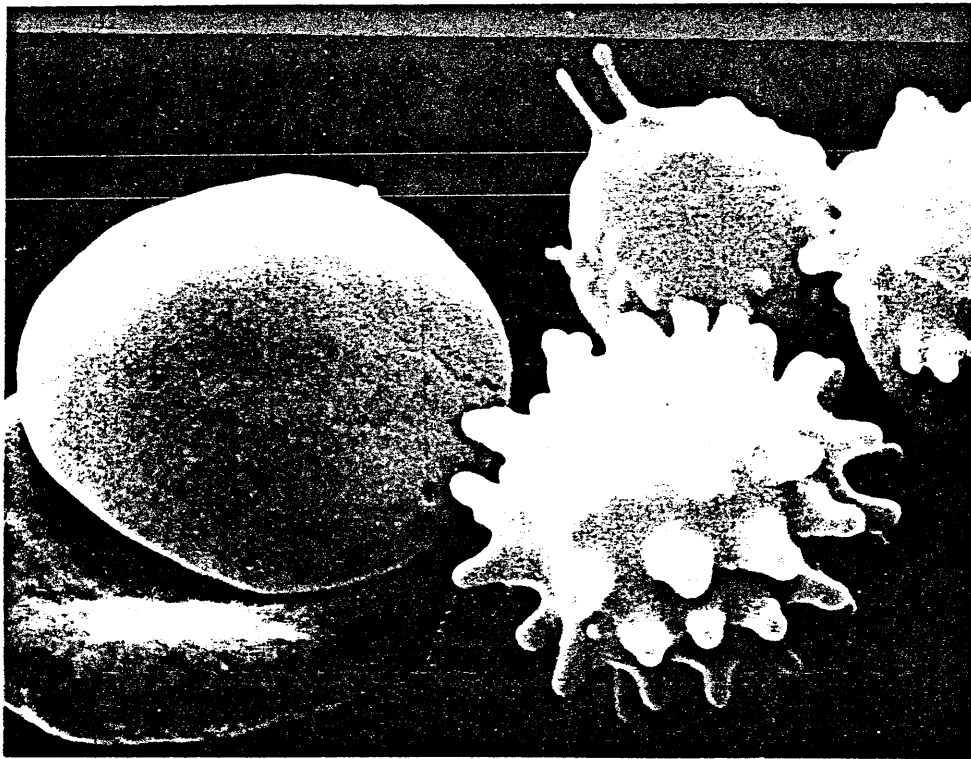


Figure 1. A scanning electron micrograph showing a red cell in crenated form, (lower right).

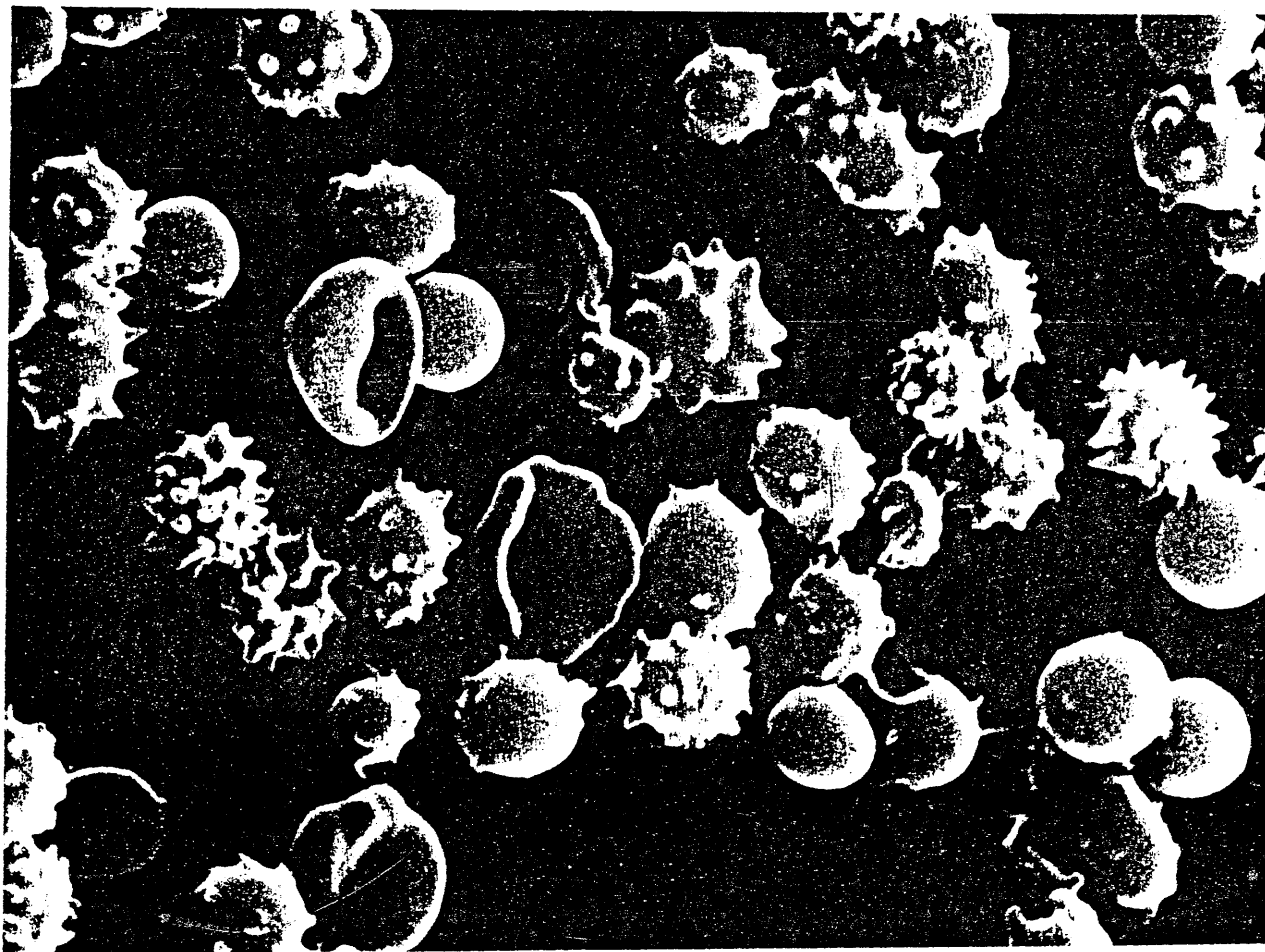


Figure 2. A scanning electron micrograph showing many red cells in crenated form.

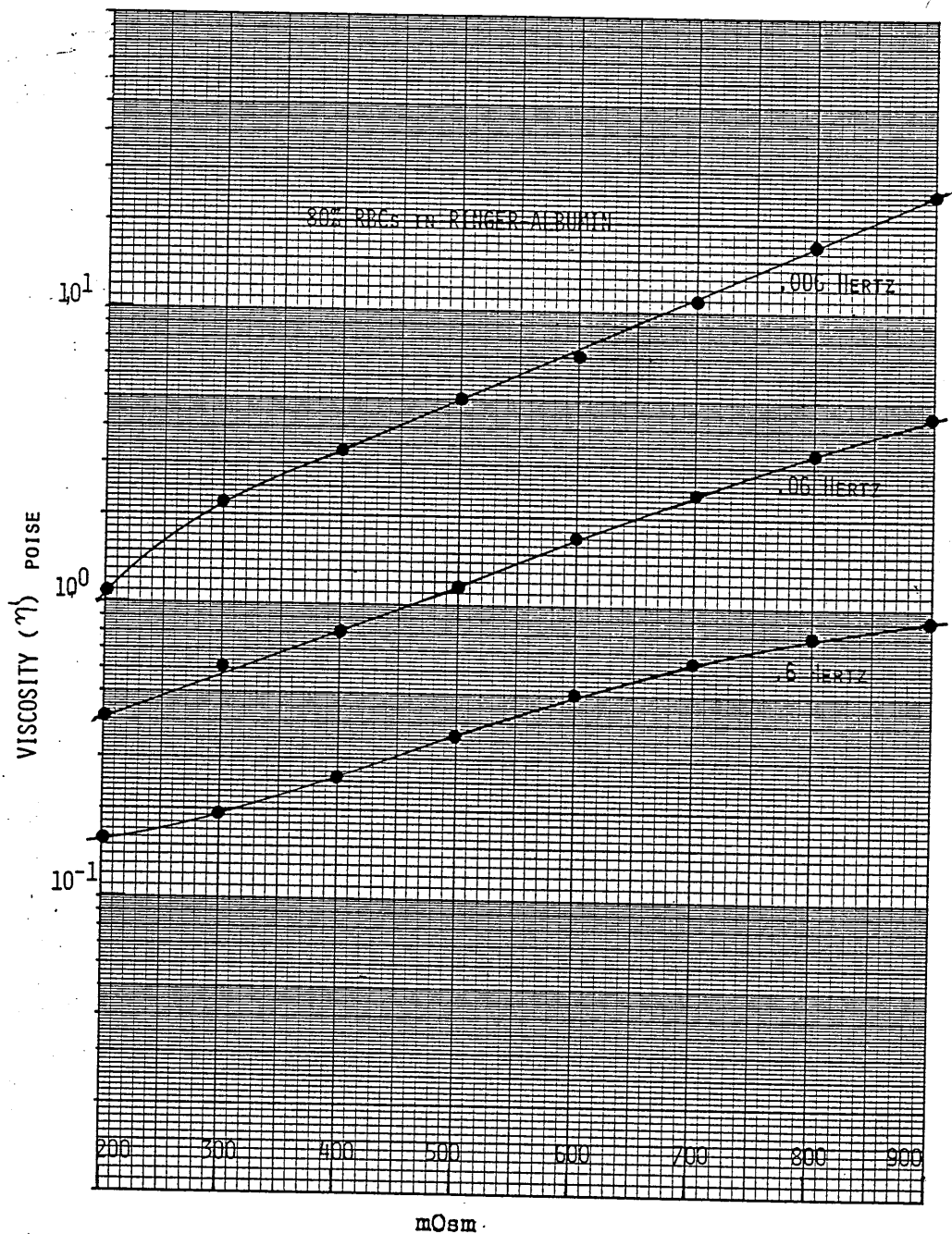


Figure 3. A plot of Viscosity (η) versus Osmolarity of percent RBCs in Ringer-albumin solution showing the effect of changing osmolarity and frequency.

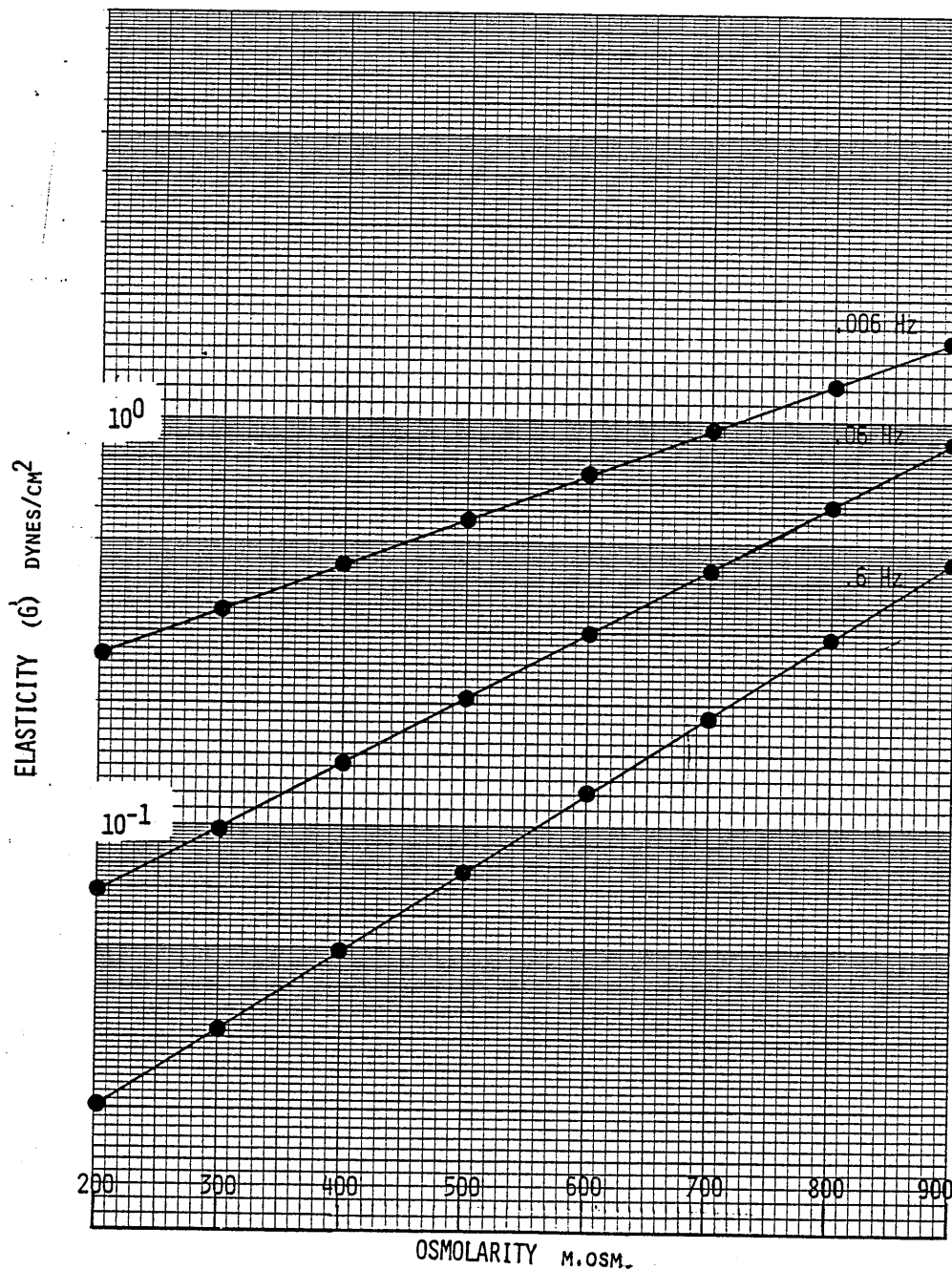


Figure 4. Elasticity (G') versus Osmolarity of 80 per cent RBCs in Ringer-albumin solution showing the effect on the elastic modulus of changing osmolarity and frequency.

The effects of deoxygenation on the viscoelastic properties of sickle cell RBCs in suspension and sickle hemoglobin

The pathophysiological manifestations in sickle cell disease are caused by the change in rheological behavior of the HbSS red cells as the normal deoxygenation process occurs during their travel through the circulation. When the HbSS cell is fully oxygenated, it behaves similarly to the normal HbAA red cell and most of the HbSS cells have the usual discoid shape. Chien et. al. 1970 (1). Deoxygenation of the HbS molecules causes them to crosslink into a rod like structure and the red cell membrane distorts into an elongated crescent or sickle shape and becomes inflexible, White et. al. 1963 (4). Figure 5 is a scanning electron micrograph of a tethered sickled red cell showing this crescent form and Figure 6 shows deoxygenated hemoglobin molecules aggregated together in typical rod like structures.

The normal red cell is readily deformable and is capable of moving through the narrow channels of the microcirculation that are much smaller than its own diameter, Cokelet et. al. 1968 (5). The deoxygenated red cell in sickle cell disease, however, is less deformable, as a result, these cells have a longer transit time in some blood vessels, and hence more oxygen is extracted from each cell, causing a vicious cycle. The cell in this case may not pass through the smaller blood vessels at all. This causes the surrounding tissues to become



Figure 5. A scanning electron micrograph of a sickled red cell showing the typical crescent form.

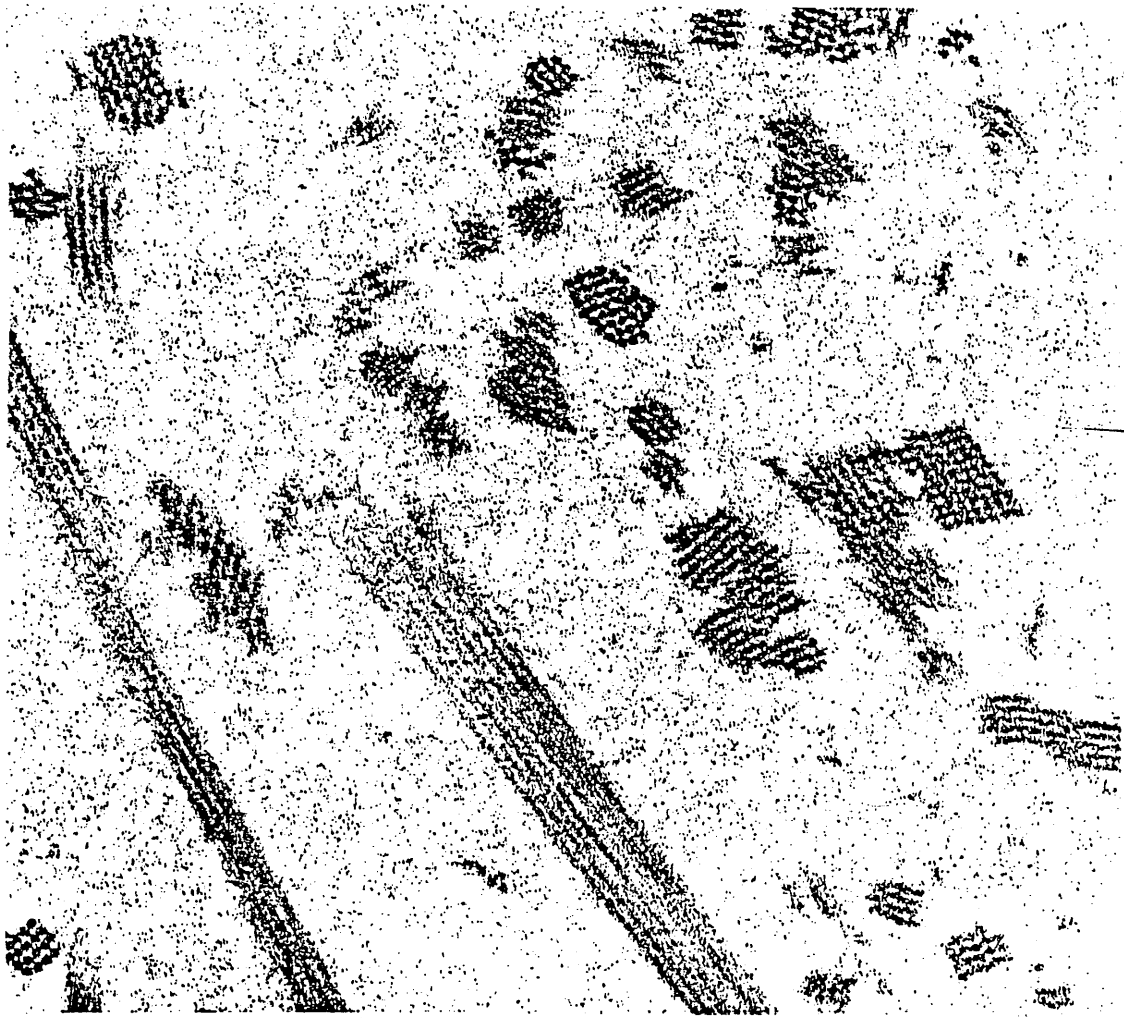


Figure 6. A scanning electronmicrograph of deoxygenated hemoglobin showing aggregated Hb molecules in typical rod-like structures.

starved of nutrients and oxygen, and the pathophysiological signs and symptoms of sickle cell disease then results.

This study was performed to characterize the effects of controlled deoxygenation on the viscoelastic behavior of packed HbSS red cells and also HbS solutions measured under oscillatory shear, and to investigate the feasibility of correlation between the rheological properties of the HbSS RBCs and the onset of crises in sickle cell disease.

The Rheogoniometer was fitted with a cone and plate geometry (Chapter II, Page 18 Figure 5) of 7 cm. diameter with a $\frac{1}{2}^\circ$ cone angle which was used in the oscillatory mode. An "I" beam form torsion with a constant (Kt) of 5.0 dynes.cm/micron was used.

The sample temperature was maintained at 37°C.

Blood samples were drawn from the antecubital vein of normal human subjects (AA) and patients with SS disease, with EDTA used as an anticoagulant. The blood samples were centrifuged to remove the buffy coat, and the red blood cells (RBCs) were washed and suspended in buffered Ringer/albumin solution to yield the desired cell concentration. The Ringer/albumin solution contained 0.5 percent human serum albumin and 25 mEq/l HCO_3^- . RBCs suspended in plasma can undergo aggregation at low shear conditions owing to intercellular bridging by fibrinogen and globulins, Fahraeus 1929; Chien 1975, (6,7), whereas RBCs suspended in Ringer/albumin solution remain dispersed at all shearing conditions, Chien 1975 (8).

For the preparation of hemoglobin solution, the RBCs were washed three times with the Ringer solution (no albumin). The packed cells were lysed by vigorous shaking in a vortex mixer following the addition of glass beads and toluene. After the centrifugal removal of the supernatant toluene and membrane debris, the hemoglobin solution was transferred to centrifuge tubes with the aid of toluene washing and centrifuged at 25,000 r.p.m. for 30 min at 5°C. After the removal of the remaining toluene and any residual membrane debris, the lysate solution of hemoglobin was used for viscosity measurements.

A rotary-type tonometer was used for the control of gas tensions, Usami et.al. 1975 (6). The CO_2 concentration in the gas mixture for tonometry of RBC suspensions was kept at 5.6 percent. The percentages of O_2 and N_2 in the gas mixture were varied to obtain various levels of $p\text{O}_2$. The values of $p\text{O}_2$, $p\text{CO}_2$ and pH of the samples were determined with the use of a blood gas analyzer system (Model 213, Instrumentation Laboratories, Lexington, MA) thermostated at 37°C . Oxygen saturation was determined with the use of an Instrumentation Laboratory Co-oximeter (IL-182). The equilibrated sample was anaerobically transferred into the viscometer. The measurement of gas tensions of cell suspensions and hemoglobin solutions after viscometry yielded results which agreed well with the values obtained before viscometry.

The hematocrit (Hct) of the red cell suspensions was determined by centrifugation at 15,000 g for 5 min in a microcentrifuge and corrected for fluid trapping as determined by an ^{125}I -albumin dilution-technique, Chien et al 1965 (9). The cyanmethemoglobin method was employed for the measurement of hemoglobin concentration (Hb). MCHC was calculated from Hb/Hct .

The measurement of viscosity

Oscillatory studies were performed at 0.01 Hertz on concentrated cell suspensions with a hematocrit of 90 percent, in which there was relatively little suspending medium. The dynamic viscosity (η') of AA cell suspensions was independent of O_2 saturation, whereas the η' of SS cell suspensions was strongly dependent on O_2 saturation.

When fully oxygenated, η' of SS cell suspensions was only slightly higher than that of AA cell suspensions, but at 35 percent O_2 saturation, the η' of SS cell suspensions was almost 10 times higher than that of AA cell suspensions. This is shown in Figure 7. Figure 8 shows the effect of deoxygenation on the dynamic elasticity (G'), of AA and SS RBCs suspended in Ringer/albumin solution at 90 percent Hct measured at 0.01 Hertz. The elastic modulus of the SS cells is also very sensitive to deoxygenation, and G' increases rapidly below an O_2 saturation of

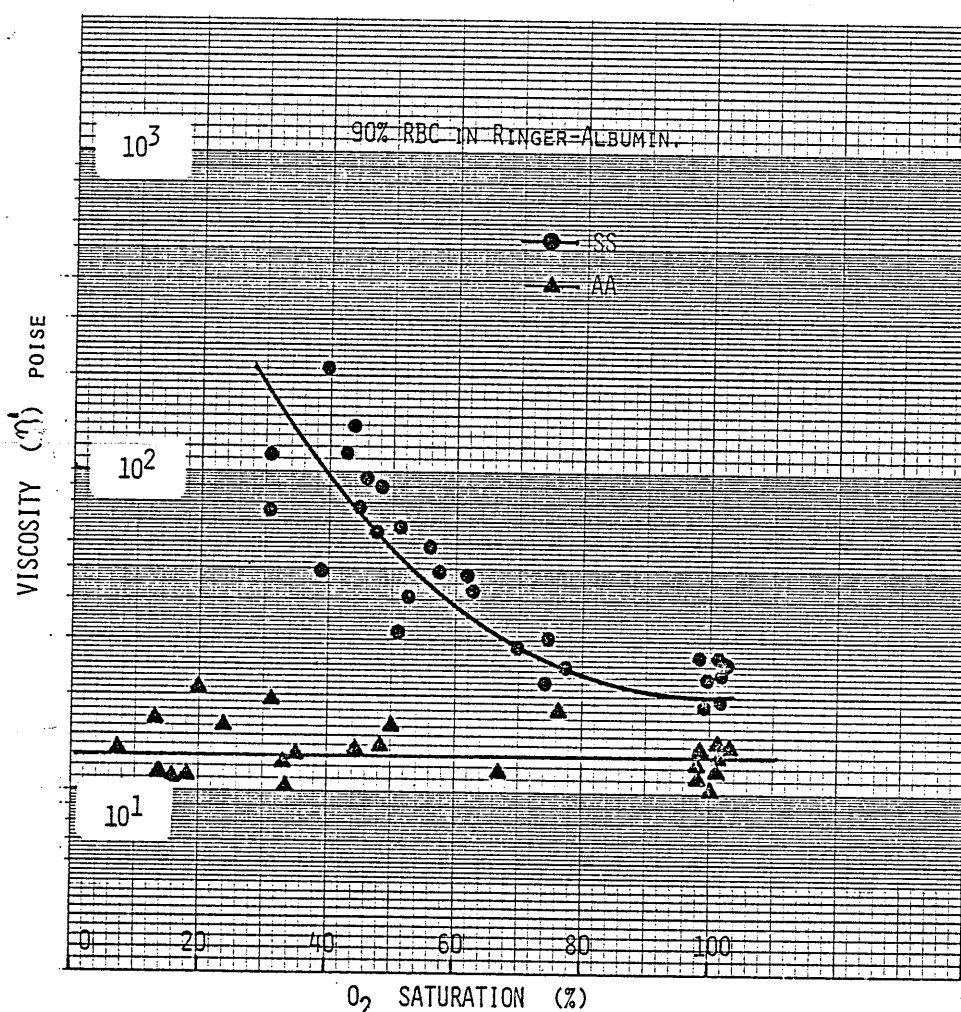


Figure 7. The viscosity (η') of SS and AA cell suspensions in Ringer-albumin at a concentration of 90 percent as a function of O_2 saturation. Data were obtained at a frequency of 0.01 Hertz.

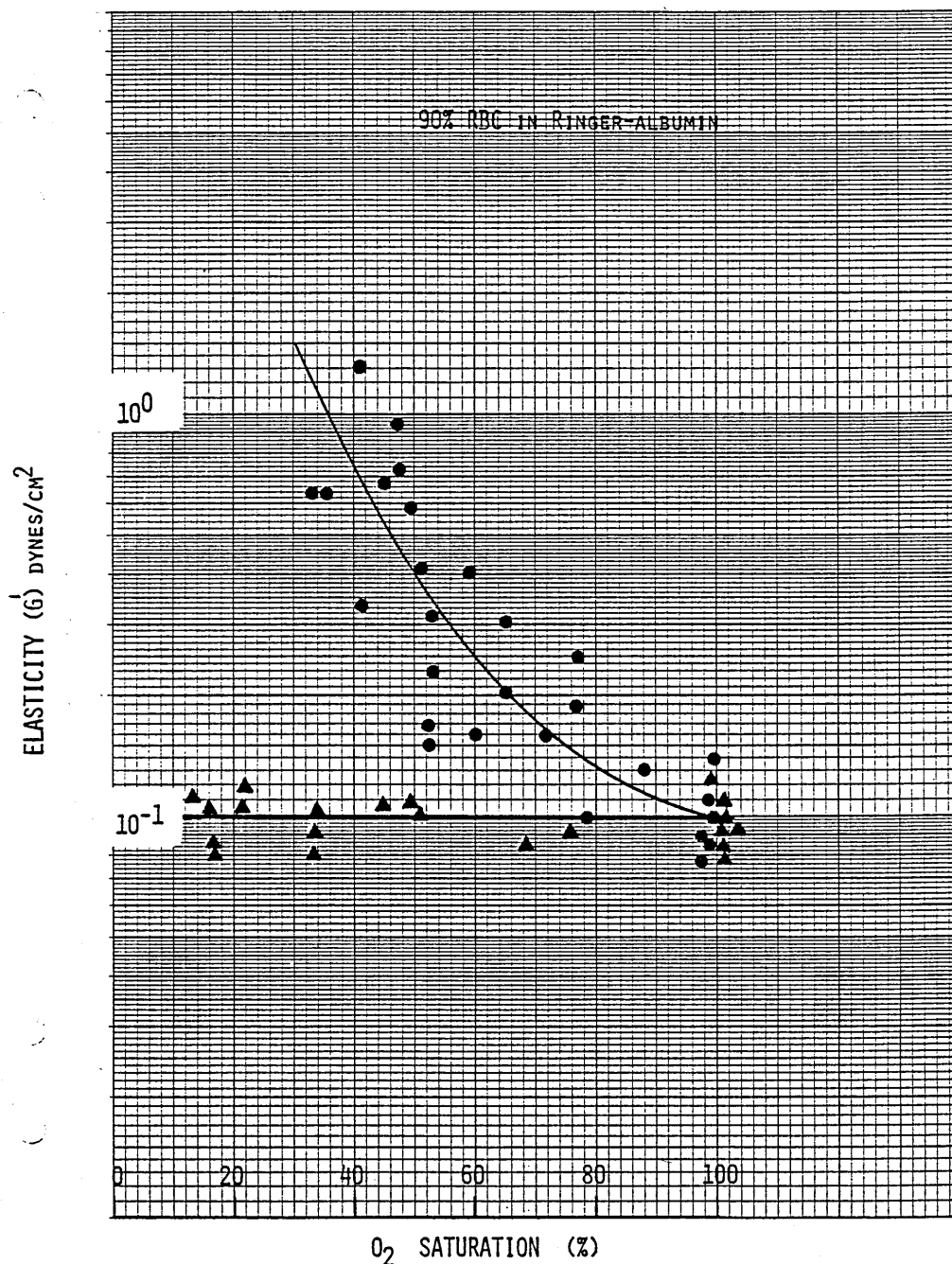


Figure 8. The dynamic elastic modulus (G') of AA RBCs (\blacktriangle) and SS RBCs (\bullet) versus O_2 saturation measured in oscillatory shear at 0.01 Hertz.

85 percent. Whereas the G' of AA cells is unchanged as the oxygen level is reduced.

Studies on the dynamic viscosity (η') of hemoglobin solutions (HbA and HbS) were performed at a hemoglobin concentration of 32g/dl. When fully oxygenated η' was independent of frequency and there were no significant differences between HbA and HbS solutions.

When O_2 saturation of HbS solution was reduced to below 80 percent, the viscosity began to increase and became frequency dependent. With further reduction in O_2 saturation, η' increased progressively. The effect of O_2 saturation on η' of hemoglobin A and S solutions at a frequency of 0.01 Hertz is shown in Figure 9.

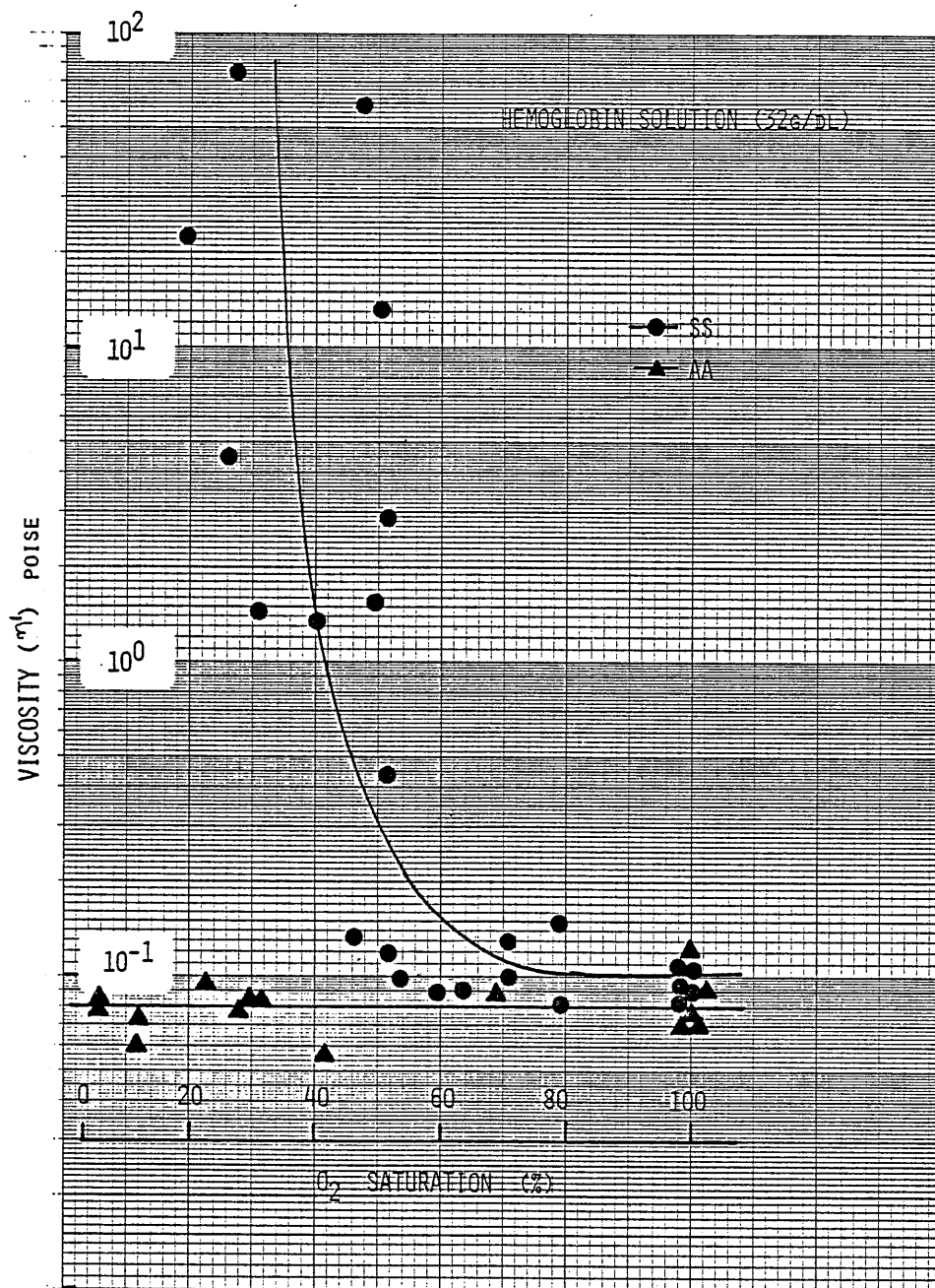


Figure 9. The viscosity (η') of HbS and HbA solutions at a concentration of 32g/dl as a function of O_2 saturation. The data was obtained at a frequency of 0.01 Hertz.

The elastic component (G') was not detectable with either HbA or HbS at 100 percent O_2 saturation. Hemoglobin A had no measurable G' even with decreases in O_2 saturation below 10 percent. Hemoglobin S, however, began to show an elastic component when it was deoxygenated below 80 percent O_2 saturation, and further decreases in O_2 saturation caused steep increases in G' . This is shown in Figure 10.

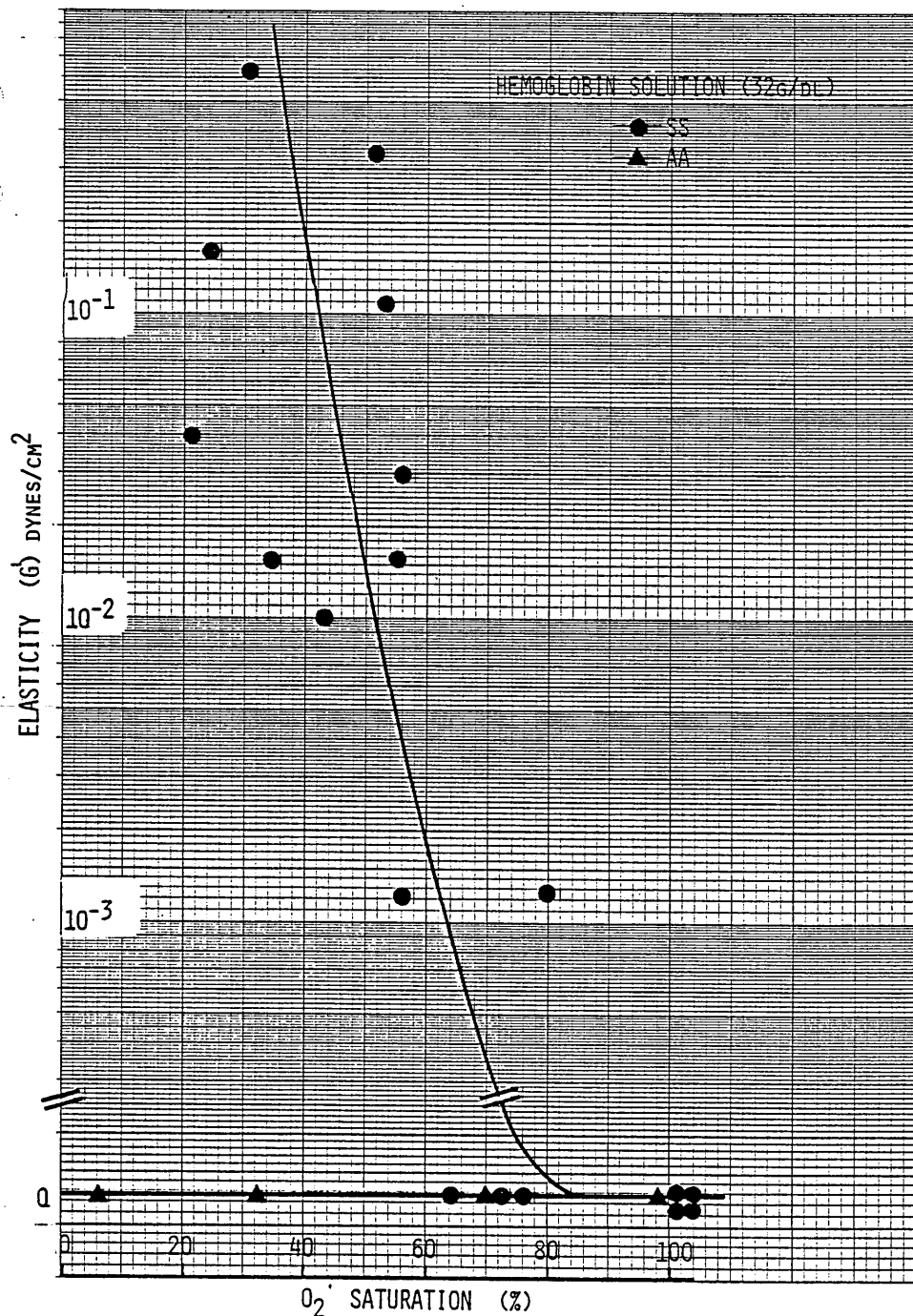


Figure 10. The elasticity (G') of HbS and HbA solutions at a concentration of 32g/dl as a function of O_2 saturation, measured at a frequency of 0.01 Hertz.

Figures 11 and 12 are plots of η' and G' versus O_2 saturation, of 90% SS RBCs, from patients who are in an active stage of the disease exhibiting such complications as maleolar ulcer, pulmonary infection, aseptic necrosis of the femoral head and congestive heart failure, etc. These η' and G' values are compared to those of patients who are in a quiescent stage, with none of these manifestations. Those in an active stage show a considerable increase in both η' and G' . This may cause decreased blood flow in the smaller arteries and capillary veins which would give rise to the pathological conditions described above.

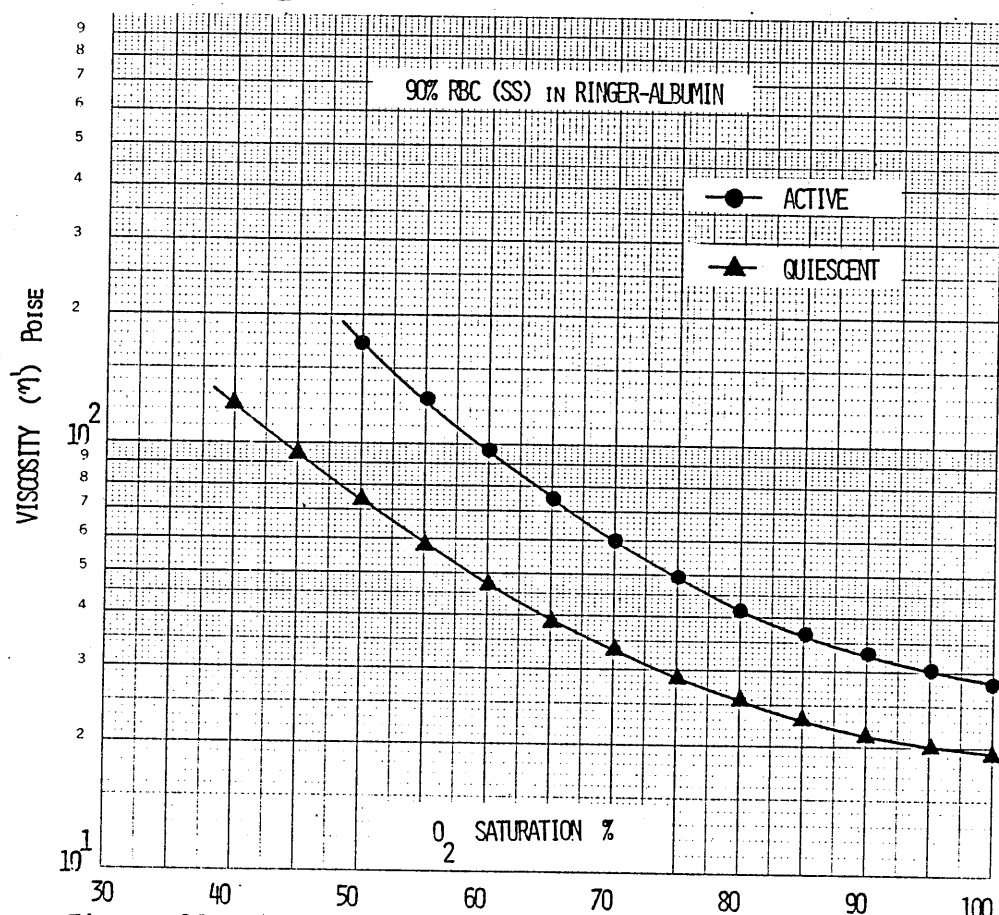


Figure 11. A comparison of viscosity (η') versus O_2 saturation of 90% SS RBCs from sickle cell patients in an active and quiescent phase of the disease.

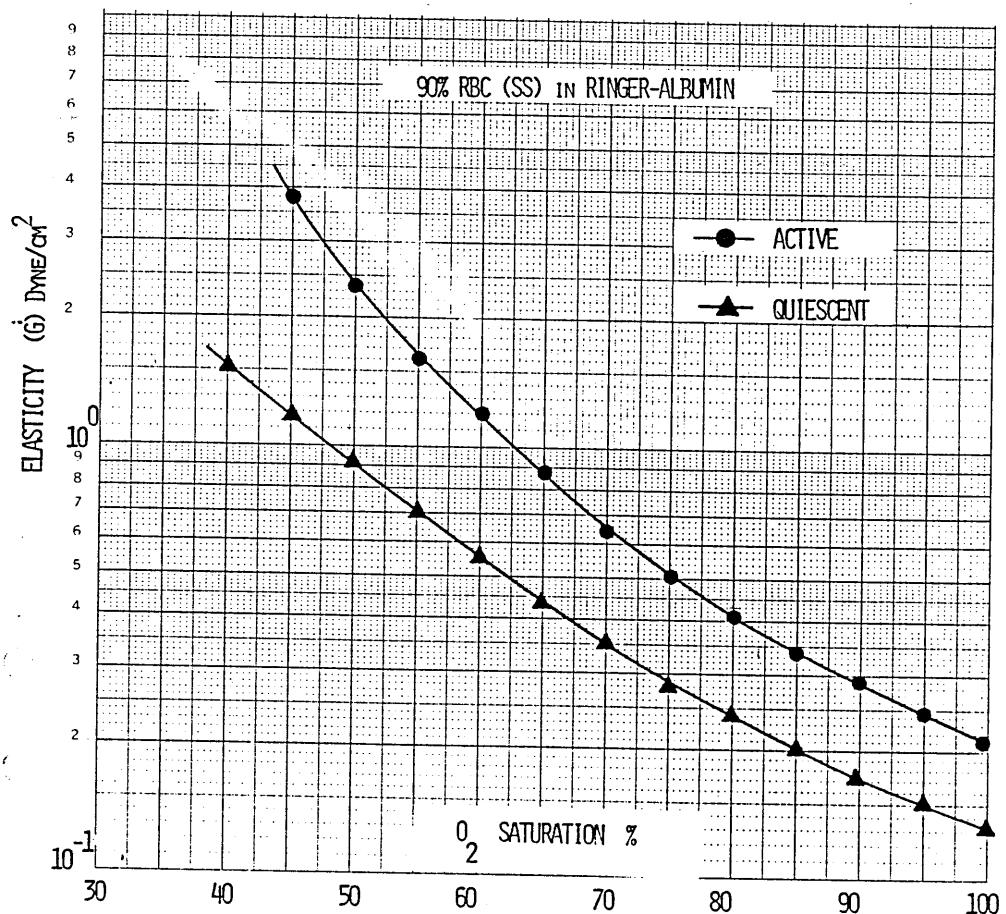


Figure 12. A comparison of the elasticity (G') versus O₂ saturation of 90% SS RBCs from sickle cell patients in an active and quiescent phase of the disease.

Discussion

When fully oxygenated, HbS and HbA solutions at the same concentration have comparable values of η' and G' measured in oscillatory shear. Therefore, the higher η' and G' values for oxygenated SS red cell suspensions when compared to oxygenated AA red cell suspensions cannot be attributable to qualitative differences in oxygenated HbS and HbA, but rather to the higher MCHC in the SS cells. Usami et al. 1975 (8), Chien et al. 1971, (10). At 90 percent hematocrit, the hemoglobin concentration is approximately 31g/dl for AA cell suspensions and 33g/dl for SS cell suspensions. Since oxygenated HbS and HbA solutions had no measurable G' , the G' values in the oxygenated, concentrated SS and AA cell suspensions can be at-

tributable to the cell membrane and the packaging of the hemoglobin solution into cellular units.

Decreases in O_2 saturation to less than 10 percent have no significant effects on the viscosity of HbA solutions and AA red cell suspensions. A decrease in O_2 saturation of HbS solutions below a critical level causes an increase in η' and G' . This critical level of O_2 saturation is strongly dependent on the hemoglobin concentrations, and is 80-85 percent saturation at 30-35g/dl.

Although the critical levels of O_2 saturation at which η' and G' begin to rise are similar for HbS solutions and SS cell suspensions, the magnitude of these curves are not the same. The effects of deoxygenation on viscoelastic properties of HbS solution at 32g/dl and SS cell suspensions at 90 percent hematocrit are compared in Figures 13 and 14. At high levels of oxygenation, the η' of SS cell suspension is 30 times higher than η' of HbS solutions. With progressive deoxygenation, the η' and G' values of HbS solutions increase to approach the corresponding values for the SS cell suspensions. These results indicate that the cell membrane is a major factor in determining the viscoelastic behavior of the cell suspensions. When η' and G' of the internal contents of the red cell, rise as a result of the gelation of HbS following deoxygenation, the gelation becomes the dominating factor determining the viscoelastic behavior of the SS RBC suspensions. The experimental data can be used for theoretical analysis of the relative roles the cell membrane and internal fluid play in the overall rheological behavior of the cell. Therefore, rheological studies on the effects

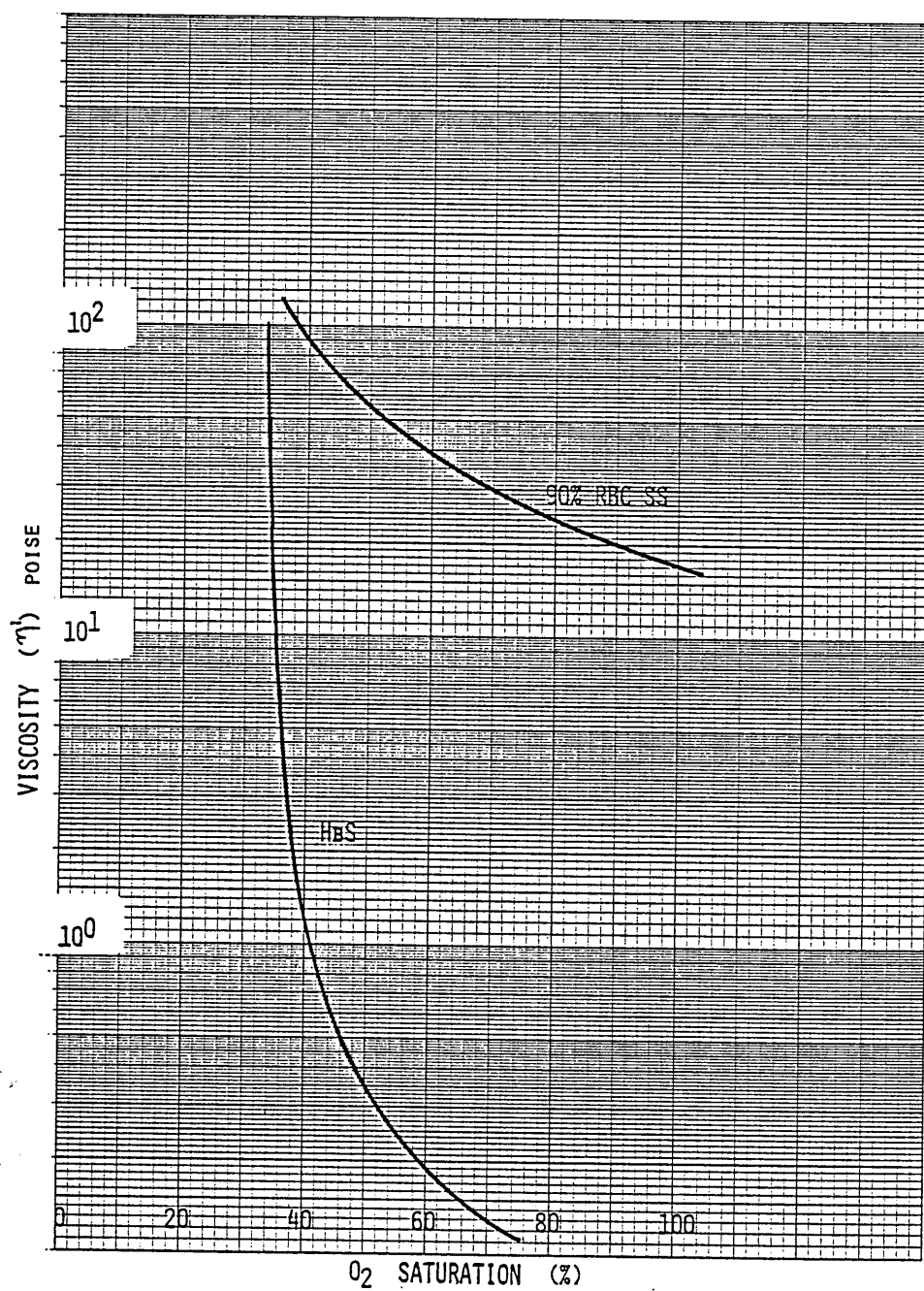


Figure 13. A comparison of the viscosity (η') versus O_2 saturation of 90% RBCs in Ringer-albumin and a HbS preparation at 32 g/dl. at a frequency of 0.01 Hertz.

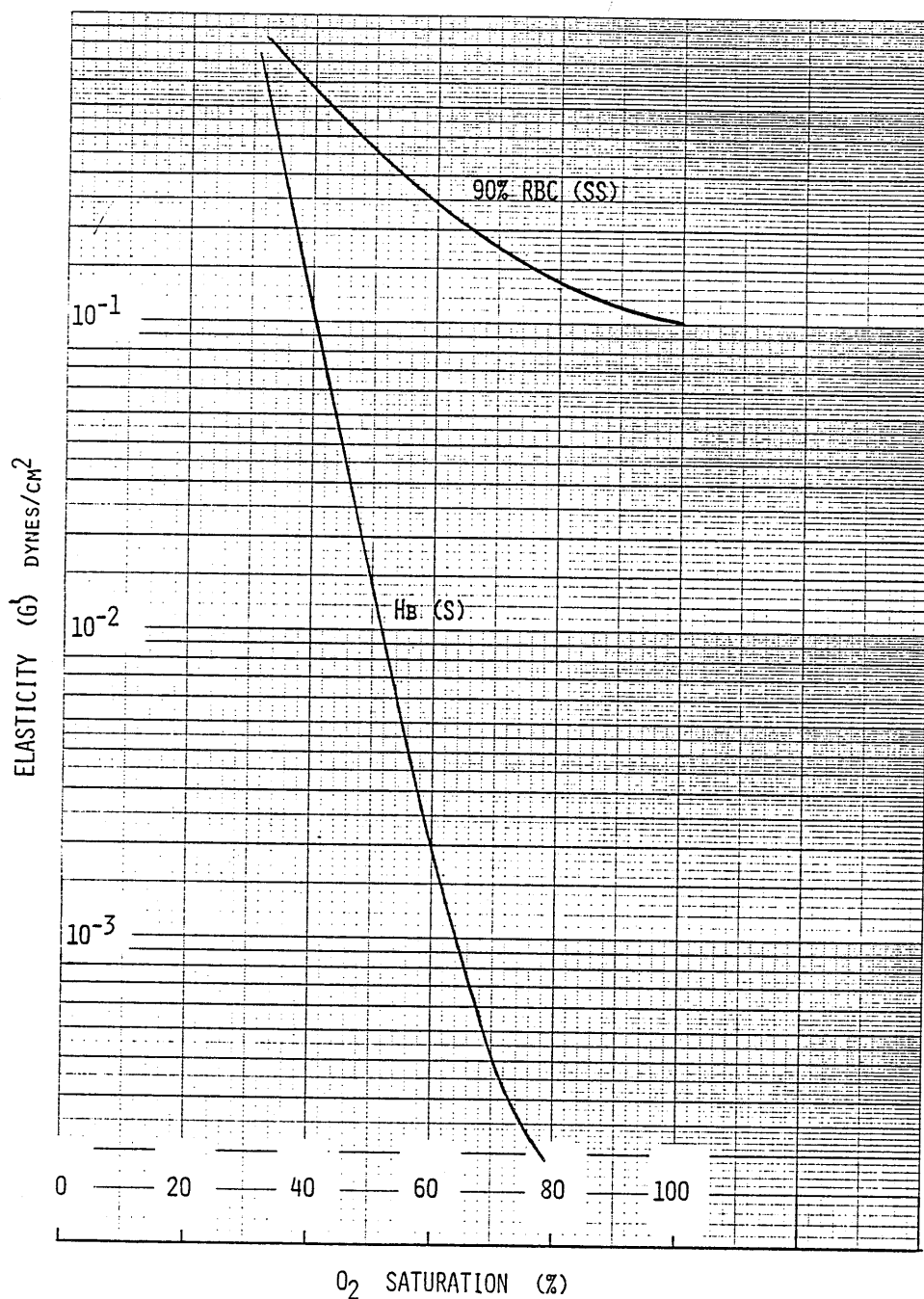


Figure 14. A comparison of the elastic modulus (G') versus O_2 saturation of 90% RBCs in Ringer-albumin and a HbS preparation at 32g/dl at a frequency of 0.01 Hertz.

of deoxygenation on SS cells and HbS solutions not only serve to elucidate the pathophysiology of sickle cell disease, but also may provide unique experimental information to elucidate the roles of individual components of the red blood cell play in determining its flow behavior.

The present study indicates that the deoxygenated HbS has a shear thinning property, as its η' and G' are reduced by several orders of magnitude when the oscillation frequency and the shear rate is raised. This shear thinning behavior points out the importance of maintaining an adequate blood flow and sufficient shear stress in sickle cell patients. If the blood flow through a region is reduced, due to greater rigidity of SS RBCs, the low flow state may enhance the probability of microvascular obstruction as a result of a greater loss of O_2 from the SS cell due to the longer transit time through tissue.

The Rheology of Whole Blood and suspensions of Leukocytes in Leukemia.

The rheology of whole blood and suspensions of white cells obtained from patients suffering from leukemia has been studied. The influence of erythrocytes and plasma proteins, in the presence of normal numbers of leukocytes, on normal blood viscosity has been described.

The influence of leukocytes on the viscosity of normal blood is minor because of their small numbers, but in leukemic patients, the leukocytes are greatly increased in numbers and affect the blood rheology adversely from the point of view of the dynamics of the circulation. However, leukemia patients, while having high leukocrits, generally have low hematocrits, which acts as a compensat-

ing mechanism. Leukopheresis (a treatment to remove excess white cells from the circulation) is used to reduce the leukocrit, and the effect of this treatment on the viscosity and elasticity of leukemic blood is investigated.

Methods

Blood rich in white blood cells (WBCs) was obtained from both chronic lymphocytic leukemia (CLL) and chronic myelocytic leukemia (CML) patients. White blood cells were also obtained from sedimented leukopheresis treatment packs.

Suspensions of WBCs from both CLL and CML patients were prepared in a special Tris saline buffer (TSA) comprising of 500ml of 0.9% NaCl with albumin (2.5g) and EDTA (0.5g) added. The pH was adjusted to 7.4 with Tris.

The WBCs from the leukopheresis packs were centrifuged and the plasma and the bag fluid was discarded. The WBCs were then washed at least three times and resuspended in the TSA buffer, and the cells were allowed to sediment. The bottom layer in the tube was discarded to remove clumps and any dead WBCs, which sediment more quickly. The WBCs were resuspended in TSA at the desired concentrations for measurement in the rheogoniometer.

Measurements were made of apparent viscosity (η_{app}) in steady shear, and the viscosity (η') and elasticity (G') in oscillatory shear, of suspensions of WBCs in TSA at various concentrations. The η' and G' of whole blood prior to and after leukopheresis treatment were also determined and the data compared, so that the effect of this therapy on the rheology of the patient's blood can be

ascertained. Preparation of RBCs in plasma were made at a constant hematocrit (40%), to which WBCs were added at various concentrations and measured in both steady and oscillatory shear. The data obtained is compared to RBCs in plasma at concentrations equal to the overall concentration of the WBC and RBC mixtures. A trapping correction factor of 0.75 was used to correct the leukocrit of the WBC suspensions determined by the microhematocrit tube method. The sample temperature was maintained at 37°C.

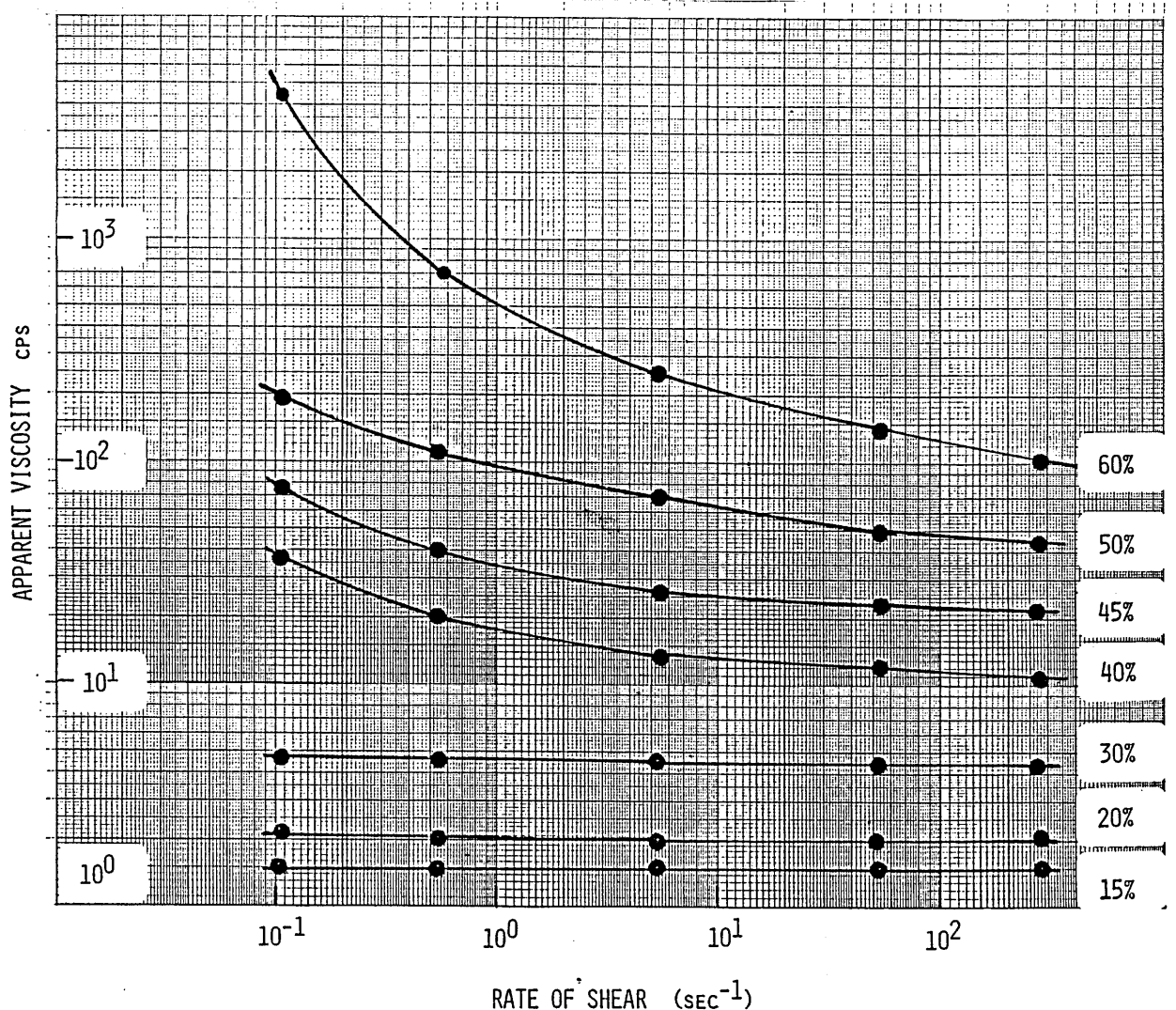


Figure 15. The Apparent Viscosity versus Rate of Shear, of suspensions of white blood cells (WBC) in a tris saline albumin (TSA) buffer solution, showing the effect of concentration. At low leukocrits the viscosity is Newtonian, but at a concentration of 40% and above, it becomes markedly non-Newtonian.

Results

Figure 15 shows η_{app} versus rate of shear for WBC suspensions in TSA at various concentrations from a CML patient. At low leukocrits, the samples exhibit Newtonian behavior up to about 40% concentration, after which the viscosity becomes markedly non-Newtonian. Figure 16 is a plot of η_{app} measured in steady shear at 0.01 sec^{-1} versus concentration for WBCs suspended in TSA from both CLL and CML patients. Figures 17 and 18 are plots of the viscosity (η') and elasticity (G'), measured in oscillatory shear of suspensions of WBC in TSA from a patient with CML. The plot of η' versus frequency indicates that there is a critical concentration (40-50%) where a change of slope occurs. Figures 19 and 20 are plots of dynamic viscosity (η') and dynamic elasticity (G') versus concentration, measured in oscillatory shear at 0.01 Hertz, of white cells from both CML and CLL patients.

Figure 21 is a plot of viscosity versus frequency in oscillatory shear, of a blood sample from a patient who underwent leukopheresis treatment. Blood samples were drawn both prior to and after the treatment. The WBC concentration was reduced in the post sample and there was also a slight decrease in RBC concentration. These decreases in cell concentration were accompanied by a lowered viscosity, which would be beneficial to the patient's circulatory system.

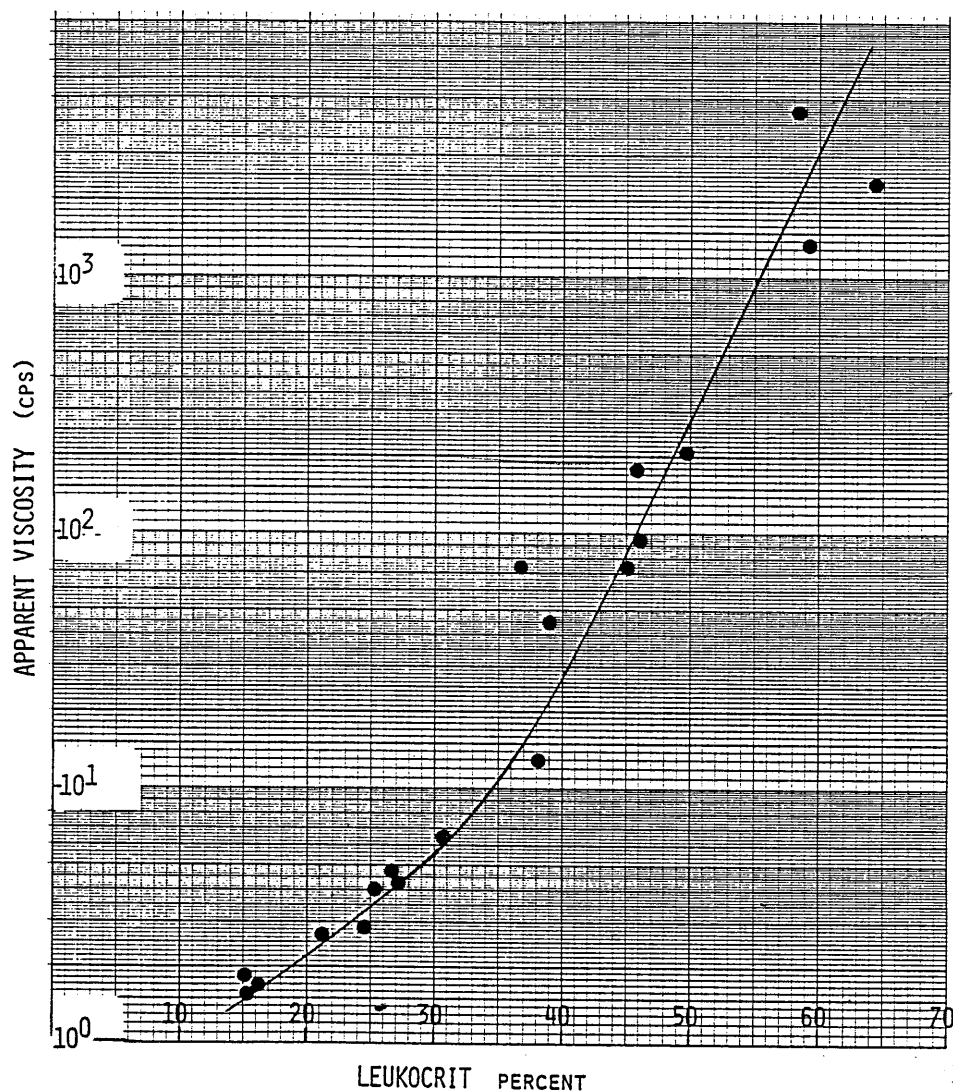


Figure 16. A plot of apparent viscosity versus leukocrit from both CLL and CML measured at 0.01 sec^{-1} . A change of slope occurs at between 30 and 40 percent concentration.

Discussion

High concentrations of leukocytes in the blood of leukemia sufferers are detrimental to the microcirculation because of the danger of local occlusions. This risk can be reduced by leukaphoresis treatment, as the removal of excess leukocytes brings about a considerable drop in viscosity on the patients blood, and will improve blood flow and reduce the cardiac load.

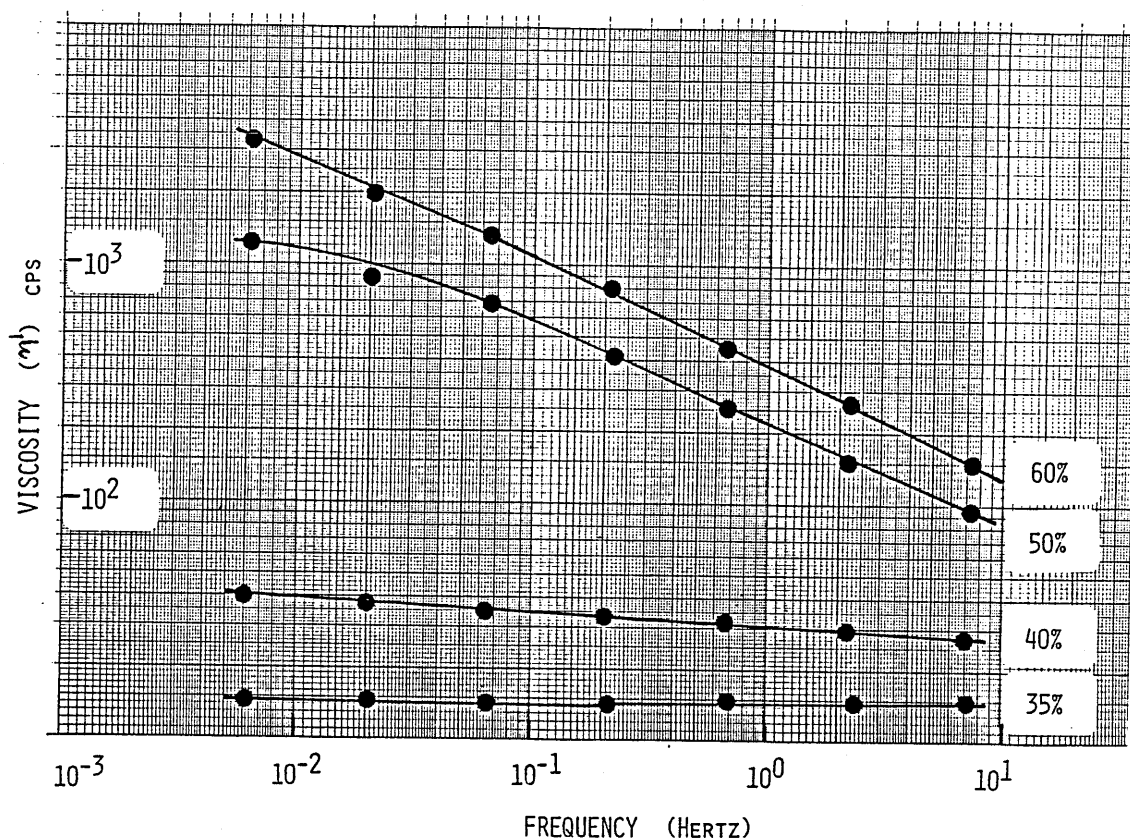


Figure 17. Viscosity (η') versus frequency in oscillation, of suspensions of WBCs from a CML patient, showing the effect on η' of increasing WBC concentration.

The rheological properties of single leukocytes, both normal and also in leukemia have been reported by Schmid-Schönbein et al. and La Celle et al. 1981 (11,12), using the micropipette method. La Celle et al. found that the deforming pressure required to aspirate the cells a certain distance into the pipette was little changed between normal and abnormal cells. Lichtman 1970 (13), reported that normal and leukemic lymphocytes were similarly deformable in a flow channel and that relaxation times were similar. Cokelet and Lichtman 1981 (14), reported rheological measurements of mixtures of normal red cells and WBCs from leukemia patients. In preparations of WBCs in plasma, they found a critical leukocrit of 30%,

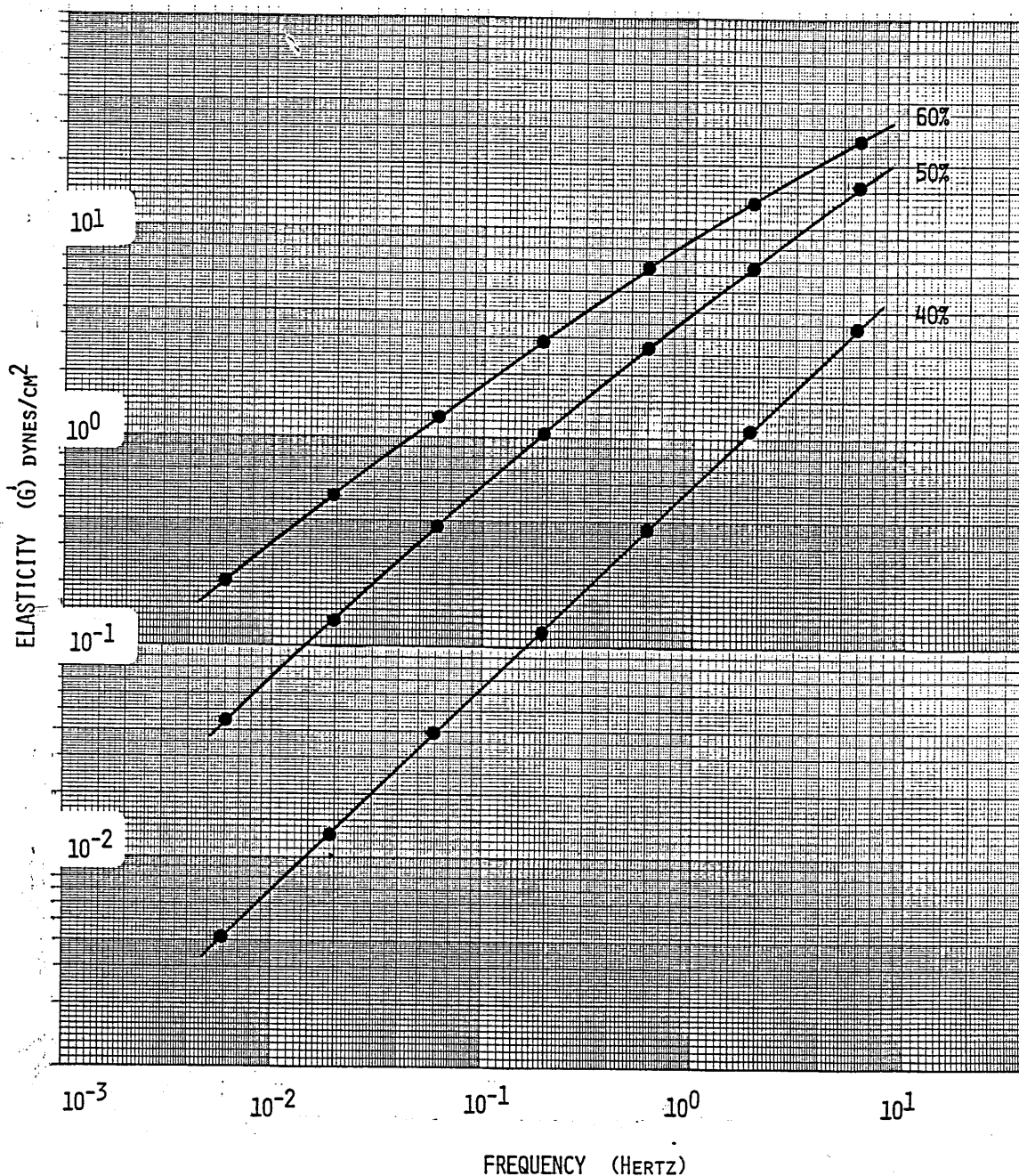


Figure 18. The elasticity (G') versus frequency in oscillatory shear, of WBCs from a CML patient resuspended in TSA at a concentration of 40, 50 and 60 per cent.

below which the apparent viscosity was a linear function of leukocrit percentage. Above this value, the viscosity increased rapidly with increasing WBC concentration. This was also found in this study, and may be due to the increasing crowding, causing increased cell to cell contacts during flow. The extreme surface roughness and stickiness of leukocytes would cause cell entanglements or

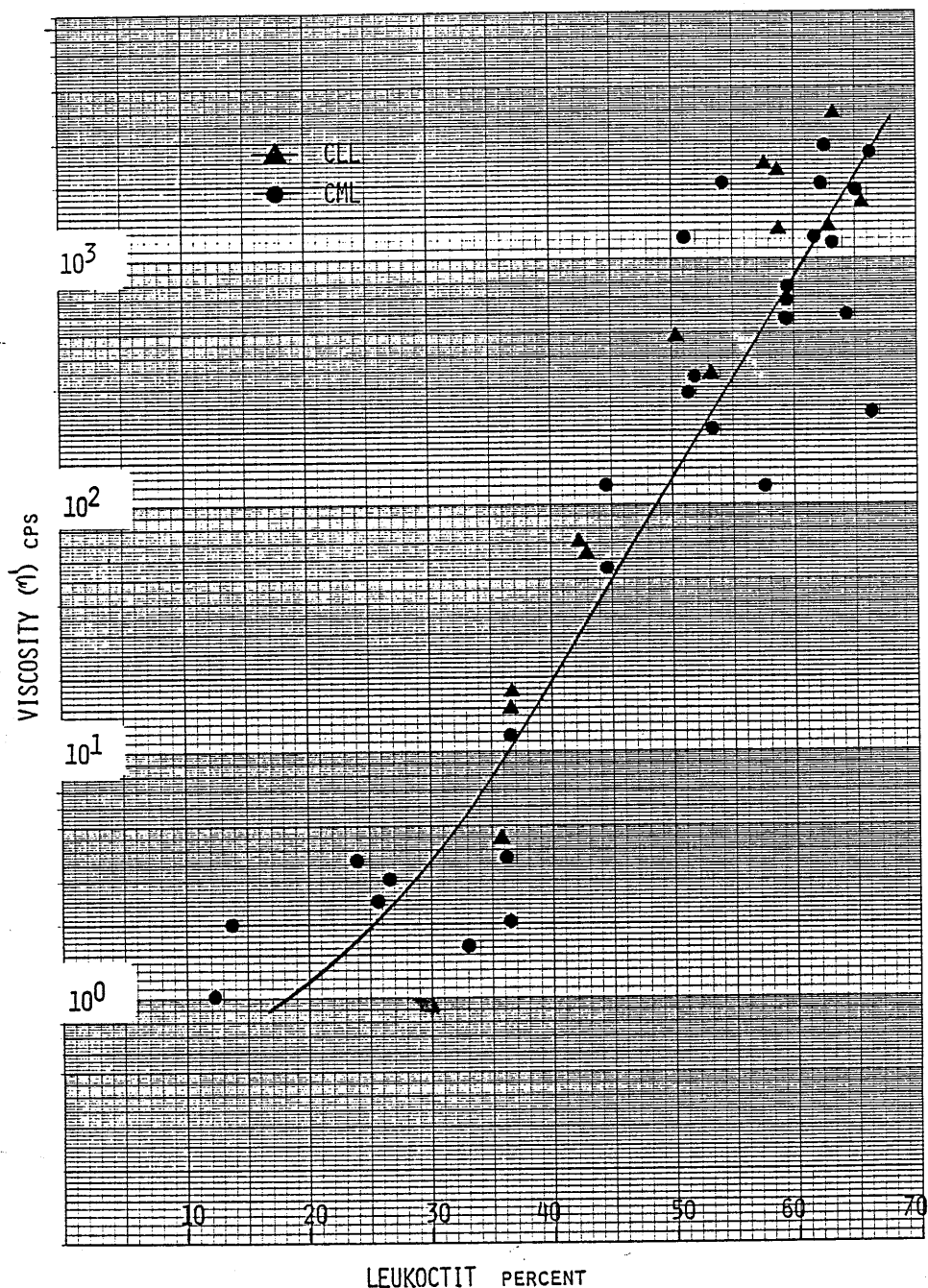


Figure 19. The viscosity (η) measured in oscillatory shear at 0.01 Hertz, of WBCs from patients with CML and CLL resuspended in TSA, showing the effect of increasing leukocrit.

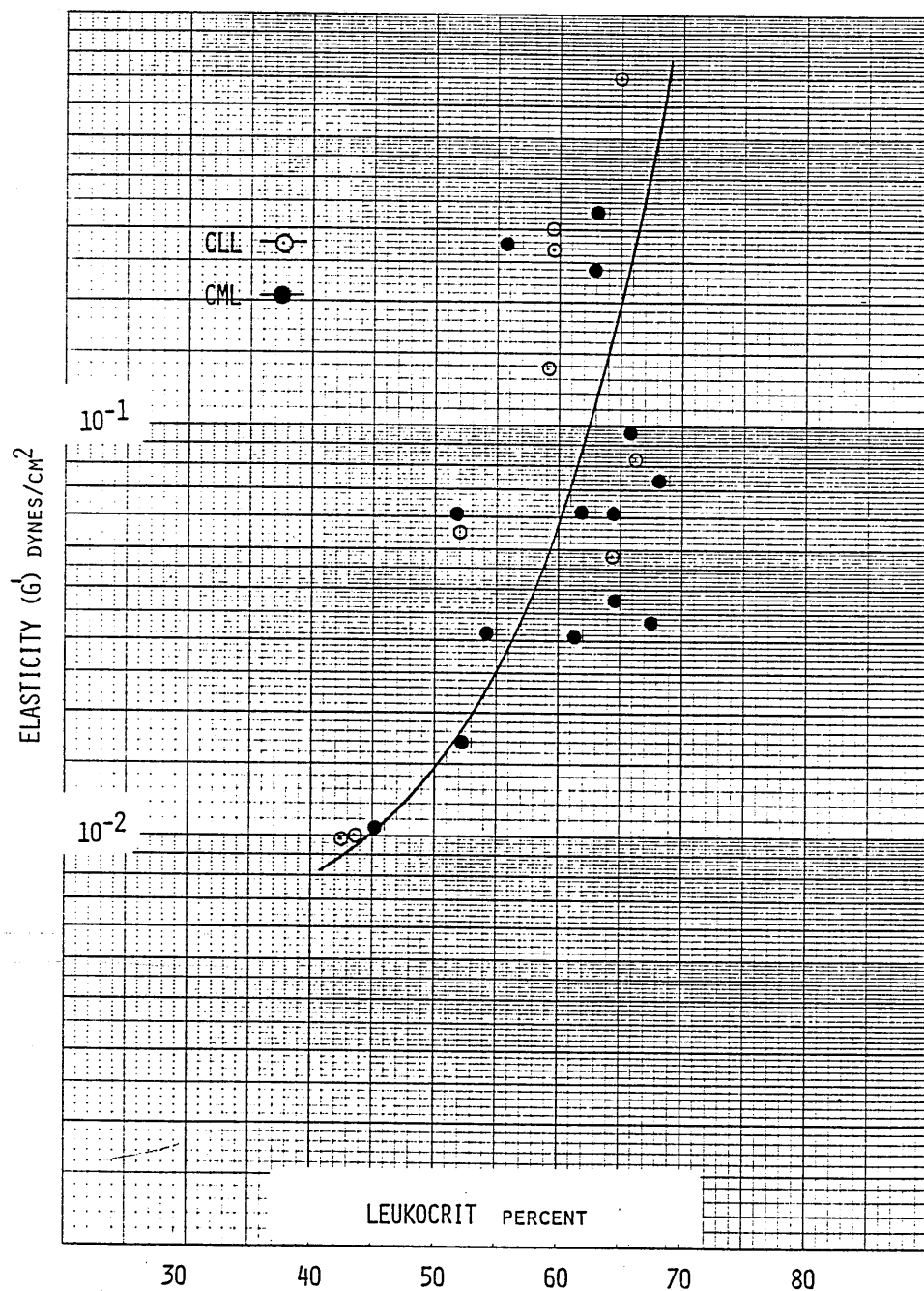


Figure 20. The Elasticity (G) measured in oscillatory shear at 0.01 Hertz, of WBCs in TSA of patients with CML and CLL showing the effect of increasing WBC concentration.

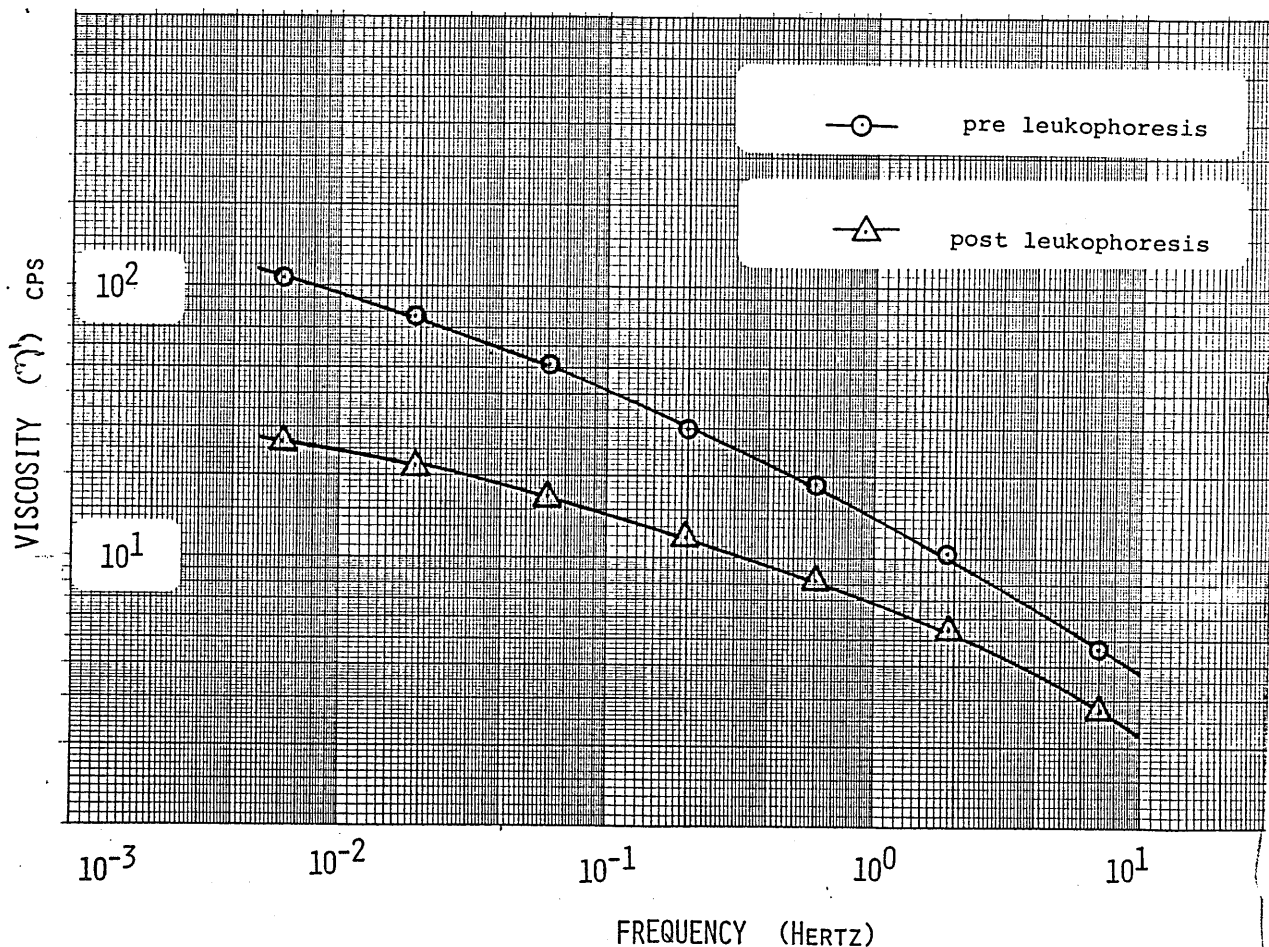


Figure 21. Viscosity (η') versus frequency, showing the effect on whole blood viscosity of leukophoresis treatment. The values of hematocrit and leukocrit measured in the pre-leukophoresis blood sample were 35 and 16 per cent. In the post leukophoresis blood sample the values were 33 and 12 per cent.

possibly rouleaux like arrangements to develop including long contact periods, as cells passed each other causing increased flow resistance. It should be noted that it is above 40% concentration that an elastic component becomes measurable, perhaps indicating that only when strings of cells or perhaps clumps are present will an elastic modulus be recorded.

Figure 22 is a scanning electronmicrograph of WBCs showing surface projections. The cell itself is spherical, 7.4 microns in diameter, with a less deformable

center or cytoplasm surrounded by a soft membrane. Chien 1981 (15), reports the rigidity of the individual WBC is higher than that of the single RBC, and this fact is reflected in this study on cell suspensions. Figures 17 and 18 confirm that the dynamic moduli (η' and G') of WBCs are greater than that of normal red cells suspended in a similar buffer preparation when above 30% concentration when compared to data from RBCs presented on pages 87 and 88.

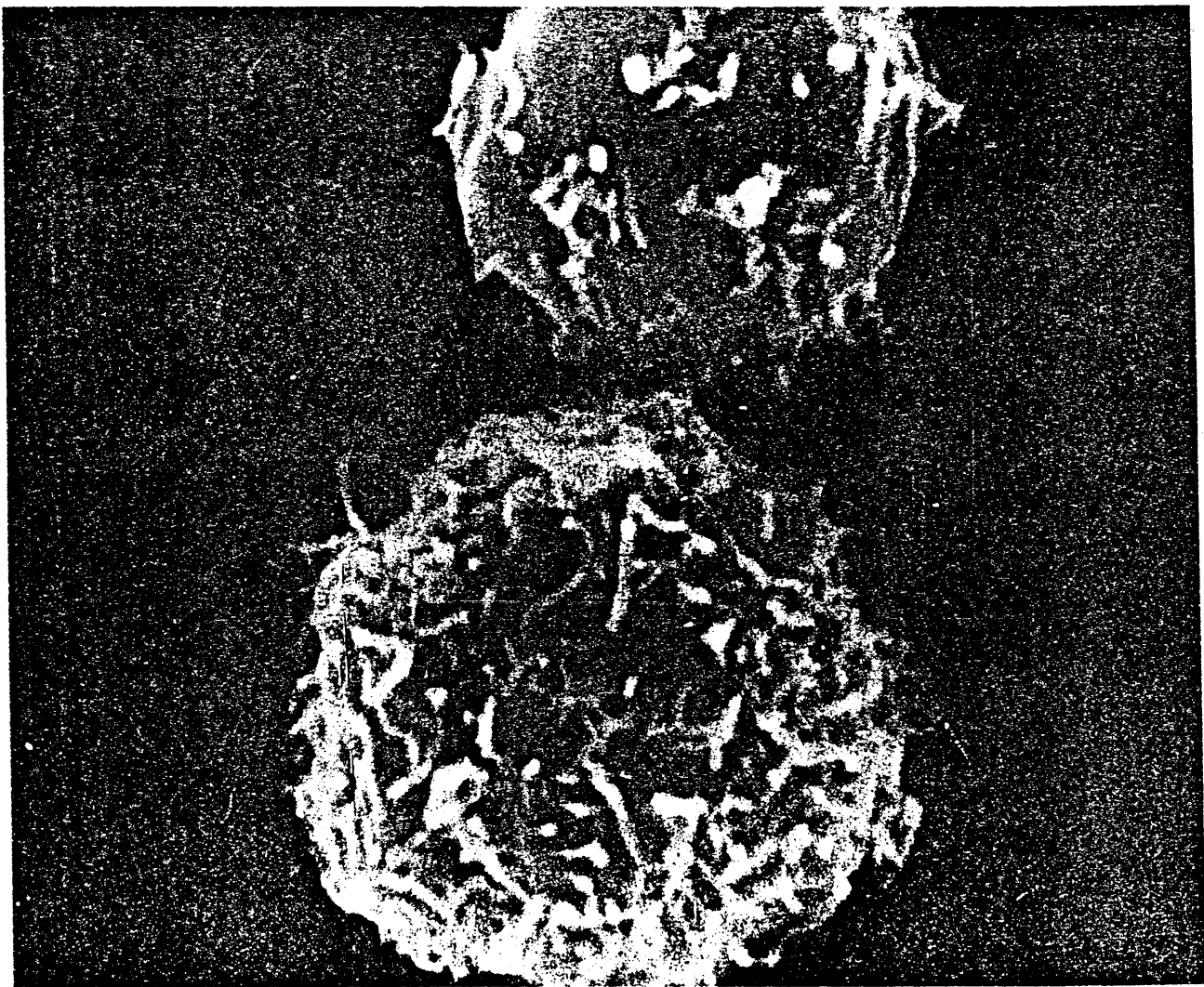


Figure 22. A scanning electron micrograph of white cells from a patient with CLL, showing the extreme surface roughness of the membrane.

CHAPTER V.

RHEOLOGICAL MEASUREMENTS OF SURFACE LAYERS OF BLOOD PROTEINS AT INTERFACES.

Introduction.

Surface layers of some blood proteins form spontaneously at solid-liquid, liquid-air, and liquid-liquid interfaces in systems of fibrinogen, albumin and in some cases γ globulin when in solution, and also from plasma (1-10). The measurement of the rheological properties of these surface layers has largely been avoided by most investigators, with the exception of July 1970 (11), because they considered them to be artefacts (12-14).

Figure 1 shows a plot of viscosity measurements, in steady shear, of human plasma using a Couette geometry with and without a detachable guard ring. Newtonian characteristics were found with the guard ring in place and average viscosity was 1.3 centipoise. However, when the guard ring is removed and the experiment is repeated, a non-Newtonian flow curve is measured, with a marked elevation of the apparent viscosity at the lower shear rates. From these two curves, we can deduce that a layer of plasma proteins, possibly a cross-linked gel, forms at the liquid-air interface.

Figure 2 is a plot of measurements obtained when fibrinogen is dissolved in 0.9 percent NaCl, to give a fibrinogen concentration of 0.4%. The solution is mea-

sured in steady shear, using a Couette type geometry, with and without a guard ring. With the guard ring in place, only Newtonian viscosity is measured. Without the guard ring, non-Newtonian characteristics are found and the

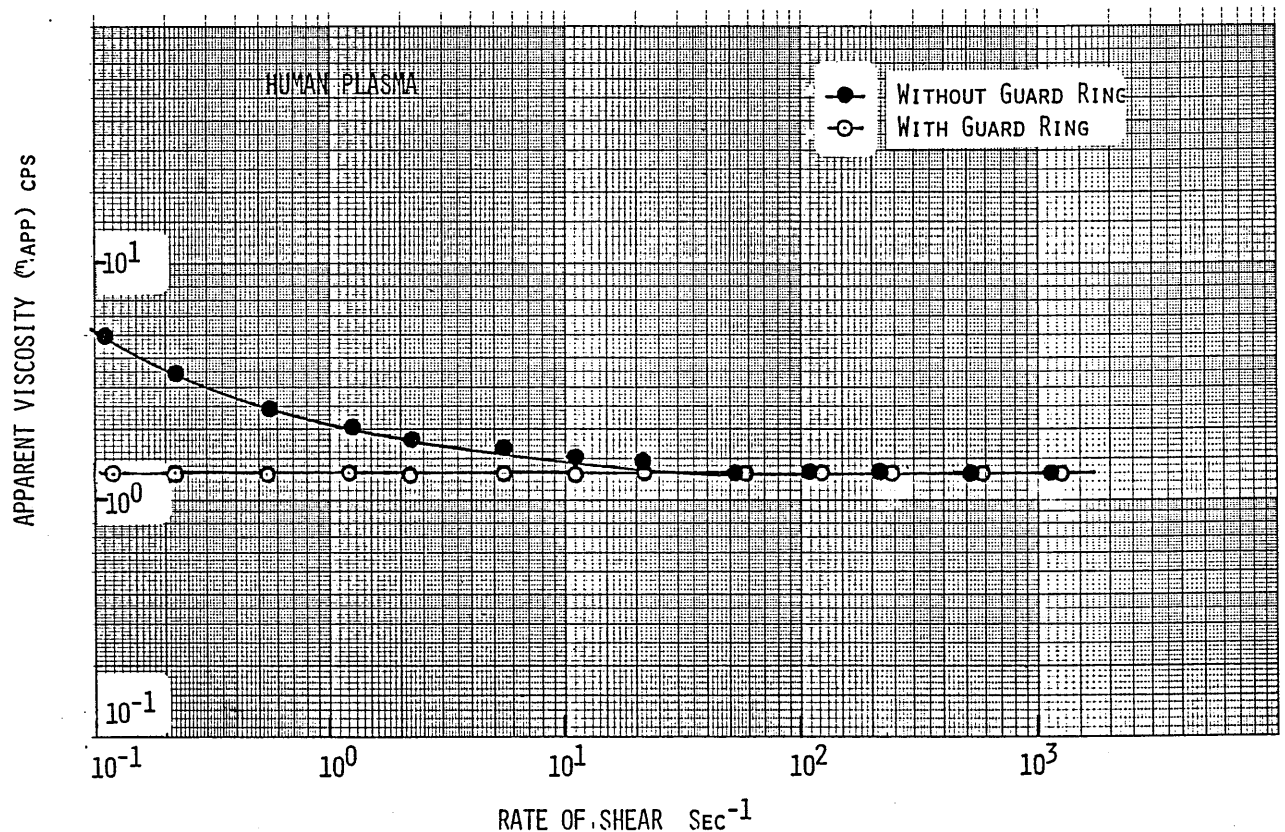


Figure 1. Apparent Viscosity, measured in steady shear of normal human plasma plotted against Rate of Shear. The measurements were made with (—○—) and without (—●—) a detachable guard ring.

apparent viscosity is markedly increased at low shear rates, indicating that the fibrinogen solutions produce surface layers of considerable strength at the air interface.

Copley and King 1973 (15), investigated the effect of human red cells and platelets on the rigidity of surface layers formed from human plasma. They found that as red cells are added to plasma in increasing numbers, the surface layers become weaker and vanish altogether when a hematocrit of 40% was reached. The addition of platelets instead of red cells, however, considerably increased the rigidity of the surface layer.

The viscosity and elastic modulus of surface layers of purified fibrinogen preparations in varying concentrations exhibited considerable strength even at concentrations as low as 0.0004 percent. This demonstrates that fibrinogen forms strong surface layers at interfaces even in very small concentrations.

The thickness of fibrinogen surface layers, measured by ellipsometry, was found by Smith and Morissey 1975 (16), to vary under certain conditions from 200 to 600 Å. If the thickness of these layers when measured in the Rheogoniometer experiments were within these values, then the bulk viscosity and elasticity of the layers could be calculated. If a surface layer thickness of 200 Å was used for these calculations, then viscosity values of up to 10^8 poise would be indicated, confirming that these layers have extremely high rigidity.

The surface layers of fibrinogen may be likened to gel structures, and may be of major significance in relation to surface induced thrombosis. Tooney and Cohen 1977 (17,18), have found that gels of native fibrinogen with fibrinopeptides intact, form aggregates similar to fibrin without thrombin interaction. In view of these findings, and earlier findings with protamine sulfate, by Stewart and Niewarowski 1969 (19) and Stewart 1971 (20), it is considered probable that fibrinogen molecules can aggregate without thrombin action, and without the liberation of fibrinopeptide A.

Copley 1971 (3), proposed a new concept of the genesis of thrombosis. This was further substantiated by Copley and King 1976 (22), by their surface rheological studies. This process begins by the adsorption of fibrin-

ogen on to the vessel wall and this is followed by a growth process of the adsorption of more fibrinogen and then other plasma proteins layer upon layer, until the lumen of the blood vessel is either partially or completely obstructed. It is only after this process is initiated, that other clotting processes in vivo, such as the aggregation of platelets and red cells, and the formation of fibrin, resulting in the formation of a so-called "mixed thrombus".

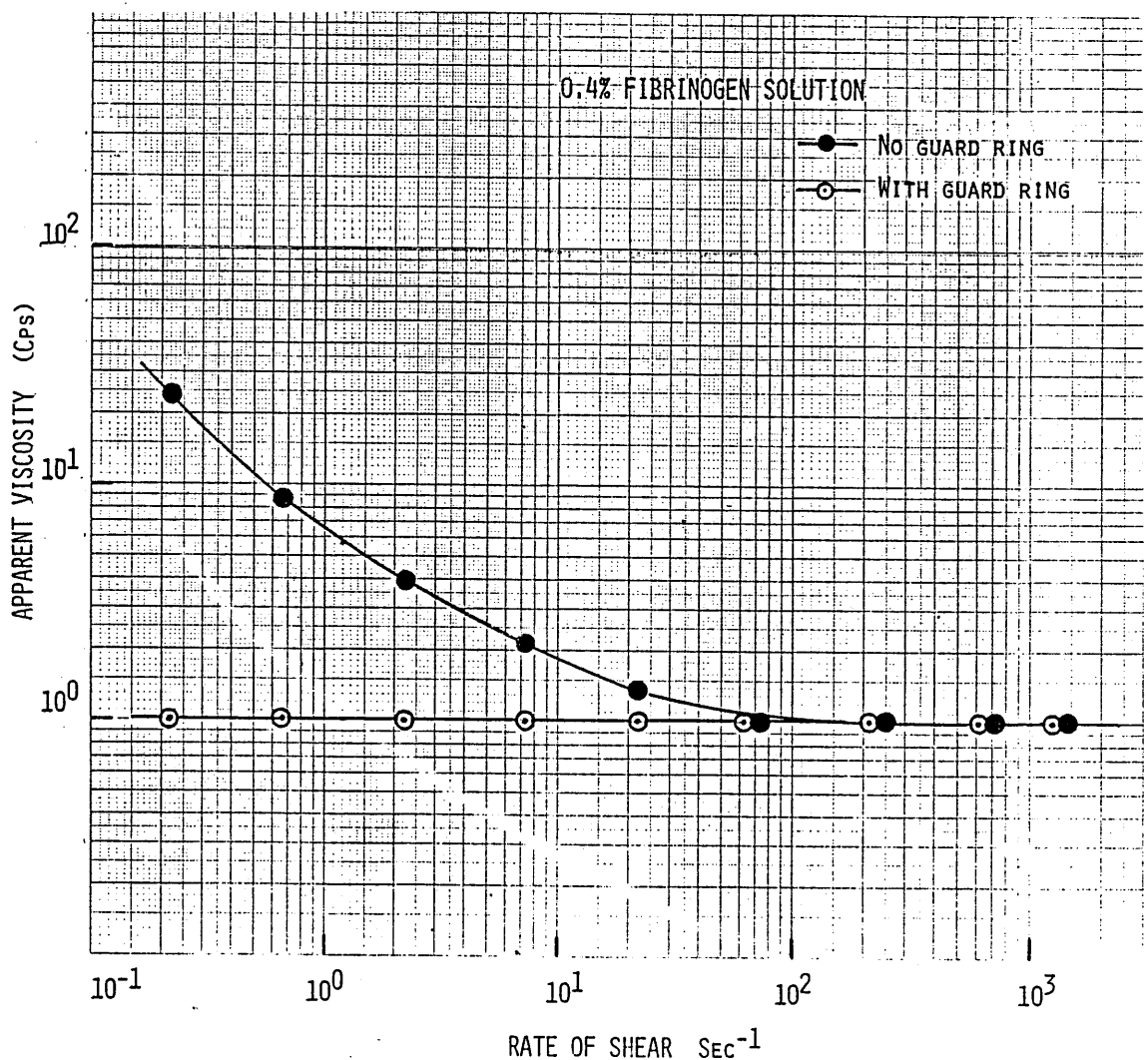


Figure 2. Apparent Viscosity, measured in steady shear with and without a guard ring, of a solution of 0.4% human fibrinogen.

It is surmised that it is not the first layer of contact of fibrinogen with the endothelial cells, but the surface gel of fibrinogen which is important in the initiation of thrombosis formation. Thus the findings on the viscoelasticity of surface layers of systems of highly purified fibrinogen preparations are of particular significance with regard to studies on the arrest of hemorrhage and also in the development of thrombosis, (23-25).

In order to investigate this phenomenon further, the rheology of surface layers of fibrinogen at different concentrations and also with the addition of other substances used as an anticoagulant, such as heparin, or those having the reverse effect, such as calcium, have been studied.

The measurement of the viscoelasticity of surface layers of solutions of highly purified fibrinogen from different species

Surface rheological studies of highly purified fibrinogen were made using the "Ring in Ring" geometry described in Chapter 2, page 22, together with the Rheogoniometer used in oscillatory shear. Figure 3 is a representation of a typical recorder trace when measuring surface layers of a 0.4% fibrinogen solution at a frequency of 0.06 Hertz.

No torque output from the torsion head could be recorded at any frequency when physiologic saline only was measured. In this case, therefore, formulas for a double wall Couette geometry, omitting the layer thickness, can be used for the direct calculation of the two dimensional surface viscosity (η_s^I) and surface elasticity (G_s^I) of the

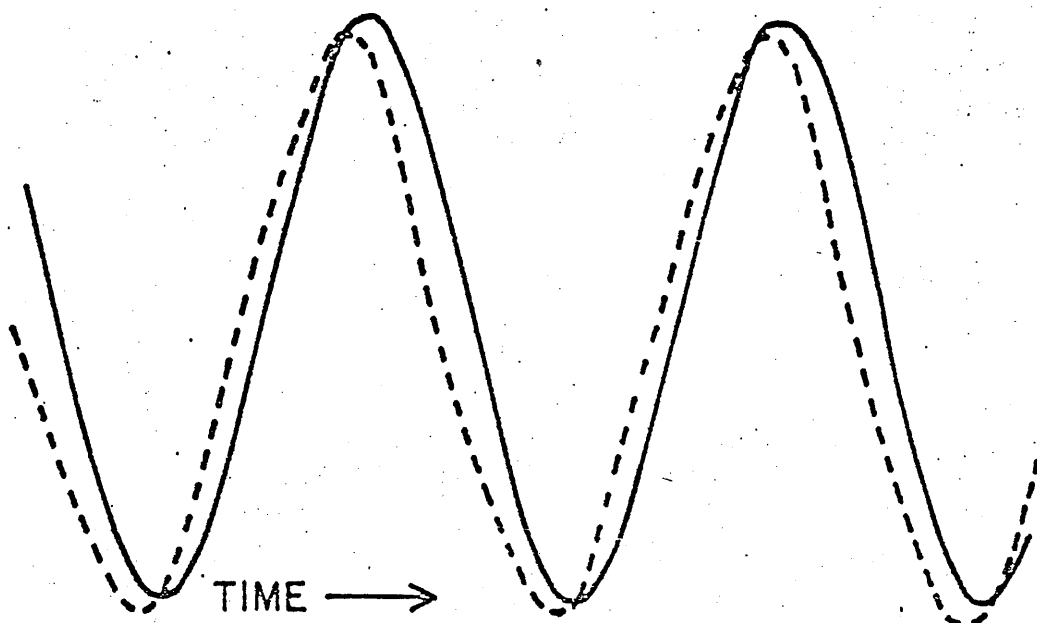


Figure 3. A typical recorder trace, obtained during an oscillatory experiment using the "Ring in Ring" geometry, of surface layers of a 0.4% solution of human fibrinogen, at a frequency of 0.01 Hertz. The solid trace indicates the input motion, while the dotted trace indicates the output from the torsion head. The phase difference between the two traces is 15 degrees.

layer without any correction for extra torque derived from substrate fluids. The subscript 's' is used to denote the surface property values when they are calculated in the absence of a measured film thickness.

Fibrinogen solutions were prepared in 0.9% saline at a concentration of 0.4%. Fibrinogen from sheep, bovine and human species were obtained from commercial sources. The temperature in all these studies was maintained at 25°C.

Figures 4 and 5 show the surface viscosity (η_s^I) and surface elasticity (G_s^I) which were obtained in dynamic shear. The η_s^I of all preparations was similar while the G_s^I of the sheep fibrinogen gave higher values.

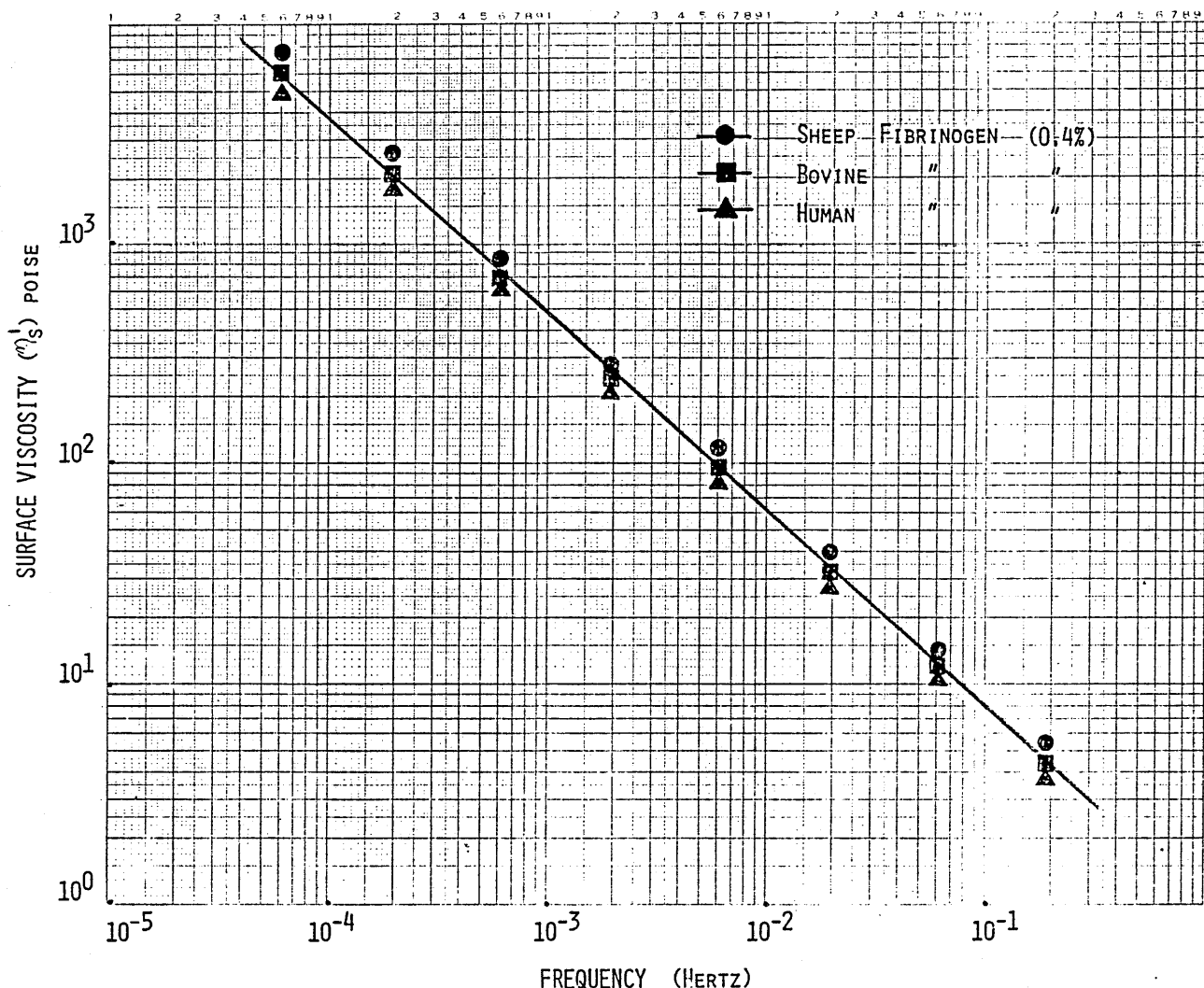


Figure 4. Surface Viscosity (η'_s) measured in oscillatory shear at very low frequencies, of surface layers of solutions of fibrinogen from human, bovine and sheep.

Measurements of the viscoelasticity of surface layers of solutions of human fibrinogen at varying concentrations

Highly purified fibrinogen (98-100% clottability) of human origin (IMCO, Stockholm), prepared by the method of Blomback and Blomback (26), was used in all experiments. Solutions of fibrinogen were prepared at the various concentrations using a Tris/saline buffer with pH adjusted to 7.2. An oil cover (Lubinol) was used to prevent evaporation of the test sample during the particularly long time experiments at the very low frequency employed.

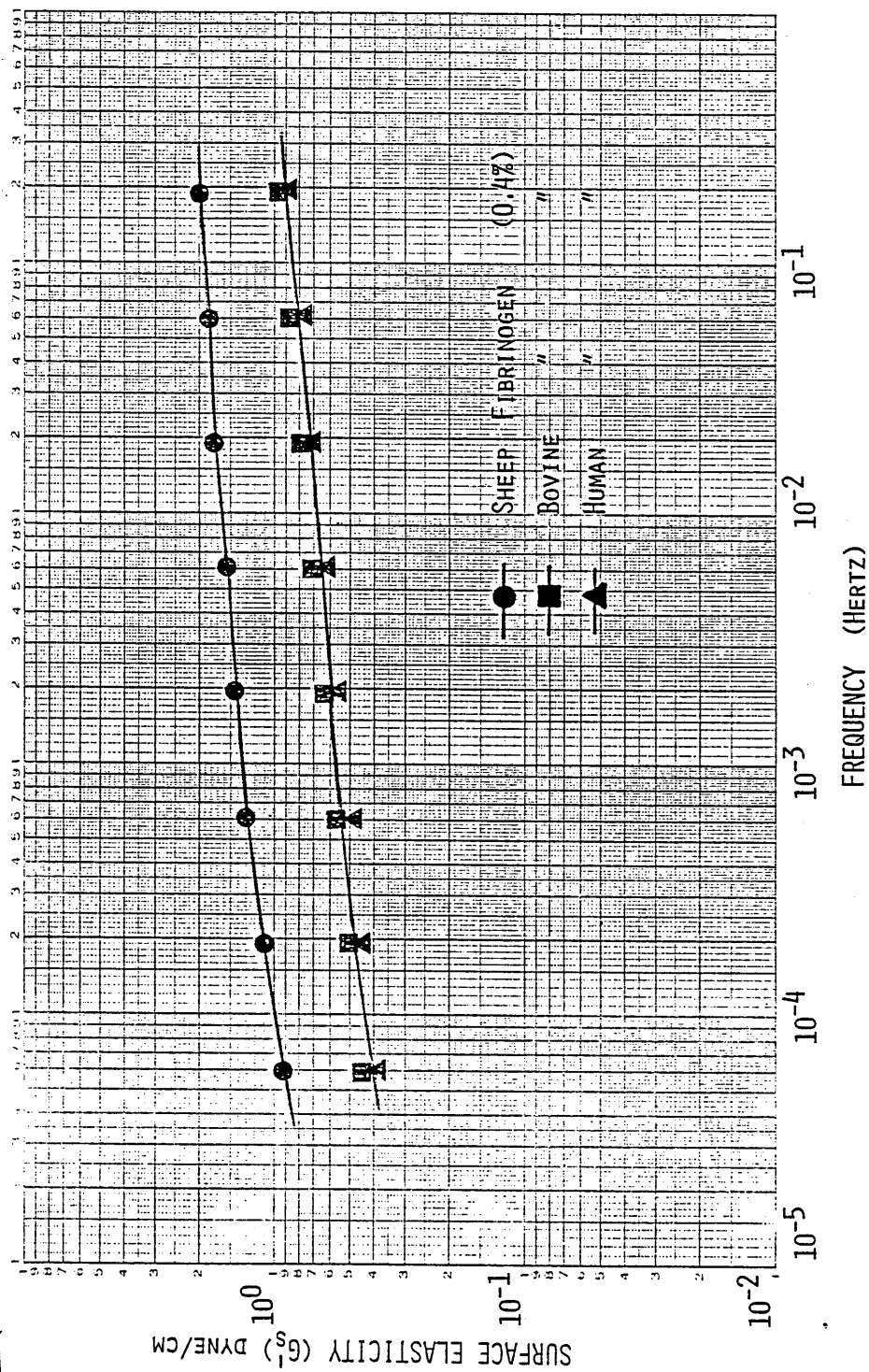


Figure 5. Surface Elasticity (G_s') measured in oscillatory shear at very low frequencies, of solutions of fibrinogen from human, bovine and sheep.

The η_s^I and G_s^I in dynamic shear, using frequencies from 2.0×10^{-5} to 2.0×10^{-1} Hertz, were measured using human fibrinogen concentrations of 0.0004 to 0.4%. The data obtained are shown in Figures 6 and 7. As can be

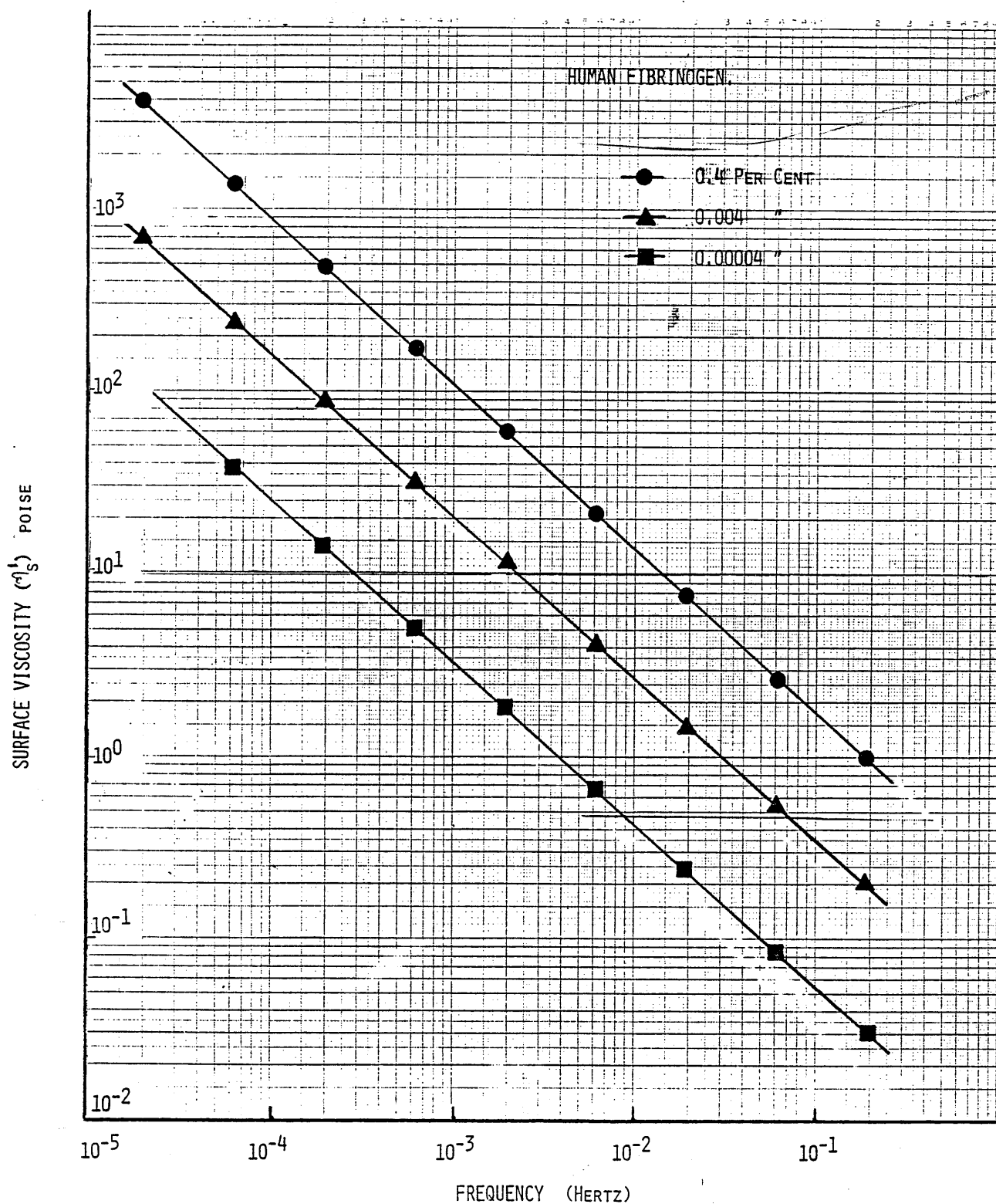


Figure 6. Surface viscosity (η_s^I) measured in oscillatory shear, of surface layers of preparations of human fibrinogen at concentrations of 0.4, 0.004 and 0.00004 percent.

seen in Figure 6, the viscosity (η'_s) decreases with decreasing fibrinogen concentration, as well as with the increase of frequency.

Figure 7, shows the elastic modulus (G'_s) of surface layers of human fibrinogen in the different concentrations employed, plotted against frequency. These measurements show that fibrinogen, even in very small concentrations, provides considerable rigidity at an interface.

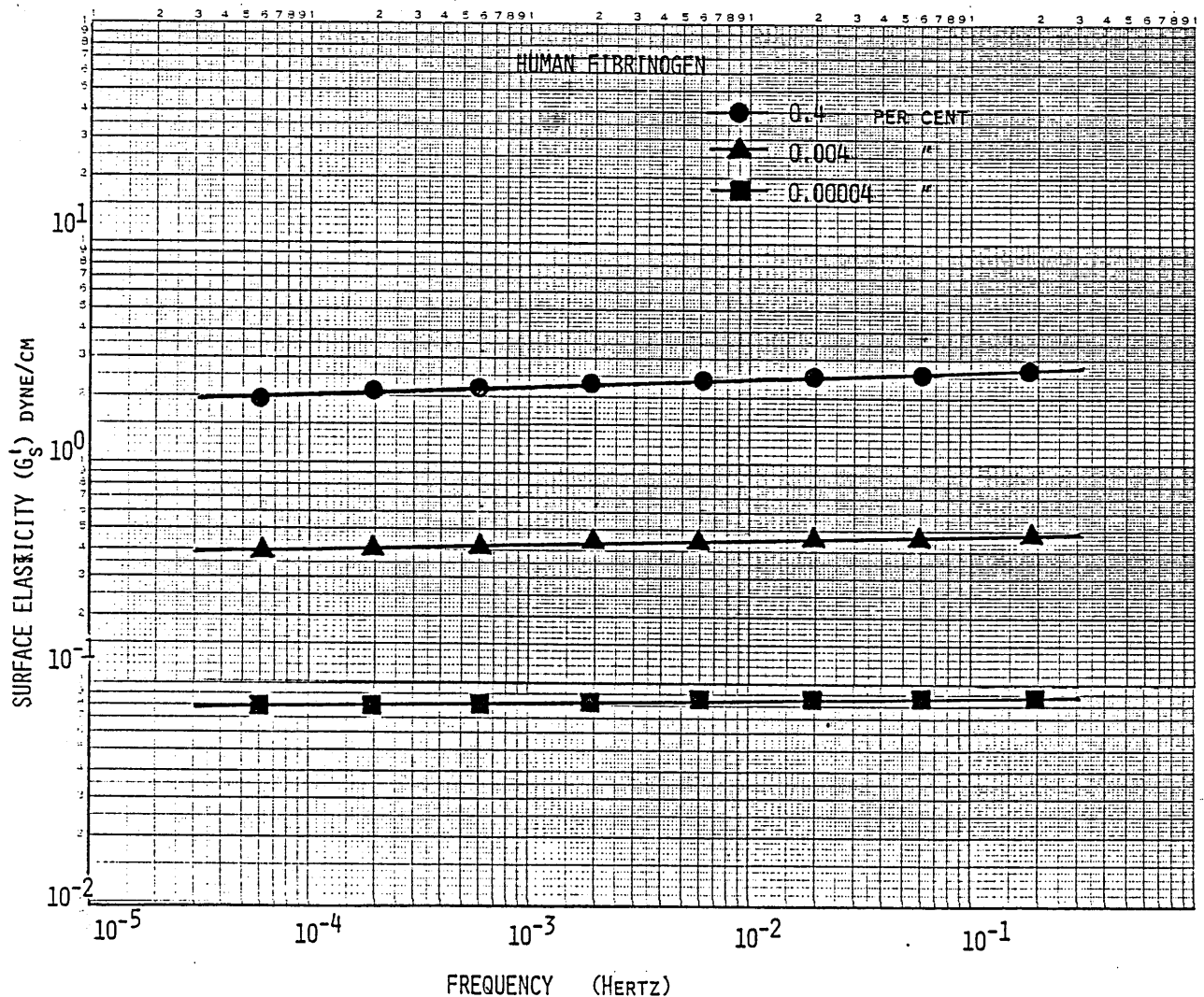


Figure 7. Surface Elasticity (G'_s) measured in oscillatory shear, of surface layers of preparations of human fibrinogen at concentrations of 0.4, 0.004 and 0.00004 per cent.

The action of highly purified γ globulin and β lipoprotein on the viscous and elastic moduli of fibrinogen surface layers

Figure 8 shows the effect of 0.1 and 1.0 percent of highly purified γ globulin on the elastic modulus of surface layers of 0.4% fibrinogen. At the lower concentration of 0.1%, γ globulin reduces G'_s slightly, while the high concentration (1.0%) decreases G'_s markedly.

Figure 9 shows the effect on the surface layers when highly purified β lipoprotein in concentrations of 0.025 and 0.25 percent is added to a 0.4 percent human fibrinogen solution. The 0.025% β lipoprotein decreases markedly the elastic modulus when compared with the fibrinogen control. When 0.25% β lipoprotein is added, the

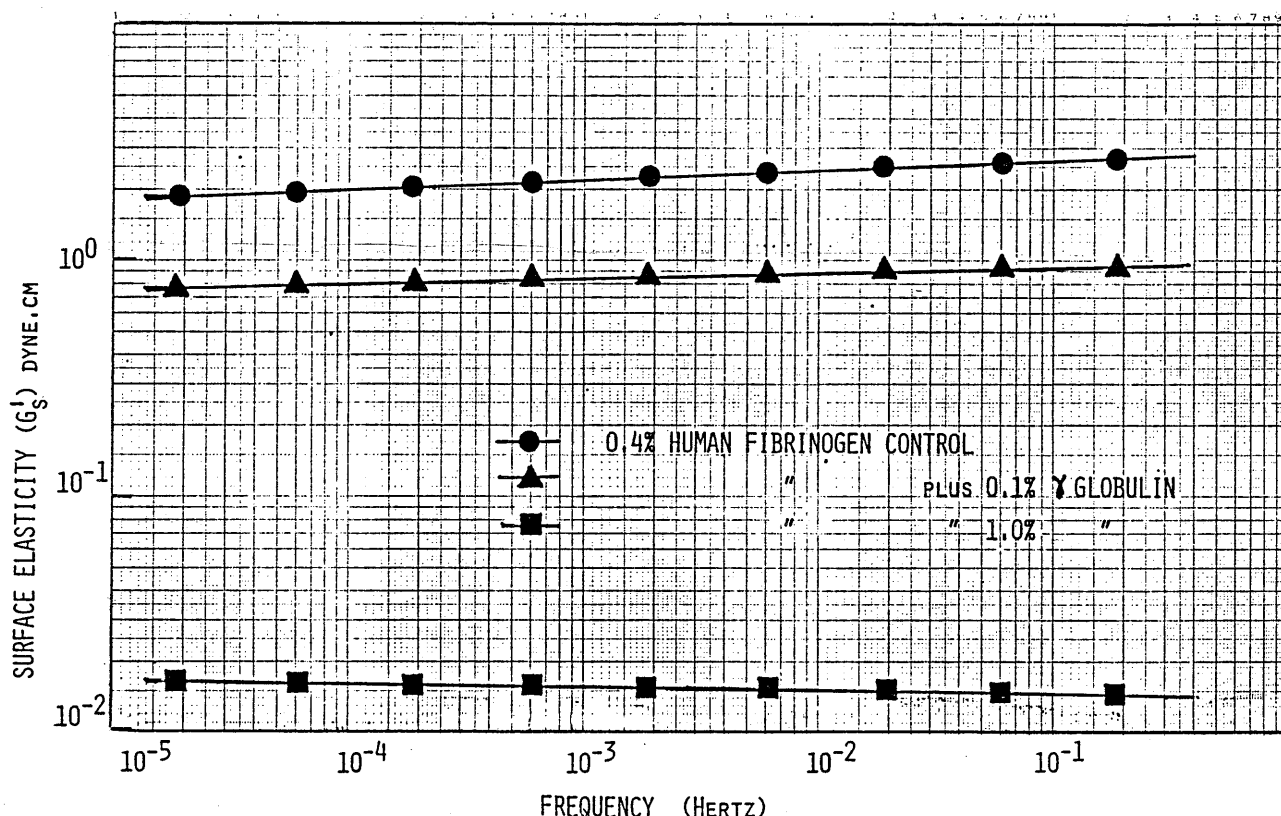


Figure 8. The effect on G'_s of a surface layer of a 0.4% fibrinogen solution, when γ globulin at 0.01 and 1.0% concentration is added.

surface layer is eliminated altogether. It can be interpreted from these findings that β lipoprotein interferes with the bonding of the fibrinogen molecules resulting in weak formations of fibrinogen layers, or none at all.

When measured alone, the β lipoprotein solutions in saline do not form measurable layers and no surface measurements from such preparations can be obtained. However, when added to fibrinogen solutions, they can be demonstrated to have a considerable reducing action on surface layer formation.

The effect of pH on the elasticity of surface layers of fibrinogen

The purified preparation of human fibrinogen (IMCO, Stockholm) was again used for these studies.

A 0.4 percent solution was prepared in a saline buffer. The pH was controlled by the addition of trace amounts of HCl, or Tris, and pH was adjusted to values over the range of 3 to 8.6. The Rheogoniometer was used in the oscillatory mode at a frequency of 0.06 Hertz. This frequency is chosen as it is low and unlikely to disturb the development of the surface layer.

Figure 10 shows the elasticity (G_s^1) of surface layers of 0.4 percent fibrinogen plotted against changing pH. As pH is lowered, the elastic modulus increases, while at pH 8.6 the value is the lowest. The curve exhibits a plateau over the range 6.8 to 7.6.

The buffering capacity of blood is such that the normal pH varies only slightly between 7.35 and 7.4. Only in severe cases of acidosis was the pH found to fall as low as 7.0, and conversely, in severe alkalosis to rise

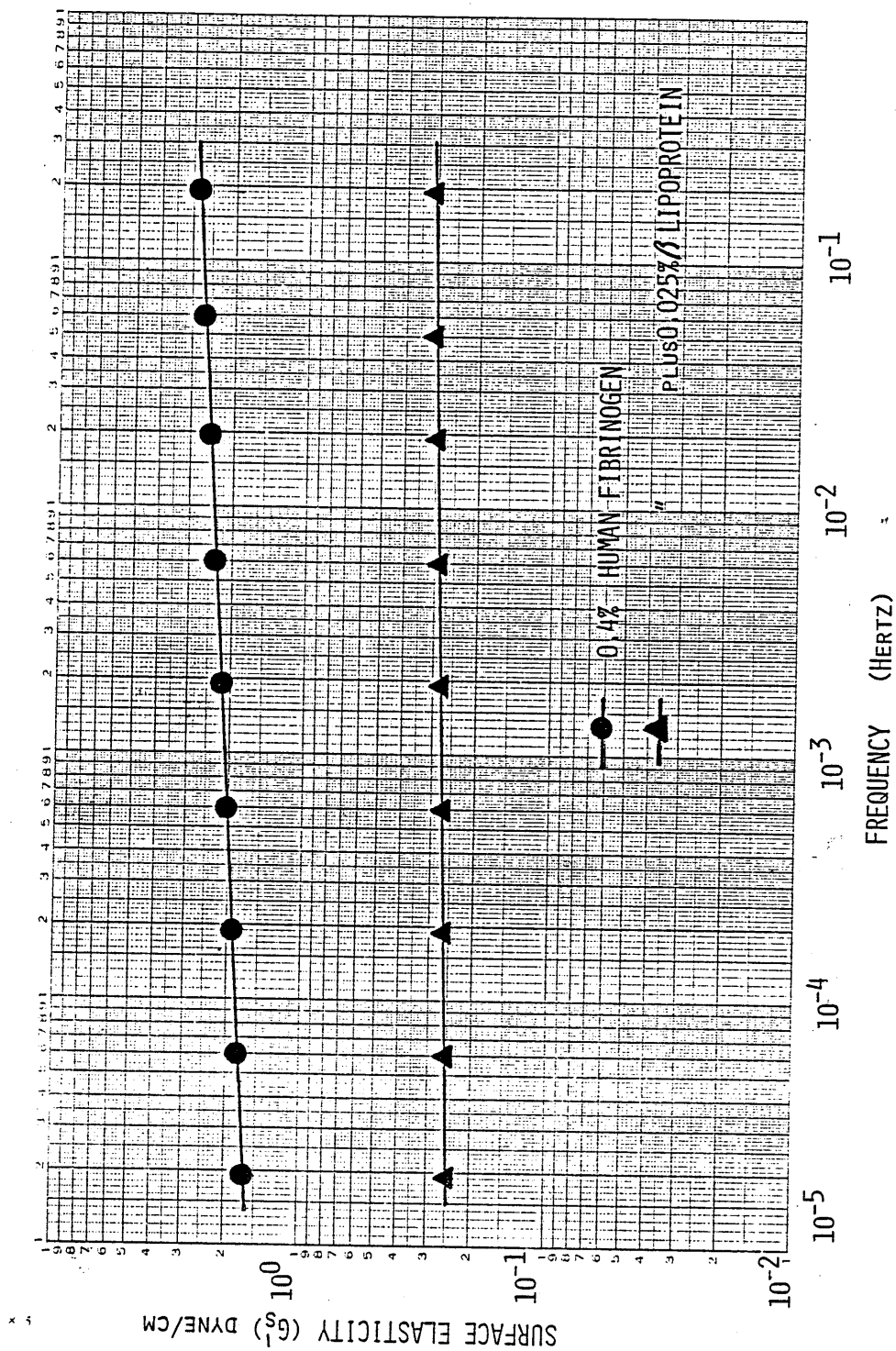


Figure 9. The effect on G_s of the surface layer of a solution of 0.4% fibrinogen when 0.25% lipoprotein is added at a concentration of 0.025% and 0.25%. The addition of 0.25% eliminates the layer altogether.

beyond 7.7. It would appear, therefore, that large changes in pH do not occur in the circulation and that these changes in pH would have negligible effect on the normal rigidity of fibrinogen molecules found at a surface.

McLaren and Seaman (27,28), in discussing surface pH on a microscopic scale, found that the value of the pH will be lower for a negatively charged surface than the bulk value, whereas for a positively charged

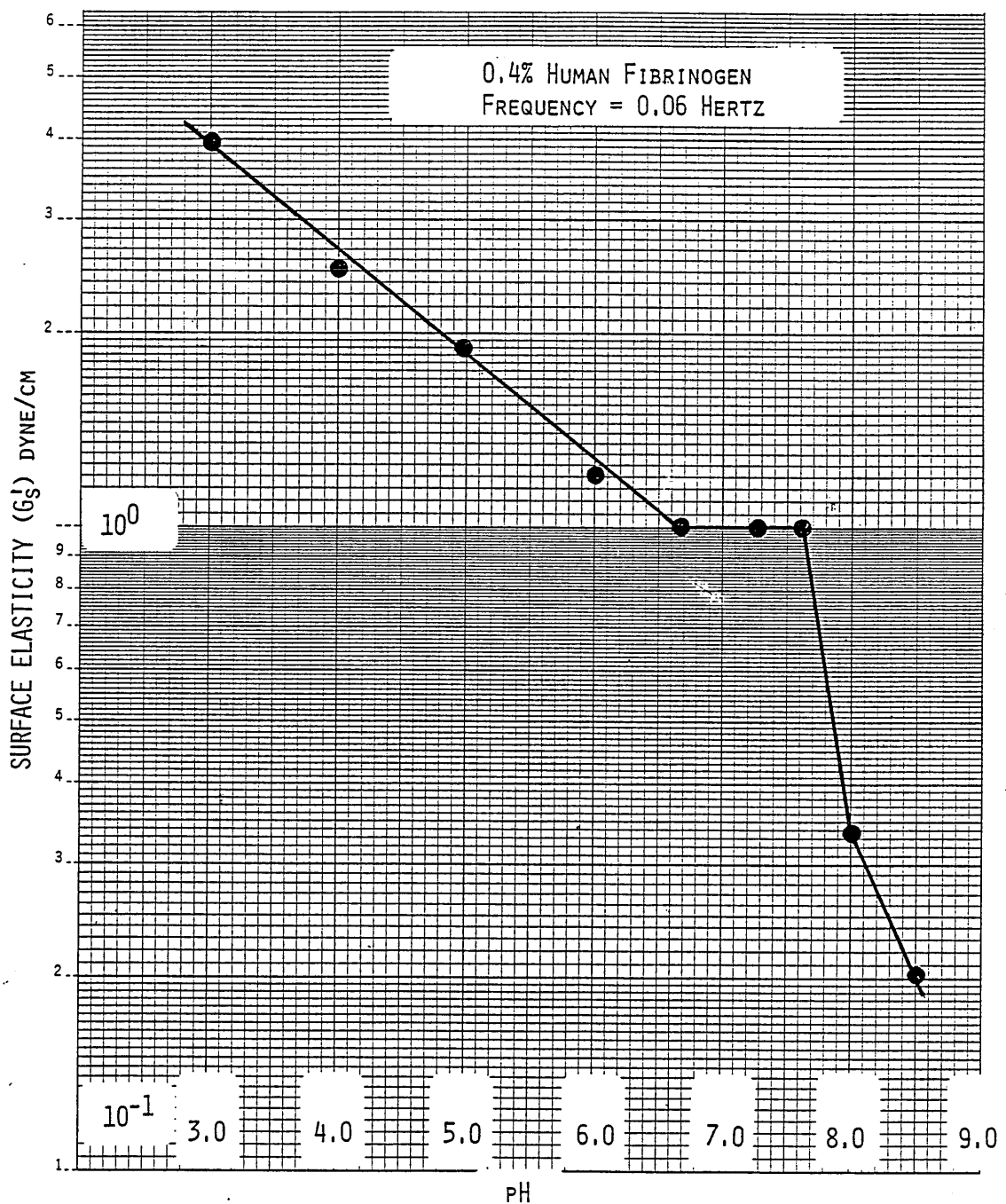


Figure 10. The effect of pH on G_s^i of surface layers of a preparation of 0.4% fibrinogen. As pH is lowered, G_s^i increases, while at pH 8.6 it is weakest. There is a plateau over the pH range 6.8 to 7.6 which are approximately physiological normal values.

surface, the pH would be higher. According to Seaman, charges can occur in patches, arrays or clusters and in such microregions, the pH could be 2 or 3 pH units lower than in the bulk, and would vary in different areas of the red cell depending on the local potentials. If the potential was to change as much as $\pm 200\text{mV}$, then the pH could change as much as 8 pH units. This would mean that a pH of from between 3 to 11 could possibly be attained locally. Virtually all cell surfaces carry a net negative charge under physiological conditions, so in general, surface pH values would be lower than the bulk values. A discussion of the underlying theory relevant to the concept of surface pH, has been given in a review by McLaren and Babcock (29). Surface pH and surface and bulk dissociation constants have been discussed by Seaman (30). The distribution of charge at a biological surface is obviously an effective means of controlling enzyme activities and ensuring that enzymes with very different pH optima, are able to function at the same time in the same biological system (31). Dintenfass and Burnard (32-33), found that the blood pH affects the viscosity of blood, particularly at high hematocrit. A 30 fold increase of rigidity of red cells at low pH is responsible for the increase in viscosity. This was also described by Teitel and Nicolau 1964 (34), Murphy (35), and by Schmid-Schönbein et al. 1975 (36).

The inhibitory action on fibrinogen surface layer formation by certain heparins, dextrans and sodium hyaluronate preparations.

The fibrinogen surface layer is considered to be a gel structure. It was, therefore of interest to find

out whether heparin, which is known to have an anticoagulant action, primarily by its affinity to antithrombin, would also have an antagonistic action to the gelation of surface layers of fibrinogen where thrombin does not play a role. The focus of this study is on the elastic modulus of these fibrinogen surface layers, since the elastic modulus is a function of the crosslinking, and its magnitude provides data concerning the organization of a thromboid (thrombus-like) structure. Heparin has an antigeloplastic action as well as an antithrombin effect. "Gelo-plastic" is defined as a general term, meaning the promotion of gelatin, while "antigeloplastic" signifies inhibiting gelation. The therapeutic action of heparin as an antithrombotic agent is considered to be due to its anticoagulant action.

The term "antithrombotic" is a term for the inhibition of any of the processes in the formation of a mixed thrombus, similar to that of mixed clotting, as well as for the inhibition of the further development of the pathologic condition of thrombosis. The term "antithrombotic" is therefore used for the inhibition or prevention of any of the three clotting processes in vivo, leading to thrombosis. Its use is applicable as well to any agent which would counteract any hemorheological and hemodynamic disturbances which would augment the propagation of the mixed thrombus and lead to the pathological condition of thrombosis.

Heparin is a mucopolysaccharide, and is prepared from lung tissue or intestinal mucosa, is not a uniform substance and it is therefore, difficult to obtain preparations of the same anticoagulant activity. In this

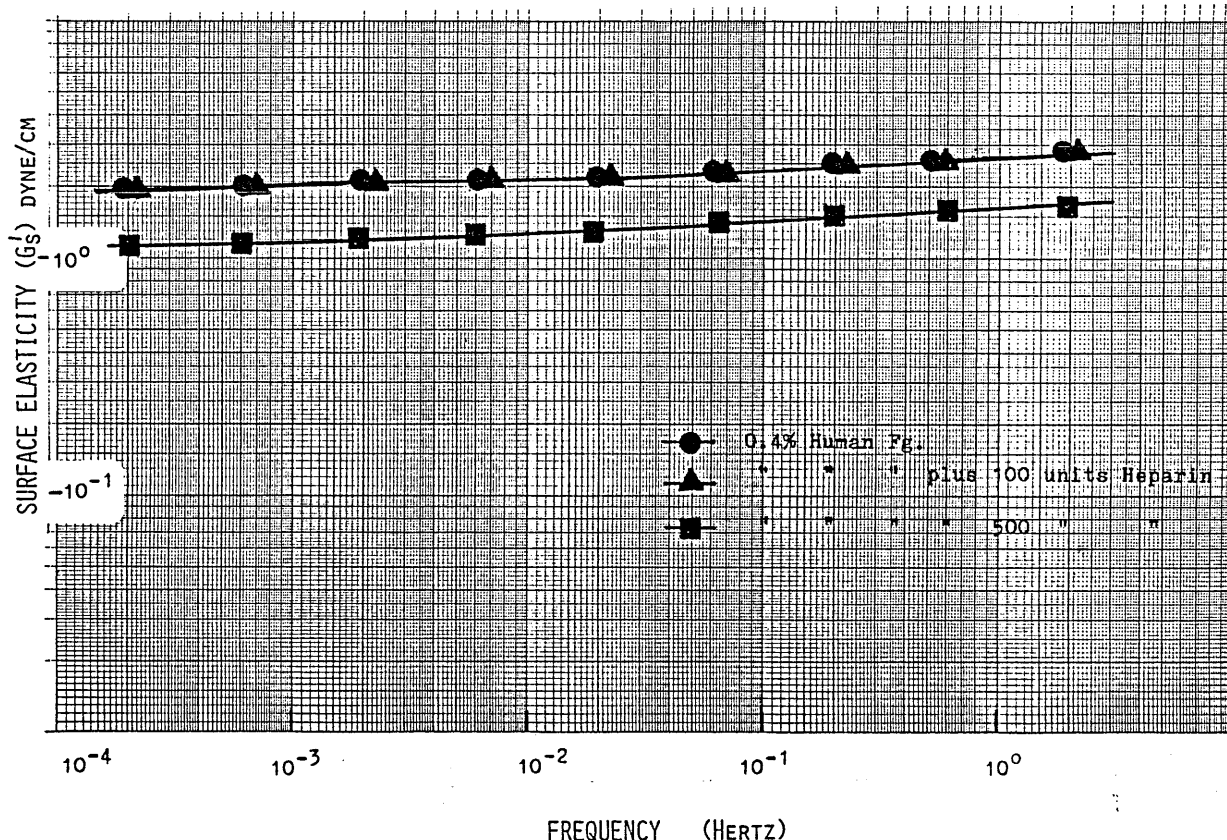


Figure 11. Comparisons of the surface elasticity (G_s^1) of surface layers of 0.4% human fibrinogen as control, compared with a 0.4% fibrinogen preparations to which 100 and 500 NIH units of heparin are added.

respect the effect, on the elastic modulus of fibrinogen surface layers, of the different heparins of different manufacturers and specially prepared heparins of various researchers has been investigated. It can be shown that there are certain heparin preparations, irrespective of their anticoagulant activity, which have a weakening effect on the elastic modulus of fibrinogen surface layers.

Figure 11 shows the effect of 100 and 500 NIH units of one of these heparin preparations (Organon) on the elastic modulus (G_s^1) of surface layers of human fibrinogen. While the 100 NIH unit does not weaken the G_s^1 component, the addition of 500 NIH units does weaken the structure. It appears that this particular preparation has a low antigeloplastic activity, as far as surface gels of fibrinogen are concerned.

Figure 12 presents an experiment with a heparin prepared by Lindahl (Sweden). This heparin does not show an affinity for antithrombin. Nevertheless it effects a marked lowering of the elastic modulus of a fibrinogen surface layer. This experiment demonstrates that there appears to be no relationship between what is considered to be anticoagulant activity, and the surface antigelo-plastic action of some of these heparins. This finding can be interpreted as confirmation that a heparin preparation which has no affinity for antithrombin, can still

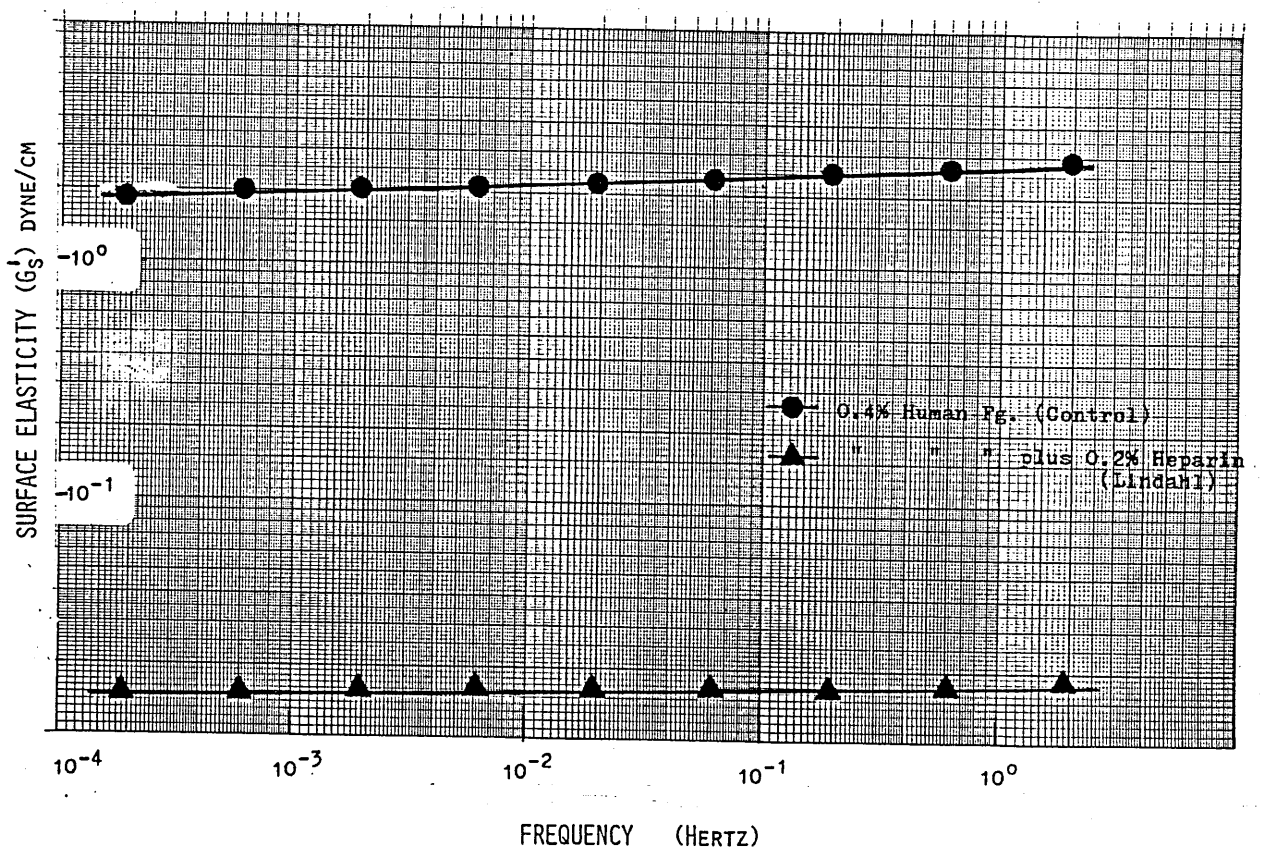


Figure 12. A plot of the Surface Elasticity (G_s') of 0.4% Human Fibrinogen compared with a 0.4% fibrinogen plus 0.2% heparin prepared by Lindahl. This heparin preparation does not show any affinity for antithrombin, but still considerably weakens G_s' .

have an antithrombotic effect.

Figure 13 shows the effect of two different low molecular weight heparin fractions (Lasker) on the G_s' of a fibrinogen solution. Both have a high affinity for anti-thrombin. It can be seen that the heparin, preparation B,

has no effect on the surface elastic modulus (G_s^1). The second heparin, preparation A, has a considerable weakening effect. This example demonstrates that these heparin preparations, while they have similar anticoagulant activity, do not necessarily have a high or even similar surface antigeloplastic activity. It is considered that the heparin preparation that had the strong effect on the surface layer, has a strong antithrombogenic action in contrast to the other one. It would appear, therefore, that the measurement of the antithrombin activity of a heparin may not completely evaluate its performance as an antithrombotic agent. Its antigeloplastic activity in inhibiting the formation of fibrinogen surface gels should be evaluated as well.

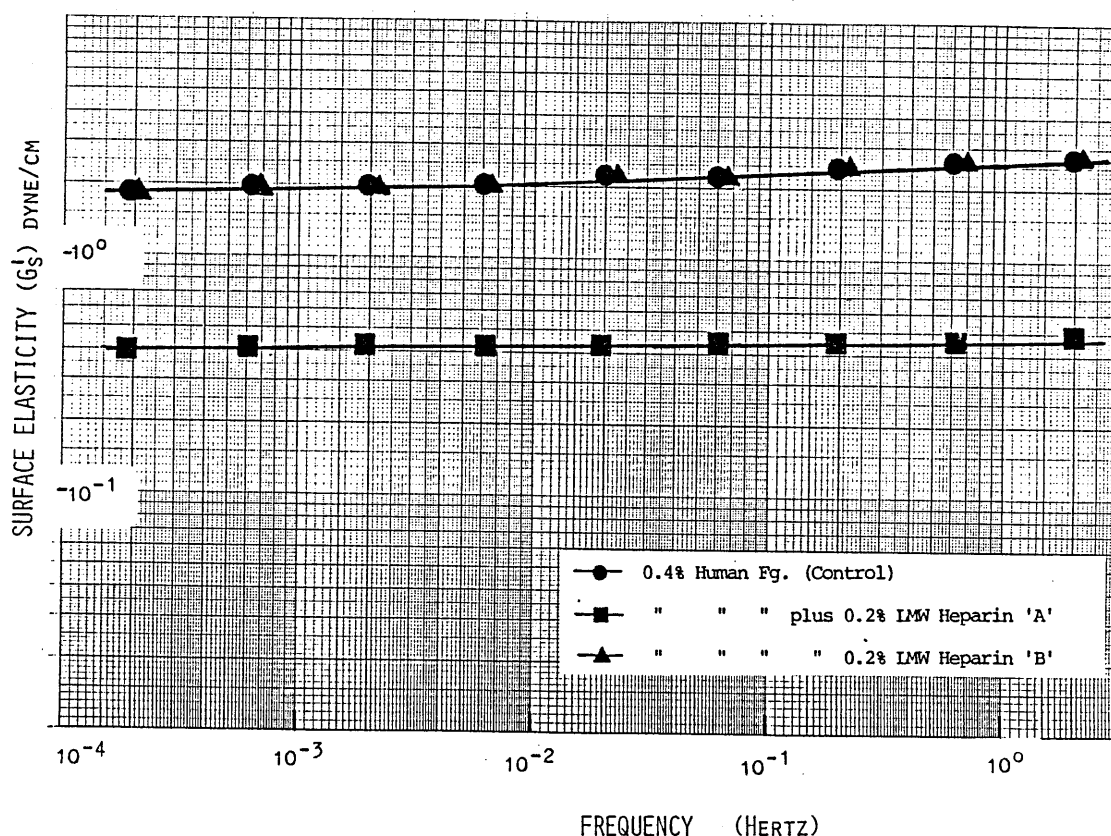


Figure 13. The effect on surface elasticity (G_s^1) of surface layers of 0.4% human fibrinogen when two different low molecular weight heparin fractions are added.

Figure 14 shows data obtained with a preparation of sodium heparin and a calcium heparin (Choay). The sodium heparin does not decrease the G_s^1 of the fibrinogen surface layers. The calcium preparation on the other hand increases the G_s^1 . These findings are not surprising as calcium can be shown to be a gelation promoting agent in coagulation studies (37-39). The calcium heparin preparation has a high affinity for antithrombin, but it appears that, in spite of this activity, it may not be as

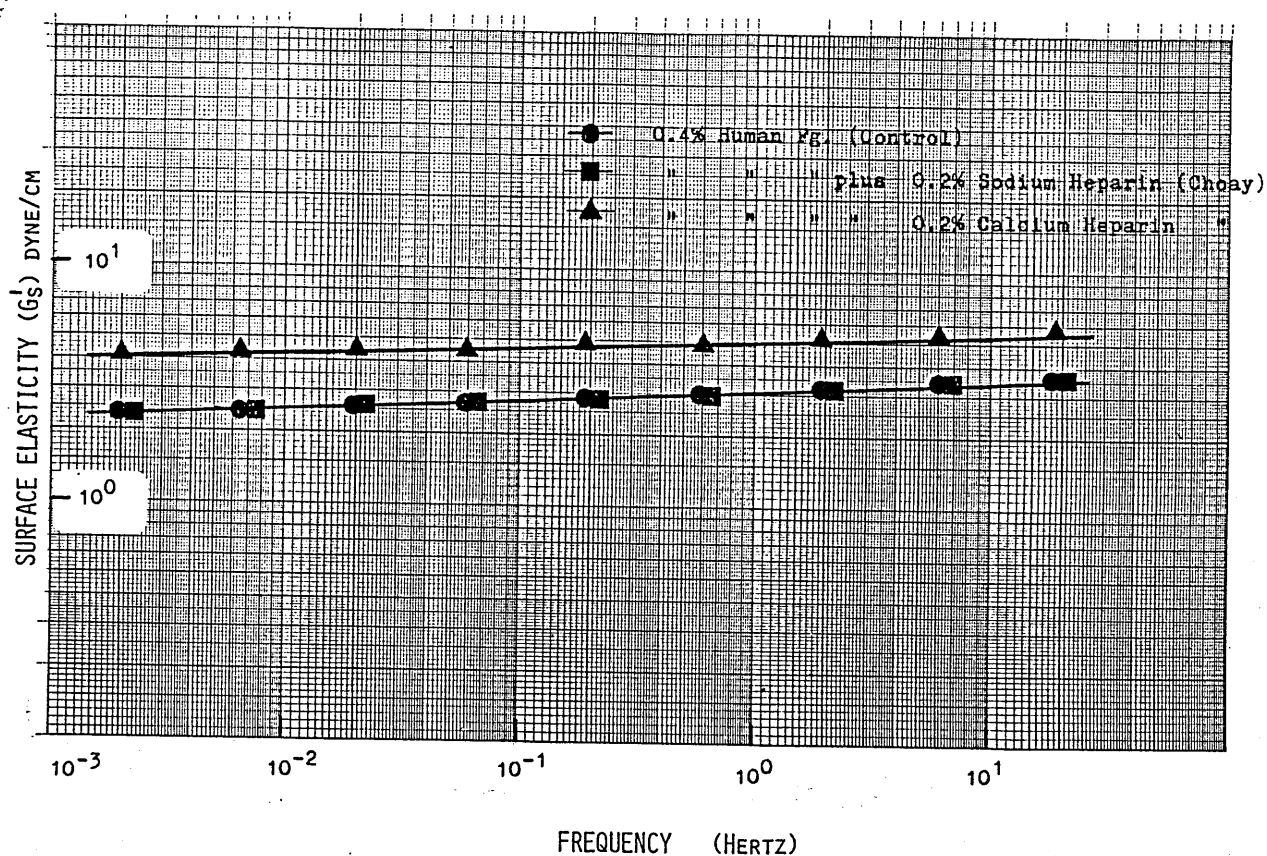


Figure 14. Plots showing the effect on G_s^1 of surface layers of 0.4% fibrinogen solutions when a sodium heparin and calcium preparations (Choay) are added.

effective in antithrombotic therapy, as the heparin preparation containing calcium does not inhibit surface fibrinogen gel coting. These findings may open a new field of study regarding the efficacy of an antithrombotic agent because the therapeutic action of such an agent may not merely depend on its anticoagulant action or on its affinity for antithrombin.

Figure 15 shows a plot of the viscous and elastic moduli of surface layers of fibrinogen versus frequency as control, together with a second plot of η_s' and G_s' of the surface layer of a fibrinogen preparation to which 5mM Ca Cl₂ has been added. This increases the viscous and elastic moduli of the surface layer by approximately 30 percent.

Low molecular weight depolymerization products prepared from commercial heparin demonstrated a strong inhibitory action on fibrinogen gel clotting. Figures 16

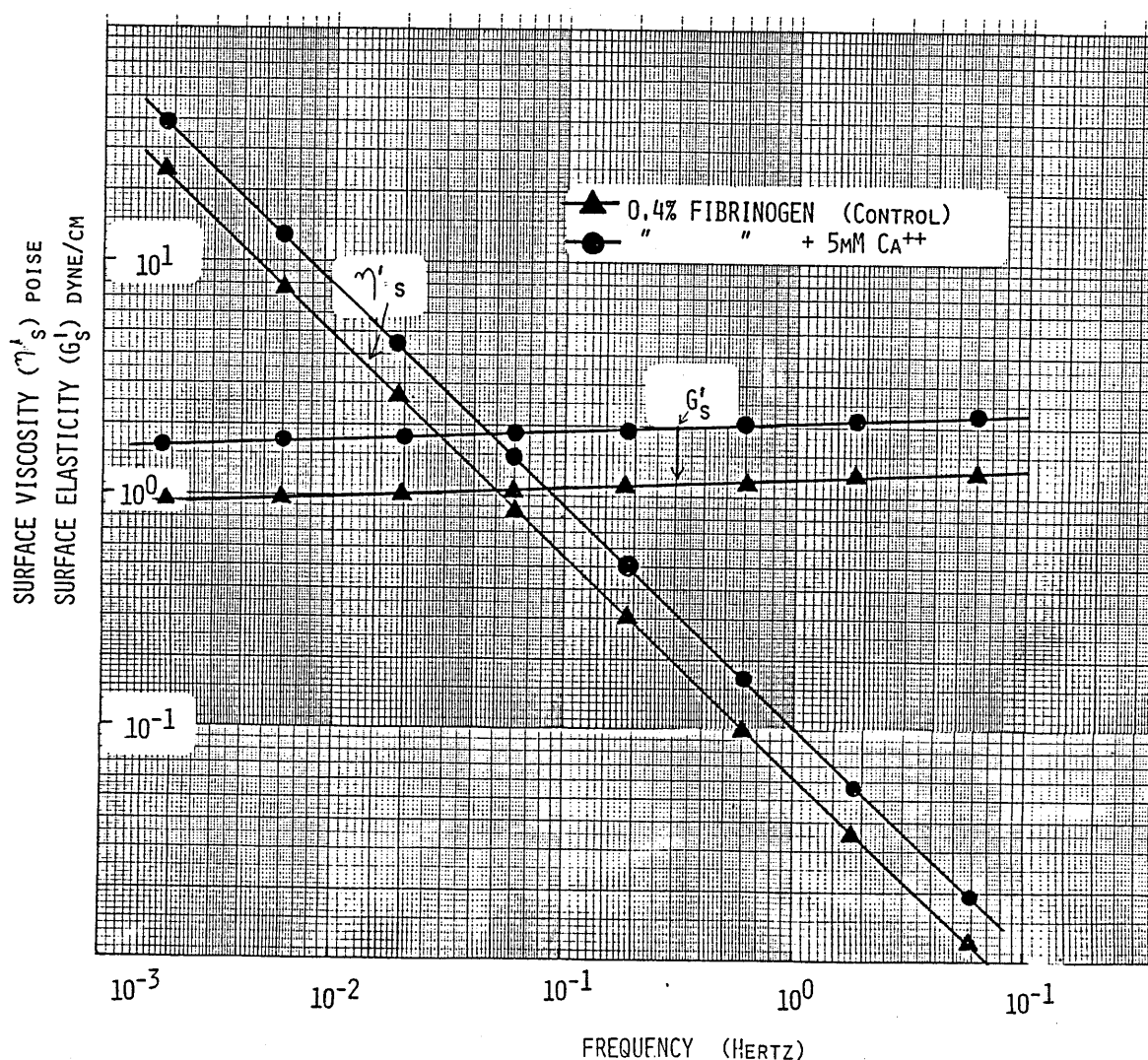


Figure 15. The viscosity (η_s') and elasticity (G_s') moduli versus frequency, of surface layers of a 0.2% fibrinogen solution in a tris-saline buffer of pH 7.4, compared with a similar preparation containing the addition of 5mM Ca Cl₂.

and 17 show surface viscosity and surface elasticity values of layers of fibrinogen to which low molecular weight derivatives of a heparin fraction from another source, were added. Heparin of 4400, 5300 and 5900 MW were added at a concentration of 0.2% to preparations of 0.4% human fibrinogen. The preparation of 4400 MW weakened the layer by about 30 percent, while the 5300 and 5900 MW

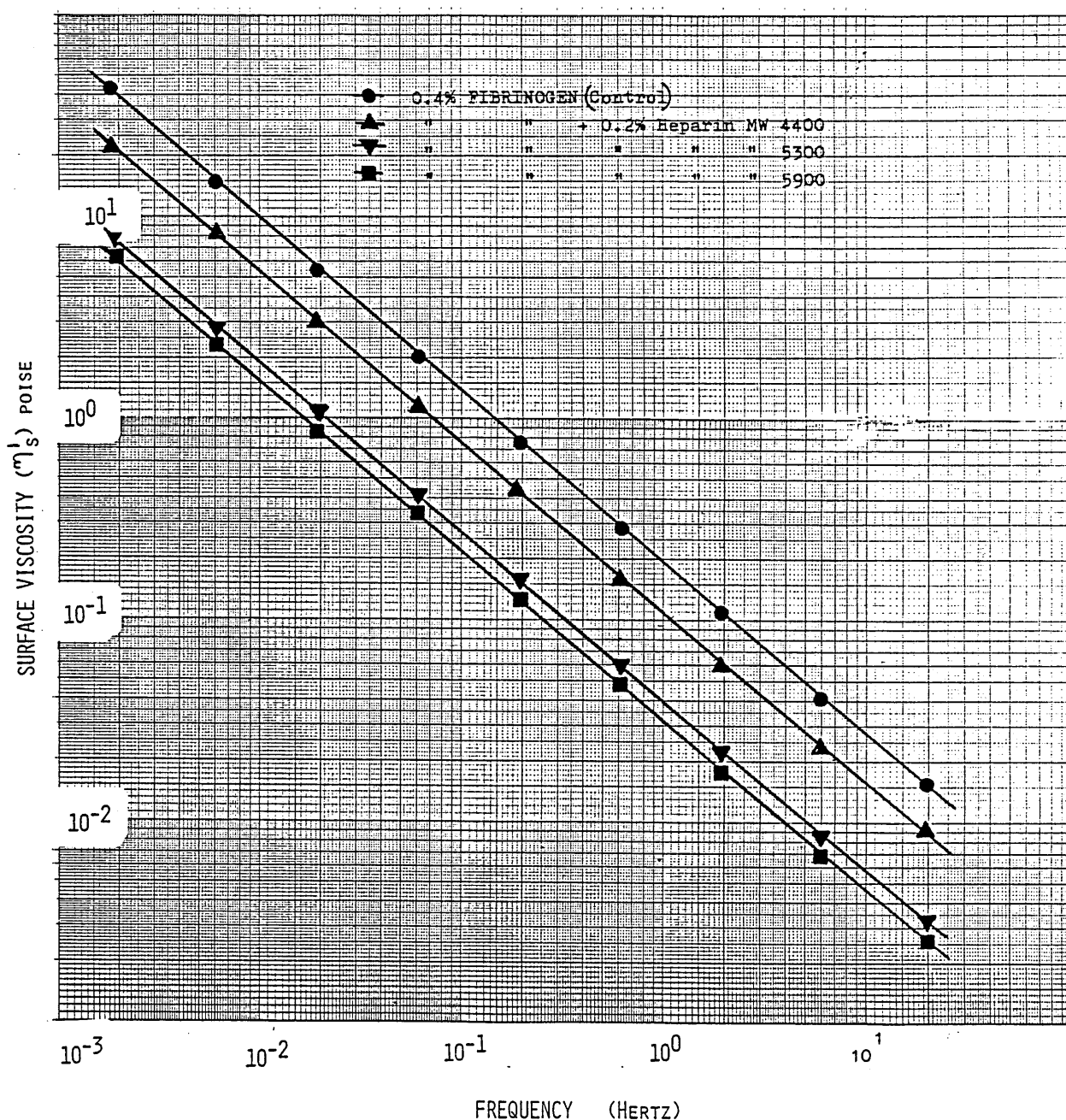


Figure 16. Surface viscosity (η_s'), versus frequency of a 0.4% fibrinogen solution as control, compared with three fibrinogen preparations to which heparin depolymerisation products of MW 4400, 5300 and 5900 have been added.

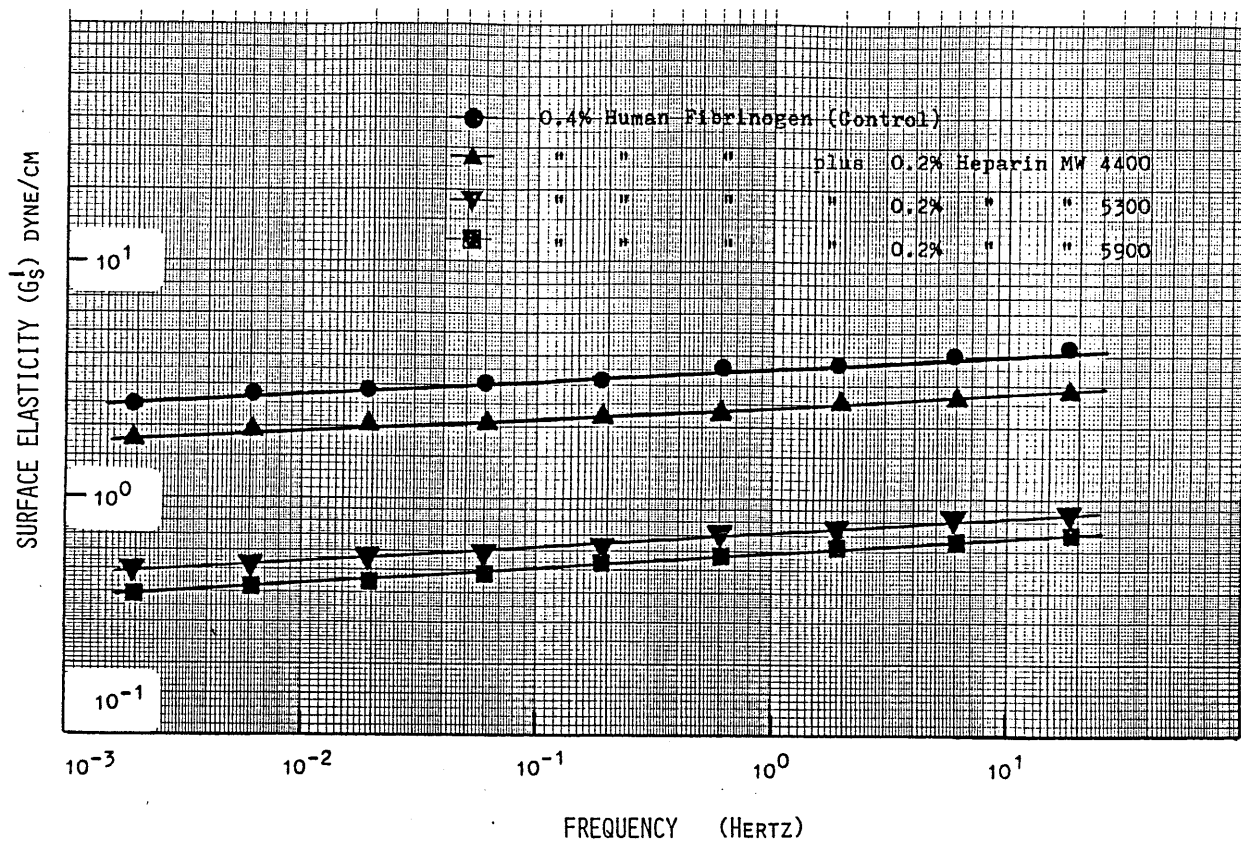


Figure 17. Surface elasticity (G_s') versus frequency of a 0.4% fibrinogen solution as control, compared with 0.4% fibrinogen solutions to which heparin depolymerisation products of MW 4400, 5300 and 5900 have been added.

preparations showed decreases of about 75 percent.

Ockelford et al. (40) reported recently a lack of relationship between the in-vivo antithrombotic effect of low molecular weight heparin employing experimentally thrombosed animal models, and extra vivum anti-thrombotic action. They concluded from their findings that "other properties of low molecular weight herapins contribute to their antithrombotic effectiveness" since this activity, measured extra vivum, is not always predictive of in vivo antithrombotic efficacy. The marked decrease in viscous and elastic moduli of surface layers of fibrinogen/LMW heparin systems, appears to show that the antithrombotic efficacy of these heparins, observed by Ockelford et al. is due to their antithrombogenic action.

Morrison et al. 1968 (41), reported in vivo findings in rabbits, of marked antithrombotic action of chondroitin-4-sulfate (chondroitin A), which is one of several natural glycosaminoglycans. Bjornson et al. 1982 (42), showed chondroitin sulfate A to have certain anti-coagulant properties, but that its antithrombotic action could not be fully explained.

Figure 18 shows the effect on the surface elasticity of fibrinogen systems when chondroitin is added. Chondroitin A, B and C was found to reduce the elastic moduli by about 40 percent when compared to the fibrinogen control, confirming the findings of Morrison that chondroitin A has antithrombotic action. Similar antithrombotic action may be expected to be shown by other glycosaminoglycans.

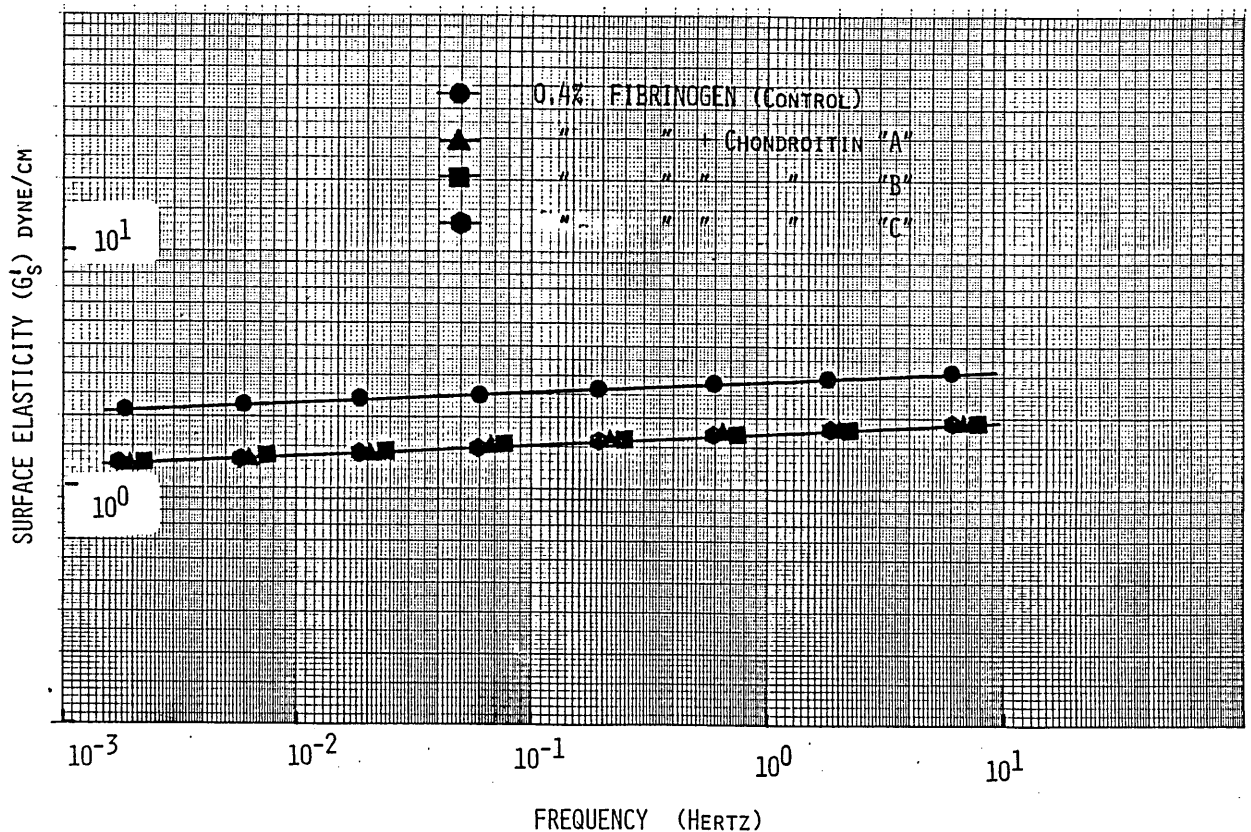


Figure 18. The elasticity (G_s') of a surface layer of a 0.4% solution as control, compared with fibrinogen solutions to which chondroitin A, B and C were added.

In the study of another substance, Dextran with MW 20,000 was found to reduce the viscosity and elasticity of surface layers of fibrinogen by about 50 percent as compared to the fibrinogen control. This is shown in Figure 19. Figure 20, shows that dextran sulfate MW 17,000, caused a decrease in elasticity of fibrinogen surface layers, also by 50 percent. Figure 21 shows the reducing effect on the viscous and elastic modulus of these fibrinogen surface layers when sodium hyaluronate was added, as compared to the fibrinogen control curve.

The oral administration of antithrombotic agents such as low molecular weight depolymerization products of

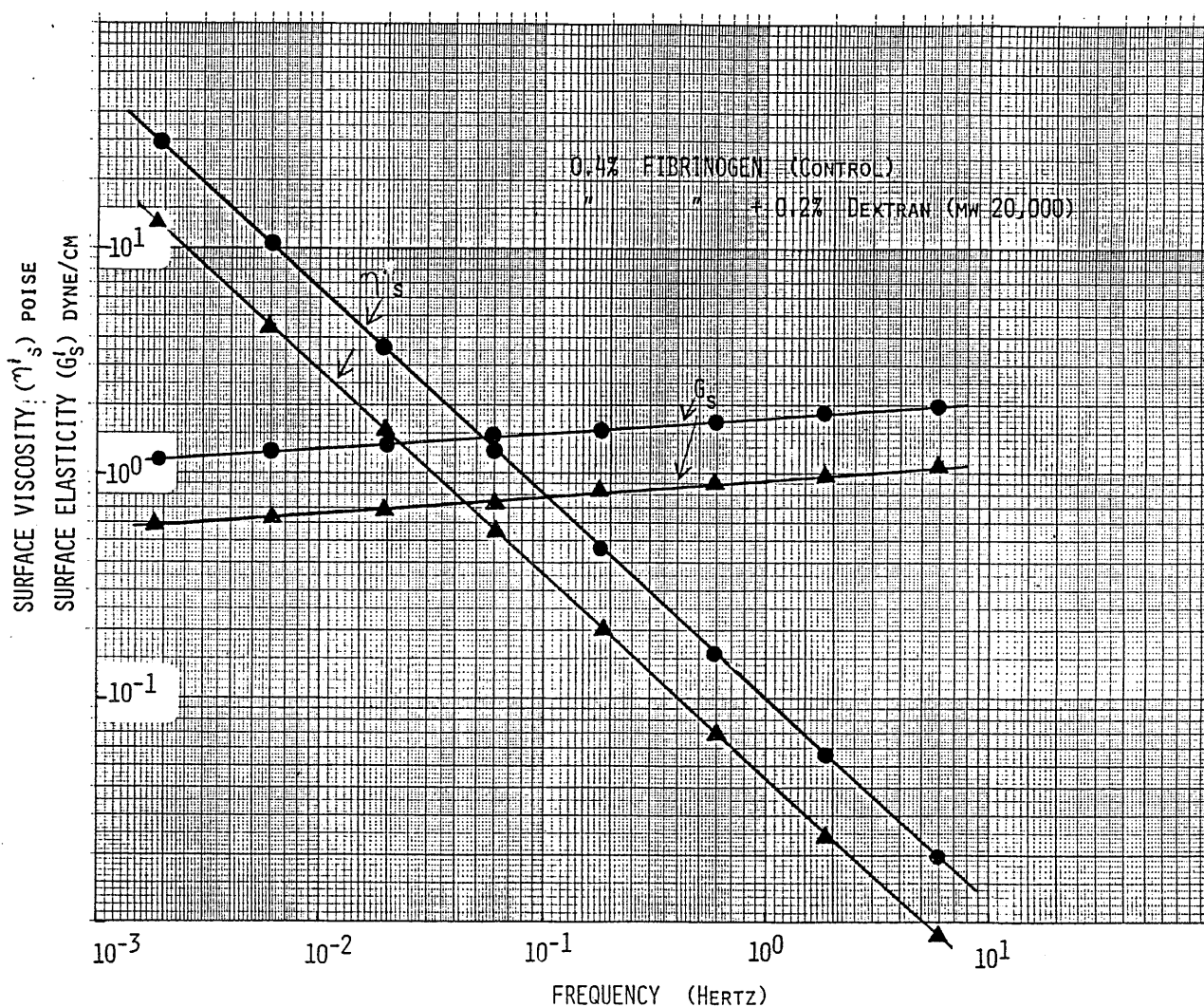


Figure 19. The viscous (η'_s) and elastic moduli (G'_s) of surface layers of a 0.4% solution of human fibrinogen plus 0.2% dextran, MW 20,000 compared to a 0.4% human fibrinogen preparation as control.

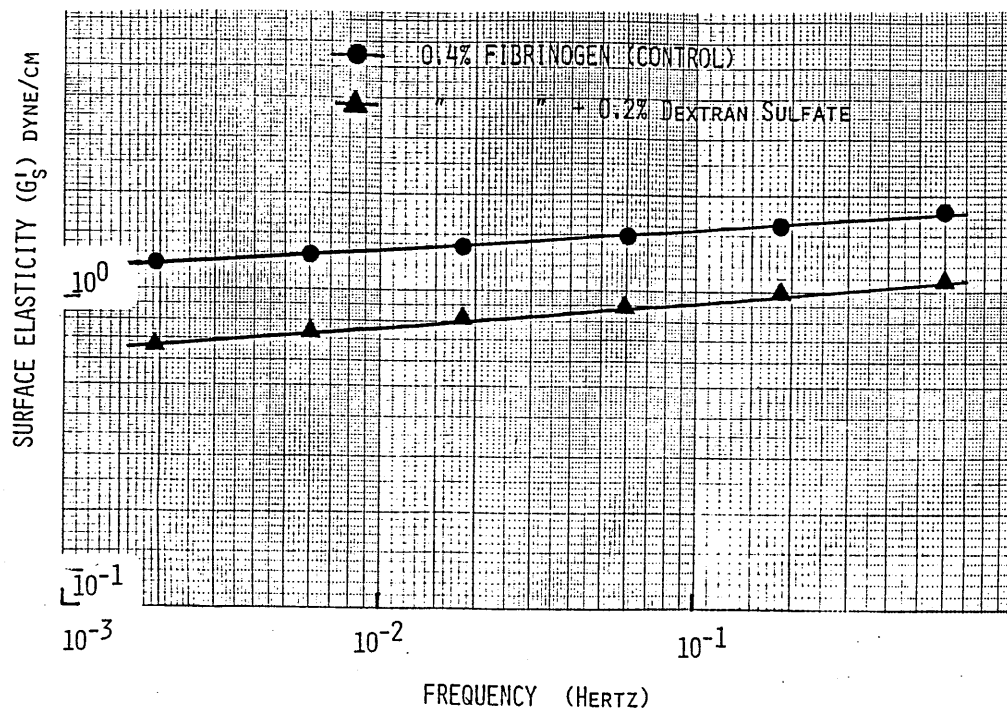


Figure 20. Surface elasticity (G'_s) of surface layers of 0.2% fibrinogen solution plus 0.2% dextran sulfate (MW 17,000) compared to 0.2% fibrinogen solution as control.

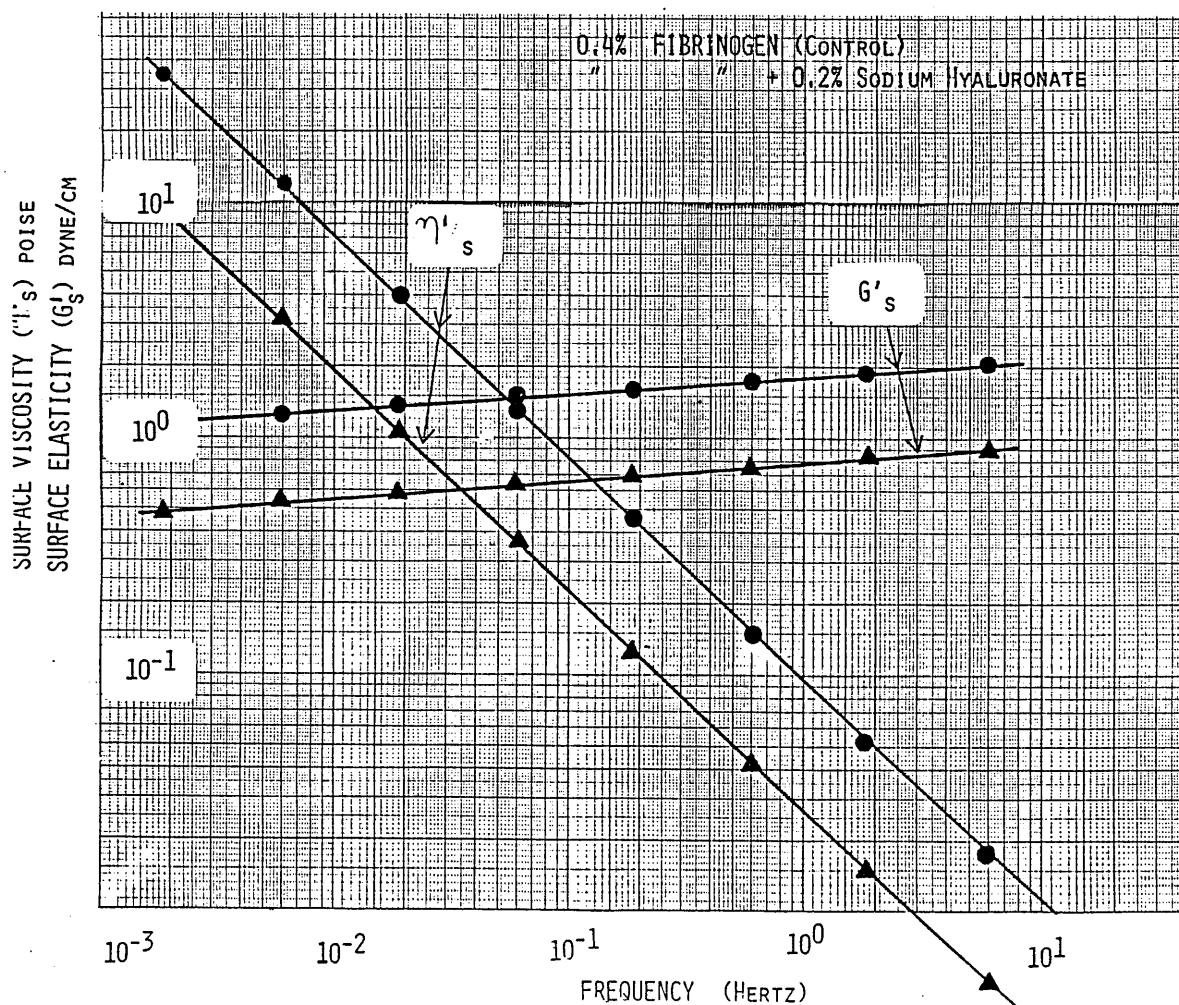


Figure 21. The viscous and elastic moduli of 0.2% sodium hyaluronate plus 0.2% human fibrinogen solution surface layers, compared to a 0.2% fibrinogen solution as control.

heparin, or other low molecular weight glucosaminoglycans, and the intravenous administration of certain dextran preparations may prove to be an important and new approach, to the prevention of thrombotic conditions. Thus the investigation of fibrinogen surface gels may prove to have clinical value as a diagnostic tool and also for establishing the value of an antithrombotic agent.

The Rheology of Surface Films of Extrinsic and Intrinsic Red Cell Membrane Proteins

Extrinsic Protein

The rheological properties of extrinsic red cell proteins, spectrin and actin (S+A) that line the inner surface of the red cell membrane were studied from the point of view of their possible role in the red cell membrane structure and function. The amount of S+A that is normally present in the membrane, can form at least one monolayer and probably two when one considers that other membrane components (e.g., band 4.1 protein) are intermixed with it. The magnitude of the rheological parameters of the S+A when spread as a film, is close to the analogous parameters of the red cell membrane itself, and then, must make a large contribution to the physical proportion of the intact red cell membrane.

Preparations and methods

Solutions of spectrin and actin was prepared from membranes of human erythrocytes obtained from out-

dated blood bank blood. Following centrifugation and removal of the plasma and buffy coat, the erythrocytes were washed with cold isotonic buffer (39mM KCl). Washed packed cells were hemolyzed in 12 volumes of 8mM Na- Po_4 , pH 7.4, for 30 minutes at 4°C, and the ghost membranes isolated, Dodge et al. 1963 (43). The ghost cells were stored frozen at -20°C overnight, and then extracted with 10 volumes 0.1mM sodium EDTA (pH 8.0) for 20 minutes at 37°C. Centrifugation at $78 \times 10^3 g$ (30 min. at 4°C) yielded a clear supernatant (typical protein concentration 0.2 mg/ml) which was a 1:1 mixture of spectrin (bands 1 and 2) and actin (band 5) as judged by the Coomassie Brilliant Blue bands seen after SDS-polyacrylamide gel electrophoresis.

The "Ring in Ring" geometry, described in Chapter II page 22 was used with the Rheogoniometer for measurements of the rheological properties of the protein layers in oscillatory shear. The protein is carefully layered over 4 ml of saline added to the trough. 1 ml of decane is layered over the protein, and the upper ring is then lowered so that it just penetrates the protein layer. All studies were performed at 25°C. The frequency of oscillation was varied from 1.9×10^{-3} to 1.9 Hertz and the amplitude of oscillation was set at 0.04 radians. The oscillatory motion of the lower ring, and the angular displacement of the upper ring were fed to the PDP 11/10 (Digital) computer. From the phase shift and the amplitude ratio between the input and the output sinusoidal motions, the viscous and elastic components (η_s^1 & G_s^1) were calculated.

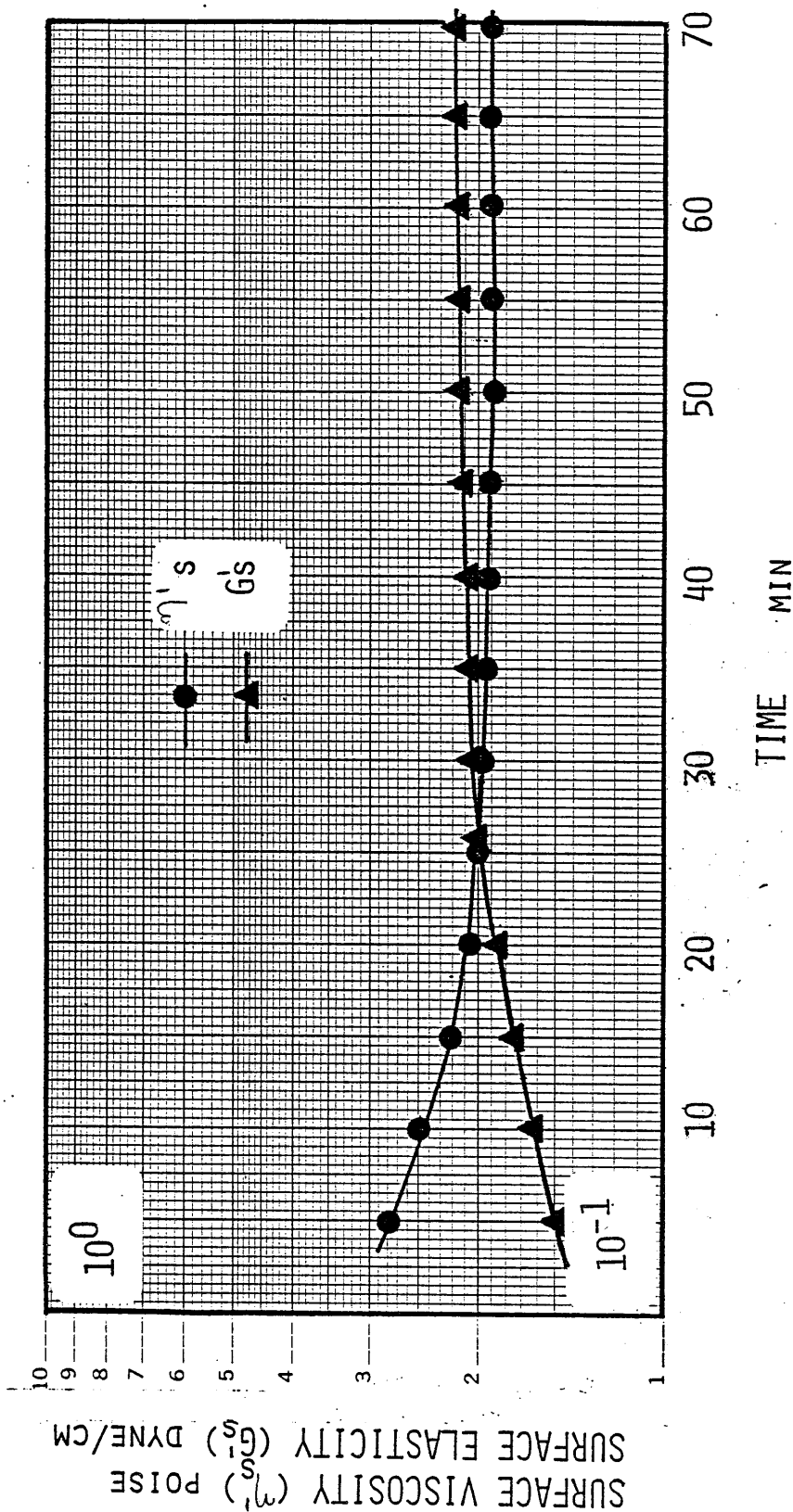


Figure 22. The Surface Viscosity, (η_s) and the Surface Elasticity, (G_s) of spread Spectrin/Actin surface films, plotted as a function of time, showing the effect of age on the surface film.

Figure 22 shows the viscosity (η_s') and the elasticity (G_s') of the spread S+A film plotted against time. Figures 23 and 24 show the effect on η_s' and G_s' of increasing film thickness and surface concentration. These are estimated assuming a partial molar volume of protein on a surface equal to that in solution, ($1.3 \text{ cm}^3/\text{g.}$) combining this figure with the value for the surface concentration of a close packed S-A film, ($1.4 \times 10^{-7} \text{ g/cm}^2$) a thickness of 18\AA is obtained.

Discussion

In a recent review, Kirkpatrick 1976 (44), has indicated that spectrin is an important structural element of the red cell membrane that exists in the form of a network. According to this view, the spectrin is not close packed, but there are strong links between the molecules themselves and other proteins that are present in the same layer (e.g., actin). Using the available value for total erythrocyte membrane proteins per cell and the known area of a cell, the average surface concentration of total proteins is:-

$$\frac{10^{-12} \text{ g/cell}}{140 \text{ m}^2/\text{cell}} = 7.1 \text{ mg/m}^2$$

The average surface concentration due to the spectrin and actin mixture (SxA), which is approximately one-third of this value, would be 2.4 mg/m^2 . The latter figure, a measure of the surface concentration on the inner face of the erythrocyte membrane, is equivalent to an area of $0.42 \text{ m}^2/\text{mg.}$ of S+A.

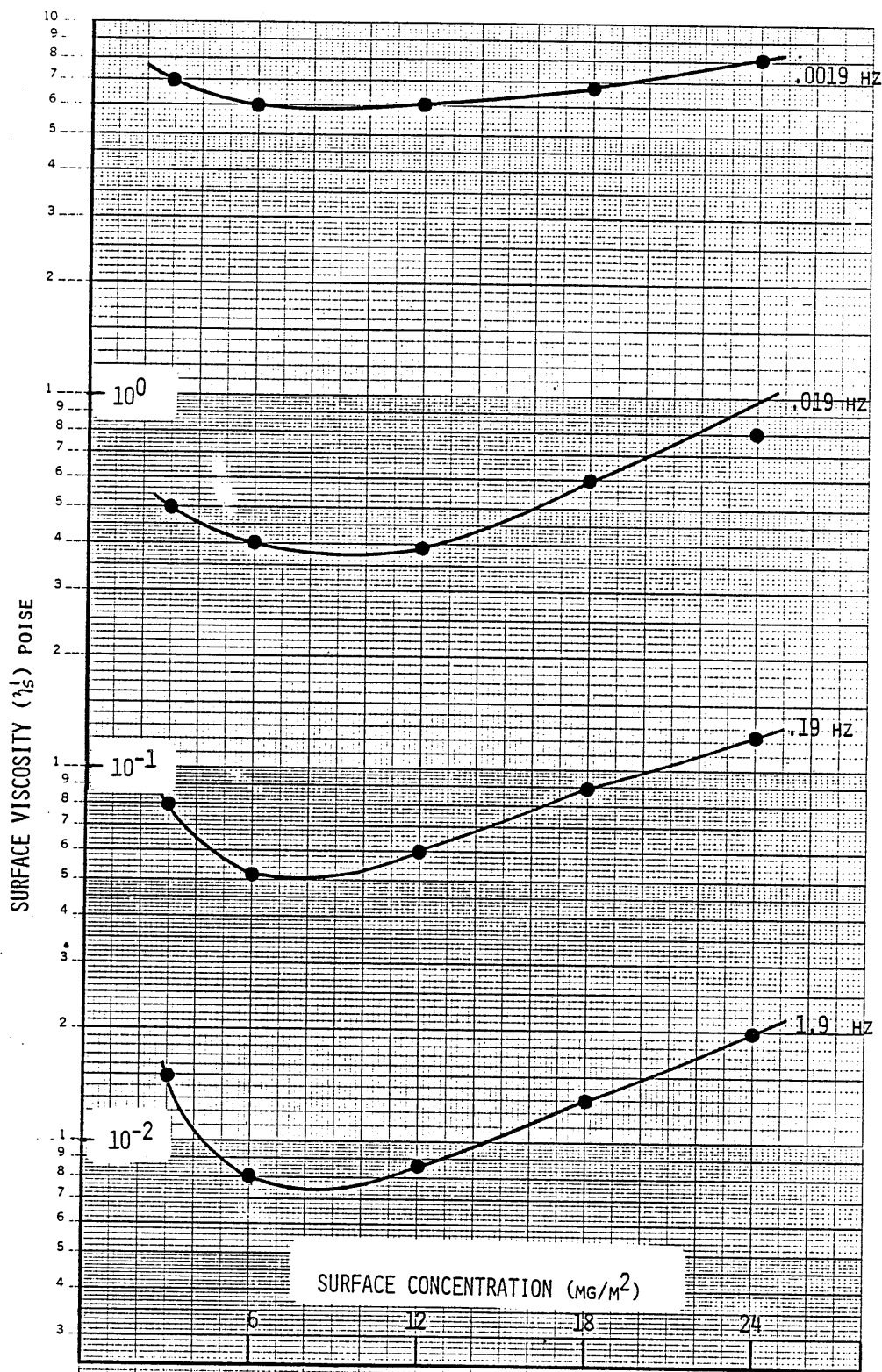


Figure 23. The surface viscosity, (η_s') of spread Spectrin-Actin surface films as a function of surface concentration.

If the S+A on the inner face of the erythrocyte membrane does form a close packed monolayer, the mechanical properties of the S+A layer should reflect those of the membrane. The measured properties of the S+A film do in fact, compare reasonably well to those made on intact erythrocyte membranes, Chien 1977 (45). The extensional elastic modulus of the membrane is given as about 10^{-2} dyn/cm. The membrane viscosity, at low frequencies is of the order of 10^3 dyne.sec/cm². The viscosity of the S+A films vary with frequency, and at low frequencies the values are of the order of $10^2 - 10^3$ dyne.sec/cm². Those values confirm that the properties of a S+A film at the inner face of the erythrocyte can account for much of the observed properties of the intact cell.

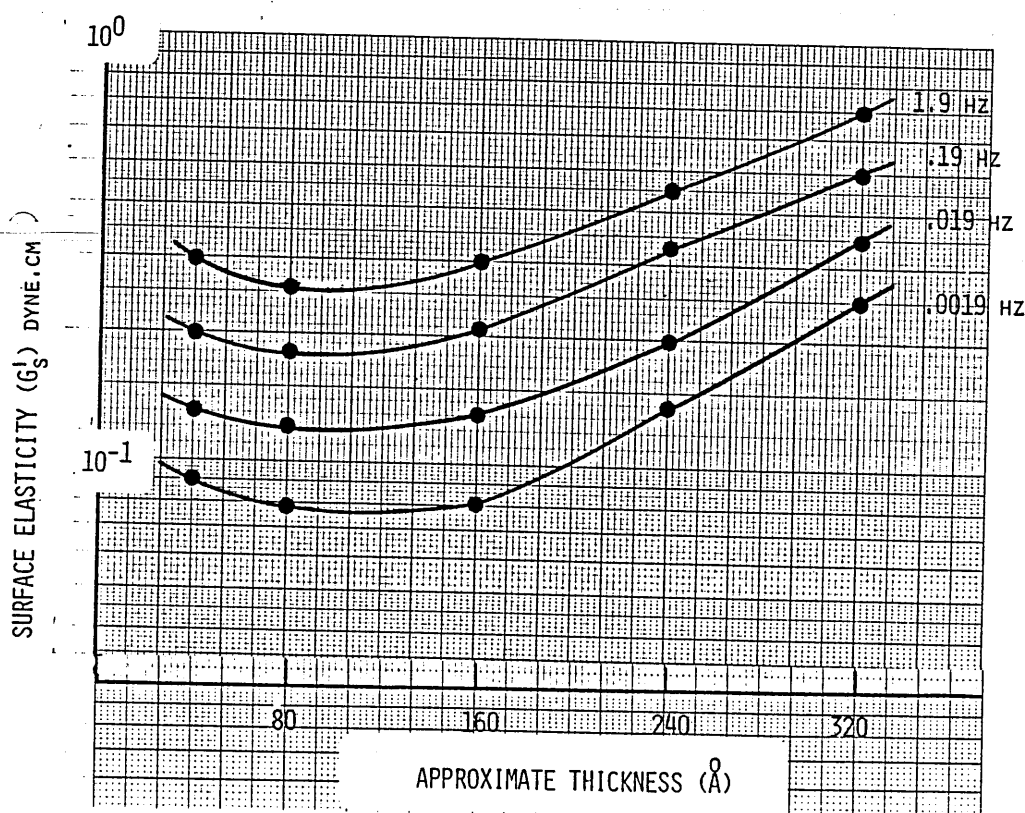


Figure 24. The surface elasticity, (G'_s) of spread spectrin/actin surface films plotted as a function of the approximate film thickness in angstroms at four different frequencies.

Intrinsic Red Cell Membrane Proteins

Intrinsic membrane proteins (IMP), the proteins which are present in the red cell membrane proper, were prepared from red cell membrane ghosts. These preparations primarily contained polyacrylamide gel bands 3, 4, 6 and 7. The measured surface isotherms varied depending on the relative amounts of protein, and was dependent on the average molecular weight. The molar volume ($1.3 \text{ cm}^3/\text{g}$) was multiplied by the amount of protein spread, to calculate the average thickness of the protein that was deposited at the interface, and the number of equivalent layers of protein could then be estimated.

The IMP films are spread in the "Ring in Ring" geometry and measured in the same way as the extrinsic proteins.

Figure 25 shows the surface viscosity (η_s^l) plotted as a function of the protein layer thickness. It can be seen that η_s^l varies inversely with the frequency. η_s^l is also dependent on the layer thickness, but shows a plateau between 80 and 160 Å. Figure 26 is a plot of surface elasticity (G_s^l) plotted in the same way. The dependence on layer thickness is again apparent, but G_s^l is less dependent on frequency. Figure 27 is a plot of η_s^l and G_s^l , of the layer at an estimated thickness of 100 Å, plotted against frequency. The viscosity (η_s^l) decreases with frequency, while the elasticity (G_s^l) increases with frequency.

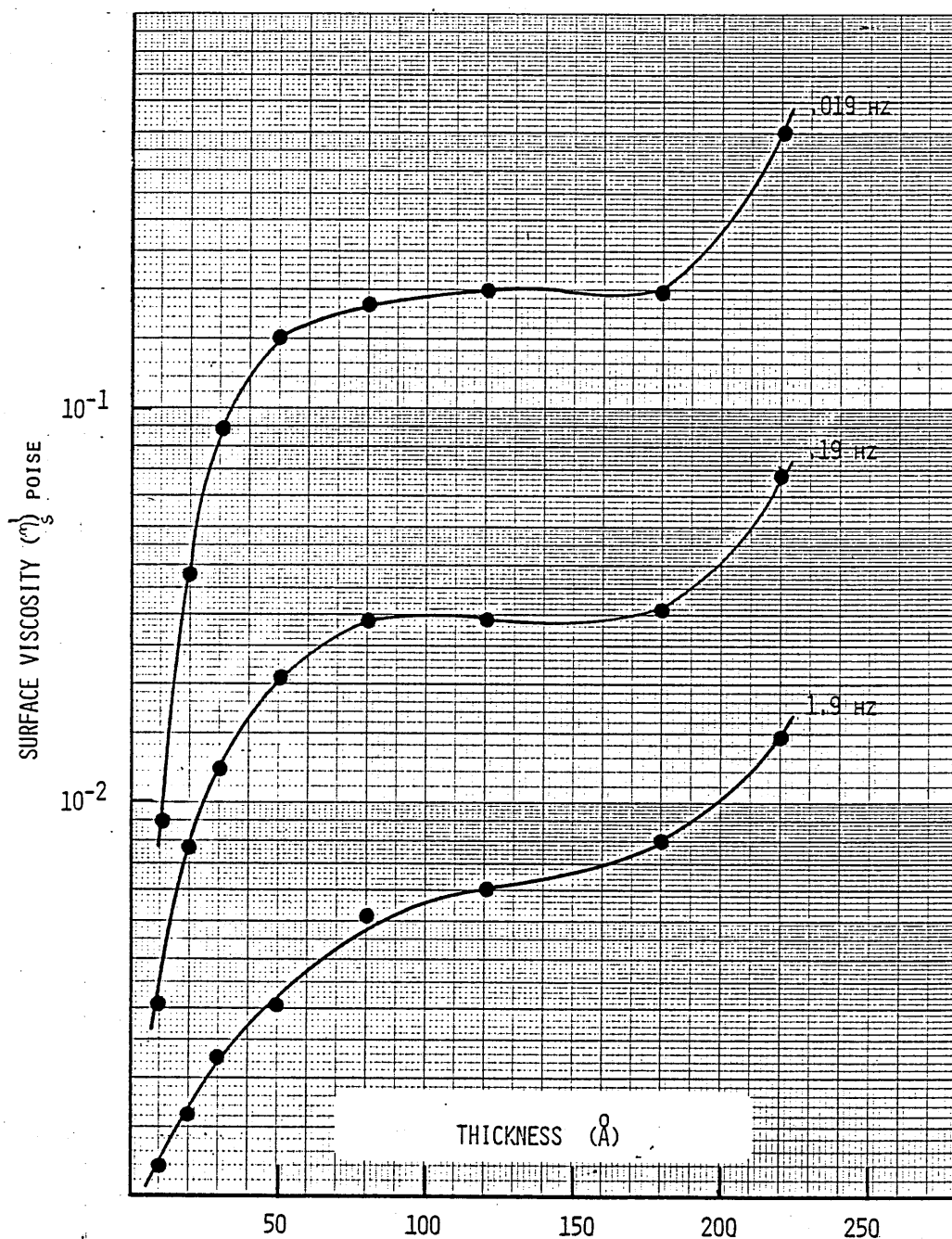


Figure 25. The surface viscosity (η_s^i) of spread layers of intrinsic red cell membrane proteins plotted as a function of the thickness of the film, at three different frequencies of oscillation.

Discussion

If a comparison is made between the data obtained for the intrinsic and extrinsic membrane proteins, it will be seen that the viscous and elastic moduli of IMP are lower by a factor of about five, but they have the same dependence on frequency and a similar dependence on

film thickness above 150A.

The extrinsic (S+A) films are composed of molecules that are present at the inner face of the red cell membrane and are thought to have an important role in maintaining structural integrity. It is surprising that the IMP, which are probably random structures embedded in

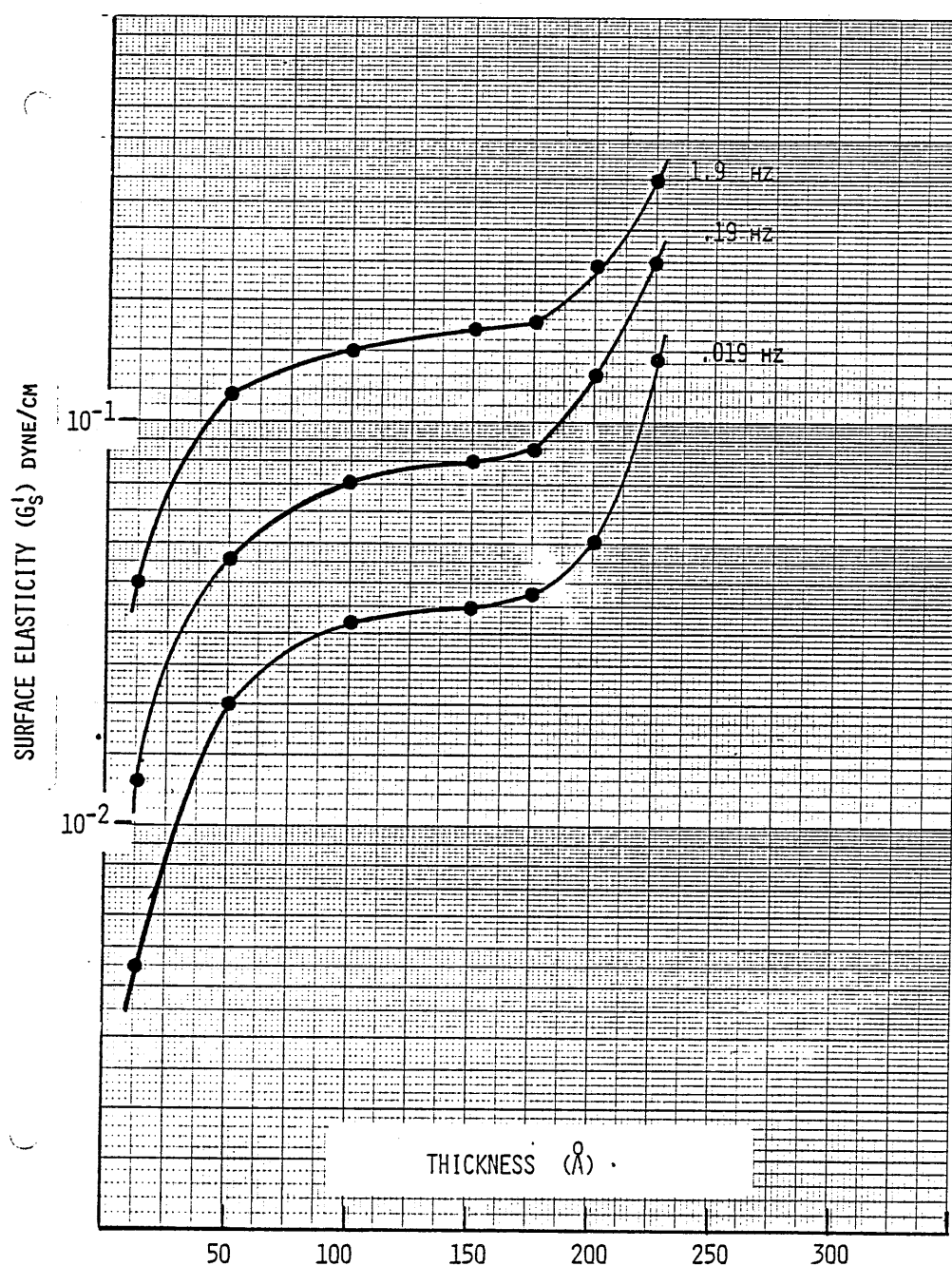


Figure 26. The surface elasticity (G'_s), of surface layers of intrinsic red cell membrane proteins, plotted as a function of the estimated thickness of the film at three different frequencies.

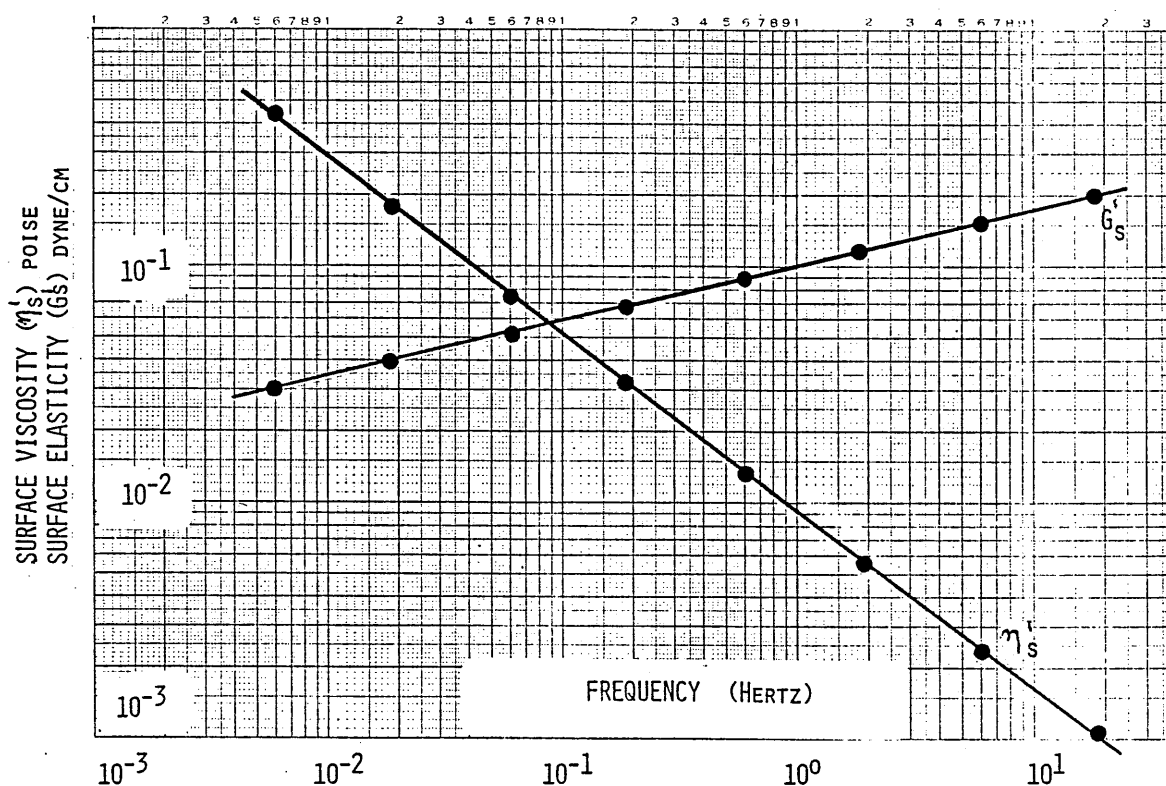


Figure 27. The surface viscosity (η'_s) and the surface elasticity (G'_s) of spread layers of intrinsic red cell membrane proteins of approximately 100Å thick, plotted as a function of frequency.

the membrane surface, have such high values of viscosity and elasticity when isolated and formed into a surface membrane. As the IMP are interacted with the lipid part of the membrane, as well as with the S+A, they also may play an important role in the mechanical integrity of the red cell.

CHAPTER VI

CONCLUSIONS AND PHYSIOLOGICAL SIGNIFICANCE

The primary purpose of the circulatory system is to transport nutrients to cells via the arterial vascular system. This transfer is mainly accomplished in the capillary vessels where oxygen and other nutrients such as glucose, amino acids and proteins diffuse through the vessel wall and enter the cells in the tissues. Metabolic wastes and cellular by-products are removed by similar routes through the venous side of the circulatory system. Its efficiency of this task is controlled by the pumping action of the heart, the condition of the vasculature and the rheological characteristics of the flowing blood. The major determinants of the viscoelastic properties of blood are the red cell concentration, the deformability of the red cell, and the degree of aggregation of the red cells, the plasma viscosity and the rate of flow.

To establish the roles of these parameters, rheological measurements have been made of preparations of blood components covering a wide range of compositional change and widely different flow conditions. From these measurements, master flow curves have been constructed using the average values of the viscous and elastic moduli derived from both steady and oscillatory shear experiments as a function of hematocrit and the composition of the suspending media.

The red cell deformability is a major contributor to the rheological properties of whole blood at high flow rates. As a general rule, the greater the deformability of the red cell, the lower the viscosity. The measurements of viscoelasticity made in the present study on red cell suspensions in Ringer-albumin solutions at controlled cell concentrations reflect primarily red cell deformability.

At low shear rates the red cell is not deformed, and in effect behaves as a solid body. This is one reason for the higher viscosity values measured at low shear rates.

The deformability of the red cell is determined by the viscosity of the internal fluid (hemoglobin solution), the geometric characteristics of the cell, and also the mechanical properties of the red cell membrane.

Another major contributor to the rheological characteristics of whole blood is the aggregation of the red cells. The extent of the aggregation is controlled by the bridging force of the proteins in the plasma, particularly fibrinogen, which forms electrical bonds between the external surfaces of the red cells, connecting them one to another.

Since the studies of Fahraeus, the mechanism of red cell aggregation has been the subject of great interest and investigation. Red blood cells (RBC) are monodispersed when suspended in isotonic salt solutions, and as the surface of the RBC is negatively charged, the aggregating force exerted by the bridging macromolecules must overcome the electrostatic repulsive force before cells could be aggregated.

As these aggregates of red cells can be broken down and dispersed by mechanical shearing forces at high flow rates, their effect on the rheological properties of blood occurs chiefly at low flow rates. The reversible aggregation of RBC therefore is the microrheological basis for the elevation of blood viscosity at low flow rates. If aggregation is unnaturally elevated by increased adhesion forces due to abnormalities in proteins, or in high levels of these macromolecules, disturbances in the microcirculation may occur which could have pathophysiological consequences.

For red cells to remain attached to one another in rouleaux formation during flow the bridging force must over-

come the electrostatic repulsion force as well as the mechanical shearing force. The bridging force is a function of the absorption force per bond, and the number of bonds per molecule and the number of bridging macromolecules between each cell. The electrostatic repulsive force is a function of the surface charge density, the composition of the fluid medium and the intercellular distance between cells. The mechanical shearing force is a function of the shear rate and the viscosity of the suspending medium. This confirms that electrochemical forces controlling red cell aggregation are a major factor affecting blood viscosity and may have wider implications in areas such as platelet aggregation, and interactions between vessel wall and other blood cellular elements.

In certain circumstances the presence of rouleaux in the circulation may be helpful. Fahraeus noted that in some smaller veins and arteries, "plug flow" was observable. Plug flow, sometimes called "bolus flow" occurs when a continuous stream or bolus of red cells, attached one to another flows in a continuous chain, and there is a slip at the vessel wall. This has the effect of allowing a large volume of red cells to pass through the vessel in a short time, which would have the effect of raising the available oxygen supply and of nutrients.

Since the RBCs are monodispersed in Ringer solution, but form aggregates when in the presence of macromolecules as found in plasma, the effect of rouleaux formation on the viscosity and elasticity of RBC preparations can be ascertained by comparing the behavior of red cell suspensions in these two types of suspending media. The contribution of the rouleaux formation and the red cell membrane to the elastic modulus of red cells resuspended in plasma at various

hematocrits has been separated by comparing the elastic modulus of red cells resuspended in Ringer-albumin which does not contain macromolecules, with that of RBCs resuspended in plasma which does. The difference in elasticity can be attributed to the presence of aggregates of red cells. The effect of these aggregates on the viscous and elastic modulus of RBCs in plasma preparation is also clearly evident when these preparations are subjected to pulsatile flow. The superimposed steady shear has the effect of breaking down the rouleaux formations into smaller lengths or groups, and this has considerable effects in reducing the viscous and elastic moduli by a factor of ten at low frequencies. This is further evidence that the high viscosity and elasticity measured in whole blood when subjected to oscillatory shear at low frequencies can be mainly attributed to rouleaux formations.

An apparent yield stress was measured in steady shear in the RBCs suspended in plasma, but not in preparations of washed cells in Ringer solution at normal red cell concentration. The yield stress could only be measured in the presence of rouleaux formation, and is not measurable when the red cells were singly dispersed, unless at a high cell concentration. This finding indicates that in areas of the circulating system where rouleaux formations exist during flow, a yield stress would have to be overcome when blood flow restarts after stasis. The inability to restart flow readily which may occur in instances of reduced cardiac output, or in instances of vascular disturbances, could give rise to prolonged stasis times which could lead to the development of pathological conditions.

A normal stress was measured in red cells resuspended in plasma at 50 percent hematocrit and above, but only when

subjected to higher shear rates, when the red cell membrane is deformed. This indicates that the red cell membrane is capable of storing energy. This is probably derived from a network of elastic fibers made up of spectrin-actin molecules arranged in strands on the underside of the red cell membrane. This network may be chiefly responsible for the shape recovery process which occurs after the red cell has been deformed during its passage through the microcirculation. No reliable measurement of normal stress could be made below a hematocrit of 50%. It is envisioned that at lower hematocrits the normal stress is weak due to the reduced crowding of the red cells, and reduced elongation of the red cell membrane due to the lower shear stress. This will cause only weak "hoop stresses" to develop which are not readily measurable as they become lost in instrument and background electronic noise. The normal stress curve may be extrapolated, however, to cover physiological hematocrits and a probable value of normal stress can be estimated, which indicates that normal stress could be present in some parts of the circulatory system during normal flow conditions.

The physiological significance of the existence of a normal stress is difficult to interpret, as the vessel walls are already under stress due to the action of the heart. The addition of a small amount of stress normal to the direction of flow is not thought to have significant effects, however this stress may be partly responsible for migration of RBC towards and away from the vessel wall, which can be seen in visual observation of flowing blood in the circulation, and in model systems.

The measurement of sedimentation rate is a standard clinical test and an accelerated sedimentation rate is used as an indication of the presence of a pathological condition.

The sedimentation rate of red cells has been shown to be accelerated by an increased degree of aggregation. The effect of shear on the aggregation of healthy RBC has been investigated and measured indirectly by comparing the rate of sedimentation at various rates of shear. It was found that the application of rates of shear below 0.01 sec^{-1} , did not affect the sedimentation rate, and it is surmised that the shear stress at these low levels was below the yield stress value of the aggregated blood, and flow does not occur within the network of red cells. At shear rates of 0.01 sec^{-1} and above, the shear stress is high enough to disturb the rouleaux network, and clumps of red cells are able to sediment at an increasing rate. Peak sedimentation rate is seen at 0.1 sec^{-1} , indicating that the most favorable conditions for sedimentation such as size of red cell clumps and flow rate, exist. At 10 sec^{-1} the imposed strain energy is high enough to disaggregate the red cells and keep them in suspension without sedimentation.

These findings would indicate that only in area of the circulation where comparatively low flow rates exist (below 10 sec^{-1}) would the presence of significant amounts of rouleaux be found which may give rise to bolus flow with slip at the vessel wall.

Clotting profiles of non-anticoagulated whole blood have been followed with time, employing the dynamic mode of the rheogoniometer using small vibration amplitudes and low frequencies. These low frequencies and amplitudes were chosen so that the natural rate of the clotting process was not altered. The measurement of the viscous and elastic moduli during the clotting process is of clinical importance, as variations of these parameters reflect the changes in clot structure. This technique therefore should be particu-

larly suitable for monitoring the progress of patient therapy for clotting disorders. It can also contribute to a more precise evaluation of the contribution of various factors, e.g. platelets, fibrinogen, prothrombin and hematocrit etc., to the clotting process in research investigations.

The rheological implications of changes in the shape of the red cell have been studied. The red cells were prepared in hypo- and hypertonic salt solutions from 200m Osm to 800m Osm. The red cell is in normal osmotic equilibrium in plasma which has an osmotic pressure corresponding to that of an aqueous solution containing 0.9 percent sodium chloride (300m Osm). In this condition the red cell retains its usual discoid shape. If they are suspended in a solution of lower tonicity, they swell and assume a spherical form, and if the osmotic pressure is low enough, hemolysis occurs, and the hemoglobin is eliminated through the membrane, leaving the red cell membrane as a ghost cell. With hypertonic osmolarities above 300m Osm, the red cell shrinks and can assume a crenated form. The shrinkage of the red cell will increase the concentration of hemoglobin and therefore the internal viscosity of the red cell, causing a change in the ratio of the internal to external fluid viscosity. This has the effect of reducing the red cell deformability. A plot of viscosity and elasticity vs. osmolarity shows a gradual increase with higher osmolarities. These results indicate that the elevation of internal viscosity and the ensuing increase in rigidity of the red cell is the factor leading to the increases in rheological moduli of these suspensions.

In sickle cell disease, changes in shape of the red cell also occur, when the hemoglobin oxygen level is reduced as it travels through the microcirculation. Deoxygenation of the hemoglobin molecules causes them to cross link into rod-like

structures within the red cell. As a result, the membrane is distorted into a crescent or sickle shape, and the cell becomes much less flexible. The cell in this condition may not pass through some areas of the microcirculation and tissue becomes starved of nutrients and oxygen, and the pathophysiological symptoms of sickle cell disease result.

In the present study the rheological behavior of red cell preparations of sickle cell sufferers were compared with those of normal subjects at the same hematocrits. At O_2 saturations of 100 percent, the viscosity and elasticity of these materials was similar. As O_2 saturation was lowered below 80%, however, the sickle cell preparations showed large increases in viscosity and elasticity, while the normal controls remained essentially constant. Comparisons of normal and sickle cell hemoglobin preparations showed very large differences, as much as X 1000, when O_2 was lowered to 40 percent. This very large increase in viscosity and elasticity is possibly the causative factor for the rheological changes which lead to the clinical manifestations of sickle cell disease. The rheological properties of preparations of red cells from sickle cell patients were compared between those who were in a quiescent stage of the disease and those who were exhibiting the severe clinical manifestations which are apparent when in the active stage. It was found that there were considerable increases both in viscosity and elasticity of those in the active stage, which is further confirmation that the cause of these pathophysiological manifestations is related to changes in the rheological characteristics of the blood itself.

White cells, or leukocytes, protect the body from infections and many diseases. In conditions of good health, their concentration in the blood is small when compared to that of

the red cells and their impact on the rheological properties of blood is minimal. In a state of infection, however, the number of white cells can increase, although perhaps still not enough to significantly change the bulk rheological properties of the blood. If the white cells exist in very large numbers, or if a significant fraction of white cells become attached to the blood vessel walls, the flow in those vessels may be affected.

In Leukemias, the numbers of white cells found in the circulation can assume massive proportions and their effect on the rheology of the whole blood of leukemia sufferers may be considerable, and some of the clinical manifestations in leukemias can be attributed to microcirculatory disturbances.

The viscosity and elasticity of preparations of white cells resuspended in plasma or in buffer solutions at various concentrations have been studied. The effect of leukophoresis treatment on the rheologic properties of their whole bloods was also investigated.

It was found that the viscosity and elasticity of preparations of white cells in plasma and also buffer solutions were essentially a linear function of the leukocrit up to 35% concentration. Above this value, the two parameters increased rapidly in an exponential manner. This may be due to increased crowding, causing cell entanglements to develop as a result of the interactions of the white cells, and the extreme surface roughness of the membrane surface. Above a concentration of 40 percent, an elastic component was measurable in these preparations. This is perhaps due to the interactions among the white cells, including clumping, leading to a capacity of storing strain energy.

The bulk viscosity and elasticity of white cells were found to be much higher than similar preparations of red

cells. This indicates that the white cells have greater rigidity than the red cells.

Leukophoresis is a treatment used in leukemia, to remove excess white cells from the circulation. The effect of this treatment was found to cause a considerable drop in viscosity of the patients blood which would reduce the danger of microvascular occlusions due to leukostasis and improve blood flow and reduce the cardiac load.

A discussion of the rheological properties of blood would be incomplete without considering the blood vessels which transport the blood throughout the circulatory system. The blood and blood vessel together can be considered to constitute a single entity. The interface between the blood and the vessel wall is crucial to the proper performance of this system. An analysis of this complex system indicates that it is in the capillary bed that the exchanges of nutrients necessary for the maintenance of tissue integrity occur. The capillaries are composed mainly of an uninterrupted layer of endothelial cells which lay along the direction of flow. Nutrients and other substances are transported through and between the endothelial cells from a largely immobile layer of plasma in contact with the endothelium. The transport processes occur by three mechanisms. Blood gases such as oxygen and carbon dioxide can diffuse through the endothelial cells across their entire surface. Water and solutes such as glucose and amino acids pass through intercellular spaces between the endothelial cells. Larger proteins pass through vesicles at the cell surface to the other side of the cell. From there the nutrients and other substances diffuse through the membranes of the tissue cells. Metabolic wastes, hormones and other cellular products are transported by the same routes back from the tissue cells into blood plasma to be

carried into the venous side of the circulating system.

The blood capillary vessel wall consists of several structures, and consists of in total: (a) predominantly immobile layer of plasma or plasmatic zone, (b) a possible layer of fibrinogen or fibrin overlaying the endothelial cells, (c) the endothelial cell proper, (d) the basement membrane, and (e) the adventitial tunic.

It is in the cell-free part of the circulating blood (the plasmatic zone) in proximity to the blood vessel wall, that processes can occur which initiate thrombosis. Fibrinogen is a surface active protein, and it has been proposed by Copley(1) that fibrin in submicroscopic dimensions lines the endothelial cells. Thus the circulating blood is separated from the endothelial cells by the endothelial fibrin lining. It is the nature of this endothelial lining that has great importance in any considerations regarding the flow of blood and the genesis of thrombosis. The concept of thrombosis is generally based on the processes of clumping of blood cellular elements and the coagulation of plasma by the polymerization of fibrinogen into fibrin. According to Copley the process of thrombus formation begins with the adsorption of fibrinogen onto the vessel wall. The primary process of fibrinogen aggregation and deposition on the vessel wall is considered to occur rapidly. The deposition of these proteins at interfaces has been investigated in this study using the modified Rheogoniometer. The measurement of the viscosity and elasticity of these protein layers using a special technique developed for this purpose, has confirmed that these protein layers have surprisingly high moduli particularly when the probable thickness of these layers is considered.

It was found that substances such as dextran, dextran sulfate, sodium hyaluronate, chondroitin A, B and C reduced

the rigidity of surface layers of fibrinogen. Sodium heparin in general, lowered the rigidity of surface layers formed on fibrinogen solutions. Some other heparin preparations, however did not. The action of heparins will need to be examined in detail with regard to the mechanism of their action, and the agent responsible for their anticoagulant activity with regard to fibrinogen surface layers will need to be isolated. It is hoped that the data reported, will stimulate new work on heparins and its action. It is clear, however, that the method, used to investigate the viscoelasticity of fibrinogen surface layers, or gels of surface layers, can be valuable in investigating a wide range of materials, such as these glucosaminoglycans, to elucidate their extent of their anticoagulant action.

The erythrocyte is the single most important component of blood dominating its rheological properties. Its particular shape, shape memory, and deformability are the major contributing factors controlling the rheological properties of blood. Therefore it is the mechanical properties of the single red cell, or more appropriately the red cell membrane itself, that most concern us in such a study as this. Other researchers (2,3,4) have demonstrated that there is a network of fibers made up of chains of spectrin-actin (S + A) molecules on the underside of the red cell membrane, which is chiefly responsible for maintaining the red cell integrity and membrane shape, and possibly contributes to the elastic memory that is demonstrated by the cell. The rheological properties of S + A protein films need therefore to be elucidated if an understanding of the rheological properties of the membrane is to be achieved. The surface rheological measurements of spread S + A layers has confirmed that the viscosity of a S + A film is of the order of 10^2 to 10^3 dyn. sec/cm², while the extensional membrane viscosity is of

the order of 10^3 dyn. sec/cm². The extensional elastic modulus of the intact membrane is given as about 10^{-2} dyn.cm. while the S + A film is of the order of 10^{-1} dyn.cm. at low frequencies. From these comparisons there appears to be good agreement regarding orders of magnitude, particularly when one considers that the S + A film properties would probably be lowered significantly in the presence of membrane lipids. This investigation suggests therefore that the properties of an S + A film at the inner face of the erythrocyte membrane can account for some of the observed properties of the intact red cell.

It can be concluded that the application of the Weissenberg Rheogoniometer, with the modifications described in this thesis, has demonstrated that it is an excellent tool for the investigation of the flow properties of whole blood and preparations of blood components in suspension. It is unique in its wide range of available shear rates which can be used in steady, oscillatory and pulsatile flows. This has enabled the elastic component, as well as the viscous modulus of blood and preparations of blood cellular components to be measured, in normal and in diseased states.

The application of the Rheogoniometer to the study of the rheological properties of blood, has widened the knowledge of the flow properties of these materials, particularly by the measurement of the elastic modulus. This study has further demonstrated that the combination of the science of rheology and biology may help to solve the intricate problems encountered in a study of the dynamics of the circulating system in normal and abnormal states. These studies therefore, can be expected to benefit and serve the well-being of our species.

APPENDIX I.

THE NEW WEISSENBERG RHEOGONIOMETER.

Description

Figure 1, is an illustration of the new Rheogoniometer. The drive unit consists of two one horse power synchronous motors driving planetary gearboxes mounted on a base frame. The gearbox of the planetary type gives 60 selectable output speeds in equal ratios of $1.0 \times 10^{-0.1}$ (1:1.259 reduction). Internally the gearbox unit is in two parts, the first giving five steps of approximately 1:1 to $1.0 \times 10^{-5.5}$ (1:316200 reduction) and is driven by the output of the first part. The gear change mechanism, associated with each part of the gearbox, shows a number indicating the speed reduction to which that side of the gearbox is set. By adding these two indices together, a figure is obtained which expresses the overall speed reduction of the gearbox approximately as a power of ten. This ratio may be expressed as a platen speed by reference to a table. It can be seen that by use of the two parts of the gearbox, 60 steps of gear reduction of from 1×10^0 (1:1) to $1.0 \times 10^{-5.9}$ (1:792,000) are available.

Needle roller bearings are used throughout the gearbox to eliminate the tendency towards stick slip motion which is often troublesome where journal bearings are employed at very low speeds.

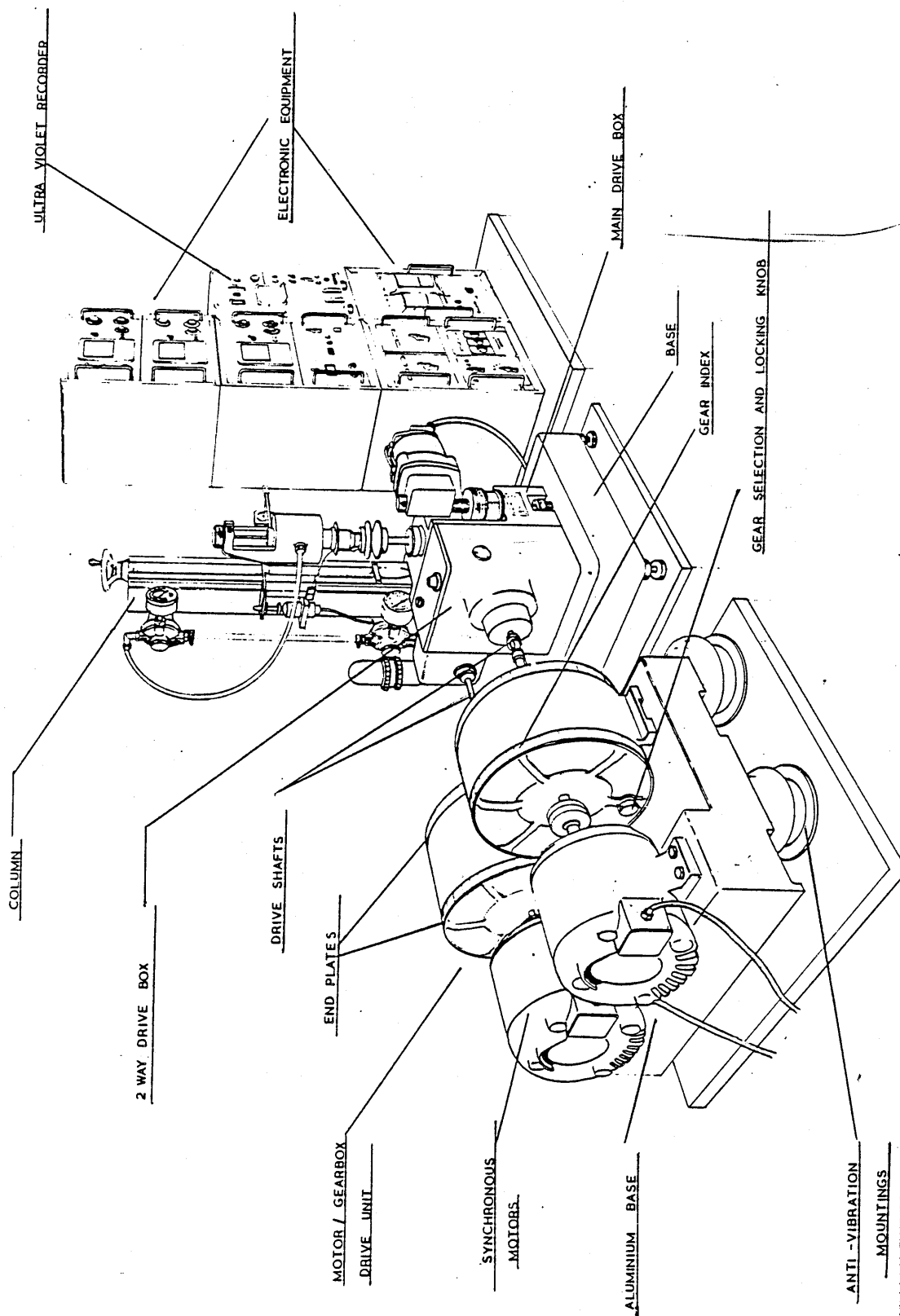


Figure 1. An illustration of the complete assembly of the new Rheogoniometer.

Torsion Measuring System

The torsion head is mounted on the column of the Rheogoniometer and carries the top platen. It owes its extreme sensitivity to an air bearing, and its wide range of available shear stress to five interchangeable torsion bars.

The rotor of the air bearing which carries the top platen consists of a stainless steel tube of 2.50 cm. in diameter and 125 microns in wall thickness. This thickness is chosen to be the thinnest in section consistent with strength in order to reduce the inertia of moving parts when making a measurement. Fig. 2 is an illustration of the torsion measuring system.

The stator of the air bearing consists of two brass bushes mounted axially 5 cm. apart within the main casting of the torsion head. Each bush has an inner diameter 10 to 15 microns larger in diameter than the rotor, so as to give a slight clearance. There are six 0.4mm holes drilled radially and equally spaced around the center of each bush. Air under pressure is forced through these radial holes, the air being supplied from a gallery in the casting behind each bush. When air pressure is applied, the rotor is held accurately in the center of the bearing with a high degree of rigidity, and, since there is no contact of the bearing surfaces the rotor is virtually frictionless.

There are a series of five torsion bars that may be used of varying stiffness. The top of the torsion bar is held rigidly in a clamp at the top of the air bearing casting, and the bottom is clamped to the top of the air

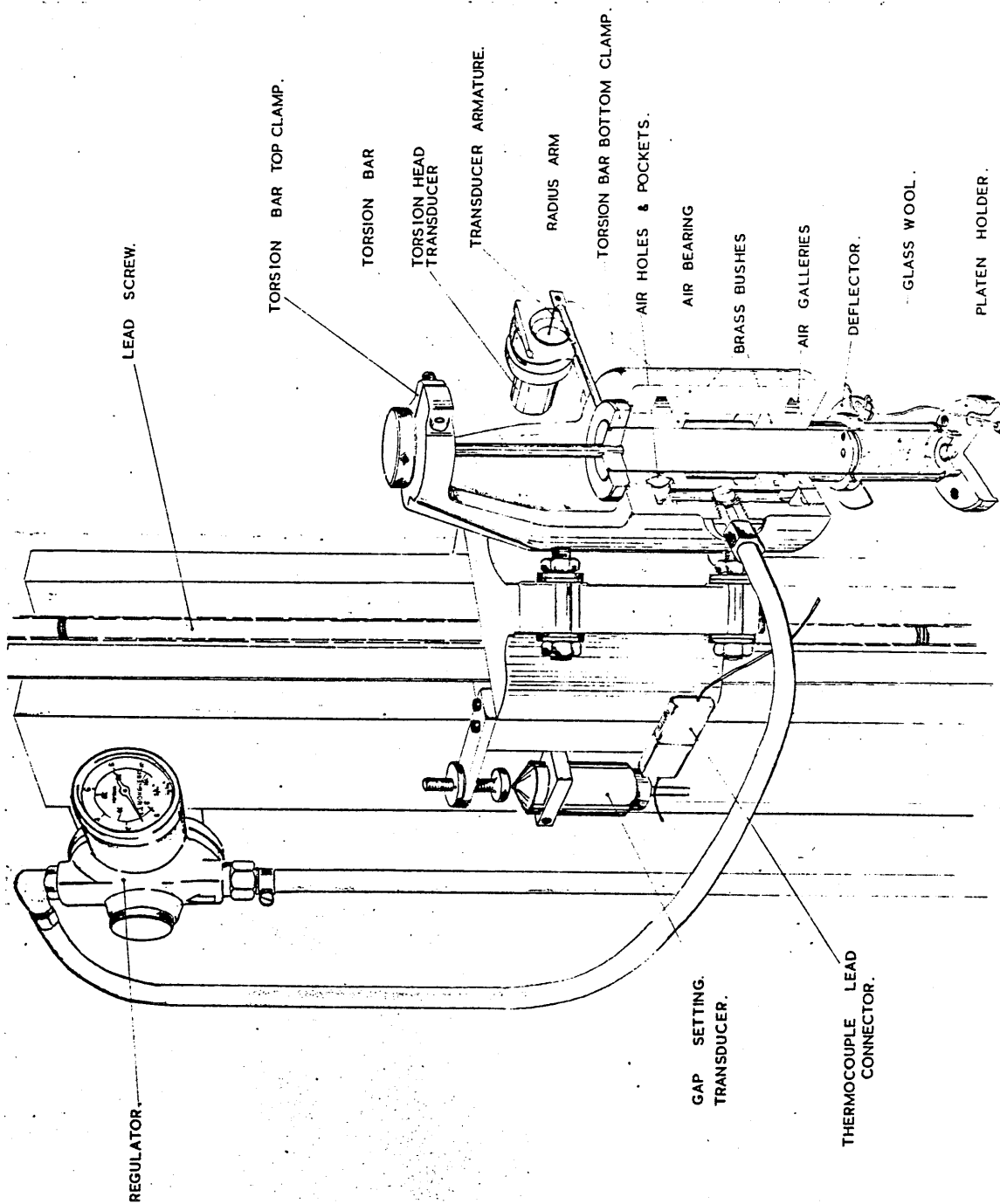


Figure 2. A cut away section of the torsion measuring system.

bearing rotor. The clamp at the lower end of the torsion bar carries a 10cm. radius arm. At the other end of this arm the armature of the torsion transducer is fitted. The displacement of the armature is displayed on the appropriate transducer meter. This can be converted into units of torque, by multiplying the displacement by the torsion bar constant, the torque produced by the test material on the top platen is then known.

Normal Force Measuring System

In order to measure the force normal to the axis of rotation (Weissenberg effect) usually present when measuring viscoelastic fluids, a system consisting of a shaft carrying a diaphragm is employed. The shaft rests on a leaf spring which registers a deflection when a force is felt on the shaft. This unit comprises the lower platen assembly. An illustration of this unit is seen in Fig. 3.

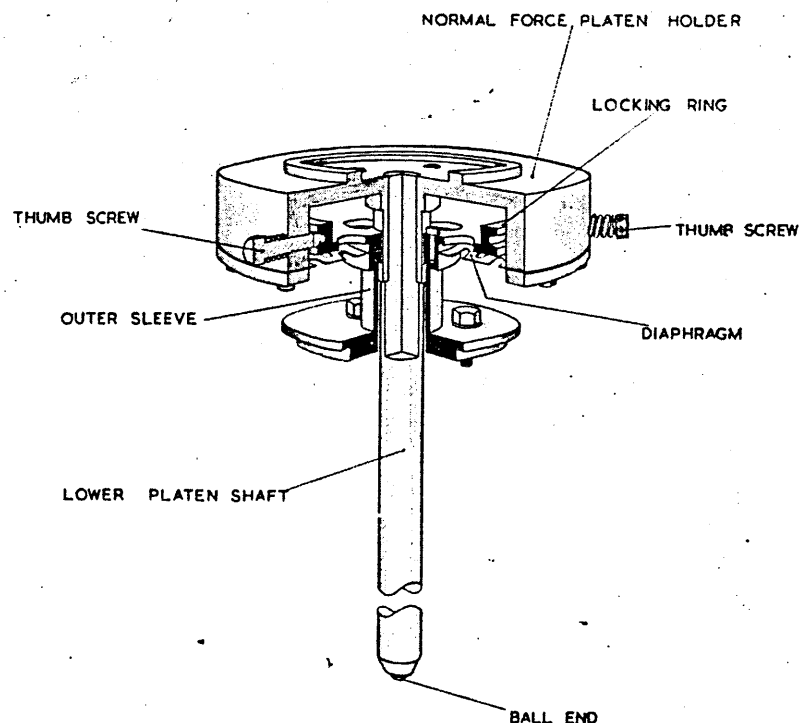


Figure 3. A sketch of the Normal Force Diaphragm assembly.

If normal force is present during a material test, the lower platen will be forced downwards, the diaphragm and leaf spring allowing movement. This movement is measured by a transducer mounted directly under the ball end of the assembly. The spring is calibrated by

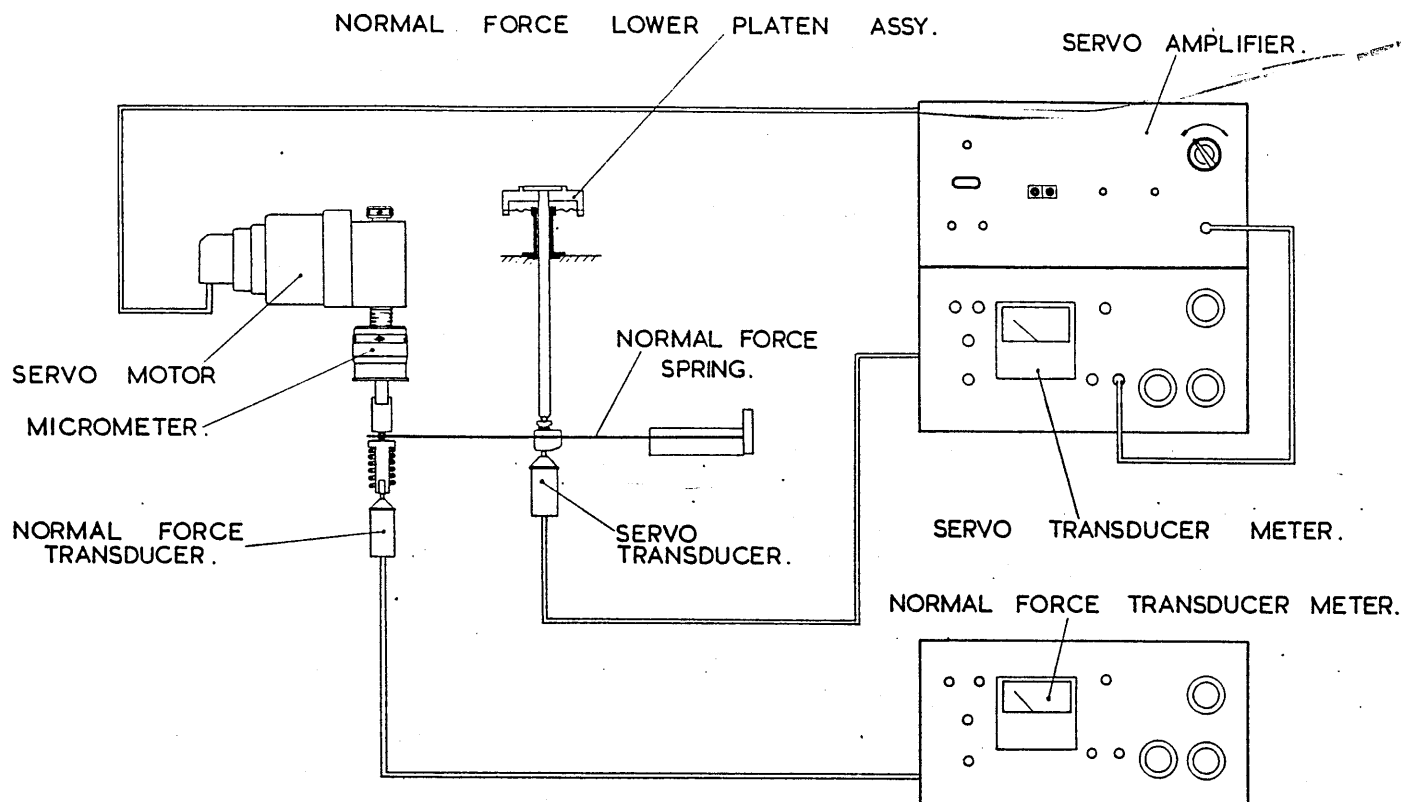


Figure 4. A schematic layout of the Normal Force measuring system.

adding known weights and so the movement can be related to force. During measurements of normal force, it is important to keep the gap between the platens constant as appreciable increase in gap size, will a) reduce the rate of shear, and b) cause both tangential and normal stress to give low readings. In order to maintain a constant gap, a null point serve system is used. The information signal (displacement of the lower platen) derived from the transducer mounted beneath the normal force pivot bearing

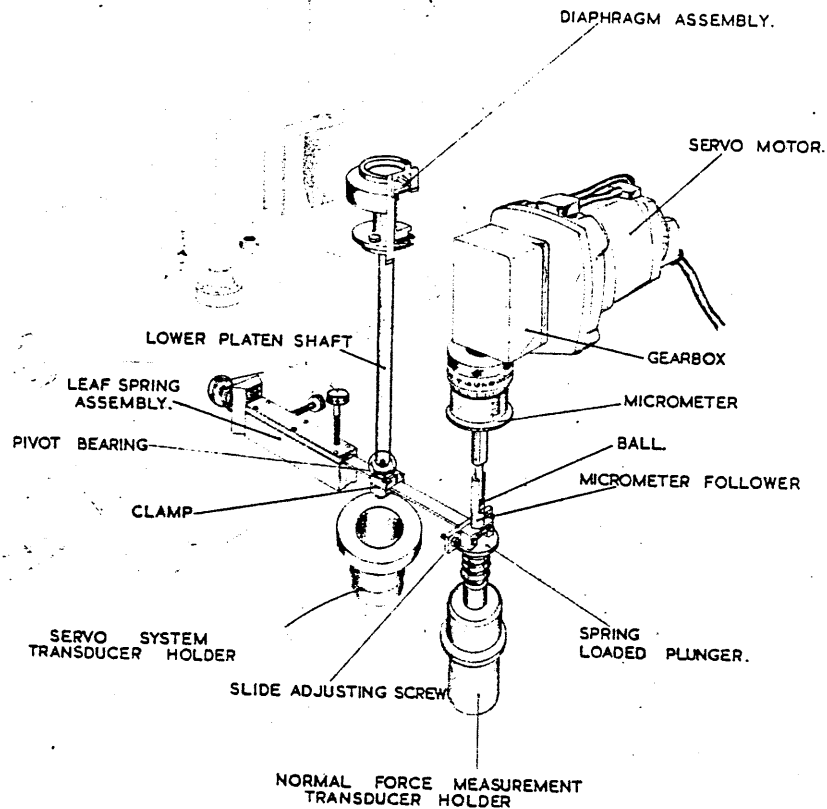


Figure 5. A sketch of the mechanical parts of the Normal Force measuring system.

is fed via its amplifier into a servo amplifier. The servo motor is driven by this amplifier and rotates a micrometer which positions the free end of the normal force spring until there is a zero output reading from the transducer mounted under the pivot bearing. This ensures that the gap between the cone and plate remains constant throughout the test. A reading of the deflection of the free end of the normal force spring now becomes an indication of the amount of normal force. The method of calibration of the normal force system is to apply weights to the lower platen and record the change of position of the free end of the normal force spring. Fig. 4 is a schematic layout of this system and Fig. 5 is an illustration of the mechanical arrangement of the normal force system

Oscillatory Mechanism

The drive for the oscillatory mechanism is taken from the 60 speed gearbox unit into the side of the Rheogoniometer. This drives a cam which is offset by $1/8$

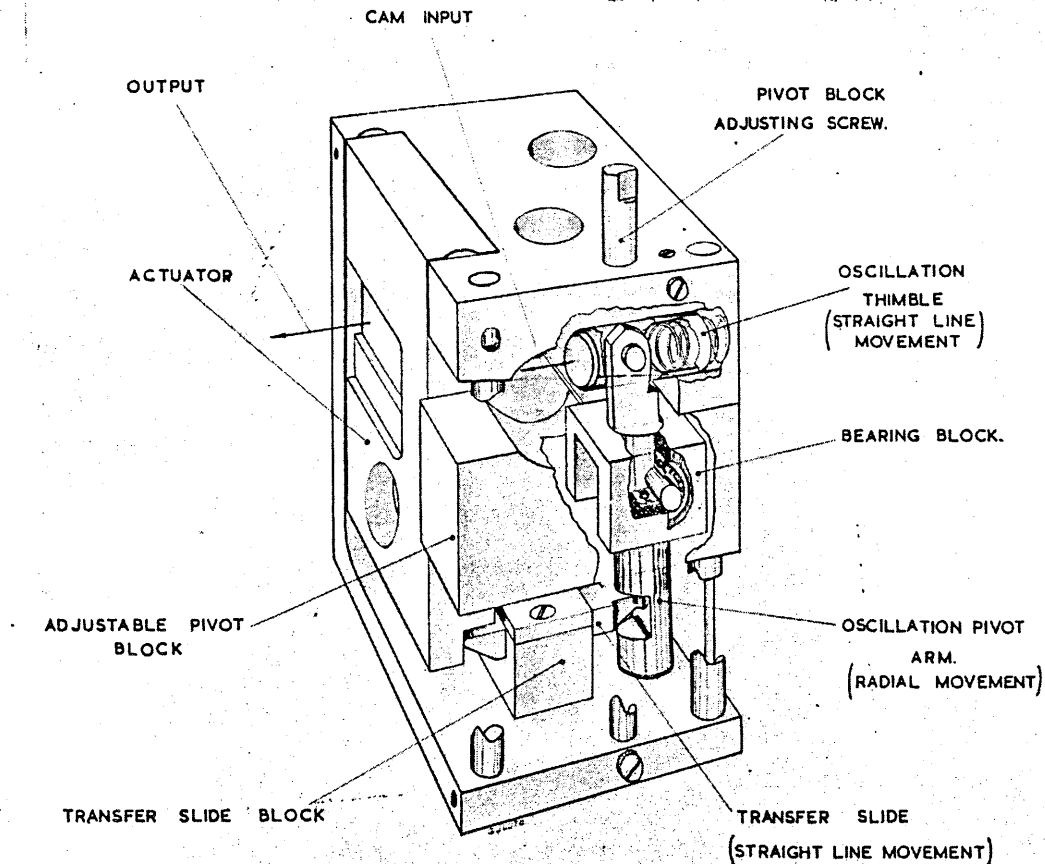


Figure 6. A schematic arrangement of the variable sine wave generator.

inch from center. A spring loaded oscillation thimble rests on this cam and the motion of the cam is taken through the "Variable Sine Wave Generator" (VSG) to the end of the worm shaft. An illustration of this unit is shown in Fig. 6. Fig. 7 is an illustration of the rotational and oscillatory motion transfer system. The VSG imparts a sinusoidal motion to the axis of the worm shaft. The worm and wheel then acts as a rack and pinion and im-

parts the oscillatory motion directly to the platen. By altering the control at the top of the main body, the amplitude of oscillation can be varied between 10 and 1,500 microns (.0003 and .045 radians), by varying the position of the pivot block.

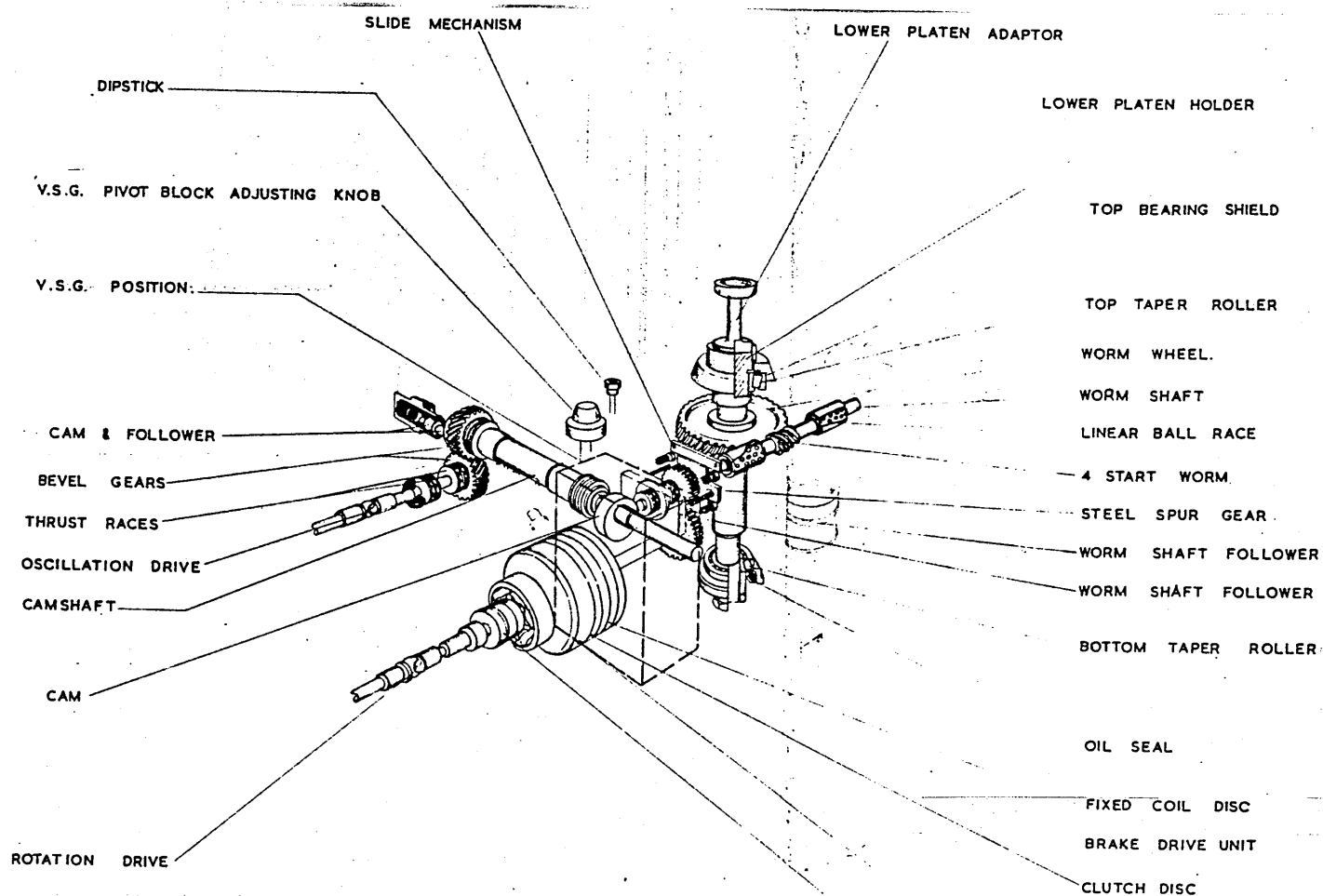


Figure 7. Arrangement of the gearing for oscillatory and rotational motions.

Electronic Measuring and Recording Equipment

a) Transducers and transducer amplifiers.

The transducer amplifiers receive their signals from variable inductance displacement transducers. The transducer converts the physical quantity being measured into a change in an electrical bridge circuit which is supplied with a constant amplitude carrier frequency with-

in the transducer amplifier. The output of the transducer meters is converted to a D.C. voltage and is available to drive recorders, oscilloscopes, etc.

There are two types of transducers used with the Rheogoniometer, but they are electrically similar. In each transducer there are two stator coils mounted side by side on the same axis, and a cylindrical armature is held within the coils. As the armature moves axially the increase of inductance of one coil and the decrease in the other is measured. Five transducers are used on a full Rheogoniometer and they are used for measurement of tangential stress, normal stress, oscillation input, amplitude and phase difference. Others are used as ancillaries and are used for Gap Setting, and Normal Force Servo Control.

b) Temperature control.

A chamber which fits around the platens, supplies a temperature controlled environment allowing testing to be made from sub zero to 350°C.

c) Test geometries.

The usual geometry that is used for rheological measurements with the instrument is the cone and plate, but parallel plates, couette type geometries and other combinations such as cone in cone, and the Couette/Cone plate system.

Material Testing Techniques

It would be difficult to describe here the varied techniques used to measure every material in every circumstance, and very little can be said about the spec-

ial handling methods some materials require and the order and manner in which rheological tests are carried out. As a general rule, however, it is best to start with low rotational speeds and work upwards through a range of increasing shear rates. A number of readings should be taken, so that a curve can be drawn. This is important even if the test value of viscosity at only one point is

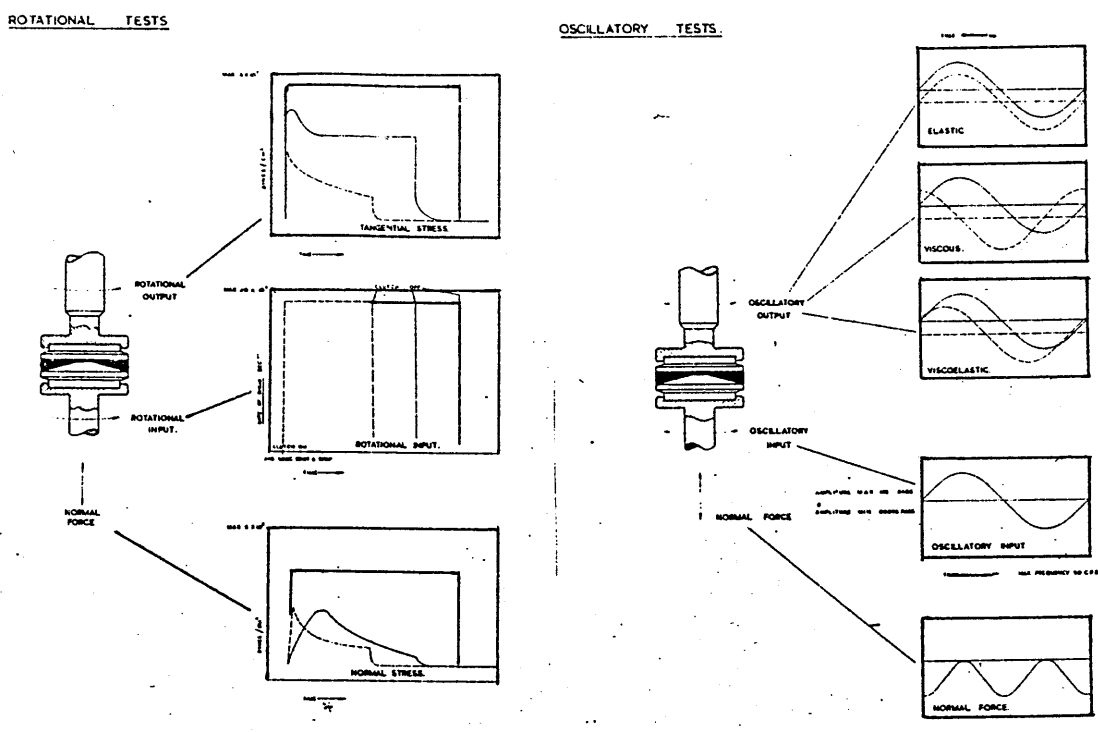


Figure 8. A representation of the steady and oscillatory shear modes.

required. A range of values should be taken to extend approximately at equal amounts of shear rate or temperature at either side of the point of interest. This greatly reduces experimental error and also indicates whether adjacent conditions are critical. Data information should be taken from the completed curve, rather than individual points, in order to make the appropriate calculation. Fig. 8 is a diagrammatic illustration of

the various measurements that can be made. A number of material tests have been carried out to demonstrate the data that may be obtained with the new Rheogoniometer. Figures 9, 10, 11, and 12, are plots of data that have been obtained using well known materials whose rheological characteristics are probably not so well known.

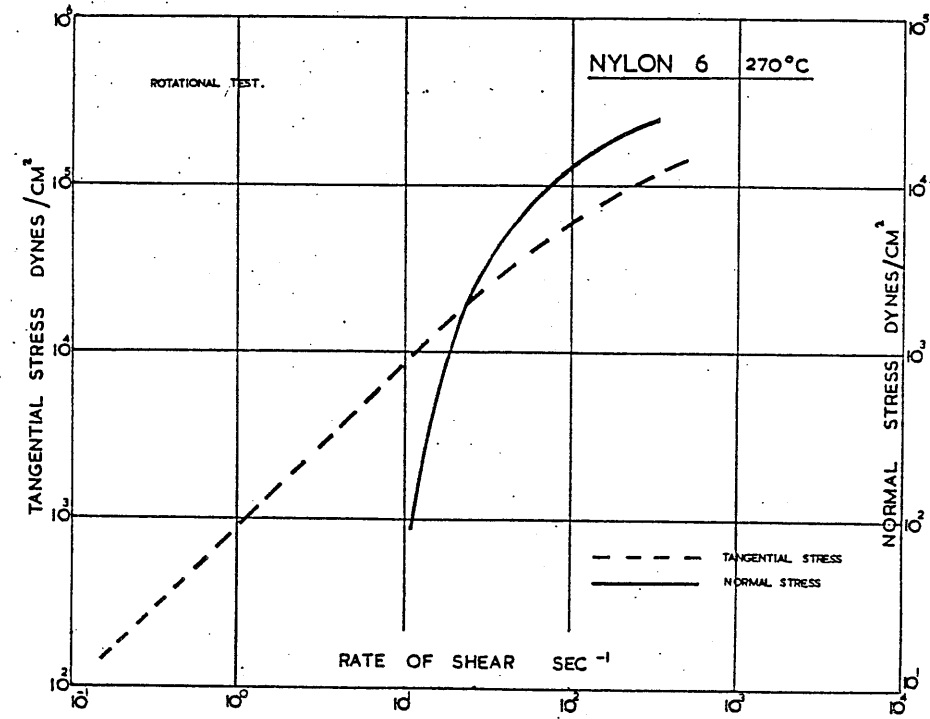


Figure 9. A plot of Tangential and Normal Stress versus Shear Rate for Nylon 6. at 270°C.

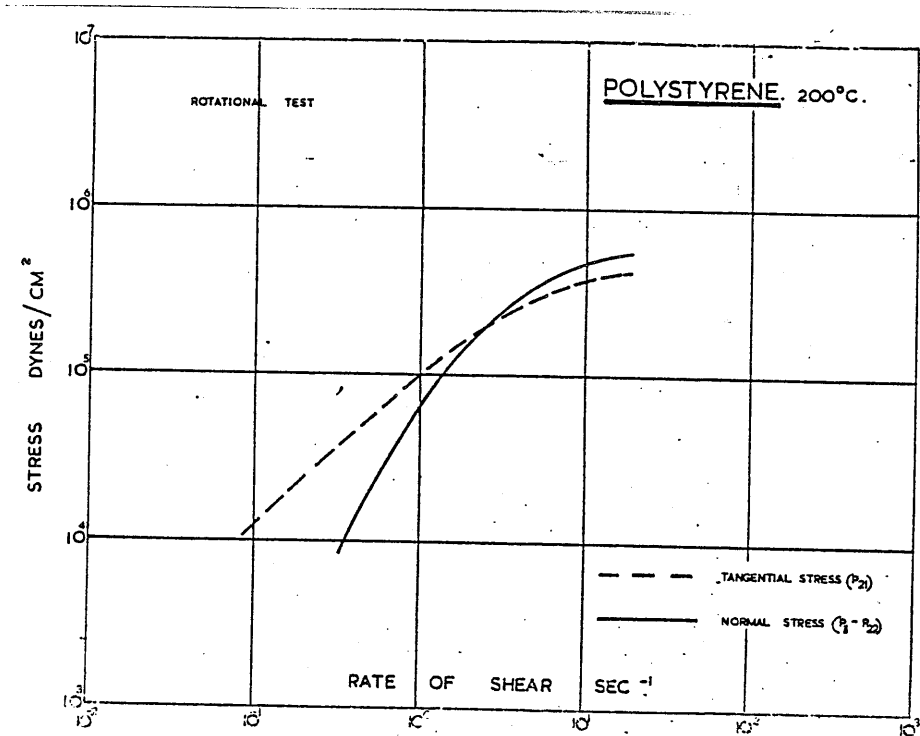


Figure 10. A plot of Tangential and Normal Stress versus Shear Rate for Polystyrene at 200°C.

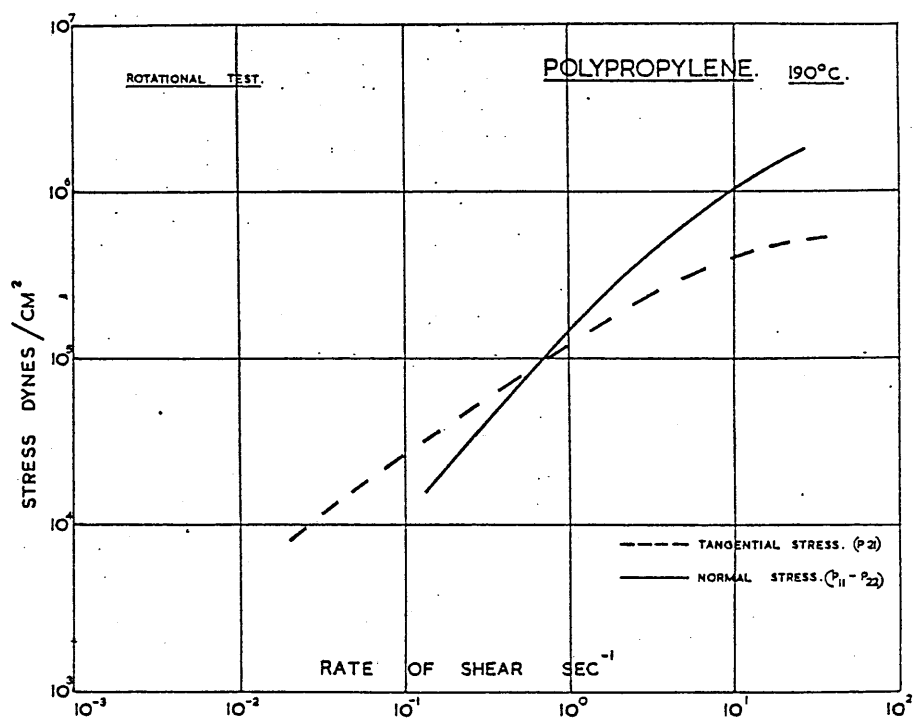


Figure 11. A plot of Tangential and Normal Stress versus Shear Rate for Polypropylene at 190°C.

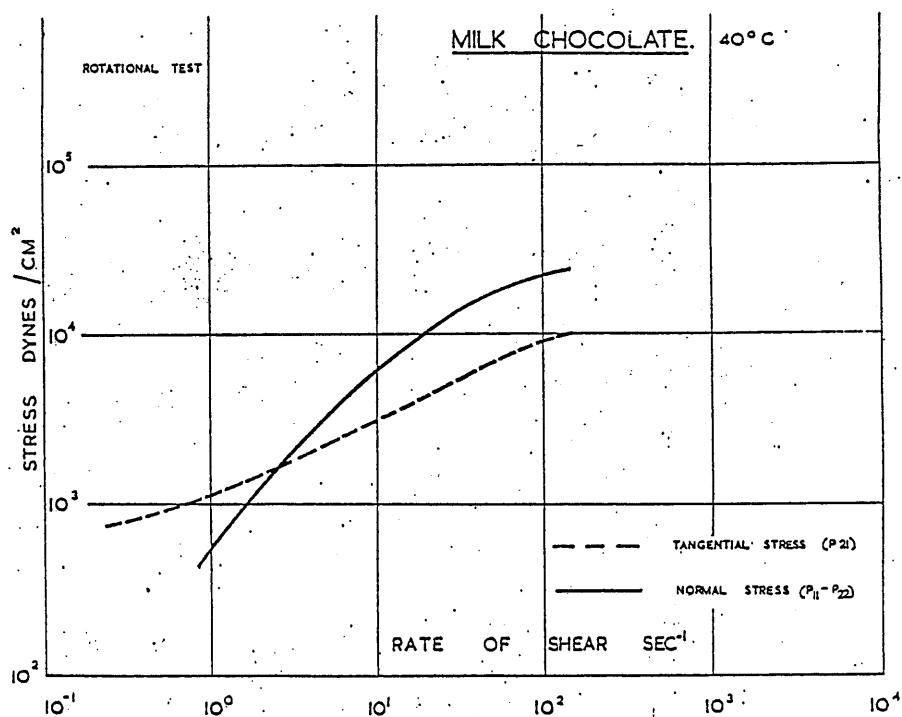


Figure 12. A plot of Tangential and Normal Stress versus Shear Rate for Milk Chocolate at 40°C.

APPENDIX II.

PROGRAM FOR THE DETERMINATION OF AMPLITUDE RATIO AND PHASE

ANGLE IN OSCILLATORY FLOW.

```

RHEODX      BASIC W01B-02

10 GOSUB 920
15 PRINT " "
17 PRINT "ENTER FREQUENCY"; INPUT F1 IF F1=0 THEN 1154
18 IF 01=100 TO 19 PRINT "ENTER INPUT RANGE"; INPUT 01
19 PRINT "ENTER OUTPUT RANGE"; INPUT 02
20 IF F1>1.00000E-03 GO TO 22 VE1=5 GO TO 30
22 IF F1>.01 GO TO 24 VE1=4 GO TO 30
24 IF F1>.100 TO 26 VE1=3 GO TO 30
26 IF F1>1.00 TO 28 VE1=2 GO TO 30
28 E1=1
30 IF F1>7.500 TO 32 NR3=256 GO TO 39
32 IF F1>100 TO 34 NR3=128 GO TO 39
34 IF F1>=3000 TO 36 NR3=64 GO TO 39
36 R3=32
39 C1=1.00000E+06/107*(E1-1)
46 PRINT "PRESS CR KEY TO START SAMPLING"; INPUT V1#
47 R1=INT(C1/(R3*F1)+.5)
48 DIM A(256), D1(512), D2(256)
49 CALL "USE"(A)
50 I9=1
52 CALL "SETR"(E1,1,R1)
55 CALL "RTS"(A,0,2,R3,2)

```



```

58 FOR I=1 TO R3
59 CALL "LED"(I)
60 CALL "RDB"(A,Z)
62 IF Z<000 TO 60
63 D1(I)=Z*2/4095-1
64 CALL "RDB"(A,Z)
65 IF Z<000 TO 64
66 D2(I)=Z*2/4095-1
70 NEXT I
75 FOR I=1 TO R3
76 IF I9=200 TO 77 \A(I)=D1(I)\GO TO 78
77 A(I)=D2(I)
78 NEXT I
102 I1=1
103 N2=2*R3\N4=N2-1
106 FOR I=1 TO N4 STEP 2
107 J=(I+1)/2
110 D1(I)=A(J)
114 NEXT I
115 FOR I=1 TO N4 STEP 2
117 K=I+1
118 D1(K)=0
119 NEXT I
140 J=1
150 FOR I=1 TO N2 STEP 2
160 IF (I-J)>=000 TO 230
170 T1=D1(J)
180 T2=D1(J+1)
190 D1(J)=D1(I)
200 D1(J+1)=D1(I+1)
210 D1(I)=T1
220 D1(I+1)=T2
230 M=N2/2
240 IF (J-M)<=000 TO 300
250 J=J-M

```

```

260 M=M/2
270 IF (M-2)>=0 GO TO 240
300 J=J+M
310 NEXT I
320 M1=2
330 IF (M1-N2)>=0 GO TO 476
331 CALL "LED"(M1)
340 I2=2*M1
345 P=3.14156
350 FOR M=1 TO M1 STEP 2
360 H1=P*I1*(M-1)/M1
370 W1=COS(H1)*W2=SIN(H1)
380 FOR I=M TO N2 STEP I2
400 J=I+M1
410 T1=W1*D1(J)-W2*D1(J+1)
420 T2=W1*D1(J+1)+W2*D1(J)
430 D1(J)=D1(I)-T1
440 D1(J+1)=D1(I+1)-T2
450 D1(I)=D1(I)+T1
460 D1(I+1)=D1(I+1)+T2
465 NEXT I
466 NEXT M
470 M1=I2
475 GO TO 330
476 PRINT '---'
480 PRINT 'HARMONIC', 'REAL COEFF', 'IMAG COEFF', 'AMP', 'PHASE'
481 04=0\PRINT ' '
482 FOR I=3 TO 9 STEP 2
483 04=04+1
485 D1(I)=D1(I)*2/R3
487 D1(I+1)=D1(I+1)*2/R3
490 P1(04)=SQR(D1(I)*D1(I)+D1(I+1)*D1(I+1))
491 IF D1(I)<0 GO TO 496
493 IF D(I+1)<0 GO TO 494 \P1(04)=90\GO TO 503
494 P1(04)=270
495 GO TO 503

```

```

496 P1(04)=ATN(D1(I+1)/D1(I))*180/P
497 IF D1(I)>000 TO 503 \P1(04)=P1(04)+180\GO TO 503
499 IF D1(I+1)>000 TO 503 \P1(04)=P1(04)+360\GO TO 503
500 GO TO 503
503 PRINT 04,D1(I),D1(I+1),A1(04),P1(04)
504 IF I9=200 TO 515
505 A2(04)=A1(04)\P2(04)=P1(04)
510 IF I9=100 TO 530
515 REM CORRECTIONS
516 P1(04)=P1(04)+.1*F1
520 A1(04)=(A1(04)*G2)/(A2(04)*G1)/3.2
521 IF A1(04)>000 TO 522 \A1(04)=-A1(04)
522 P1(04)=P2(04)-P1(04)
523 IF F1<F900 TO 525 \GO TO 527
525 IF P1(04)>000 TO 530 \P1(04)=P1(04)+360\GO TO 530
527 IF P1(04)<000 TO 530 \P1(04)=P1(04)-360\GO TO 530
530 NEXT I
535 I9=I9+1
540 IF I9<=200 TO 75
545 GOSUB 1130
550 PRINT ' ' \PRINT ' '
600 PRINT 'FREQUENCY',F1\PRINT ' '
605 PRINT ' ' \PRINT ' '
610 PRINT 'HARMONIC', 'AMP. RATIO', 'PHASE ANGLE'
611 I=1
612 PRINT I,A1(I),P1(I)
614 PRINT ' ' \PRINT ' '
615 O1=1\GO TO 17
920 PRINT "HELLO MY NAME IS DAGNEY. WHAT IS YOUR NAME";\INPUT M1#
930 PRINT "ENTER DATASET NUMBER";\INPUT V1#
940 PRINT "ENTER SAMPLE TYPE";\INPUT V2#
950 IF V2#="OIL"GO TO 980
960 PRINT "ENTER HEMATOCRIT";\INPUT V3#
970 GO TO 990
980 PRINT "ENTER NOMINAL VISCOSITY";\INPUT V3#
990 V1#='DX1:DAT'&V1#

```

```

1000 OPEN V1$ FOR OUTPUT AS FILE #1
1006 PRINT #1: '\PRINT #1:'
1007 PRINT #1: 'VISCO-ELASTIC EXPERIMENT\PRINT #1:'
1010 PRINT #1: 'DATE: ' ; DATE$
1020 PRINT #1: 'SAMPLE: ' ; V2$
1030 IF V2$="OIL" GO TO 1060
1040 PRINT #1: 'HEMATOCRIT: ' ; V3$
1050 GO TO 1070
1060 PRINT #1: 'NOMINAL VISCOSITY: ' ; V3$
1070 PRINT #1: 'ENTER NAT. FREQ. IN HERTZ' ; '\INPUT F9
1080 PRINT #1: 'NATURAL FREQUENCY OF TORSION BAR: ' ; F9; " HERTZ"
1090 PRINT #1: 'ENTER STIFFNESS CONST. IN DYNES-CM/MICRON' ; '\INPUT F9$
1100 PRINT #1: 'STIFFNESS CONST. OF TORSION BAR IN DYNES-CM: ' ; F9$
1101 PRINT #1: 'ENTER INPUT AMP. IN MICRONS' ; '\INPUT F9$
1103 PRINT #1: 'INPUT AMP. IN MICRONS: ' ; F9$
1110 PRINT #1:
1120 PRINT #1: 'INPUT RANGE", "OUTPUT RANGE", "FREQ.", "AMP. RATIO", "PHASE ANGLE"
1125 RETURN
1130 PRINT #1:
1140 PRINT #1: G1, G2, F1, A1(1), P1(1)
1150 RETURN
1154 PRINT #1: '\PRINT #1:'
1155 PRINT #1: 'THIS EXPERIMENT WAS INITIATED BY ' ; M1$
1160 CLOSE #1

```

READY

APPENDIX III.

PROGRAM FOR THE DETERMINATION OF AMPLITUDE RATIO AND PHASE

ANGLE IN PULSATILE FLOW.

```

RHEOSO      BASIC W01B-02

10 GOSUB 920
15 PRINT ' '
17 PRINT "ENTER FREQUENCY";\INPUT F1\IF F1=0 THEN 1154
18 PRINT "ENTER SHEAR RATE";\INPUT S1
19 PRINT "ENTER OUTPUT RANGE";\INPUT G2
20 IF F1>1.00000E-03GO TO 22 \E1=5\GO TO 30
22 IF F1>.01GO TO 24 \E1=4\GO TO 30
24 IF F1>.1GO TO 26 \E1=3\GO TO 30
26 IF F1>1GO TO 28 \E1=2\GO TO 30
28 E1=1
30 IF F1>7.5GO TO 32 \R3=256\GO TO 39
32 IF F1>10GO TO 34 \R3=128\GO TO 39
34 IF F1>30GO TO 36 \R3=64\GO TO 39
36 R3=32
39 C1=1.00000E+06/10^(E1-1)
46 PRINT 'PRESS CR KEY TO START SAMPLING';\INPUT W1#
47 R1=INT(C1/(R3*F1))+.5)
48 DIM A(256),D1(512),D2(256)
49 CALL "USE"(A)
50 I9=1
52 CALL "SETR"(E1,1,R1)
55 CALL "RTS"(A,0,2,R3,2)

```

```

58 FOR I=1 TO R3
59 CALL "LED"(I)
60 CALL "RDB"(A,Z)
62 IF Z<000 TO 60
63 D1(I)=Z*2/4095-1
64 CALL "RDB"(A,Z)
65 IF Z<000 TO 64
66 D2(I)=Z*2/4095-1
70 NEXT I
75 FOR I=1 TO R3
76 IF I9=200 TO 77 \A(I)=D1(I)\GO TO 78
77 A(I)=D2(I)
78 NEXT I
102 I1=1
103 N2=2*R3\N4=N2-1
106 FOR I=1 TO N4 STEP 2
107 J=(I+1)/2
110 D1(I)=A(J)
114 NEXT I
115 FOR I=1 TO N4 STEP 2
117 K=I+1
118 D1(K)=0
119 NEXT I
140 J=1
150 FOR I=1 TO N2 STEP 2
160 IF (I-J)>=000 TO 230
170 T1=D1(J)
180 T2=D1(J+1)
190 D1(J)=D1(I)
200 D1(J+1)=D1(I+1)
210 D1(I)=T1
220 D1(I+1)=T2
230 M=N2/2
240 IF (J-M)<=000 TO 300
250 J=J-M
260 M=M/2

```

```

270 IF (M-2)>=0 GO TO 240
300 J=J+M
310 NEXT I
320 M1=2
330 IF (M1-M2)>=0 GO TO 476
331 CALL "LED"(M1)
340 I2=2*M1
345 P=3.14156
350 FOR M=1 TO M1 STEP 2
360 H1=P*I1*(M-1)/M1
370 M1=COS(H1)\M2=SIN(H1)
390 FOR I=M TO N2 STEP I2
400 J=I+M1
410 T1=M1*D1(J)-M2*D1(J+1)
420 T2=M1*D1(J+1)+M2*D1(J)
430 D1(J)=D1(I)-T1
440 D1(J+1)=D1(I+1)-T2
450 D1(I)=D1(I)+T1
460 D1(I+1)=D1(I+1)+T2
465 NEXT I
466 NEXT M
470 M1=I2
475 GO TO 330
476 PRINT '
480 PRINT 'HARMONIC', 'REAL COEFF', 'IMAG COEFF', 'AMP', 'PHASE'
481 O4=0\PRINT '
482 FOR I=1 TO 9 STEP 2
485 D1(I)=D1(I)*2/R3
487 D1(I+1)=D1(I+1)*2/R3
490 A1(O4)=SQRT(D1(I)*D1(I)+D1(I+1)*D1(I+1))
491 IF D1(I)>0 GO TO 496
493 IF D1(I+1)<0 GO TO 494 \P1(O4)=90\GO TO 503
494 P1(O4)=270
495 GO TO 503
496 P1(O4)=ATN(D1(I+1)/D1(I))*180/P
497 IF D1(I)>0 GO TO 503 \P1(O4)=P1(O4)+180\GO TO 503

```

```

499 IF D1(I+1)>0GO TO 503 \P1(04)=P1(04)+360\GO TO 503
500 GO TO 503
503 PRINT 04,D1(I),D1(I+1),A1(04),P1(04)
504 IF I9=260 TO 515
505 A2(04)=A1(04)\P2(04)=P1(04)
510 IF I9=160 TO 530
515 REM CORRECTIONS
516 P1(04)=P1(04)+.1*F1
520 A1(04)=(A1(04)*G2)/(A2(04)*G1)/3.2
521 IF A1(04)>0GO TO 522 \A1(04)=-A1(04)
522 P1(04)=P2(04)-P1(04)
523 IF F1<F9GO TO 525 \GO TO 527
525 IF P1(04)>0GO TO 530 \P1(04)=P1(04)+360\GO TO 530
527 IF P1(04)<0GO TO 530 \P1(04)=P1(04)-360\GO TO 530
530 04=04+1
531 NEXT I
535 I9=I9+1
540 IF I9<=260 TO 75
545 GOSUB 1130
550 PRINT ' ' \PRINT ' '
600 PRINT 'FREQUENCY',F1\PRINT ' '
601 PRINT 'SHEAR RATE',S1
605 PRINT ' ' \PRINT ' '
610 PRINT 'HARMONIC',AMP.RATIO', 'PHASE ANGLE'
611 I=1
612 PRINT I,A1(I),P1(I)
614 PRINT ' ' \PRINT ' '
615 01=1\GO TO 17
920 PRINT "HELLO MY NAME IS DAGNEY. WHAT IS YOUR NAME";\INPUT M1#
930 PRINT "ENTER DATASET NUMBER";\INPUT V1#
940 PRINT "ENTER SAMPLE TYPE";\INPUT V2#
950 IF V2#="OIL"GO TO 980
960 PRINT "ENTER HEMATOCRIT";\INPUT V3#
970 GO TO 990
980 PRINT "ENTER NOMINAL VISCOSITY";\INPUT V3#
990 V1#='DX1:DAT'&V1#
1000 OPEN V1# FOR OUTPUT AS FILE #1

```



```

1006 PRINT #1: " \PRINT #1: "
1007 PRINT #1: "VISCO-ELASTIC EXPERIMENT \PRINT #1: "
1010 PRINT #1: "DATE: "; DAT$
1020 PRINT #1: "SAMPLE: "; V2$
1030 IF V2$="OIL" GO TO 1060
1040 PRINT #1: "HEMATOCRIT: "; V3$
1050 GO TO 1070
1060 PRINT #1: "NOMINAL VISCOSITY: "; V3$
1070 PRINT #1: "ENTER NAT. FREQ. IN HERTZ \INPUT F9
1080 PRINT #1: "NATURAL FREQUENCY OF TORSION BAR: "; F9; " HERTZ"
1090 PRINT #1: "ENTER STIFFNESS CONST. IN DYNES-CM/MICRON \INPUT F9$
1100 PRINT #1: "STIFFNESS CONST. OF TORSION BAR IN DYNES+CM: "; F9$
1101 PRINT #1: "ENTER INPUT AMP. IN MICRONS \INPUT F9#
1103 PRINT #1: "INPUT AMP. IN MICRONS: "; F9#
1104 PRINT #1: "ENTER INPUT RANGE \INPUT G1
1105 PRINT #1: "INPUT RANGE: "; G1
1110 PRINT #1: "
1120 PRINT #1: "OUTPUT RANGE". "FREQ. ". "SHEAR". "AMP. RATIO". "PHASE ANGLE"
1125 RETURN
1130 PRINT #1: "
1140 PRINT #1: G2. F1. S1. A1(1). P1(1)
1150 RETURN
1154 PRINT #1: " \PRINT #1: "
1155 PRINT #1: "THIS EXPERIMENT WAS INITIATED BY "; M1$
1160 CLOSE #1

```

READY

REFERENCES

Chapter I.

1. Weissenberg, K. Abhdlg. Preuss. Ak.d. Wiss. No.2 1931.
2. Weissenberg, K. Arch. Sci. Phys. et Nat.V.17, 1. 1934.
3. Weissenberg, K. Proceedings 1st Int. Cong. Rheol. Holland, 1948. Amsterdam, North Holland Publishing Co., 1949. I. 29-46.
4. Weissenberg, K. A course of ten lectures on the principles of continuum mechanics, as seen in the light of a general theory of transformation. (Columbia University, 1964). Office of Naval Research, Project #064-446. (Technical Report #18).
5. Freeman, S.M., and Weissenberg, K. Nature, 161, 324. 1948.
6. Weissenberg, K. Proceedings 1st Int. Cong. Rheol. Holland 1948. Amsterdam, North Holland Publishing Co., 1949. II. 114-118.
7. Roberts, J. Proceedings 2nd Int. Cong. Rheol. Oxford. I. 91, 1953.
8. Jobling, A. PhD. Thesis, Cambridge University, 1955.
9. Roberts, J. Personal communication to R.G. King, 1960.
10. King R.G. Rheogoniometer Techniques. Bognor Regis, Farol Research Engineers, Ltd., 1964.
11. Grossman, P.U.A. Ph.D. Thesis, Cambridge University, 1958.
12. Grossman, P.U.A. J. Scient. Inst. 35, 131, 1958.
13. Grossman, P.U.A. Koll; Zs. 174, 97. 1961.
14. Grossman, P.U.A. The Karl Weissenberg 80th Birthday Celebration Essays. Ed. J. Harris. Kampala, Nairobi Dar Es Salaam. East African Literature Bureau. 57-64, 1973.

Chapter I (continued)

15. Giesekeus H. The Karl Weissenberg 80th Birthday Celebration Essays. Ed. J. Harris. Kampala, Nairobi, Dar Es Salaam. East African Literature Bureau. 103-112, 1973.
16. Lodge, A.S. The Karl Weissenberg 80th Birthday Celebration Essays. Ed. J. Harris. Kampala, Nairobi, Dar Es Salaam. East African Literature Bureau. 81-101, 1973.
17. Scott-Blair, G.W. The Karl Weissenberg 80th Birthday Celebration Essays. Ed. J. Harris. Kampala, Nairobi, Dar Es Salaam. East African Literature Bureau. 113-126, 1973.
18. Weissenberg, K. The testing of materials by means of the Rheogoniometer. Bognor Regis, Farol Research Engineers, Ltd., 1964.
19. Walters, K. Basic concepts and formulae for the Rheogoniometer. Bognor Regis, Sangamo Controls, Ltd., 1968.

Chapter II.

1. Weissenberg, K. Proc. Ivth Int.Cong.Rheol. IV (Ed. A. Copley) New York. Interscience Publishers. 19, 1965.
2. Scott-Blair, G.W. "Deformation and Flow in Biological Systems" Ed. A. Frey-Wyssling. North Holland Publishing Co., Amsterdam, p. 447. 1952.
3. Copley, A.L., Scott-Blair, G.W., Glover, F.A. and Thorley, R.S. Kolloid Ziet. 168, 101. 1960.
4. Whitmore, R.L. "Hemorheology and Hemodynamics". Bio-rheology 1, 201. 1963.
5. Dintenfass, L. "Thixotrophy of Blood at very low rates of shear". Kollid Zeit. 180, 160. 1962.

Chapter II (continued)

6. Wells, R.E. "Rheology of Blood in the Microvasculature"
New Engl. J. Med. 270, 832. 1964.
7. Gregersen, M.I., Perie, B., Usami, S. and Chien, S.
Proc. Sec. Exptl. Biol. Med. 112, 883, 1963.
8. Muller, H.G. Nature Vol. 195. 4838, 235. 1962.
9. Fahraeus, R. Physiol. Rev. 9, 2. 241. 1929.
10. Singer, S.L. Ann. Ref. Biochem. 43. 805. 1974.
11. Katchalsky, A., Kedem, O., Klimausky, C. and DeVies, A.
The Flow Properties of Blood and other Biological Systems. 155-164. A.L. Copley and G. Stainsby, eds.
Pergamon Press, Inc., New York, N.Y.
12. Rand, P.R. Biophys. 4. 303. 1964.
13. Hochmuth, R.M. et al. Biophys. J. 13. 747. 1973.
14. Evans, E.A., La Celle, P.L. Blood 45. 29. 1973.
15. Chien, S., Sung, K.P., Skalak, R., Usami S., and
Tozeran, A. Biophys. J. 24. 463. 1978.
16. Lesner, A. Biorheology 6. 284. 1970.
17. Thurston, G.B. Biophys. J. 12. 1205. 1972.
18. Chien, S., King, R.G., Skalak, K., Usami, S. Biorheology
12. 341-346. 1975.

Chapter III

1. Chien, S., et al. Biophys. J. 24. 463 1978
2. Brooks, D. E., et al. Biorheology 11. 69-77. 1974
3. Lessner, A., et. al. Biorheology 6. 284. 1970
4. Silberberg, A., and Mijulieff, P. F. J. Polymer
Science. Part A-2 8. 1089. 1970

Chapter III (continued)

5. Thurston, G. B. Biophys. J. 12. 1205. 1972
6. Thurston, G. B. Biorheology 9. 165. 1972
7. Chien, S.; King, R. G.; Skalak, R.; Usami, S. Bio-rheology, 12. 341-346. 1975
8. Ponder, E. "Hemolysis and Related Phenomina". Grune and Stratton, Pub. New York 1948
9. Pranker, T. A. J. "The Red Cell". Blackwell Pub. Oxford. 1961
10. Huang, C. R., et.al. Biorheology, 12. 279 1975
11. Dintenfass, L. Blood Microrheology. Appleton-Century-Crofts, New York, London. 1971
12. Cokelet, J. R., et. al. Trans. Soc. Rheology. 1. 303. 1963
13. Copley, A. L., and King. R. G. Experientia. 21. 81. 1970
14. Copley, A. L., and King, R. G. Biorheology, 12, 5-10, 1975
15. King, R. G. Rheol. Acta 4, 265 1965
16. Fahraeus, R. Acta Med. Scand: 55, 1. 1921
17. Fahraeus, R. Acta Med. Scand: 161, 151 1958
18. Ruhenstroth-Bauer, C.; Brittinger, G.; Granzer, E.; and Nass, G. Deutsche Med. Wehnschr:85, 808 1960
19. Gomulkiewicz, J. Studia Biophyca:35, 21 1973
20. Boyd, J. J. M., and Sanderson, J. J. Plasma Dynamics, Barnes and Noble, New York 1969
21. Cutler, J. W. Am. J. Med. Sci.:183, 643 1932
22. Reichel, H. Blutkörperchensenkung, Springer-Verlag, Vienna 1936

Chapter III (continued)

23. Westergren, A. Acta Med. Scand.:54, 247 1921
24. Fahraeus, R. Rheol. Acta.:1, 656 1961
25. Macfarlane, R. G. "An Enzyme Cascade in the Blood Cutting Mechanism, and its Function as a Biochemical Amplifier." Nature. London, 202, 498 1964
26. Macfarlane, R. G. "The Basis of the Cascade Hypothesis of Blood Clotting." Thromb. Diath. Haemorrh. 15, 591 1966
27. Hartert, H. "Blutgerinnungastudien mit der Thrombelastographie, einen neuen Untersuchungsverfahren." Klin. Wachr. 26, 577 1948
28. Hartert, H. "Die Thrombelastographie in der Differentialdiagnose der Hamorrhagischen Diatheses." Schweiz. med. Wachr. 79, 318 1949
29. Hartert, H. "Uber einen strukturbilden Fakto in den Thrombocyten." Klin. Wachr. 27, 789 1949
30. Hartert, H. "Thrombelastographische Untersuchungen zur Fibrinolyse." Klin. Wachr. 28, 77 1950
31. Hartert, H. "Thrombelastographische Unterschuhungen zur Retraktion." Klin. Wachr. 28, 78 1950
32. Die Thrombelastographie. "Eine Methode zur physikalischen Analyse des Blutgerinnungavorganges." Z. exper. Med. 117, 189 1951.
33. Hartert, H. "Eine neue Theorie der Retraktion des Blutgerinnnsels. Schweiz. med. Wachr. 81, 1248 1951
34. Thrombelastographische Kriterien der echten Thrombocytopathien und thre diagnostische Anwendung. Schweiz. 81, 1253 1951

Chapter III (continued)

35. Hartert, H. "Thrombelastographische Untersuchungen bei der Milzexstirpation an Fällen von Morbus Werlof." Schweiz. med. Wachr. 81, 1253 1951
36. Hartert, H. "Idiopathische Hypoprothrombinaemie mit Hemorrhagien." Z. klin. Med. 1949, 635 1952
37. Hartert, H. "Physiologische und methodische Grundlagen der Thrombelastographie." Dtsch. Arch. klin. Med. 199, 284 1952
38. Hartert, H. Die Thrombocytopathien. Dtsch. Arch. klin. Med. 199, 293 1952
39. Hartert, H. Plasmatische Gerinnungsdefekte. Dtsch. Arch. klin. Med. 199, 402 1952
40. Hartert, H. Vasculare hamorrhagische Diathesen; Blutungen ohne hamorrhagische Diathesen; Differentialdiagnose der hamorrhagischen Diathesen. Dtsch. Arch. klin. Med. 199, 414 1952
41. Das Thrombelastogram. Verh. dtsch. Ges. Inn. Med., Wiesbaden 562 1952
42. Hartert, H. Eine neue Theorie der Retraktion. Verh. dtsch. Ges. Inn. Med., Wiesbaden 530, 1952
43. Hartert, H. L'evaluation de la fonction des plaquettes par la thrombelastographie. Proc. 4. Congr. Soc. Europ. Hematol, Amsterdam, 64 1953
44. Hartert, H. Eine Retraktions-Cofaktor im Serum. Klin. Wschr. 32, 139 1954
45. Vecchietti, G. La fibrinolisi attivata con streptochinasi nel periodo post-operative. Valutazione trombelastografica. Riv. ostetr. ginec. 9, 137 1954

46. Kaulla, K. N.; Weiner, M. Studies of coagulation and fibrinolysis by new techniques of continuous recording. Blood, 10, 362 1955
47. Jurgens, R. Koronarthrombose und Gerinnung. Verh. dtsh. Ges. Kreislaufforsch. 21, 77 1955
48. Bock, H. E.; Gross, R. Grose und kleine Blutungen in der Inneron Medizin. Dtsch. med. Wschr. 81, 1451 1956
49. Beller, F. K.; Koch, F.; Mammen, E. Thrombelastographische Untersuchungen bei isolierten Störungen der Vor-und 1. Phase der Gerinnung Blut 2, 112, 1956.
50. Gross, R.; Ludwig, H. Hochdosierte Prednison und Prednisonolbehandlung bei Blutkrankheiten. Klin. Wschr. 34, 1117 1956
51. Satake, K. Blutgerinnung und Thrombelastograph. Japanese Med. J. 1743, 29, 1957
52. Marchal, G.; Duhamel, G.; Leroux, M.; Chenderovitch, J.; Goglin, J. Deux cas de splénomégalie myéloïde avec thrombocythémie hémorragipare. Action du myélan. Intérêt des thrombo-elastogrammes. Sang 23, 245 1957
53. Leroux, M. La place du laboratoire dans le diagnostic et le traitement des thromboses. Therapie. 10, 259 1955
54. De Nicola, P. Thrombelastography. Charles C. Thomas, Springfield, Ill. USA. 1957
55. Deutsch, E. Veränderungen und Wechsel der Gerinnungswerte bei Auftreten einer thrombotischen Erkrankung. Thrombose und Embolie, Basel. 433 1954

Chapter III (continued)

56. Marx, R. Über den Wert der Bestimmung von Blutgerinnungsfaktoren und kinstanten ("Hepatocoagulogramme") für die Beurteilung von Leberkrankheiten. *Arztl. Laboratorium* 2, 309 1956
57. Hartert, H.; Lasch, H. G.; Pfisterer, J. Charakterisierung und Funktion eines Retraktions-Cofaktors. *Throm. Diath. haem.* 1, 445 1957
58. Winckelmann, G. Fehlermöglichkeiten bei der Beurteilung von Thrombelastogrammen. *Folia haemat. Neue Folge* 2, 102 1958
59. Hartert, H. Thrombelastographie. *Proc. VIIth Congr. Internat. Soc. Hematol. Rome. Il Pensiero Scientifico, Roma.* 216-225 1959
60. Hartert, H. Stuart factor and thrombelastography. In: *New blood clotting factors.* I. S. Wright,; F. Keller; F. Streuli, Eds. *Thromb. Diath. Haem. Suppl. ad Vol IV.,* 43 1959
61. Hartert, H. Thrombelastography: Physical and physiological aspects. In: *Flow Properties of Blood.* A. L. Copley and G. Stainsby, Eds. Pergamon Press, Oxford-New York 186-196 1960
62. Hartert, H. Comparative laboratory studies on the effect of anticoagulants and fibrinolysins. In: *Anticoagulants and Fibrinolysins.* Macmillan, Toronto, Canada 389 1961
63. Hartert, H. Effect of anticoagulant therapy on thrombogenesis. In: *Anticoagulant Therapy in Ischemic Heart Disease.* E. Sterling-Nicol, Ed. Miami 51-55 1964

64. Hartert, H. Thrombelastography. In: Thrombosis and Bleeding Disorders. N. U. Bang; F. K. Beller; E. Deutsch; E. F. Mammen, Eds. Academic Press. Thieme - New York-London 70-76 1970
65. Fischbacher, W. Beitrag zur Fibrinolyse. Thesis, Zurich. 1960
66. Caprini, J. A.; Kwaan, H. C.; Zuckerman, L.; and Verduin, R. Thrombelastographic patterns of Ancrod and thrombin, fibrin formation and dissolution. Thrombosis Research, 4:199 1974
67. Caprini, J. A.; Eckenhoff, J. B.; Ramstrack, L.; Zuckerman, F. F. and Mockros, L. F. Contact activation of heparinized plasma. Thrombosis Research, 5:379 1975
68. Zuckerman, L.; Ramstrack, J. M.; Vagher, J. P.; Caprini, J. A.; Mockros, L. F. Neutralization of heparin by cellular blood elements. Thrombosis Research. 7:149 1975
69. Caprini, J. A.; Zuckerman, L.; Cohen, E. and Vagher, J. P. The identification of accelerated coagulability. Thrombosis Research. 9:167 1976
70. Caprini, J. A.; Eckenhoff, L.; Zuckerman, L. F.; Mockros, L. F. and Verduin, R. The influence of celite on heparinized plasma. Clin. Research. 548 1976.
71. Haid, M.; Zuckerman, L.; Caprini, J. A.; Kurtider, S. and Vagher, J. P. Thrombelastographic changes in carcinoma. J. Of Medicine, 7:304 1976

Chapter III (continued)

72. Zuckerman, L.; Cohen, E.; Vagher, J. P.; Woodward, E. and Caprini, J. A. Comparison of Thrombelastography with common coagulation tests. Thrombosis and Hemostasis. 10:234 1976
73. Hartert, H. Rheo-Thrombelastographie, ein neuer Globalgerinnungstest. Proc. SIV. Tagg. Dtsch. Arb. Gemeinschaft fur Blutgerinnungsforsch. Stuttgart 1970
74. Hartert, H. Rheo-Simulation. Proc. SV. Tagg. Dtsch. Arb. Gemeinschaft fur Blutgerinnungsforsch. Marburg 1971
75. Hartert, H. Rheo-Simulation: A new method for the assay of clotting process and the effect of factor XIII. Biorheology 11, 355 1974
76. Marchal, G.; Leroux, M. E. and Samama, M. "Atlas de Thrombodynamographie" Edition Information, Service de Propaganda. Paris 1962
77. Dintenfass, L. The effect of velocity gradient on the clotting time of blood and on the consistency of clots found in vitro. Circulation Research, 18:349 1966
78. Dintenfass, L. Dynamics of Blood Coagulation. Haematologia, 1:387 1967
79. Dintenfass, L. Blood Microrheology. Appleton-Century-Crofts, London 1971

Chapter IV.

1. Whitmore, R. L. "The Rheology of the Circulation." Pergamon Press, Oxford, London, New York. 1968

2. Dintenfass, L. "Blood Microrheology." Appleton-Century-Crofts, London, New York 1971
3. Chien, S.; Usami, S. and Bertles, J. F. J. Clin. Invest. 44. 623 1970
4. White, J. G. and Heagan, B. "Sickle Cell Disease. Diagnosis, Management, Education and Research." C. V. Mosby, St. Louis, MO 104 1963
5. Cokelet, S. R. and Neisselman, N. J. Science. 162 275 1968
6. Fahraeus, R. The suspension stability of blood. Physiol. Rev. 9, 241 1929
7. Chien, S. Biophysical behavior of red cells in suspensions. In: The Red Blood Cell. D. MacN. Surgenor, ed. Vol. II. Academic Press, New York, pp. 1031-1133, 1975
8. Usami, S.; Chien, S.; Scholz, P. M.; Bertles, J. F. Effect of deoxygenation on blood rheology in sickle cell disease. Microvascular Res. 9, 324 1975
9. Chien, S.; Dellenback, R. J.; Usami, S.; Gregersen, M. I. Plasma trapping in hematocrit determination: Differences among animal species. Proc. Soc. Exper. Biol. Med. 119, 1155 1965
10. Chien, S.; Usami, S.; Dellenback, R. J.; Bryant, C. A. Comparative hemorheology hematological implications of species differences in blood viscosity. Biorheology 9, 35 1971
11. Schmid-Schönbein, G. W. et al. Passive mechanical properties of Human Leukocytes. Biophys. J. 36 243 1981

Chapter IV (continued)

12. La Celle, P. L.; Bush, R. W. and Smith, B. D. "Viscoelastic Properties of Normal and Pathological Human Granulocytes and Lymphocytes." In: "White Blood Cells." U. Bagge; G. V. R. Børn; P. Gaentgens, Eds. Martinus-Nijhoff, Publ. The Hague-Boston-London, p. 32 1982
13. Lichtman, M. A. "Cellular deformability during maturation of the myeloblast." N. Engl. J. Med. 283: 943 1970
14. Cokelet, G. R. and Lichtman, M. A. "Rheology of Leukocyte Suspensions." In: "White Blood Cells," U. Bagge; G. V. R. Born; P. Gaentgens, Eds. Martinus-Nijhoff, Pub. The Hague-Boston-London, p. 46 1982
15. Chien, S. In Symposium on Recent Developments in Microcirculation Research. E. Davis and G. A. Marcel, Eds. Excerpta Medica Acta. Amsterdam-Oxford-Princeton, pp. 54-69 1981

Chapter V.

1. Copley, A. L. "On Biorheology." Biorheology, 9:141, 1972; Abstract, 1st Internat. Congress of Biorheology, Lyon 1972
2. Copley, A. L. "Hemorheological Aspects of the Endothelium-Plasma Interface." Abstracts, VIII Congr. European Soc. Microcirculation, Aberdeen, Scotland. Aug. 26-Sept. 1, 1972

3. Copley, A. L. "Non-Newtonian Behavior of Surface Layers of Human Plasma Protein Systems and a New Concept of the Initiation of Thrombosis." *Bioheology*, 8:79 1971
4. Copley, A. L. "Rheogoniometrically Measured Viscosity Profiles of Plasma Protein Systems and a New Concept of the Genesis of Thrombosis." Abstracts, 25th Int. Cong. Physiol. Science, July 25-31, 1971, Munich, W. Germany.
5. Copley, A. L. and King, R. G. "Rheogoniometric Study of Viscosity of Fibrinogen and Plasma-Fibrinogen Systems." *Federation Proc.* 30:480 1971
6. Copley, A. L. and King, R. G. "Viscous Resistance to Thromboid (Thrombus like) Surface Layers in Systems of Plasma Proteins Including Fibrinogen." *Thrombosis Research* 1:1 1972
7. Copley, A. L. and King, R. G. "The Action of Human Red Blood Cells and Platelets on Viscous Resistance of Plasma Protein Systems." *Biorheology* 9:147 1972
8. Copley, A. L. and King, R. G. "Viscous Resistance Lowering Action of Highly Purified Gamma Globulin on Surface Layers of Fibrinogen and other Plasma Proteins." Abstracts, IV. Congress of the International Society on Thrombosis and Hemostasis, Vienna, 19-22 June, 1973

Chapter V (continued)

9. Vroman, L.; Adams, A. L.; Klings, M.; Fischer, G. C.; Munoz, P. G. and Solensky, P. P. "Reactions of formed Elements of Blood with Plasma Proteins." In: "The Behavior of Blood and its Components at Interfaces." L. Vroman and E. F. Leonard, Eds. Ann. N. Y. Acad.-Sci. 283, 65-76 1977
10. Vroman, L.; Adams, A.; Klings, M.; and Fischer, G. "Fibrinogen, Globulins, Albumin and Plasma at Interfaces." Adv. Ehem. Series, 145, 255-289 1975
11. Joly, M. "Etude par Viscometrie Superficielle de la deformabilite des macromolecules." Proc. 5. Internat. Congress on Rheology, Kyoto, Japan, 1968. Ed. S. Onogi, Tokyo Press: Baltimore, MD and Manchester, England. University Book Press, Vol. 2, p. 191 1970
12. Wells, R. B. and Merrill, E. W. "Shear Rate Dependence of the Viscosity of Whole Blood and Plasma." Science, 133:763 1961
13. Chien, S.; Usami, S.; Taylor, H. M.; Lundberg, J. L. and Gregersen, M. I. "Effects of Hematocrit and Plasma Proteins on Human Blood Rheology at Low Shear Rates." J. Appl. Physiol. 21:81 1966
14. Brooks, D. E.; Goodwin, J. W.; Seaman, G. V. F. "Interactions among Erythrocytes under Shear." J. Appl. Physiol. 28:172 1970
15. Copley, A. L. and King, R. G. "The Action of Human Red Blood Cells and Platelets on Viscous Resistance of Plasma Protein Systems." Biorheology, 10 533 1973
16. Smith, I. E. and Morrison, B. W. Personal Communications 1975

17. Tooney, N. M. and Cohen, C. "Microcrystals of a Modified Fibrinogen." *Nature* 237, 23-25 1972
18. Tooney, N. M. and Cohen, C. "Crystalline States of a Modified Fibrinogen." *J. Molecular Biol.*, 110, 363-385 1977
19. Stewart, G. J. and Niewiarowski, S. "Nonenzymatic Polymerization of Fibrinogen by Protamine Sulfate: An Electron Microscopic Study." *Biophys. Acta.* 194 462-469 1969
20. Stewart, S. "An Electron Microscope Study of the Polymerization of Fibrinogen and its Derivatives." In: *Fibrinogen Degradation Products.* M. Verstraete; J. Vermylen; and M. B. Donati, Eds., pp. 165-178. *Scand. J. Hematol. Suppl. No. 13.* Munksgaard, Copenhagen 1971
21. Copley, A. L. "Non-Newtonian Behavior of Surface Layers of Human Plasma Protein Systems, and a New Concept of the Initiation of Thrombosis." *Biorheology*, 8, 79 1971
22. Copley, A. L. and King, R. G. "Polymolecular Layers of Fibrinogen Systems and the Genesis of Thrombosis." In: *Hemorheology and Thrombosis.* A. L. Copley and S. Okamoto (Eds.) Pergamon Press, 393-409 1976
23. Copley, A. L.; King, R. G.; Kudryk, B. and Blomback, B. "Viscous Resistance of Surface Layers of Highly Purified Fibrinogen Systems." *Proc. VII Internat. Congr. Rheology*, Gothenberg, Sweden 1976

24. Copley, A. L. "New Hemorheological Findings on Surface Layers of Fibrinogen Systems and their Relationship to Thrombogenesis." Symposium on Hemorheological Aspects of Thrombosis. 16th Int. Cong. Hematol. Kyoto, Japan. Abstracts, Main Topics and Symposia, p. 156 1976
25. Copley, A. L. "On the Endoendothelial Fibrin Lining and on Fibrinogen Clotting without Thrombin Action, Their Significance in Health and Disease." Gazette Medicale de France (Paris) 1978
26. Blomback, B. and Blomback, M. "Purification of Human and Bovine Fibrinogen." Arkiv. Kemi. 10:415-443 1956
27. McLaren, A. D. and Seaman, G. V. F. "Concerning the Surface pH of Clays." Soil Science Soc. American Proc., 32:127 1968
28. McLaren, A. D. "Enzyme action in structurally restricted systems." Enzymology, 21:356-364 1960
29. McLaren, A. D. and Babcock, K. L. "Some characteristics of enzyme reactions at surfaces." In: Subcellular Particles, T. Hayashi, Ed. New York; Ronald Press, pp. 23-36 1959
30. Seaman, G. V. F. "Electrokinetic Behavior of Red Cells." In: The Red Blood Cell, Vol. 2. New York; Academic Press, pp. 1135-1229 1975
31. Seaman, G. V. F. Personal Communication, 12th August 1980.
32. Dintenfass, L. "Viscosity of Blood at high hematocrits measured in microcapillary viscometers." In: Hemorheology, A. L. Copley, Ed. pp. 197-209.

33. Dintenfass, L. and Burnard, E. Med. J. Australia, 1:1072 1966
34. Teitel, P. and Nicolau, C. T. In: Proc. Sympos. of Molecular Biology and Pathology, Bucharest 1964
35. Murphy, J. R. "Erythrocyte shape and Blood Viscosity." In: Hemorheology, A. L. Copely, Ed. pp. 469-478.
36. Schmid-Schönbein, H.; Volgar, E.; Weiss, J. and Brendhuber, M. Vasa 4:263-270 1975
37. Chambers, R, and Zweifach, B. W. J. of Cellular and Comparative Physiology, 15:225 1940
38. Shea, L. L.; Hermans, J.; McDonagh, J.; McDonagh, R. P. and Carr. M. "Effects of calcium ion and covalent cross-linking on the formation and elasticity of fibrin gels." Thrombosis Research, 6, 225-265 1975
39. Copley, A. L. "Some problems in hemorheology." In: Proc. 5th Int. Cong. on Rheology. S. Onogi, Ed. Tokyo-Baltimore-Manchester: University of Tokyo Press, 2, 3-25 1970
40. Ockelford, P. A.; Carter, C. J.; Mitchell, L. and Hirsh, J. "Discorance between the anti-Xa activity and the antithrombotic activity of an ultralow molecular weight heparin fraction." Thrombosis Research, 23:401-409 1982
41. Morrison, L. M.; Rucker, P. G. and Ereshoff, B. H. "Prolongation of thrombus formation time in rabbits given chondroitin sulfate 'A'/" J. Atherocler. Res. 8. pp. 319-327 1968

Chapter V (continued)

42. Bjornson, T. D.; Nash, V. P. and Schaten, R. "The Anticoagulant effect of Chondroitin-4-sulfate." Thrombosis Research, 27:15-21 1982
43. Dodge, J. T.; Mitchell, C. and Hanahan, D. J. Arch. Biochem. 110, 119 1963
44. Kirkpatrick, F. H. Life Science, 19, 1 1976
45. Chien, S. Blood Cells, 3, 71 1977

Chapter VI.

1. Copley, A.L. The Endothelial Fibrin lining as the crucial barrier and the role of fibrin gels in controlling transcapillary transport. Biorheology 21, 1984. (In Press).
2. Kirkpatrick, F.H. Life Science, 19. 1. 1976.
3. Blank, M. in "Membranes and Diseases" (L. Bolis, J.F. Hoffman, and A. Leaf, Eds.) 81-88. Raven Press, New York, 1976.
4. Singer, S.L. Ann. Ref. Biochem. 43. 805. 1974.